Risk Modelling of Safety Critical Systems for Life Extension in Offshore Oil and Gas

The University of Nottingham

Thomas Shuttleworth

Supervisor:
Darren Prescott

Abstract

On the United Kingdom Continental Shelf over half of the platforms are operating beyond their design life in a stage that is known as Life Extension (LE). Their extended life is due to the fact that fields that the platforms are extracting from are productive enough to continue to produce oil and gas at a rate that remains profitable to the operator. The rate of production is typically reduced in this stage and therefore the financial pressure on the platform is increased. Through the ageing of the installation the assets on the platform have undergone deterioration, to manage this operators have performed inspections and maintenance actions to control the condition of the assets, this is known as Asset Management (AM). Through the LE stage the deterioration rate of the assets has the potential to increase, meanwhile the financial pressure is increasing and as such there arises a problem of performing AM tasks such that it is optimised financially. Furthermore, due to the volatile fluids handled on-board it is imperative to ensure that the operation of the platform remains safe, therefore, a decision on performing AM tasks must also consider the probability and consequences of a loss of containment.

This thesis aims to construct a model for the production, generation and firewater deluge systems of an offshore oil and gas platform that simulates the AM of the assets involved in these systems. This will measure the performance of the platform through metrics representing different key indicators, these include the whole-life production availability, the AM expenditures and the risk of fires and explosions. A case-study platform known as Beryl B, is selected, this platform is an appropriate target as it is currently operating in a LE stage. The design of the systems are taken from this platform such that they appropriately reflect a real-world design. The key outcome of the research is the construction of a model for determining the performance of AM strategies and furthermore, an optimisation algorithm for the finding optimal strategies.

The primary technique of this research is a Petri Net (PN), this was selected as it can easily model system structures and interdependencies between arbitrary nodes. A novel extension to the traditional PN was created for this work which combined discrete and continuous elements to produce a hybrid technique. The net is used to model the degradation, AM and production of the platform throughout its life. The discrete

net simulates instantaneous, constantly timed and stochastically timed events, which include periodic inspections, maintenance, and stochastic degradation. Additionally, the system structures are represented in the discrete net such that faults can be connected to represent redundancies and system failures. Whereas, the continuous net simulates the constant flow of oil and gas through the production vessels throughout the platform's life to determine production quantities. The hybrid net allows for these parts to be connected, this is utilised such that the flows are dependent on the asset's conditions and failures. This forms a powerful technique for simulating the assets of an oil and gas processing platform, considering degradation, inspection, maintenance and production.

The oil and gas within the production vessels are volatile fluids that can ignite and cause damage or loss of life, it is therefore imperative that the frequency of leaks and the possible escalation are well understood. To this end, a consequence analysis technique is applied to the problem with the purpose of evaluating the risk of possible escalations following a loss of containment event. Specifically, three escalations are considered which are caused by ignitions in different situations, these are jet fires, pool fires and explosions. The consequence analysis is integrated into the PN through its simulation of asset degradation, this is such that when a leak failure mode occurs for a production vessel the consequence analysis evaluates risk profiles based on the initiating conditions. The initial conditions of the analysis are dependent on the vessel's dimensions and fluid contents and thereby give unique results for each vessel. Combined, this can evaluate the performance of a given AM strategy on the platform's through metrics relating to production quantities, AM expenditure and consequence frequencies and magnitudes.

This model is extended by the addition of an optimisation algorithm to determine optimal AM strategies for the platform from a whole-life perspective. Specifically the Non-Dominated Sorting Genetic Algorithm II (NSGA-II) is applied to the problem, this is a multi-objective evolutionary algorithm. A multi-objective algorithm was selected as the platform's objectives are not directly comparable, these were selected to quantify the production, cost and risk associated with a strategy. The algorithm produced a set of solutions that approach the Pareto surface, this does not require any preference to be made between the objectives, instead a user can select after the solutions have been generated. By examining the solutions through the generations the evolutionary progress can be seen to produce a solution set which is simultaneously diverse and near-optimal.

Acknowledgments

This PhD could not have been completed without the assistance, guidance and support of several individuals.

Firstly, I would like to express my gratitude to my supervisor Dr Darren Prescott who has mentored me throughout this PhD. His knowledge and advice has been invaluable in guiding my research and the completion of this thesis. Without his persistent help, this research would not have reached its goal. I am also thankful for Professor John Andrews for organising this research and trusting in me to perform it.

I am indebted to the University of Nottingham for the opportunity to perform my undergraduate and graduate studies. I wish to express my appreciation to Lloyd's Register Foundation for the support and funding, without which this research would not have been possible

Throughout my research my partner Alex has been a constant support, her positive words have encouraged me and enabled me to stay motivated in my research. I would also like to thank my parents, whose lifetime of support has allowed me to reach this point. Without their limitless love and backing I could have never achieved this PhD.

Contents

List of Figures

List of Tables

Acronyms

AM Asset Management.

BN Bayesian Network.

BOP Blowout Preventer.

CFD Computational Fluid Dynamics.

ETA Event Tree Analysis.

FTA Fault Tree Analysis.

GA Genetic Algorithm.

HSE Health and Safety Executive.

HSPN Hybrid Stochastic Petri Net.

HVAC Heating Ventilation and Air Conditioning.

LE Life Extension.

LFL Lower Flammable Limit.

MC Monte Carlo.

MP Markov Process.

MTTF Mean Time To Failure.

MTTR Mean Time To Repair.

NSGA-II Non-Dominated Sorting Genetic Algorithm II.

OREDA Offshore and Onshore Reliability Database.

PN Petri Net.

PSA Petroleum Safety Authority.

UFL Upper Flammable Limit.

UKCS United Kingdom Continental Shelf.

Chapter 1

The Offshore Oil and Gas Industry

1.1 Introduction

The majority of the discovered large and accessible offshore oil and gas fields are already being exploited by existing platforms, many of these platforms are old enough that they are reaching or have surpassed their design life, typically this is approximately 25 years (Stacey, Birkinshaw, and Sharp 2008). In some cases platforms continue to produce oil and gas economically, for these platforms it is advantageous to continue operating and enter into a Life Extension (LE) stage. These platforms are subject to advanced ageing with many of the assets lacking historical data on the effects of the advanced ageing on their condition. Therefore it is important to ensure that the Asset Management (AM) strategy is sufficiently maintaining assets during LE such that expenditure is minimised while maximising production and reaching the required safety standards.

In this thesis a model is constructed to analyse the effects of the AM strategy on a platform's assets' conditions, the safety system's reliabilities and the production level of a platform. The methodology followed in this research can be divided into four parts. Firstly, a Petri Net (PN) technique is used to model the life-cycle of an offshore platform's production, firewater deluge and power supply systems. This evaluates the performance of the platform, some of the key points are: production quantities, frequency and location of hydrocarbon leaks, safety system availability and AM expenditures. Secondly, a consequence analysis technique is developed, this is paired with the hydrocarbon leak information from the PN to produce a risk profile

for the platform. This analysis produces probability density functions of the magnitude of three possible events that can be caused by a leak: a jet fire, a pool fire and an explosion. Together these two parts produce a framework for trialling AM strategies on a simulated platform. Thus this leads to an opportunity to optimise the AM strategy using this model. The third part uses an evolutionary algorithm with multiple objective functions to determine a set of solutions near the optimal trade-off surface.

An advanced PN technique is at the core of the model, this is used to construct a network that simulates the life-cycle of a platform. This is chosen because of its ability to include stochastically sampled transition times and furthermore its capacity to implement interdependencies simply between elements of the model. The PN simulates several AM processes such as the degradation of components, periodic inspections and maintenance actions. The characteristics of inspection timing and maintenance decisions are given by the AM strategy, the net is designed such that a variety of AM strategies can be simulated. Furthermore, the net simulates degradation of components that result in a loss of containment of hydrocarbons, this is used to determine a frequency of leak from each component. The technique that was used in this research and is known as a Hybrid Stochastic Petri Net (HSPN), which can model both discrete and continuous processes. The flow of fluids through the platform's production train is modelled using the continuous part of the net. The assets covered by this research are in the production train, firewater deluge and power systems. These were selected as they were deemed to be the most important for the operation and safety of the platform. Through the Monte Carlo (MC) method, numerous simulations of the HSPN are performed, from which the model's results are generated.

The frequency and location of a hydrocarbon leak are found from the HSPN, to form a risk profile a consequence analysis technique is used. The initial conditions of the analysis are based on the vessel's dimensions, the fluids it contains and the module it is located in. Additionally some of the initial conditions are based on stochastically sampled variables such as the leak hole size and the leak hole height. As these are stochastically sampled a MC method is used to determine the distribution of results. The basis of the analysis is the calculation of the mass discharge rates of fluids from the vessels through incremental time-steps, this allows gas concentration and oil pool areas to be determined. In turn these allow the frequency and magnitude of a fire or explosion to be calculated. Therefore the consequence analysis determines the consequences of a leak scenario given by the HSPN.

The HSPN and consequence analysis provide a framework for trialling AM strate-

gies and evaluating their performance from many perspectives, such as production quantities, safety system availability and risk profile. Thus to determine the best AM strategy an optimisation technique can be used.

An evolutionary algorithm is used as an optimisation technique, in particular the Non-Dominated Sorting Genetic Algorithm II (NSGA-II) is used. This is applied as a multi-objective algorithm with several objective functions based on production, AM expenditures and risk. This algorithm breeds a population of solutions through successive generations to determine fitter solutions. A non-crowding process increases the spread of solutions across the objective space. The algorithm produces a set of solutions that a user can choose from after seeing the shape of the dominant solutions in objective space.

This chapter aims to present the reader with an introduction to the offshore oil and gas industry, the place of AM within it, a description of the aim, objectives and finally an outline of the thesis. Beginning with a background of the offshore oil and gas industry, Section 1.2 examines the history, present and future direction of the industry. Section 1.3 gives a brief overview of the production processes that take place on a platform in extracting well-fluids from a reservoir to exporting oil and gas. Next the hazards found on platforms are discussed in Section 1.4, relating to this some of the safety systems are discussed in Section 1.5. To examine the failures of these safety systems some of the most significant accidents and incidents in the industry are presented in Section 1.7. Introductions to AM and LE are presented in Section 1.8 and Section 1.9 respectively. The perspective of the state of the industry from regulatory bodies are examined in Section 1.10. Finally the direction of the thesis is discussed, the aims and objectives are presented in Section 1.11 and an outline of the thesis is given in Section 1.12.

1.2 Background of the Offshore Oil and Gas Industry

The offshore oil and gas industry has developed into a huge industry which is currently presented with a number of challenges. In this section the history, current state and future of the industry are discussed.

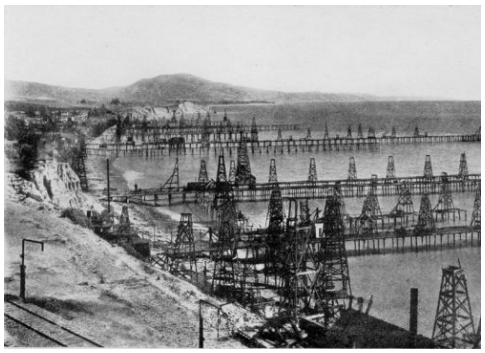

Figure 1.1: The first offshore oil wells, drilled off of piers in Santa Barbara, California. Image from Office of Response and Restoration n.d.

Figure 1.2: The first offshore drilling taking place out of the sight of land in 1947. Image from GEO ExPro n.d.

1.2.1 History

The offshore oil and gas industry can trace its origin back to 1896 when the first offshore oil drilling started just off the coast of California in Santa Barbara (Wilder 1998). Drilling was not new to Santa Barbara, onshore wells were already a common sight throughout the county as can be seen in Figure 1.1. When the offshore drilling began it consisted of little more than the construction of 400 metre long piers off the coast with wells periodically drilled along them in a water depth of a mere 10 metres. They drilled to roughly 130 metres below the sea floor before striking oil. With the offshore drilling industry in its infancy the technology used was largely borrowed from the onshore industry. The local populace considered the piers an eyesore but nevertheless they remained until a storm destroyed them in 1942, by which time they had been abandoned.

The industry continued to grow, by 1945 political pressure about the ownership of offshore oil in the waters surrounding the USA made President Truman extend USA claims for oil from 3 miles offshore to the edge of the continental shelf, defined to be a minimum of 200 nautical miles from the nearest USA shoreline (National Academies of Sciences, Engineering, and Medicine and others 2016). This allowed for the ongoing progression of the offshore oil and gas industry. By 1947 a new landmark was reached, the first drilling out of sight of land began. The Ship Shoal 32 achieved this in the Gulf of Mexico at 17 kilometres from the Louisiana coast (Priest 2007), as seen in Figure 1.2. Despite the increased distance from the shore, the platform was in shallow water, a depth of only 6 metres.

1.2.2 Present Day

Offshore drilling has moved into deeper water and new types of platforms are in use. When drilling in shallow water, fixed platforms are used, these sit on legs reaching down to the sea floor. When drilling in deeper water, new floating platforms were designed and constructed, a common type of floating platform is the semi-submersible. These structures are outfitted with drilling equipment and are capable of movement, albeit slow, reaching a top speed of around 4 knots. Modern semi-submersibles act as floating mini-cities, providing accommodation and all necessities to provide for a large crew, requiring only periodic visits from a supply ship.

The industry is increasingly moving towards drilling in deeper waters. The platform Perdido currently holds the record for the deepest floating platform at 2,450 metres in the Gulf of Mexico (Shell Global n.d.). Deepwater drilling presents several challenges, at the well the water pressures are hundreds of times atmospheric pressure and the temperatures are also very high, these both pose challenges to the equipment at the well. In these depths the cost of a well can easily run into excess of $100 million (Skogdalen, Utne, and Vinnem 2011). It is believed that the global production of oil is near at its maximum, most of the large oil and gas fields have already been discovered and exploited, with new discoveries being predominately smaller fields which are more challenging to produce from.

1.2.3 Future

Offshore platforms were typically built with a design life of 25 years, some of these platforms are continuing to produce oil and gas due to the field's yield being higher than expected or through new technologies increasing the recovery rate. It is important to streamline the operation of the platform so that the platform remains economic, in this extended life it is also important to maintain a safe environment as assets undergo ageing beyond their design lives. The future of the industry is uncertain, there is increasing demand for green energy, however in the near future a mix of energy generation sources will still be required to meet demand.

1.3 Offshore Production Processes

There are several different types of platforms and vessels in operation around the world. Some of these only extract the well-fluids to be processed at a nearby platform or onshore whereas others both extract and process for export. In this research we are considering a platform which both extracts and processes the well-fluids to produce an output of oil and gas (Speight 2014; Arnold and Stewart 1999; Devold 2013).

The extraction of hydrocarbons begins at the wellhead, this is a piece of equipment that is mounted on top of the well leading to the reservoir. In the offshore industry this wellhead can be mounted either sub-sea or topside on the platform. Generally a topside wellhead is used by fixed platforms or very stable platforms, whereas a sub-sea wellhead is used by less stable platforms and vessels. The reservoir is connected to the platform through a riser, this is a large conduit that connects the reservoir to the platform. Its purpose it to retrieve the well-fluids and transport then to the platform. The centre of a riser is used for the transport of hydrocarbons to the platform, the rest of the space in the riser is used for control of the well, including supplying power to sub-sea systems and for fluid lines to control the well pressure.

Once the well-fluids reach the platform they begin their journey along the process train. This consists of a series of assets that splits the fluids into a water, an oil and a gas stream for export. The primary asset for splitting the fluids is known as a separator, this a large pressure vessel that through the process of gravitational settling divides the fluids into layers. The oil and water separate into layers in the vessel, an interface-controller controls the rate at which the fluids leave the vessel to maintain the correct amount of water to function. Meanwhile the gas rises to the top of the vessel and a pressure control valve controls the rate at which the gas leaves.

Another significant process on the platform is the compression of the gas, this process consists of a series of scrubbers and compressors. The scrubbers remove remaining fluid from the gas, this is returned to the separators to be processed again. Each compressor increases the pressure of the gas so that the gas is under high-pressure by the end of the chain. This aids in the ability to store and export large quantities of gas.

An offshore platform is composed of a variety of modules, in this research we are interested in the production modules. Typically these are divided into three modules: wellhead, separation and compression. The wellhead module consists of production headers and the gas injection and gas lift wells. The separation module consists of

the assets relating to the separation of the well-fluids into water, oil and gas, these are the separators and related assets. The compression module is composed of assets that increase the pressure of the gas and remove any excess fluids, this contains the scrubbers, compressors and related assets.

1.4 Hazards

The processing of oil and gas is an inherently dangerous process due to the handling of large volumes of volatile fluids at high temperatures and pressures, this compounded with the difficulties of constructing, maintaining and operating an offshore structure creates a unique set of hazards. Some of the main hazards are discussed in this section.

1.4.1 Helicopter Crashes

Platforms are typically in part supplied by helicopter. There is a risk that the helicopter will crash on take-off or landing, the causes include human error, poor maintenance, environmental conditions or mechanical failure (MNSL 1993). A crash can cause structural damage, if the crash occurs on the Helideck the consequences are expected to be far lower than if the crash occurs elsewhere on the platform.

1.4.2 Structural Failure

On the United Kingdom Continental Shelf (UKCS) the majority of offshore platforms are fixed steel jacket structures. The failure of a platform's structure can cause a collapse of the platform. This failure can be brought about through shock damage, such as a ship collision, or can be accumulated damage through corrosion, fatigue, bacterial growth or other processes (NORSOK 2008).

1.4.3 Kicks and Blowouts

Kicks are the flow of well fluids into the well-bore during drilling, this happens when the pressure supplied by the drilling mud is insufficient to contain the fluid. If the kick is not contained then it can develop into the uncontrolled release of well fluids to the surface, this is known as a blowout (Xiaozhen 2012). The fluids from a blowout can be ignited threatening the safety of the platform, additionally the fluids can leak into the

surroundings causing an environmental issue. A blowout was the cause of the largest oil spill in the history of the industry, this is discussed in Subsection 1.7.3.

1.4.4 Fires and Explosions

A leak of hydrocarbons will lead to a fire or explosion in the presence of an ignition source. If it is an oil leak then if ignited it will result in a pool fire, a gas leak that is immediately ignited will result in a jet fire (Lees 2012). The principal hazard of both jet fires and pool fires are the thermal radiation. As a platform is often tightly packed it is likely for a jet fire to impact an object, increasing the probability of escalation. If the gas accumulates to form a gas cloud before it is ignited then it may result in an explosion. An explosion produces heat and over-pressures which can escalate the scenario by rupturing other vessels and igniting additional fluids. Both fires and explosions can cause significant damage to the assets, the platform and personnel. In this thesis the safety systems modelled will be in relation to the hazards posed by fire and explosions.

1.5 Safety Systems

An offshore platform contains several safety systems to minimise the probability and consequence of the hazards described previously. In this section some of the main safety systems are discussed.

1.5.1 Heating Ventilation and Air Conditioning

Offshore platforms are fitted with a HVAC system. This is composed of ventilation ducts located throughout the platform, the attached systems act to supply air at a temperature, pressure and humidity suitable for working and living conditions. Further, the installation's HVAC works as a safety system, the main goal of a HVAC system is to maintain a safe working environment. The accumulation of gas in an area creates a risk of explosion following an ignition source, to prevent this risk the HVAC system creates a pressure differential from hazardous areas prone to gas build-up, venting away through pressure control. The pressure differential causes the removal of gas from the area and the subsequent venting away, this aims to keep the accumulation of gas below the lower explosive limit. Additionally the venting system has chemical and carbon-activated filters that remove airborne contaminants. There are also fire

and gas detectors in the vents, such that following the detection of a fire or gas leak a control system can command the HVAC system to respond so as to minimise the hazard. The vents are fitted with fire and gas dampers which prevent the propagation of fire, smoke and hazardous gases through the vents, these dampers may close following a detection to minimise damage to the installation, prevent the escalation of a hazard and maintain a safe environment for personnel and aid their evacuation.

1.5.2 Blast and Fire Walls

In areas where the probability of oil release is above a threshold fire walls are located, these are designed to be fire resistant and to prevent or slow the spread of a fire to other regions of the installation. Similarly in areas in danger of a gas leak blast walls are located, in the event of a gas explosion these walls are designed to resist the blast.

1.5.3 Coatings

Fire resistant coatings are used to allow assets to withstand higher temperatures by increasing their thermal protection. Coatings can be applied to assets of most shapes and as such they are particularly useful for assets that are vulnerable to increasing the fire risk under high temperature such as hydrocarbon carrying pipes or pressurised hydrocarbon vessels. Coatings can undergo deterioration from several different causes, cement based coatings often experience cracks which then can grow in size, generally this only damages the top layer but allows for other deterioration mechanisms to access the lower layers. The damaging of a coating's topcoat can lead to water ingress which can then significantly damage the coating's thermal protection within 10 years. Furthermore offshore installations are exposed to harsh weathering conditions and these can cause erosion of coatings that are exposed to the weathering.

1.5.4 Emergency Blowdown System

A blowdown is the rapid depressurisation of hydrocarbon carrying vessels to flare. A control system can trigger this to minimise the effects of a leak or fire by removing the hydrocarbon inventory from the vessels within the hazardous area. The purpose of this is to reduce the pressure to a safe level, to do this blowdown valves are opened, this sends gas to the flare system. The flare is used to ignite and burn off the excess hydrocarbons until a time at which the pressure is at a safe level.

1.5.5 Emergency Shutdown System

Isolation valves are fitted through the platform's piping networks which can be closed to contain hydrocarbon inventories. When activated the emergency shutdown system can close isolation valves to minimise the quantity of hydrocarbons available to be released in an incident to prevent escalation. The emergency shutdown system can activate a depressurisation by the emergency blowdown system if necessary.

1.5.6 Isolation System

Isolation valves are fitted through the platform's piping networks. A leak can be minimised through the closing of isolation valves, these limit the quantity of hydrocarbons available to the leak but, depending on the valves closed, may also force the cessation of production. Isolation valves can be manually activated but can also be automatically activated by a control system following the detection of a hydrocarbon leak or a fire.

1.5.7 Blowout Preventer

A Blowout Preventer (BOP) is a large high-pressure valve with the purpose of sealing wells to prevent an uncontrolled hydrocarbon leak, known as a blowout, as discussed in Subsection 1.4.3. A BOP stack is constructed of several individual BOPs placed on top of each other. Each BOP is designed to be capable of closing the well without the assistance of any of the other BOPs but due to the potential of high pressure leaks on a failure several BOPs are present for redundancy. A BOP can be activated manually from the control room but also has an automatic activation if the riser fails to supply the BOP with power and control fluids. Further, a remotely controlled vehicle can dive to a sub-sea BOP to activate a manual lever as a final option to close the well. A BOP stack is located at the wellhead and therefore can be located either sub-sea or topside dependent on the location of the wellhead.

1.6 Safety Systems Modelled in this Research

The scope of this research covers three of the safety systems, these were selected to represent some of the most critical systems to maintaining a safe operating environment. The three safety systems are:

1. Fire and gas detection system.
2. Firewater deluge system.
3. Emergency power system.

These are discussed in detail in the following sections.

1.6.1 Fire and Gas Detection System

Offshore installations employ the use of a large number and type of fire and gas detectors throughout the installation, there are several types of fire and gas detectors that are used (Norsk-Olje-&-Gass 2001). The most common types are introduced below, a platform will use a mixture of these detectors connected to a control system for detection of a hazard and potential activation of a fire protection system such as a firewater deluge system.

- Smoke detectors - A smoke detector is a point detector that requires smoke to travel by convection into its chamber for the detection to occur.
- Heat detectors - A heat detector works by a heated element exposed to the air, the rate at which heat is dissipated is measured by the changing electric conductivity of the element which allows for the change in temperature to be measured. This can detect a fire by measuring the change in the air temperature following a nearby fire producing heat. Further a heat detector can be used to detect hazardous gases, the different heat capacities of hazardous gases means it conducts heat at a different rate to normal air and as such the change in temperature can be used to determine gas quantities. This is only effective when the hazardous gas has a large difference in specific heat capacity with the surrounding air.
- Flame detector - Flames emit infra-red light, which a sensor in the detector can identify as a flame. A flame detector often detects a fire more quickly than smoke or heat detectors as it senses emitted light whereas smoke and heat detectors need to wait for convection. Other hot objects are sources of infra-red radiation and as such can cause false positives. The sensor's accuracy is decreased by hydrocarbon or water films on the lens and additionally radiation from the sun can interfere with detections.
- Catalytic gas detectors - These detectors house a catalyst which lowers the activation energy for a reaction between the hazardous gases and air. When this reaction takes place, the catalyst is heated which in turn changes the electrical

resistivity of a wire embedded inside the catalyst, this change is then used to measure the amount of hazardous gas in the air. Other gases found in small quantities, such as H_2S, can poison the catalyst leading to inaccurate readings. To counter this the detectors require periodic calibration and replacement.

- Infra-red gas detectors - A beam of infra-red light is emitted along a path which then passes through air whereupon gases absorb frequencies of the infra-red spectrum, a sensor placed at the end of the path then receives the absorption spectrum and can determine how much of various gases are present. This allows for a measurement of the quantity of hazardous gases. There are two types of infra-red detectors, firstly there are infra-red line detectors which emit the beam through an open path to a sensor or a mirror, secondly there are infra-red point detectors which emit the beam in localised housings through a gas permeable region into a sensor. Sometimes the sun can be aligned with the detector such that radiation may enter the sensor and interfere with the beam. Additionally, open-path detectors can suffer from alignment issues or give false readings if an object is in the path of the beam.
- Ultrasonic detectors - The venting of gas from a pressurised asset or pipeline generates ultrasound which can then be detected by a acoustic sensor, the rate of the leak can then be determined by the ultrasonic waveform. This can be triggered by false signals due to other ultrasonic sources.

Detectors are spread throughout the platform, this allows the location of a detection event to be determined and thus the response of the safety system can target the relevant area.

1.6.2 Firewater Deluge System

An offshore platform is outfitted with many fire and gas detectors that are connected to a control panel, the firewater deluge system may be activated in some situations, this system releases water into an area to combat a fire or explosion risk (ISO 1999).

The firewater ringmain is a large pipe circling the installation filled with pressurised water, with the purpose of providing water to fire-fighting systems. The ringmain is designed to take a route such that it takes advantage of any fire protection and to avoid potentially hazardous areas as much as is possible. The firewater ringmain is fitted with pressure sensors such that under a low pressure a pump will automatically start to maintain water pressure.

An installation is required to have a minimum of two fire water pumps that draw from the sea and into the firewater ringmain (DNV 2015). These pumps are required to be located in separate areas of the installation such that in the event of a damaging event in the vicinity of one pump the others may continue to function. Additionally, it is required that with one failed pump the firewater ringmain must still be supplied at maximum capacity through the other pumps.

The firewater pumps are driven by either a diesel generator or an electric motor powered by the installation's main power supply. This setup such that under the failure of the installation's power the firewater ringmain will still be supplied at maximum capacity through the diesel driven pumps.

A deluge system is similar to a sprinkler system in that it disperses water into an area. A sprinkler is designed such that its nozzles are blocked by a bulb that shatters under heat thus releasing the water onto the fire, contrastingly a deluge system's nozzles are dry and connected via piping to a firewater ringmain. A deluge valve connects the deluge piping to the firewater ringmain. When the deluge system is activated the deluge valve is opened, flooding the deluge piping and releasing firewater into the area. This method of fire water distribution allows for a higher rate of water flow into the area than a sprinkler system would supply.

The deluge system cannot only be used directly onto a fire but can also be sprayed on nearby assets, such as a hydrocarbon containing pressure vessel, to provide thermal protection to it. Furthermore, the deluge system can be used to lower the probability of explosions, following the detection of a high gas concentration by a detector the deluge system is activated, the resulting extra humidity in the area decreases the probability of ignition. Therefore the deluge system may be used both to control fires and to prevent the ignition of gas leaks with the potential to lead to a fire or explosion.

Typically, a control system does not cause the opening of deluge valves following a detection event from a single detector, rather following this detection the firewater pumps are started. If a second detection event occurs in the same area from a different detector then the deluge valves will be opened, consequently causing the inflow of water into the area. Typically a platform will have a delay of up to 30 seconds between the valve being activated and water being dispersed from the nozzles.

The deluge piping branches to deluge nozzles at many points such that the dispersal of water into an area is from many points, covering the area. The deluge system is affected by a variety of deterioration mechanisms. Offshore installations' deluge

systems are designed such that they can supply firewater at the minimum required rate even when some of the deluge nozzles have failed. Deterioration of valves in the deluge system may cause more widespread failures of entire deluge areas.

1.6.3 Emergency Power System

A platform is supplied with electricity through generators, these are typically either driven by gas or diesel, where the gas would be taken from the production process. Generally the main power of the platform is supplied by generators with a degree of redundancy, such that at least one of the generators can be not operational while the full power load can still be handled by the other generators (DNV 2015). The emergency power system supplies electrical power for essential safety systems. When the main power supply fails, the emergency power system starts to operate automatically. In normal operation the main power supply takes the load of these essential safety systems. Platforms are fitted with emergency generators to supply these systems when the main power fails. These are typically diesel driven with a dedicated fuel tank with enough fuel to operate continuously for 24 hours.

1.7 Accidents and Incidents in the Offshore Industry

The offshore oil and gas industry is inherently dangerous due to its extraction and processing of hydrocarbons. Hydrocarbons pose a physical danger to nearby structures and personnel with their highly combustible nature. In addition oil released into the sea can quickly cause environmental damage to the surroundings, a large oil spill can have an impact hundreds of miles away. Several layers of safety systems exist to minimise unwanted consequences of a hydrocarbon release. The safety systems can be divided into consecutive barriers, each with the purpose to preventive successively worse outcomes of a fault (Kujath, Amyotte, and Khan 2010).

There have been several accidents in the history of the offshore oil and gas industry, many having large negative effects and gaining infamy for this. In this section three of the major industry accidents are looked into. The first major oil spill occurred in Santa Barbara and resulted in an environmental disaster that prompted public and political response. Next, the Piper Alpha disaster is examined, this event was the single largest loss of life in the history of the industry, costing the majority of the crew with a total of 167 individuals lost. Finally the largest oil spill to date is discussed, this was caused

Figure 1.3: Santa Barbara oil spill - 1969. Image from Santa Barbara Edible n.d.

by an explosion on the Deepwater Horizon platform. For each incident to develop into a disaster, safety systems failed, in this section it is explored how these failed for each incident.

1.7.1 Santa Barbara

On 28 January 1969 the first major offshore oil spill occurred in Santa Barbara, California, shown in Figure 1.3. At the time this was the largest oil spill in history and is largely perceived as the largest offshore oil spill accident until the Deepwater Horizon platform blowout in 2010.

The platform, named Alpha, was drilling a well of a depth of 1,000 metres. Standard procedure is to inject well mud into the well as oil and gas is extracted such that a safe pressure is maintained in the reservoir. The well mud failed to maintain a safe pressure, the crew noticed this and in response triggered an emergency shut-down. The purpose of the emergency shut-down was to stop the flow with the use of a BOP. Unfortunately the emergency shut-down failed to close the well due to a weakened BOP. The failure of the BOP caused the pressure to crack part of its casing and in addition break holes in the sea floor, both of these allowing the escape of oil into the sea (Clarke and Hemphill 2002).

For 11 days the well spilled oil, releasing approximately 80,000 barrels of oil and thereby causing a large environmental disaster. The oil covered 35 miles of the coast with thick oil and clean-up teams found in excess of 3,500 dead birds. It quickly became clear the scale of the accident. The response was far reaching, several envi-

Figure 1.4: Piper Alpha on fire after the gas explosion. Image from (Wikipedia 2016b).

ronmentalist groups were created, one of which led to the establishment of Earth Day. Further, President Nixon signed the National Environmental Policy Act which works to minimise the effect of man on the environment.

1.7.2 Piper Alpha

Based in the British sector of the North Sea oil field, Piper Alpha was an offshore oil and gas platform that was established in 1976. On 6 July 1988 an explosion occurred following a gas leak, this escalated and caused the destruction of the platform. An image of the fire taken from a rescue vessel can be seen in Figure 1.4. This event brought about the death of 165 of the 226 personnel aboard the platform and an additional 2 persons from a rescue vessel, all the deaths occurring within only 22 minutes.

Following an official public inquiry into the disaster the chain of events ending in the catastrophic destruction and loss of life was determined (Cullen 1993). Routine maintenance on a pump was performed but this was not completed within the day shift and was therefore left in a non-functioning state as the shifts changed. The pump's state was recorded and a note was left to not start the pump under any circumstances. As the night shift started the note was unseen and subsequently later that evening the pump was started. This caused gas to leak from the pump which quickly ignited, causing an explosion on the platform. These were a non-coherent sequence of events that caused the disaster (Andrews 2002). When constructed Piper Alpha was designed only for oil processing, not gas, and therefore the safety walls were designed to withstand fire but not explosions. During the upgrade of function of Piper Alpha to process gas the improvements to the safety walls were neglected and thus insufficient for the risk posed by gas processing. The overpressure blasted through the

firewall and created a new fire fed from the inventory of a nearby pipe.

Two nearby platforms Tartan and Claymore supplied oil to Piper Alpha for processing. The cost of shutting down this flow was significant; although informed of the fire aboard Piper Alpha the operators did not know of its magnitude and thus despite the fire both platforms decided to continue to pump oil to Piper Alpha until instructed otherwise. Unknown to them, communications between the platforms had been destroyed and no instruction would come, this acted to pour more oil onto the burning platform supplying the fire fuel. In addition to the oil link both of these platforms had a gas link to Piper Alpha and both of these ruptured during the fire and ignited. This caused catastrophic damage to Piper Alpha leading to its destruction and the death of 167 persons. The UK Government reacted to the disaster by introducing new stricter regulation on offshore safety, which caused safety upgrades across the North Sea. Financially, the impact of this disaster was estimated to be in the region of $3 billion (Pate-Cornell 1993).

1.7.3 Deepwater Horizon

The Deepwater Horizon was a semi-submersible platform in the Gulf of Mexico. It was owned by Transocean although the platform was on lease to BP from its inception and scheduled to be until 2013. The Deepwater horizon was a state-of-the-art platform, during its construction it became the single heaviest object ever lifted when its topside was placed onto the submersible section. In February 2010 it began drilling 66 kilometres off the Louisiana coast. The platform was in 1,500 metres of water and the well was a further 5,500 metres below the sea floor. On 20 April 2010 an explosion killing 11 was caused by a wellhead blowout which subsequently leaked oil into the Gulf of Mexico for almost three months becoming the worst offshore oil leak of all time and causing huge environmental damage (Council 2010). An image of the emergency response to the accident can be seen in Figure 1.5.

Following the disaster there was an extensive investigation into the cause. It was found that 8 preventive barriers were breached (Bly 2011). These are as follows:

1. Cement had been pumped down to the wellbore to prevent hydrocarbons entering the wellbore. This cement was later found to be below industry standard and had not been properly prepared or tested before use. This allowed hydrocarbons to enter the wellbore.
2. After the initial cement failure hydrocarbons penetrated the wellbore and passed

Figure 1.5: Deepwater Horizon on fire. Image from (Wikipedia 2016a).

two physical barriers into the production casing. For this to happen the barriers must both have been suffering from a mechanical failure.

3. A negative-pressure test was carried out, this test is designed to verify the integrity of the barriers. BP had no standard procedure for how to conduct this test and when the data was examined the crew identified the test as a success despite the results being indicative of a failed test.
4. As part of normal procedure the well was temporarily abandoned. During operation, drilling mud is pumped into the well to maintain pressure, as the well had been temporarily abandoned this pumping ceased. This, in combination with the hydrocarbon leak in the wellbore, allowed hydrocarbons to flow up the riser towards the platform. Data available on the platform indicated this but were not acted on for 40 minutes. At this point the hydrocarbons had passed the BOP.
5. Once this was noticed the crew forced an emergency BOP closure and activated the diversion of the incoming fluids to a mud gas separator system. The crew could have chosen to divert the fluids overboard, this was undesirable due to the environmental pollution it would have caused but may have given the crew more time to respond to the crisis.
6. The decision to divert to the mud gas separator resulted in the venting of gas onto the platform as the separator system was not designed for such a high flow situation.
7. The fire and gas system did not prevent the ignition of the hydrocarbons. In addition the HVAC system acted to transfer gas into engine rooms, introducing a source of ignition.

8. The BOP emergency closure was activated by the crew to stop the flow of hydrocarbons, unfortunately the BOP located at the sea floor received no signal to close. This had three modes of activations that all failed. The crew's emergency disconnect sequence did not activate the BOP, it is likely that the damage from explosions broke the connection to the BOP. As a backup the BOP was designed to automatically seal upon loss of hydraulic pressure, electric power and communication from top-side controls. Thus an automatic seal should have occurred but on the BOP a solenoid valve was broken in one system and in addition the backup system's batteries had insufficient charge. Finally, 33 hours after the initial explosion a remotely operated vehicle was sent to the BOP and directly activated an emergency close but this also failed to seal the well.

The failure to close the BOP allowed hydrocarbons to leak into the Gulf of Mexico. It took 87 days after the initial explosion to close the leak which in total allowed 4.9 million barrels of oil to escape. BP reacted to the spill with a mammoth response. At the height of the clean-up approximately 47,000 personnel and 7,000 vessels were involved. The disaster cost them in excess of $14 billion in clean-up operations, $15 billion paid to the US government and another $6 billion as various settlements (Ramseur and Hagerty 2013).

There have been numerous other accidents in the offshore oil and gas industry, here only three of the most severe have been examined. It is clear that the possible consequences of an accident are huge and can impact the environment, cause significant economic damage and cost lives. Therefore, it is imperative that when considering the maintenance of a platform the safety barriers must be considered. In particular, a hydrocarbon leak can cause immediate danger with fires or explosions as was seen with Piper Alpha. This research will focus on modelling the occurrence and possible consequences of hydrocarbon leaks with the purpose of ensuring these are minimised.

1.8 Asset Management

To maximise productivity and maintain safety on a platform the operator will perform AM tasks. ISO 55000 is a standard with the purpose of providing the reader with an overview of AM, it defines AM to be the 'coordinated activity of an organisation to realize value from assets' (ISO 2014). In the context of physical assets it is the processes of inspecting and maintaining the condition of assets within a system. The condition of an asset will deteriorate over time to the point of eventual failure, it is

the purpose of AM to monitor the condition of the asset and to take action to improve the condition of the asset if its condition is determined to be sufficiently degraded. The condition can be improved through repair or replacement, furthermore AM can also improve the performance of a system by modifying an asset to add additional functionality or increase its capabilities. Moreover AM can cover other elements such as the management of spare parts or the decision process to add new assets into the system to improve system performance.

An AM strategy is how an operator performs the inspection and maintenance tasks on the platform. This is defined by choices such as the threshold which an asset's condition state must be degraded beyond to trigger a maintenance action and the interval between an asset's inspection tasks. In this thesis the AM will be modelled by a set of variables that can be modified in order to investigate the impact of the AM strategy.

In any AM decision process it is important to factor the economic impact, safety requirements and system performance effects. As part of sustaining an economically profitable platform it is important to minimise the expenditure on AM tasks while maximising the production and maintaining a safe platform environment, as such in LE the efficient performance of AM tasks is necessary.

1.9 Ageing and Life Extension

Typically at construction an offshore platform is assigned a design life, this is the duration through which the platform is designed to operate. Typically platforms on the UKCS have a design life of approximately 25 years (Stacey, Birkinshaw, and Sharp 2008). It is now the case that many of these platforms are reaching or have exceeded their design life but are expected to continue operating. This can have a few causes such as the discovery of more nearby reservoirs or improvements in the quantity of fluid recoverable from the reservoirs. The year of construction of offshore installations on the UKCS is shown in Figure 1.6, it can be seen that many of these will now be nearing the end of their design life. Currently approximately half of these platforms are operating beyond their design life (DECOM 2014).

The period that a platform operates beyond its design life is known as Life Extension (LE). In this period the challenges presented to the platform's dutyholder are increased, this is due to two leading pressures. Firstly, the platforms are often op-

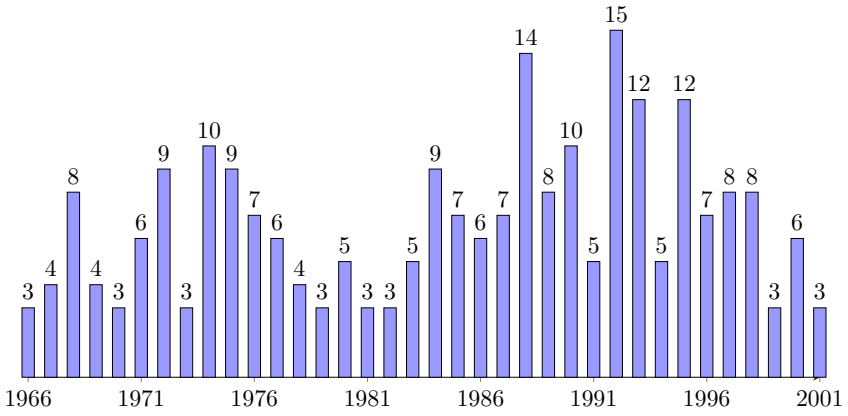

Figure 1.6: Year of construction for UKCS installations.

erating under increased financial pressure because of smaller production quantities. Secondly, the effects of ageing on the platform and its assets have accumulated and therefore to ensure an effective and safe platform there must be robust AM taking place. These pressures together make it clear that it is imperative to optimise the AM procedures to simultaneously minimise their expenditure while ensuring the high availabilities the platform's assets require. These ageing platforms present AM challenges to the industry, they must be carefully studied to decide how the current AM activities should be optimised and modified.

The challenges and issues that a platform faces in LE might not be immediately obvious. A paper published with relation to the management of safety risks brought about during LE (Holmes et al. 2009) discusses the indicators of ageing of offshore assets. The most apparent indicator is the physical degradation of assets, which corresponds to increased failure rates and therefore more production downtime and safety system unavailability. Additionally platforms often build up a large backlog of maintenance actions, in this situation it is important to prioritise these different tasks. Holmes et al. (2009) go on to highlight the relevance of ageing processes across the safety systems on the platform with particular focus on the accumulated hidden damage the assets have gained through the years of operation.

1.9.1 Asset Management in Life Extension

A major reason for platforms entering into a LE stage is the exploitation of newly found fields near to the existing platform (Stacey, Birkinshaw, and Sharp 2008). Often this carries with it a decreased profit and as such the financial optimisation of the AM

strategy is required. Therefore the AM strategy must minimise cost while achieving sufficient safety standards. Furthermore the systems of an ageing installation might undergo increased deterioration rates and as such the AM strategy must be developed with this taken into account. Due to the fast pace that modern technology develops, the control systems on an offshore platform are out-dated soon after installation (Ersdal, Hörnlund, and Spilde 2011). Therefore when the system requires maintenance it can be difficult to acquire the spare parts required to fix it. This obsolescence has the effect that to maintain a functioning control system it is necessary to upgrade it throughout the life of the platform. Several knowledge gaps relating to ageing were identified by Hokstad et al. (2010), these included a lack of understanding of the the results of testing, inspection and monitoring of process equipment with respect to degradation mechanisms. Additionally it was determined that platform operators must ensure safety throughout LE and do so in a cost-effective manner.

1.10 Regulations and Guidelines

In the UK, the Health and Safety Executive (HSE) is the body which certifies the safety of offshore oil and gas platforms . In addition, Norway has an extensive offshore industry and so their regulatory body, the Petroleum Safety Authority (PSA), is also examined. These both produce guidelines and perform industry studies on the safe operation of platforms that give valuable information on the industry's approach to safety. In this section publications which relate to the issues of AM and LE are discussed.

The HSE identifies the magnitude of the effects of ageing on plant safety, an analysis of technical integrity and electrical, control and instrumentation systems, which are approximately 60% of all recorded incidents, finds that over 50% of the incidents are a result of ageing (HSE 2010). Therefore it is necessary to effectively manage ageing through the LE of a platform so it is important to understand the physical processes and other ageing issues. The HSE provides a document with a technical viewpoint discussing ageing issues related to particular types of assets on platforms (HSE 2009). These issues include physical deterioration processes, changed operating conditions and obsolescence issues brought about by advancements in technology. The document covers all the major safety systems of an offshore platform, such as the structure, hydrocarbon containment, detection and control, deluge, passive fire protection and HVAC. The document gives guidance on how to reduce the risk introduced by ageing.

Initiated in 2011 and completed in 2013, the HSE performed a series of inspections on 33 hydrocarbon plants onshore and offshore in its Key Programme 4 study (HSE 2013), this focused on the industry's response to ageing and LE issues. It aimed to ensure that duty holders were aware of the distinction between AM in the design life and in LE and furthermore that they were correctly modifying their maintenance procedures to adapt. The report found that in the majority of cases duty holders were performing to LE standards correctly but several areas still required improvement. In particular the report found that duty holders often lacked a distinction between usual AM issues and ageing in LE issues and so the HSE recommends that the industry increase focus on maintaining safety in a LE setting. This conclusion was echoed by the PSA in a paper by Ersdal, Hörnlund, and Spilde (2011) which reviewed the outcome of a programme of technical investigations into the effects of ageing on safety in the petroleum industry. It was found that the industry seemed to lack an awareness of the effects of ageing; information on an asset's operational history was either lacking or unused in LE assessments which would assist in predicting the asset's likely deterioration.

An offshore platform is required to maintain safety throughout all phases of its lifetime including the LE stage. It is required that for all installations on the UKCS that the records of the safety critical systems are examined by an independent and competent person (Stacey, Birkinshaw, and Sharp 2008), in relation to LE it is important to verify the availability, reliability and survivability as these can all be affected by the ageing process. Similarly Norwegian regulations require that approval is given by the PSA to enter into LE, in requesting the extension the operator must include fatigue life calculations, evidence of the match between the facility and design documentation such that modifications in the future can be accounted for and the operator's additional considerations such as inspection and maintenance strategies for LE.

1.11 Aims and Objectives

It has been seen that LE and the application of AM to the platform's ageing assets is a current issue in the offshore oil and gas industry. In this section the thesis' aims and objectives for the construction of a model are discussed.

1.11.1 Aims

The primary aim of this thesis is to construct a model that can simulate the life-cycle of an offshore platform in relation to the production, safety and power systems. In particular this requires the modelling of the AM actions on the assets in these systems. This then allows the performance of various AM strategies to be evaluated. An additional aim is to create a framework for determining the risk profile of each of these AM strategies. Given a methodology for evaluating the AM strategy, the aim is then to optimise this strategy. The research aims to apply an optimisation technique for determining a solution set of AM strategies with respect to multiple objectives

1.11.2 Objectives

This research has the following objectives:

1. To develop an advanced PN model capable of modelling both discrete AM processes and the continuous fluid flows of the production train.
2. To incorporate in the PN a means to simulate the life-cycle of a platform's assets which accounts for multiple degradation mechanisms and interdependencies between assets.
3. To effectively predict the frequency of hydrocarbon leaks for production assets from the PN model.
4. To develop a consequence analysis technique to evaluate the frequency and magnitude of fires and explosions caused by a leak.
5. To simulate a platform that operates beyond its design life and into a LE stage, thereby, simulating the accumulation of a maintenance backlog and ageing assets.
6. To perform a multi-objective optimisation technique with an evolutionary algorithm to determine a set of optimal solutions to the AM strategy.

1.12 Thesis Outline

The thesis is divided into eight chapters, which are organised as follows:

- **Chapter 1** gives an introduction to the offshore oil and gas industry, discussing the historical development and challenges going into the future. A description of a typical platform's production system involved with processing well fluids into oil and gas exports is described. The variety of hazards on a platform are

discussed and the safety systems present to reduce the risk posed by fires and explosions are presented. Historical accidents and incidents are chronicled with the purpose of understanding the scenarios that can lead to a disaster and the safety barriers that failed. Due to the growing proportion of platforms operating beyond their design life, LE and the effects of ageing are discussed. The purpose and definition of AM is given and its relation to LE is presented. A summary of the regulations and guidelines that apply to offshore oil and gas platforms during LE is presented. Furthermore an introduction to the topics this thesis will explore and the research aims and goals is discussed.

- **Chapter 2** presents a literature review with the purpose of bringing the reader to the state-of-the-art position. The chapter reviews the techniques and research relating to the three main topics of this research, these are reliability models, consequence analysis techniques and optimisation algorithms. The review of these provides a basis for deciding on the choice of techniques in this research. Additionally it allows for gaps in the state-of-the-art to be identified and used to shape the direction of the work in this thesis.
- **Chapter 3** presents the system design of the offshore platforms used in this research. This includes the design of the production, firewater deluge and emergency power systems. The redundancies and relationships between different assets are described such that the requirements for system functions are understood. Further, the details of how the AM strategy is applied in this research is presented. The chapter goes on to discuss the important current issues in the industry and it is seen how they relate to this work. In addition the data sources in this research are presented and their effects on model decisions are discussed.
- **Chapter 4** presents the reader with an in-depth description of the advanced PN used to simulate the production and AM. The structure of the net is presented, it involves the modular construction of smaller nets that are then connected into larger nets to form an increasingly large and complex net. Once completed this net simulates the life-cycle of the platform assets from an AM perspective and in addition simulates the continuous production process. Through purpose-written code and a MC method results are obtained.
- **Chapter 5** presents results of the analysis of the AM strategy through simulations with the PN. This demonstrates the ability of the PN to simulate arbitrary AM strategies and to evaluate their performance. It is seen that the analysis can compare the strategies, however it cannot find the best strategies, which justifies the later use of an optimisation algorithm. An overview of the software

developed for simulating the HSPN is also given.

- **Chapter 6** describes to the reader a mathematical technique for determining the consequence of a leak of oil or gas from a pressure vessel in an offshore platform module. The technique quantifies the magnitude and probability of a fire or explosion due to a leak. It is explained how the consequence analysis is linked to the PN such that together they can form a methodology for evaluating a risk profile.
- **Chapter 7** presents a genetic algorithm optimisation of the model to determine a set of solutions to the AM strategy. The algorithm is multi-objective and aims to optimise many important variables including the production quantities, AM expenditure and frequency of fires and explosions. The algorithm selected produces a set of solutions that cover the optimal region, such that the relative importance of different objectives can be decided on after knowing the possible optimal solutions. Further, a modified approach to the optimisation is detailed which has distinct AM strategies for design life and LE and the effectiveness of this is compared with the non-modified optimisaion.
- **Chapter 8** presents a conclusion and discussion of the research performed in this thesis. This chapter reviews the modelling methodology that was developed. This critical review evaluates the strengths and weaknesses of the techniques and model design. This leads to the identification of improvements that could be made to the model. In addition this chapter presents a selection of possible areas in which future research could be performed.

1.13 Summary and Discussion

It has been seen that throughout the growth of the offshore oil and gas industry a number of incidents have occurred, Santa Barbara and Deepwater Horizon led to large oil spills causing environmental damage and Piper Alpha was destroyed by a fire with a significant loss of life. In the wake of these events actions were taken to try to prevent their recurrence, these brought about the development of resilient and effective safety systems.

The processing of oil and gas at high temperatures and pressures compounded with the challenges of an offshore environment presents a unique set of hazards. In this chapter a brief description was given of the main hazards. As an offshore platform is an isolated environment the hazards must be combatted by on-board safety systems,

the safety systems on a platform were seen to be extensive and include a firewater deluge system, emergency power generators, isolation and blowdown systems.

It was seen that it is often economical to keep a platform running beyond its design life and into a LE stage. The advanced age was seen to add financial pressure onto the platform and so onto the AM strategy, this comes due to the reduced yield and the greater likelihood of degraded assets. The HSE and the PSA both address ageing and LE in a number of documents, they found that operators often lacked a distinct AM strategy for the LE stage. The requirements to submit for LE were also summarised, this involved providing a safety case for the platform, demonstrating its fitness for continued service.

The aims and objectives of the thesis were discussed, broadly this was to construct a model of the production, safety and power systems of an offshore oil and gas platform with the purpose of finding an optimal AM strategy with respect to the production and AM expenditures while meeting safety requirements. Further, the model will simulate throughout the initial design life of a platform and a subsequent LE stage in which there will be accumulation of a maintenance backlog and ageing assets. The advanced age of the assets will increase the failure rate and therefore AM strategies must be constructed to be effective throughout the platform's life-cycle.

Chapter 2

Literature Review

2.1 Introduction

The purpose of this chapter is to present to the reader a systematic overview of literature relating to the research of this thesis. There are three fields-of-study that this research covers, the literature of these are detailed in three sections of this chapter. A wide variety of analysis techniques are seen to be used with each demonstrating strengths and limitations in different applications. The end result of this literature review is to identify the research gap that this thesis attempts to fill and to determine which techniques are the best-suited for this problem.

The first section is AM modelling, this presents an overview of literature relating to the modelling of degradation, inspection and maintenance of systems. These models typically perform analyses into areas such as inspection timings, maintenance decisions and prediction of degradation. In particular literature using the techniques: Fault Tree Analysis (FTA), Bayesian Networks (BNs), Markov Processes (MPs) and Petri Nets (PNs) are examined.

The second section is a review of consequence analysis techniques relating to hydrocarbon leaks. These have the purpose of performing a quantitative analysis of the possible events following a leak. This can be in the form of probability of escalation events, the magnitude of fires or explosions or many other quantities. Dominating consequence analysis techniques are Computational Fluid Dynamics (CFD) approaches which can vary significantly in their implementation and area of study.

The third section presents literature relating to the multi-objective optimisation. The purpose of these techniques is to determine optimal solutions to a problem with

multiple criteria. For this research those criteria include a minimisation of the risk relating to each consequence, the maximisation of production quantities and minimisation of AM expenditure. The most frequently-used technique for multi-objective optimisation is found to be evolutionary algorithms which mimic the Darwinian evolutionary process to breed successively fitter populations of solutions.

2.2 Risk and Reliability

To evaluate the safety of a complex system, reliability analysis models are often used. These analyses can be useful for identifying the subsystems and assets which have a large effect on the reliability of the system. Through modification of the identified subsystems and assets the reliability can be increased and the risk can be decreased.

An important measure of performance is the reliability, this is defined by Andrews and Moss (2002) as '*the probability that an item (component, equipment or system) will operate without failure for a stated period of time under specified conditions*', this is given by the equation,

$$\text{Reliability} = 1 - \text{Probability of Failure.}$$

The reliability, $R(t)$, can be thought as a measure of the success of the system in functioning properly during its lifecycle. The probability of failure at some time, $F(t)$, is equal to the integral of the probability density function of the failure, $f(t)$, this leads to the following equation,

$$R(t) = 1 - F(t), \tag{2.1}$$

$$R(t) = 1 - \int_0^t f(\tau)d\tau. \tag{2.2}$$

Therefore the reliability of a system depends entirely on the probability of failure at all previous times. This probability of failure can be decreased through an effective AM programme.

The risk posed by an incident can be evaluated as a simple product defined as '*the product of the consequence of a specific incident and the probability over a time period or frequency of its occurrence*' (Andrews and Moss 2002), such that,

$$\text{Risk} = \text{Consequences} \times \text{Probability of Occurrence.}$$

Thus methods to decrease the risk of an event can take two approaches. Firstly, the event's consequences could be reduced, for instance an explosion's consequences

could be reduced by erecting blast walls in the vicinity, which decrease the damage caused by an explosion. Secondly, work could be performed to decrease the probability of occurrence, for example this could be achieved by improving the safety systems to automatically isolate vessels when a gas leak is detected to reduce the gas concentration and thereby the probability of ignition. Combining both of these approaches will decrease the risk further.

A common metric for evaluating the performance of a system is the measure of its availability, $A(t)$, this is defined as '*the fraction of the total time that a device or system is able to perform its required function*' (Andrews and Moss 2002). Availability is calculated as the ratio of uptime to the sum of uptime and downtime such that,

$$\text{Availability} = \frac{Uptime}{Uptime + Downtime}.$$

Availability could be increased by modifying the system by introducing redundant components or through the implementation of a more effective AM strategy. At steady the availability can be found by evaluating the Mean Time To Failure (MTTF), given by the reciprocal of the failure rate, MTTF $= 1/\lambda$, and the Mean Time To Repair (MTTR) such that,

$$\text{Availability} = \frac{\text{MTTF}}{\text{MTTF} + \text{MTTR}}.$$

The availability can be thought of as the probability that the system is operating at any given time. The unavailability, $Q(t)$, of a system is given by, $Q(t) = 1 - A(t)$.

It is well understood in reliability engineering that often the failure rate of an asset follows a bathtub curve as shown in Figure 2.1 (Elsayed 2012). In the early life of an asset the failure rate is high due to manufacturing and installation faults, the failure rate follows an exponential decay. As the asset passes this stage it enters into its useful life period wherein the failure rate can be approximated as constant. The final stage of the asset's life is the wear-out stage where the failure rate increases with time due to ageing effects taking their toll on the asset, the failure rate follows an exponential increase.

2.3 Asset Management Modelling

The primary aim of AM is to maximise the value from assets via the performance of inspection and maintenance actions. In terms of this research this means to maximise the production and availability of assets throughout a platform operation including a life-extension stage. AM models can be used for several purposes, some frequently seen

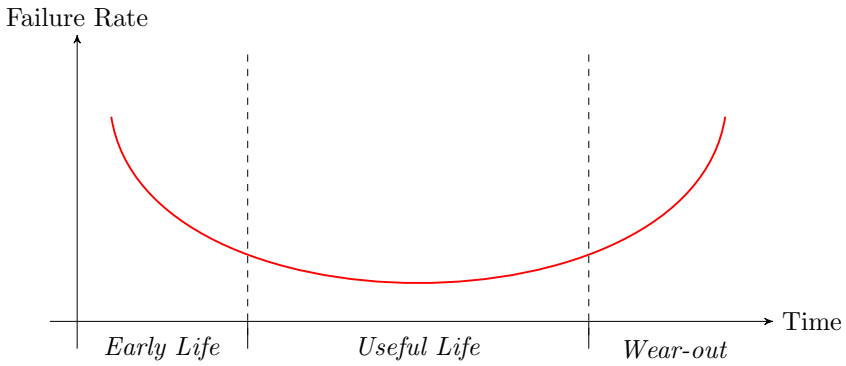

Figure 2.1: The Bathtub Curve.

purposes include prediction of future deterioration, evaluation of system availability and inspection and maintenance decision making.

One of the aims of this research is to evaluate the performance of various AM strategies applied to an offshore oil and gas platform, to achieve this a model must be constructed that can successfully simulate the degradation and AM processes on-board a platform. To determine the best possible modelling technique for this research a review of the current literature in AM modelling has been performed. The most common and successful techniques are discussed in detail and the strengths and weakness are identified. This allows a modelling technique to be selected that is the best fit for this research and thus provides a good basis for analysing the performance of AM strategies.

2.3.1 Fault Tree Analysis

Fault Tree Analysis (FTA) is one of the most widely-used tools in the fields of safety, reliability and dependability engineering due to its ease of application and suitability to many engineering problems (Baig, Ruzli, and Buang 2013). The technique was first developed at Bell Laboratories in 1962 to analyse the launch control systems of Minuteman missiles, later Boeing adopted the technique and developed it further (Clifton et al. 1999). It is an easy-to-understand and powerful technique for qualitative and quantitative analyses and has become one of the most frequently-used techniques in reliability analysis (Xing and Amari 2008).

FTA is a technique that constructs a tree-like structure of relationships between events that can cause a particular fault. Beginning with a top event, the analysis works down from the top of the tree towards the leaves. The branching points of a

Name	Symbol	Description
OR		Any of the input events must occur in order for the output event to occur.
AND		All the input events must occur in order for the output event to occur.
Voting gate		k the input events must occur in order for the output event to occur.
Basic Event		The final events on the leaves of the tree.
Intermediate Event	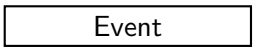	The output of a gate.
Transfer Event		This event is shared between two fault trees.

Table 2.1: The most common nodes of a fault tree

fault tree are represented by logic gates that define how the events below combine to cause the event above (Berk 2009). The top event is usually a system failure mode, the next level of nodes are all the possible events that contribute to cause the failure mode and these are connected to the top event through a logic gate. In turn each of these intermediate events has its causes evaluated creating a further set of nodes beneath it, this is repeated until the system boundary is reached and thereby the entire fault tree is constructed (Labib 2014). In doing so the relationship between basic events, which model events relating to, component failures or environmental conditions, and the top event is explicitly identified. The basic events of a fault tree are assumed to be statistically independent (Pandey 2005). This structure makes it possible to determine the combinations of basic events required to cause the top event which can be used to identify weaknesses in the system.

A fault tree is constructed of events and gates, Table 2.1 gives the names, symbols and brief description of the most common of these. Further, types of events or gates increase the modelling capabilities of the technique. A simple fault tree has been constructed, shown in Figure 2.2, to demonstrate the qualitative and quantitative analyses that can be performed.

A qualitative analysis involves determining the minimal cut sets of the tree (Kabir 2017). A minimal cut set is a set of basic events that will cause the top event which

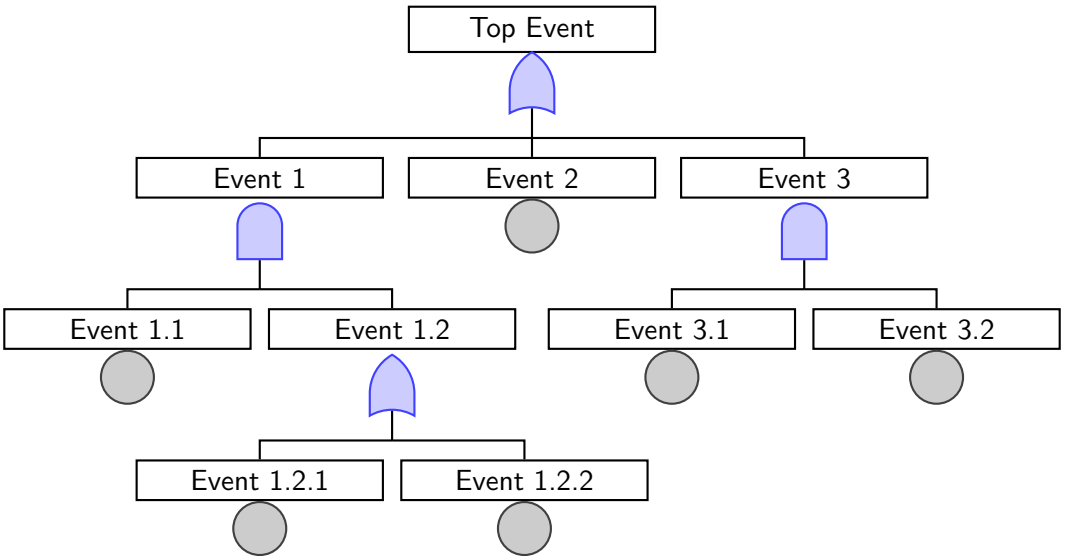

Figure 2.2: A schematic of a fault tree, showing OR gates, AND gates, basic events and intermediate events.

cannot be reduced by removing any of the basic events. This can be a useful technique for determining weaknesses in the system were improvements could be made to its design. For example, if one examines Figure 2.2 then the minimal sets can be seen to be the events numbered {1.1, 1.2.1}, {1.1, 1.2.2}, {2} and{3.1, 3.2}.

A quantitative analysis will evaluate measures such as the probability of the top event occurring. This can be determined through the union of the basic events, $\widetilde{C_i}$, in the i^{th} minimal cut set, C_i,

$$Pr(T) = Pr\left(\bigcup_{i=1}^{n} \widetilde{C_i}\right). \tag{2.3}$$

Here n is the number of minimal cut sets in the tree. Through the inclusion-exclusion rule, this can be expressed as,

$$Pr(T) = \sum_{i=1}^{2^n} (-1)^{|I_i|+1} Pr\left(\bigcap_{j \in I_i} \widetilde{C_j}\right). \tag{2.4}$$

Where I_i is the i^{th} non-empty subset of $\{C_1, C_2, \ldots C_n\}$ and $|I_i|$ is the cardinality of I_i (Yuge, Tagami, and Yanagi 2006). Rausand and Hoyland (2003) show that an upper bound for this can be given as,

$$Pr(T) \leq \sum_{i=1}^{n} Pr(\widetilde{C_i}). \tag{2.5}$$

The results of this analysis give information on the critical components of the system and in doing so provides insight into possible improvements that can be made by

reducing a basic event's occurrence rate or by adding redundancy into the system design.

In reliability analyses FTA is a frequently used tool, for instance Choi and Chang (2016) applied the analysis to a sub-sea hydrocarbon storage tank to perform a reliability and availability assessment. Through the construction of fault trees for five failure modes the basic events are identified. The probability of failure of each failure mode was determined through the evaluation of the probability of failure of the basic events through the logic gates, the technique was shown to successfully determine the system availability. Similarly Bhattacharyya and Cheliyan (2019) performed a FTA of a sub-sea production system to determine the probability of failure subject to different system designs. The results of the FTA were used to aid in an optimisation algorithm of the system design. The performance of a system is dependent on the performance of its components or basic events. Some components will be more important for the system's reliability that others. To quantify the importance of each component, an importance measure can be assigned to every basic event in a fault tree. This is a value between 0 and 1 that measures the component-reliability importance, which is defined as the probability that when a component failures it will cause the system to fail (Andrews and Beeson 2003).

In a standard FTA the relationships between the events are only modelled according to their existence and not the order of occurrence however system failure can depend on the order of occurrence of the basic events. A dynamic fault tree analysis aims to overcome this by introducing a concept of temporal dependency (Boudali, Crouzen, and Stoelinga 2009). This is achieved by the introduction of several gates that have requirements on the sequence of occurrence of the events. Thus the scope of systems that can be represented is greatly increased. Due to the temporal relationships in a dynamic fault tree, many of the methods used to analyse a standard fault tree cannot be applied. Although some of these can be approximated or similar analyses can be performed, this nevertheless can reduce the utility of a dynamic FTA (Ruijters and Stoelinga 2015). However, dynamic FTA is often used in research, for instance Rao et al. (2009) construct a dynamic fault tree to analyse an electrical supply system of a nuclear power plant. A comparison with a standard fault tree of the same system gives significantly different results, proving that accounting for temporal events is important for some systems.

In calculating the probability of the top event, a standard FTA also does not account for uncertainty. The predominant methodology to combat this weakness is the

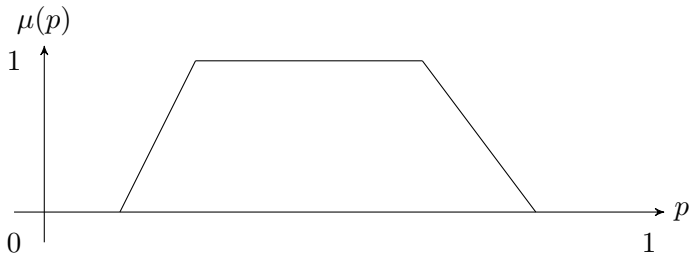

Figure 2.3: The membership function of a trapezoid fuzzy number in probability space.

use of fuzzy numbers in an extension to the technique known as fuzzy FTA (Mahmood et al. 2013). Fuzzy numbers are functions on the interval $[0, 1]$ that have some associated membership function $\mu \in [0, 1]$ where 0 represents no membership and 1 represents full membership, an example of a fuzzy number can be seen in Figure 2.3. The membership function of a fuzzy number is used to represent the uncertainty of the probability. In a fuzzy fault tree the probabilities of occurrence of the basic events are represented by fuzzy numbers, such that their uncertainty is quantified. Fuzzy mathematics is used to calculate the fuzzy probability of the intermediate and top events, thus the uncertainty in the probability of every event is known.

Fuzzy fault tree analysis has been used in the oil and gas industry to perform risk analysis. Often the fuzzy numbers are used to represent uncertainty in language, for instance Wang, Zhang, and Chen (2013) apply fuzzy fault tree analysis to an oil tank explosion scenario, where the probabilities of failure of the basic events were given by experts using language such as 'very low' or 'mildly high' which were assigned fuzzy numbers to represent the uncertainty in the statements. Similarly an analysis performed by Yuhua and Datao (2005) in relation to failure of oil and gas pipelines also applied weighting to experts' statements dependent on their experience. Through this extension the top event's probability of failure was dependent on the uncertainty in the statements.

It has been seen that a FTA is a powerful technique for examining the relationships between basic events and system failures. The gates provide a logical connection between the events, this allows for a robust construction but also limits the failure propagation to be a deterministic process which prohibits the inclusion of event dependencies with probabilistic relations. Moreover a FTA is designed to only consider a single system failure mode, to consider multiple system failure modes it is required to construct multiple fault trees which can be time-consuming.

To address the lack of temporal relationships, dynamic FTA can be used which

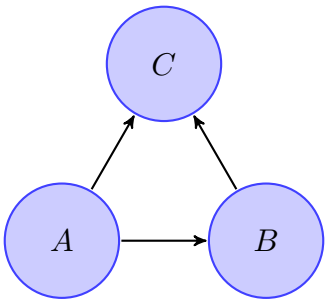

Figure 2.4: An example of a simple BN.

increases the complexity of the systems it can model. This allows for the order of when events occur to effect the behaviour of the fault tree although it does not account for the absolute time of events, only the sequence. Another extension, a fuzzy fault tree utilises fuzzy numbers so that uncertainties in event failure rates can be modelled, this is particularly useful for embedding expert opinions and uncertainty into a model. These extensions to the standard technique greatly increase the capabilities of the technique.

The structure of a fault tree can lead to drawbacks in its modelling capabilities. For instance, a FTA can only analyse a single top event, to analyse many a fault tree must be constructed for each. Additionally, it is difficult to model inter-dependencies between events in a conventional fault tree. Baig, Ruzli, and Buang (2013) note that constructing a fault tree can be time consuming and prone to human error. Automated constructions can be performed to minimise human error, these modelling approaches include diagraphs, decision tables and state diagrams (Majdara and Wakabayashi 2009). To obtain results from a fault tree, typically a Markov analysis or simulation are used, for large complex trees this can be computational expensive. Alternatively, a binary decision diagram can be used to analyse the fault tree (Remenyte and Andrews 2006).

2.3.2 Bayesian Networks

Bayesian Networks (BNs) are another technique used frequently in reliability engineering, named after Thomas Bayes for their application of Bayesian statistics. BNs were first introduced in 1985 by Julia Pearl (Pearl 1985) and have become widely used since then in a variety of fields, including in reliability analysis. In many respects, BNs are similar to FTA, however, BNs are better suited for modelling uncertainties, updating probabilities and defining dependencies between events (al. 2011).

Formally, BNs are directed acyclic graphs, the nodes are connected through arcs which represent direct causal relationships between the linked nodes (Fenton and Neil 2012), a simple example of a BN can be seen in Figure 2.4. Each node of the network is associated with a set of exhaustive and mutually exclusive states. Additionally assigned to each node is a conditional probability table, these define the probability of the node being in a state conditional on the state of the connected nodes. When new knowledge becomes available relating to the state of a node in a BN, the node can be updated through Bayesian inference (Langseth et al. 2009). Bayes' theorem is used to calculate the probability of the states of connected nodes such that, for evidence, E, the conditional probability of X is given by,

$$P(X|E) = \frac{P(E|X) \cdot P(X)}{P(E)}. \tag{2.6}$$

BNs are well suited for solving conditional probabilities. For instance, if we network in Figure 2.4 the conditional probability tables given in Table 2.2 then we can calculate a conditional probability. For simplicity each node has been assumed to have simply a true (T) or false (F) state although an arbitrary number of states could be assigned. To calculate the probability of A being true given that C is true is given by Bayes' theorem such that,

$$P(A = T|C = T) = \frac{P(C = T, A = T)P(A = T)}{P(C = T)}. \tag{2.7}$$

By summing over the possible values of A and C the probability can be obtained with the values from the conditional probability tables,

$$P(A = T|C = T) = \frac{\sum_{x\in\{T,F\}} P(C = T|B = x, A = T)P(B = x|A = T)P(A = T)}{\sum_{x,y\in\{T,F\}} P(C = T|B = x, A = y)P(B = x|A = y)P(A = y)} \tag{2.8}$$

$$= \frac{(0.2 \cdot 0.1 \cdot 0.6) + (0.7 \cdot 0.9 \cdot 0.4)}{(0.2 \cdot 0.1 \cdot 0.6) + (0.7 \cdot 0.6 \cdot 0.4) + (0.7 \cdot 0.9 \cdot 0.4) + (1 \cdot 0.4 \cdot 0.4)} \tag{2.9}$$

$$\approx 0.446 \tag{2.10}$$

BNs are an active research area in reliability engineering, some examples of literature reviews of their use in sub-fields are discussed here. For instance, Tosun, Bener, and Akbarinasaji (2017) presented a review of application of BNs in software quality prediction, Mkrtchyan, Podofillini, and Dang (2015) reviewed the use in human reliability engineering, while Langseth and Portinale (2007) provides a more general overview of their use in reliability engineering. Additionally BNs are used in similar

A	
T	F
0.6	0.4

	B	
A	T	F
T	0.1	0.9
F	0.6	0.4

		C	
A	B	T	F
T	T	0.2	0.8
T	F	0.3	0.7
F	T	0.7	0.3
F	F	1	0

Table 2.2: Conditional probability tables

fields that involve uncertainty, these include resilience engineering (Cai et al. 2018), failure diagnosis (Cai, Liu, and Xie 2016; Luo et al. 2017; Wang et al. 2018) and risk analyses (Zhang et al. 2017; Cai et al. 2020). This clearly shows that BNs are frequently used across all areas of reliability engineering, demonstrating the success and applicability of the technique.

There are several examples of the use of BNs in the offshore oil and gas industry. For instance, Abaei et al. (2018) evaluate the reliability of floating marine structures that are often used in the offshore oil and gas industry. Demonstrating the diverse utility of a BN, Wang et al. (2017) calculate the probability fire on an offshore platform by constructing a network to describe the sequence of events that cause a fire. Investigating an AM optimisation problem, Bhandari et al. (2016) construct a BN of an offshore processing facility. This determines the contribution of components to an oil and gas production accident and optimising the maintenance schedule to minimise the risk for each component.

First introduced by Murphy and Russell (2002) dynamic BNs are an extension to a traditional BN that adds the ability to include temporal relationships between nodes (Kammouh, Gardoni, and Cimellaro 2020). This is achieved by constructing a series of time slices that each contain a BN. Within each slice the BN is constructed as normal but between the nodes in each time slices there are arcs that allow for temporal dependencies to be modelled (Mihajlovic and Petkovic 2001).

Dynamic BNs are frequently used in the offshore oil and gas industry to perform analyses that require temporal dependencies, this enabled analyses to calculate values over time. For example, Cai et al. (2013) examined the human factors behind offshore blowouts where the probability of failure of the human barrier was calculated as a function of time. Alternatively it allows models to include time dependent events, Amin, Khan, and Imtiaz (2018) evaluated the availability of safety critical systems, the

authors noted how the dynamic BN enabled them to include time dependent failures. Considering sub-sea assets, Liu et al. (2015) investigated a blowout preventer using a dynamic BN, the model included common cause failures and parallel subsystems and was used to perform a reliability analysis comparing different system configurations. Ramírez and Utne (2015) apply a dynamic BN to provide preventive maintenance decision support for the LE of a firewater pump system in an oil and gas facility. This was achieved by modelling of the degradation and maintenance for a selection of strategies to evaluate the probability density functions of the maintenance cost and risk.

A BN has a clear graphical representation that makes the connection between the nodes easy to understand. A powerful part of the network is the ability for it to update when receiving new evidence, this is achieved through Bayesian inference. Furthermore, BNs are noted to have significant advantages over classical frameworks such as FTAs for failure modelling, the reasons for this include that the probabilistic relations between nodes which allows for more complex relationships to be modelled. Additionally, that the lack of structural restrictions allows dependencies to exist freely between any nodes (Langseth and Portinale 2007; Wang et al. 2011; al. 2011).

A traditional BN is limited by its lack of temporal dependency, although through the use of a dynamic BN this can be solved. A BN is an acyclic directed graph, this is necessary so that the probability calculations can be completed but introduces the limitation that a BN cannot have any feedback loops and thus cyclic relations cannot be represented (Barton et al. 2008). In addition, each node requires a conditional probability for each node it is connected to, thus the amount of data needed quickly grows as the number of connections increase and can thus necessitate an impractically large amount of input to the model. For a node with two states and n incoming arcs 2^n independent parameters must be specified, thus as n grows the amount of input data needed grows exponentially.

2.3.3 Markov Processes

In 1906 Andrey Markov published a paper (Markov 1906) introducing Markov Processes (MPs), since then MPs have been used extensively as a modelling tool (Gagniuc 2017). A MP is a directed graph, it is constructed out of a set of states linked through transitions, these are graphically represented by nodes and arcs respectively (Kijima 1997). It is a stochastic process that satisfies the Markov property, mathematically

defined as,

$$P(X_{\tau+1} = x | X_1 = x_1, X_2 = x_2, \ldots, X_\tau = x_\tau) \\ = P(X_{\tau+1} = x | X_\tau = x_\tau), \tag{2.11}$$

where X_i are random variables and x_τ are the state of the process at τ, that often, but not necessarily represents time. The Markov property is the feature that the future states of the system depend only on the current state of the system and not the history of it. Often described as the memoryless property, this has the effect that the future states and past states are independent. For example, a sequence of coin tosses are memoryless as the result of each toss does not depend on the previous toss. Typically MPs are categorised into two types, discrete-time and continuous-time. These correspond to processes which model time either in discrete steps or continuously respectively (Kirkwood 2015).

A MP is defined by its transition matrix, A, for a chain with N states the matrix is of dimension $N \times N$ with each element, $a_{i,j}$, representing the relationship between state x_i and state x_j. The matrix is of the form,

$$T = \begin{bmatrix} a_{1,1} & a_{1,2} & \cdots & a_{1,N} \\ a_{2,1} & a_{2,2} & \cdots & a_{2,N} \\ \vdots & \vdots & \ddots & \vdots \\ a_{N,1} & a_{N,2} & \cdots & a_{N,N} \end{bmatrix}. \tag{2.12}$$

For a discrete-time MP an element, $a_{i,j}$, represents the probability that the state will transition from state x_i to x_j. Each state x_τ can be given iteratively through the transition matrix by,

$$x_{\tau+1} = x_\tau A, \tag{2.13}$$

by extension an arbitrary state can be given as,

$$x_\tau = x_0 A^\tau, \tag{2.14}$$

where x_0 represents the initial state of the system.

For a continuous-time MP an element, $a_{i,j}$, represents the rate from which x_i will transition to x_j per unit time, these are restricted such that all elements where $i \neq j$ are subject to $a_{i,j} \geq 0$. Further the diagonal elements, $a_{i,i}$, are selected such that each row sums to zero, such that $\sum_j a_{i,j} = 0$, thus $a_{i,i} \leq 0$.

The transition matrix can be used to define the Kolmogorov forward equations (Kolmogoroff 1931). The probability that state i is left and state j is entered in time,

$P_{i,j}(t)$, in the time period $t + \Delta t$ is given by,

$$P_{i,j}(t + \Delta t) = \sum_{k=0}^{r} P_{i,k}(t) P_{j,k}(\Delta t). \tag{2.15}$$

If we then subtract $P_{i,j}$ and separate the $k = j$ case from the sum we obtain,

$$P_{i,j}(t + \Delta t) - P_{i,j}(t) = \sum_{k=0, k\neq j}^{r} P_{i,k}(t) P_{j,k}(\Delta t) - (1 - P_{j,j}(\Delta t)) P_{i,j}(t). \tag{2.16}$$

We can then divide by Δt and take the limit as it goes to zero,

$$\lim_{\Delta t \to 0} \frac{P_{i,j}(t + \Delta t) - P_{ij}(t)}{\Delta t} = \lim_{\Delta t \to 0} \sum_{k=0, k\neq j}^{r} \frac{P_{i,k}(t) P_{j,k}(\Delta t)}{\Delta t} - \frac{1 - P_{j,j}(\Delta t)}{\Delta t} P_{i,j}(t). \tag{2.17}$$

We obtain,

$$\frac{\partial P_{ij}(t)}{\partial t} = \sum_{k=0, k\neq j}^{r} a_{k,j} P_{i,k}(t) - a_{j,j} P_{i,j}(t), \tag{2.18}$$

$$= \sum_{k=0}^{r} a_{k,j} P_{i,k}(t). \tag{2.19}$$

This is know as the Kolmogorov forward equations. It can also be written in matrix form as,

$$P(t) \cdot A = \dot{P}(t). \tag{2.20}$$

MPs are frequently used in reliability engineering, of interest to this research is their application to degradation and AM. A common approach in reliability engineering is to create a *degradation chain* in which an asset's condition is categorised into a linear series of discrete states with a transition rate between the states, a basic example for a MP can be seen in Figure 2.5. This represents the degradation through successively more degraded conditions, typically terminating in a failure mode. Some implementations of this include extra transitions that skip over conditions and furthermore transitions that renew that state to represent maintenance.

Many papers using this technique appear in the literature, for instance, bridge deterioration was modelled by Cesare et al. (1992) with degradation chains. In this work multiple degradation mechanisms were represented, each with their own degradation chains. Shafahi, Masoudi, and Hakhamaneshi (2008) use a similar degradation chain technique applied to a railway track degradation model. This was used to predict the track condition through time, and was found to give good results. Cristaldi, Khalil,

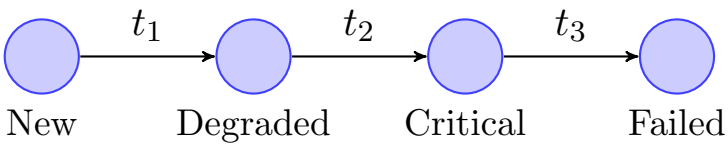

Figure 2.5: An example of a MP degradation chain.

and Faifer (2017) performed a reliability analysis for a photovoltaic module, a complete MP is constructed for all possible failure modes and is used to calculate reliability metrics such as probability of each failure mode, mean time to failure and the hazard function. Dhulipala and Flint (2020) presented a MP for evaluating infrastructure resilience under multi-hazards through use of a selection of degradation chain based methodologies. In the model, inter-dependencies between events were easily captured by the MP's structure. The technique proved to be successful in determining the time of recovery of operations and demonstrated the importance of resilience-based decision making.

Degradation chains are often used as a basis for analysing the performance of AM strategies. Gowid, Dixon, and Ghani (2014) apply a MP to a reliability analysis of a liquefaction system of a liquid natural gas production plant. This is used to optimise the maintenance to maximise reliability and minimise maintenance cost. Dharmaraja (2012) applied a MP to model degradation and preventive maintenance in an evaluation of the performance and cost under various maintenance strategies. Research performed by Li, Sun, and Ning (2014) predicted the degradation of a bridge considering multiple mechanisms which was verified against historical data. This was used to study the effectivity of different maintenance strategies. Prescott and Andrews (2013) investigated the effects of AM strategies on a railway track, which includes decisions relating to inspection, maintenance and renewal, the performance of track sections were analysed under different AM strategies. The performance of inspection strategies were evaluated by Fleming (2004) in relation to power plant piping systems. A degradation chain MP was used to form a reliability model that estimated frequency of pipe failures. Zhang, Kim, and Tee (2017) use a MP degradation chain to model the manage the maintenance of an offshore structures. The degradation of a offshore platform's compressor was examined by Cho et al. (2016) to estimate the next failure time.

MPs are frequently used in reliability analyses and have proven to be a good technique for evaluating system degradation, performance and efficiency. Several tech-

niques have used MPs to predict component degradation and failure. Some of the models in the literature do this by using degradation chain models. Furthermore, MPs are a useful modelling technique for investigating the effects of changing AM strategy parameters. In the literature it was seen that different elements of AM strategies were considered including expenditures, inspection and maintenance decisions. It was seen that MPs were capable of modelling systems composed of many components with many failure processes and interdependencies. All of these demonstrate the versatility of MPs technique to perform a wide range of modelling.

Despite the popularity and success of MPs, the technique does have its limitations. MPs require constant transition rates between states, corresponding to exponential distributions, given by,

$$f(x, \lambda) = \lambda e^{-\lambda x} : x \geq 0, \tag{2.21}$$

where λ is the failure rate. An asset's failure rate can change with time, as in the bath-tub curve (Figure 2.1), which cannot be modelled using an exponential distribution. Another limitation of a MP is of state-space explosion, this is as the number of states in the MP is given by the total number of possible combination of each asset conditions (Ever et al. 2013). Thus for a system with n assets then it will be represented with 2^n states, assuming each asset exists in 2 states. This is such that the number of states in a MP will increase exponentially as the number of assets increase making the model difficult to analyse.

2.3.4 Petri Nets

The Petri Net (PN) was first introduced in 1966 in Carl Petri's thesis (Petri 1966), since then they have been extensively used in research and several extensions have been developed (Murata 1989). The basis of a PN is an easy-to-interpret abstract mathematical graph, that simulates the change in the number of tokens in a set of nodes through discrete steps. Precisely speaking, a PN is a directed bipartite graph that is constructed of two types of nodes: places and transitions, which are connected through directed arcs. The arcs connect places to transitions and transitions to places, connections between two places or two transitions are not permitted (Reisig 2012). Further associated with each place is a non-negative integer, known as its marking, which, is the number of tokens that reside in the place. The transitions can fire which changes the markings of the places connected to the transition and thereby, through the construction of an appropriate net, many systems can be modelled. The graphical

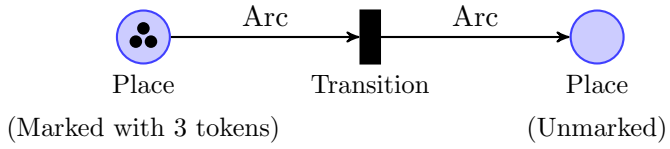

Figure 2.6: The components of a PN.

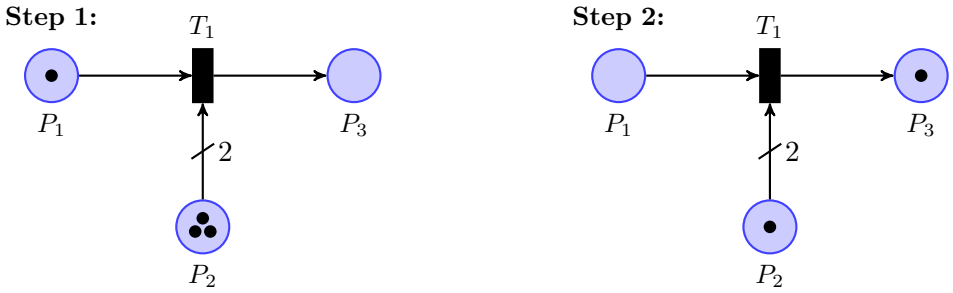

Figure 2.7: An example of the step-evolution of a simple PN.

representations of these elements are given in Figure 2.6.

In some cases an arc may contain an inscription of a positive integer, this is known as the arc's weight, an arc with no inscription has a weight of one (Wang 2012). The marking of places are increased or decreased by the firing of connected transitions. A transition fires when its incoming places have a marking greater than or equal to the connecting arc's weight. When firing, the incoming places' markings are reduced by the weight of their connecting arc and the outgoing places' markings are increased by the weight of their connecting arc.

An example of a basic PN can be seen in Figure 2.7, at step 1 transition T_1 is enabled as the incoming places P_1 and P_2 contain enough tokens to exceed the related arc weights. At step 2 transition T_1 has fired so one token has been removed from P_1 and two from P_2 due to the weight of the arcs and a token has been added to P_3. It is important to note that the tokens are not moving through the net and that the number of tokens in the net is not a conserved quantity. There are several frequently used extensions to the technique that greatly increase the modelling capabilities.

From a review of literature it was seen that stochastic PNs were a highly common technique in reliability engineering and in other fields. A stochastic PN is an extension that adds the ability to include temporal relationships. This is achieved through the addition of timed transitions, which once the enabling conditions are passed wait for some delay time before they fire (Bause and Kritzinger 1996). The timed transitions can be either a constant delay time or can be sampled from a probability density dis-

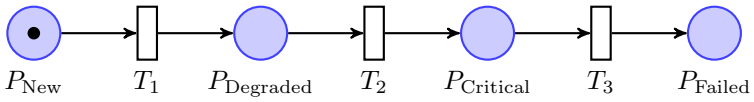

Figure 2.8: An example of a stochastic PN degradation chain.

tribution. The probability density functions of the stochastically-timed transitions are randomly sampled and for an enabled transition, i.e. one for which after the sampled time has passed, the transition will fire and remove and add tokens appropriately. This enhances the modelling possibilities, the inclusion of time and stochastic transitions allow for more complex time-dependent systems. Similar to a MPs, PNs share the memoryless property as their future is independent from the marking history (Hurson 2014). Although, in contrast a PN does not suffer the same state explosion problem and furthermore, a stochastic PN can include non-exponential transition times.

Typically, analysis of a stochastic PN involves using a MC method, this repeatedly simulates the net to investigate its time-evolution. The simulation is continued until some predefined condition is reached, this could be the total time that has passed or when a place reaches a particular marking. Throughout the MC method data about the places' markings and firings are collected to be analysed in order to determine the modelled system's behaviour.

In reliability engineering literature the degradation of a component can be modelled with a stochastic PN through a degradation chain, similar to those seen in the MP literature. An example with four conditions is shown in Figure 2.8, where three timed transitions with associated probability density distributions define the degradation rate. An example of the application of this method is given by Audley and Andrews (2013) in measuring the performance of a section of railway track throughout its life with modelling the AM of the track section, the stochastic PN model was shown to be a suitable technique due to its ability to model degradation as a stochastic process, furthermore it allows for dependencies between nodes, these abilities were used to include features such as opportunistic maintenance and interdependencies among intervention activities, which were seen to greatly influence the results. A stochastic PN approach is compared to a MP by Le and Andrews (2013) in analysing the AM of railway bridges, several comparison points between the two models were noted. It was found that the stochastic PN model held advantages over the MP, these included the use of non-constant deterioration rates which were sampled from probability density functions, features of the system operation such as the limitation of the number of

times a maintenance action can be performed can be modelled and the modularisation of the stochastic PN allows the model to be expanded easily without the problem of state explosion as in the MP.

Another extension, known as a coloured PN, introduces *coloured* tokens that can carry information, this can be of any type such as an integer or a word and can be used to define conditions on the enabling of transitions. This functionality allows for the constructing of nets that can model complex processes with relatively few places and transitions, although the complexity of the markings and transitions are increased, which in turn can increase computational time, for large nets this can be an issue. Shang and Beŕenguer (2015) create a timed, coloured PN for modelling the AM of railway track. A degradation chain is not used in this paper, instead the firing of a transition updates a real-valued condition stored within the colour information of a token by the sampling of a probability density function. Condition-based inspection and preventive inspection were both included in the model, the model was used to provide information for determining the best inspection policy. The degradation of an asset was modelled in this coloured PN without the use of a degradation chain with success, this demonstrates the versatility of the PN and its extensions as a modelling technique.

Briš (2013) applies stochastic coloured PNs as a technique for modelling AM on a subset of the production processing equipment on an offshore oil and gas platform, this research is closely aligned with the work of this thesis. The model included complicated elements such as operational loops, preventive and corrective maintenance and a single repair team. A stochastic coloured PN modelling approach was shown to be capable of including these elements, this was done through degradation chains with repair tasks controlled by transition conditions. This is a logical expression composed of information on the markings of places within the net, it has a boolean solution which when true allows the transition to fire. The use of these conditions allowed the repair tasks to be prioritised according to their effect on the production level of the platform. One of the main advantages of the PN is its graphical structure which allows for the model to be easily interpreted, although, the complexity of the transitions' conditions in this paper make it difficult to interpret.

Despite their similarity, there are many differences between Briš' paper and the PN part of the thesis' model. Some of the main elements that are covered by this thesis and not in Briš' paper include:

- Multiple degradation mechanisms per asset, with more condition states and thereby more preventative maintenance opportunities.
- Inspections, with internal and external inspections that reveal the state of conditions due to different degradation mechanisms.
- Continiuous fluid flow simulated in the PN with dependencies on the assets' state.
- More complex possible asset management strategies, where inspection intervals and maintenance decisions are defined individually.
- A larger production system with the inclusion of the power generation and firewater deluge systems with interdependencies between the systems.
- Additional model elements, such as a consequence analysis and optimisation algorithm.

So far places have been constrained to have an integer marking, another extension, known as a continuous PN, removes this restriction and allows for a marking to be any non-negative real value. Additionally, transitions are associated with a firing rate that defines the change in marking per unit time of the connected places. This extension allows for the modelling of continuous processes such as fluid flows (David 1997). In later research the traditional (discrete) PN and continuous PN were combined to form a hybrid PN that can model both the discrete and continuous processes and therefore has greater modelling capabilities (Alla and David 1998b). Hybrid PNs find use in several areas, for instance Lu et al. (2016) model the processes of an energy generation system to aid in decision-making opportunities, Ghasemieh, Remke, and Haverkort (2013) evaluate the survivability of water refinery systems subject to failures at different times and Khilwani, Tiwari, and Sabuncuoglu (2011) model supply chains to assist in evaluation of supply networks.

It has been seen that PNs are a powerful modelling technique, their abstract structure allows them to model advanced features and interdependencies easily. The graphical representation of a PN is such that each step of the simulation can be clearly seen so the PN's functions can be easily understood. From a review of the literature it was noted that stochastic PNs extensions were very common, this timed extension is often used in AM so that the degradations between discrete condition states can be given by the stochastic sampling of a probability density function. A limitation of a stochastic PN is that, generally, an analysis involves a MC method that for large or complex nets can be computationally expensive (Chemweno et al. 2018). In addition, unlike standard MC methods, PNs can have non-constant transition rates. This is vital in

this work for simulating increasing failure rates with asset age via non-constant transition rates. Additionally it was seen that coloured PN allow information to be encoded into the tokens which further permits more complicated models. Finally hybrid PNs extend the capabilities of the net to model continuous processes in addition to discrete processes.

2.3.5 Summary of Asset Management Modelling Techniques

In Table 2.3 a summary of the advantages and disadvantages of the AM modelling techniques discussed in this section is given.

In this thesis, it was decided to select a PN technique to model the AM for two main reasons. Firstly, a PN can model degradation as a discrete progression through states with a stochastic PN and it can also include interdependencies between assets through arcs between places. Secondly, the production process of an oil and gas platform is a continuous flow of fluid through the assets and so, a continuous PN can be used to model this flow. Therefore, a PN technique allows us to model the AM and production process within one modelling technique.

2.4 Consequence Analyses

Consequence analyses involve quantifying the severity of the possible eventualities of an event, for this thesis the event of interest is a hydrocarbon leak. The most frequently-reported loss-producing process-related events on an offshore oil and gas platform are fires and explosions (Chamberlain et al. 2002). The consequences of a leak can vary hugely, from no negative effects to a catastrophic loss of life and the platform. In Section 1.7 some of these catastrophic events were examined and it was seen that fluid leaks were often one of the causes. Due to this wide range of possible outcomes of a leak it is crucial to understand the probability and magnitude of each consequence. It is important to note that hydrocarbon leaks on a platform are not all the same, between vessels the pressure and quantities of oil and gas vary. Therefore the consequences of the leaks can significantly differ depending on the initial conditions and a model must reflect this. In this section literature relating to consequence analysis approaches are presented.

Modelling Technique	Advantages	Disadvantages
Fault Tree Analysis	• Easy to interpret relationships between nodes • Can be used for qualitative and quantitative analyses	• Only considers a single system failure mode • Cannot model probabilistic relationships • Basic event independence
Bayesian Networks	• Can update when receiving new evidence • No restriction on relationships between nodes	• Data requirements grow exponentially with the number of nodes • Cannot represent cyclic relationships
Markov Processes	• Readable graphic representation • Small systems can be solved exactly	• Requires constant transition rates between states • Large systems suffer from state-space explosion and must be solved analytically
Petri Nets	• Clear graphical representation • Can model abstract system and interdependencies between any places • Stochastic, coloured and continuous PNs greatly increase the techniques modelling capabilities.	• Typically require a MC method to produce solutions

Table 2.3: A summary of the advantages and disadvantages of the AM modelling techniques

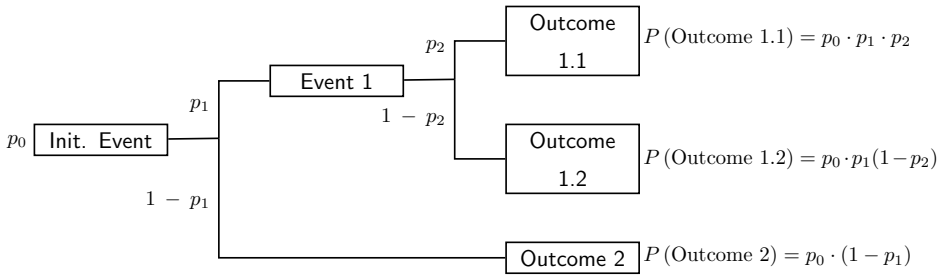

Figure 2.9: An example of ETA.

2.4.1 Event Tree Analysis

In considering the risk posed by an event it is often required to evaluate its potential consequences.Event Tree Analysis (ETA) can be used to do this (Čepin 2011). The construction of an event tree begins by specifying a single initiating event. From this event multiple possible outcomes are defined and the event branches to these. This is repeated through a series of steps to build a tree like structure. Typically an event tree is drawn from left-to-right such that the initiating event is on the left and enabling events on the right, a simple example event tree is shown in Figure 2.9. At each branching point the probabilities of the next event occurring or not occurring are specified, these are often inscribed on the connecting arc, at the end of each branch is an outcome.

An event tree can be used to determine the sequence of failures necessary for an outcome to be reached. From this information weaknesses in barrier systems to escalations can be identified and addressed. Furthermore a quantitative analysis can be performed for an event tree where the probability of each branching is known or can be estimated. The probability of occurrence of an outcome can be calculated through the product of the probabilities along the outcome's path (British Standard 2011). In the example it can be seen that 'Outcome 1.2' has a probability of occurrence of $P\,(\text{Outcome 1.2}) = p_0 \cdot p_1(1 - p_2)$.

Event trees are often used in analyses of the consequences of a hydrocarbon leak considering the barriers between a leak and a fire or explosion. For example, Alileche et al. (2017) analyse the escalation of a two-phase oil and gas release for three leak scenarios by modelling escalation barriers as branching points. It was found that the ETA provided an effective method for supporting decision making. In another paper Noroozi et al. (2013) performed a risk analysis of the effects of human error during maintenance of process equipment. The overall risk was found through considering

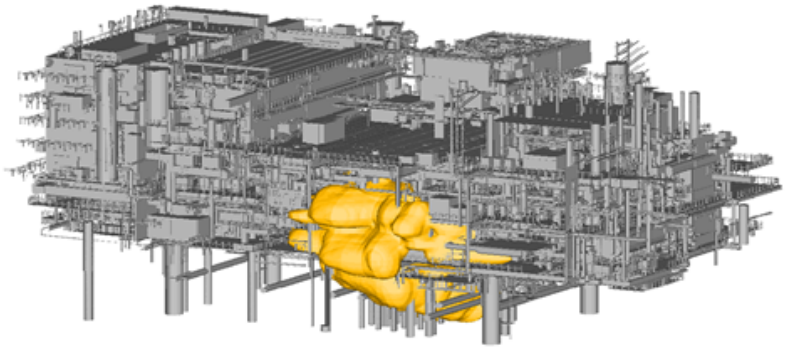

Figure 2.10: An example of computational fluid dynamics for explosion modelling.

the event tree of escalation barriers which was used to determine the contribution of human error. A fuzzy ETA can be performed to include uncertainties, Ramzali, Lavasani, and Ghodousi (2015) analysed the safety barriers in offshore drilling using a fuzzy event tree to account for uncertainty in expert judgement.

An event tree presents a methodology for determining the potential outcomes of a particular event by considering a series of barriers. This can be used to calculate the probability of the outcomes occurrence when the probability of each branching event is known. An ETA presents a relatively simple method for considering the consequences of an event, thereby making it easy to understand (Ericson et al. 2015). The construction of an event tree is based on a single initiating event, although realistically a situation might have multiple initiating events which a event tree does not account for (Clemens, Simmons, and Cincinnati 1998).

2.4.2 Computational Fluid Dynamics

Computational Fluid Dynamics (CFD) is the simulation of fluid flows through numerically solving equations that describe fluid motion. Typically the technique involves dividing the simulation domain into discrete sections and calculating the time evolution through iterative small time steps (Andersson et al. 2011). Of particular interest to this thesis is research that simulates leaks of hydrocarbons on offshore oil and gas platforms, with the possible negative escalation of this being a fire or explosion.

On an offshore oil and gas platform the consequences of greatest concern are of a fire or explosion. Therefore there is much research on modelling the escalation of a leak, although often literature focusses on either a fire or explosion. A liquid natural

gas pool fire was examined by Sun, Guo, and Pareek (2014) with the use of a CFD model. The model was used to evaluate the radiant heat flux across a processing plant, from the results an improved layout was suggested to minimise the hazards. Another CFD model was applied to a vapour cloud explosion by Tauseef et al. (2011). The use of a CFD allows for the model to consider the impact of obstacles which can cause turbulence and affect the dynamics of the mixing of fuel and oxidant. Both of these papers showed good agreement with results from other research techniques. From a review of recent literature it was found that two pieces of software for CFD modelling were frequently used, these are FDS (McGrattan et al. 2010) and FLACS (GexCon 2014). Some examples of research with these techniques include Mouilleau and Champassith (2009), Pedersen and Middha (2012), Hansen, Ichard, and Davis (2009) and Sellami et al. (2018). Crucially, the fundamental differences between these two models are that FDS models fires and FLACS models explosions, thus separating the modelling of these two escalation events (Borg, Husted, and Njå 2014). In reality fires and explosions are connected and can be consequences of the same initiating leak and thereby a model that includes both of these consequences is advantageous. Research by Dadashzadeh et al. (2013) applies an integrated analysis to examine both fires and explosions. A CFD model was used to analyse oil and gas release incidents to determine combined risk profiles for jet fires, pool fires and overpressure events.

The computational power required depends on the number of sections, the size of time steps and the complexity of the calculations. It is often the case that a significantly-detailed simulation requires a significant amount of computational power. Nevertheless, CFD is a popular technique across engineering disciplines with the oil and gas industry being no exception.

The main advantage of a CFD approach is the high degree of accuracy. It is highly successful in modelling the flow of fluids through a space and thus excels in situations where the time-evolution of a leak is needed to be known precisely.

2.4.3 Analytical Model

A risk analysis was performed by Lewthwaite et al. (2006) on an offshore platform's production vessels. A numerical model was formed that calculates the flow rates of oil and gas out of a leaking vessel into the module over time. Through this the gas concentration and oil pool size in the module are calculated, which are then used to calculate the probability and magnitude of fires and explosions. This technique

Analysis Technique	Advantages	Disadvantages
Event Tree Analysis	• Is a clear representation of the barriers to escalation	• Limited to a single initiating event
Computational Fluid Dynamics	• Produces high accuracy results	• Can be computationally expensive
Analytical Model by Lewthwaite et al. (2006)	• Computationally inexpensive compared to CFD	• Simplified simulation compared to CFD

Table 2.4: A summary of the advantages and disadvantages of the consequence analysis techniques.

considers all three major negative consequences of oil and gas leaks: jet fires, pool fires and explosions. This approach can be considered an analytical model involving a numerical simulation, compared to a typical CFD model of a similar scenario, the number of calculations needed are significantly lower, thus allowing a large amount of simulations to be performed. Therefore many different initial conditions can be easily considered and distributions of the possible outcomes can be obtained.

2.4.4 Summary of Consequence Analysis Techniques

In Table 2.4 the main advantages and disadvantages of each consequence analysis technique are summarised.

There are many vessels onboard the platform, from each of these an oil or gas leak is possible and further, the leak size or location on the vessel can vary. To produce a comprehensive consequence analysis it was decided that each of these different leak scenario should be modelled. Therefore, the consequence analysis technique must be easily applicable to each leak and relatively computationally inexpensive. It is for this reason that an analytical model based on work by Lewthwaite et al. (2006) was chosen.

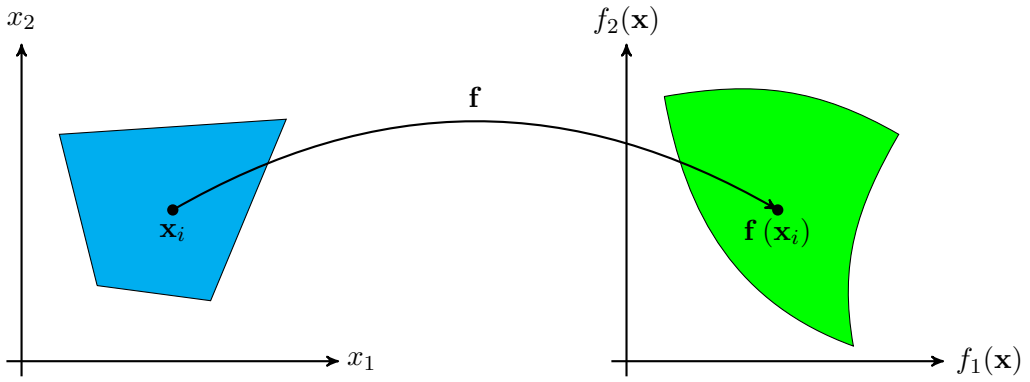

Figure 2.11: The mapping of the objective function from decision space, $\mathbf{x}$, to objective space, $\mathbf{f}(\mathbf{x})$. The filled areas represent the feasible regions of decision and objective vectors.

2.5 Multi-Objective Optimisation

Often real-world problems require that multiple objectives are simultaneously optimised. These objectives are also often in situations were they are competing for resources and thus it is not clear how to allocate the resources to best solve the problems. Further, these objectives are often difficult or impossible to directly compare such that they cannot be combined to form a single criterion through weighting or another method. Thus there is a need for multi-objective optimisation techniques that can determine solutions to these problems.

Formally a multi-objective optimisation problem can be defined in the form,

$$\text{minimise} \quad \{f_1(\mathbf{x}), f_2(\mathbf{x}), \ldots, f_k(\mathbf{x})\} \tag{2.22}$$

where we have a vector of objective functions $\mathbf{f}(\mathbf{x}) = (f_1(\mathbf{x}), f_2(\mathbf{x}), \ldots f_k(\mathbf{x}))^T$ with $k \geq 2$ elements, where $f_i : \mathbb{R}^n \to \mathbb{R}$. These act on the decision vectors $\mathbf{x} = (x_1, x_2, \ldots, x_n)^T$, with $x_i \in X$ where X is the feasible region for decision vectors, which is a non-empty set, $X \neq \emptyset$, and is a subset of the decision variable space, $X \subseteq \mathbb{R}^n$, (Miettinen 2012). The mapping of the objective function from decision space to objective space is shown in Figure 2.11.

Any solution to a multi-objective optimisation problem will satisfy each objective to varying degrees. Generally there is not a single solution that can be said to best solve the problem, to overcome this often a methodology will produce a set of solutions that each present a different compromise between the objectives (Cui et al. 2017). A good optimisation technique will determine the set of solutions that are the best pos-

sible compromises in the search space. In addition many multi-objective optimisation techniques do not require any knowledge of the workings of the problem and can treat it as a black-box, this allows for the techniques to be applied to a wide-variety of problems.

One of the aims of this thesis is to construct a methodology for determining optimal solutions to the AM strategy subject to multiple objectives including production quantities, frequency of leaks and AM expenditures. Therefore the optimisation technique used in this research is required to be a multi-objective algorithm. In recent years multi-objective optimisation in maintenance has seen a dramatic increase in popularity in research (Syan and Ramsoobag 2019a).

Pareto Optimality

A solution to a multi-objective optimisation problem is said to be Pareto optimal if there exists no solution which improves on any of the objectives without lessening at least one other objective (Miettinen 2012). For any non-trivial problem there will exist a set of points that are Pareto optimal, these are known as the Pareto front. An example of this can be seen as the blue line in Figure 2.12, this is for an optimisation problem with two objectives, x and y, that are to be minimised. The Pareto front exists in objective space, the space is spanned by the objectives and thus has the dimensionality of the number of objectives functions.

Without any further constraints it cannot be said that any of the solutions on the Pareto frontier is superior to any other. Therefore it is not enough to find a single solution to a multi-objective optimisation problem, instead a selection of solutions that span the Pareto frontier must be found. This allows for a decision maker to see the trade-off of various solution in the different criteria (Konak, Coit, and Smith 2006).

A solution to the optimisation problem exists in objective space as a vector representing its values in the objective functions. The optimisation procedure aims to determine solutions that minimise the distance to the Pareto front in objective space (Abraham and Jain 2005). Typically an optimisation algorithm is an iterative process that compares solution's objective vectors to determine the best solutions. One common method is to evaluate how many solutions Pareto dominate each solution. Intuitively, for a minimisation problem, a solution can be thought to be Pareto dominant to another solution if all of its objective values are less than the other solutions. Mathematically this can be described by a a vector function, $\mathbf{f}(\mathbf{u}) = (f_1(\mathbf{u}), f_2(\mathbf{u}), \ldots, f_n(\mathbf{u}))$,

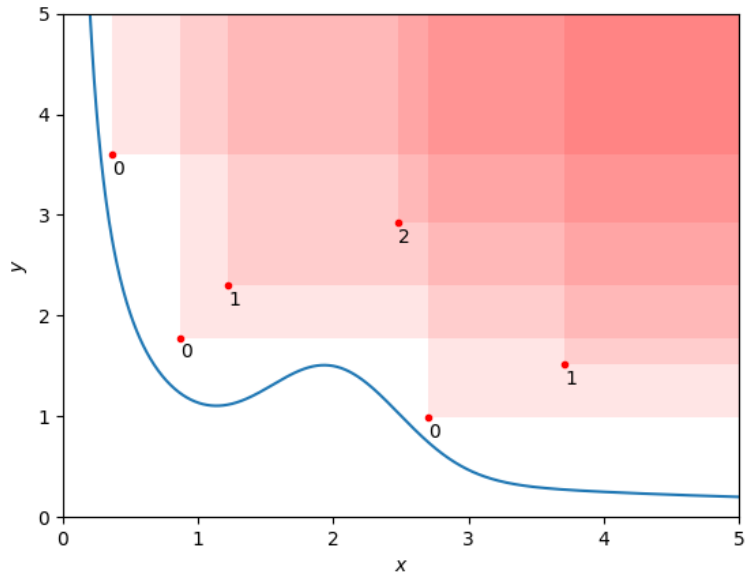

Figure 2.12: The objective space of a two-dimensional multi-objective problem. Showing the Pareto front and a set of solution points labelled with the number of solutions dominating them.

with a decision vector in decision space $\mathbf{u} = (u_1, u_2, \dots u_m) \in U$ and objective vector in objective space $\mathbf{f}(\mathbf{u}) = (v_1, v_2, \dots, v_n) \in V$. A decision vector $\mathbf{x} \in U$ is said to be Pareto dominant to $\mathbf{y} \in U$, denoted as $\mathbf{x} \prec \mathbf{y}$, if and only if,

$$\begin{aligned} &\forall i \in \{1, 2, \dots, n\} : f_i(\mathbf{x}) \geq f_i(\mathbf{y}) \\ \wedge \quad &\exists j \in \{1, 2, \dots, n\} : f_j(\mathbf{x}) > f_j(\mathbf{y}). \end{aligned} \tag{2.23}$$

From a given set of solutions, for each solution the number of other solutions which are Pareto dominant to it can be found. This number is inscribed on each solution's objective vector in Figure 2.12. There will always exist a set of solutions which are not dominated by another other solution (inscribed with zero), these are known as the non-dominated solutions and form the non-dominated front. This front comprises the best solutions from the given set.

2.5.1 Weighted Sum Method

The complexity of a multi-objective optimisation problem can be reduced into a single objective optimisation problem with the weighted sum method (Marler and Arora 2010). The method involves assigning a scalar weighting to each of the objective

functions, such that a single objective function, F, is constructed of the form,

$$F(\mathbf{x}) = \sum_{i=1}^{k} \left(f_i(\mathbf{x}) w_i \right), \tag{2.24}$$

where w_i is the weighting of the i^{th} objective function f_i. This method has converted a multi-objective problem into a single-objective problem and therefore methods for solving single-objective optimisation problems can be applied (Yang 2014). Assuming that all the weights are positive then this method will always find a Pareto optimal solution (Goicoechea, Hansen, and Duckstein 1982).

In this method the weighting of each objective function is determined at the start of the simulation, methods that require some form of expression of preference between the objective functions before the solution(s) are found are known as *A priori* methods (Hwang and Masud 2012). It is often very difficult to correctly weight these objective functions as the shape of the Pareto front is unknown. Other techniques instead find solutions across the Pareto front such that a user can select the best solution from the front without specifying any objective preferences, these are known as *A posteriori* methods.

2.5.2 Lexicographical Method

In the lexicographical method, a priority is assigned to each objective before the optimisation begins (Zykina 2004). When comparing two or more solutions the method compares their performance in the highest priority objective, if one of the solutions is significantly better then it is chosen. If the difference in their objective values is less than a predefined threshold then they are compared based on the second objective. This process is continued, decreasing through the prioritised objectives until a solution is selected.

This process requires no weighting of objectives but also will ignore any lower priority objective if a solution is considered better in one higher priority objective. This can ignore good solutions by overlooking important differences in the latter objectives. A limitation of this methodology is that the selection of the objectives' priorities may also not be apparent depending on the problem. Additionally the threshold at which objectives are considered close must be selected, this choice is not trivial and can be the source of subjectivity (Freitas 2004).

2.5.3 Goal Programming

First introduced in 1955 goal programming presented an extension to linear programming that could optimise with respect to multiple objectives (Charnes, Cooper, and Ferguson 1955). This can be considered an *A priori* method as each objective must be assigned a goal where the optimisation will aim to minimise the deviation between the objective and goal (Jones, Tamiz, et al. 2010).

Mathematically, goal programming can be formulated by assigning a goal, g_i, to each objective, $f_i(\mathbf{x})$, for $i \in \{1, 2, \ldots, n\}$ (Schniederjans 2012). A deviation is calculated for each objective given by $d_i = g_i - f_i(\mathbf{x})$. This deviation can be split into its positive and negative components, d_i^+ and d_i^-, such that $d_i = d_i^+ - d_i^-$. Finally, goal programming aims to minimise the total deviation of all objectives, thus the optimisation problem can be written as,

$$\begin{aligned} & \min \sum_{i=1}^{n} \left(d_i^+ + d_i^-\right), \\ \text{Subject to:} \quad & f_j(\mathbf{x}) + d_j^+ - d_j^- = g_j, \quad : \quad j = 1, 2, \ldots, n \\ & d_j^+, d_j^- \geq 0, \\ & d_j^+ d_j^- = 0. \end{aligned} \tag{2.25}$$

Goal programming has seen many successful applications in reliability engineering. For instance, Moghaddam (2013) optimised the preventive maintenance and replacement schedules of a manufacturing system, applying a goal programming technique to obtain a set of near Pareto-optimal solutions across the surface. There have been many developments to goal programming that have produced several variants (Colapinto, Jayaraman, and Marsiglio 2017). A variant that utilises fuzzy set theory and weightings was presented by Kundu and Islam (2019). Goal programming was used to determine an optimal solution to system reliability with minimum cost with the purpose of designing a high productivity system.

To solve this the equations of the objective vectors must be known, for any optimisation problem that there are not known for this technique cannot be applied. Another limitation of goal programming is that it is not guaranteed to find a Pareto optimal solution (Marler and Arora 2004).

2.5.4 Evolutionary Algorithms

Evolutionary algorithms are a very popular technique in multi-objective optimisation problems (Deb 2001). There are several variants of evolutionary algorithm which determine solutions with different methods, nevertheless they share common core concepts. As suggested by the name, these algorithms are inspired by Darwinian evolution such that through a series of generations a population breeds converging to fitter solutions (Pétrowski and Ben-Hamida 2017). The exact mechanics behind this vary from technique to technique. Although broadly the techniques can be split into a series of steps:

1. Create an initial population with decision vectors across the feasible region of the decision space.
2. Evaluate the objectives of each solution in the population.
3. Select a subset of the population as parents based on their objective vectors.
4. Breed the parents in turn to create a new population which have decision vectors derived from their parents' decision vectors.
5. Repeat steps 2 to 4 until an end condition is met such as a pre-defined number of generations have been completed.

Particular evolutionary algorithms will add or modify steps but generally they all share the idea of converging by breeding successful parents to produce fitter offspring.

Evolutionary algorithms can converge to a population of identical or very similar solutions because of the breeding between solutions. The degree of variance between the solutions is known as the diversity and often evolutionary algorithms implement methods for ensuring diversity is preserved (Kita 2011). One of the most common methods to achieve this is mutation, this gives a small probability of any part of the decision vector to be randomly changed when creating a child solution. This preserves some degree of variety even in a set of similar solutions. De Falco, Della Cioppa, and Tarantino (2002) note that the choice of the mutation probability is non-trivial and can have a significant effect on the algorithm's results.

Some evolutionary algorithms have mechanisms that aim to produce a population of solutions that are distant from each other in the solution space, such that the population spans the solution space (Deb 2011). Therefore the final population provides a decision-maker with a set of solutions that satisfy each objective to various degrees, with all solutions near the Pareto surface.

Within reliability engineering evolutionary algorithms have frequently been ap-

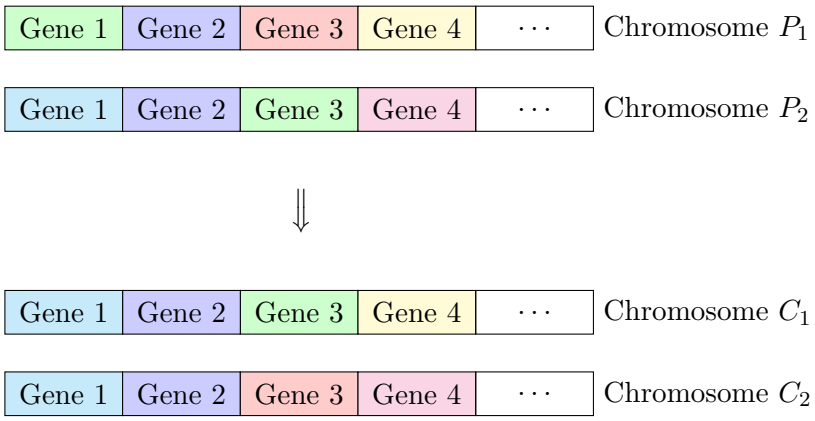

Figure 2.13: A diagram of the mating of two parent chromosomes (P_1, P_2) to produce two child chromosomes (C_1,C_2). The child chromosomes are a random mixture of the genes of the parent chromosomes.

plied (Bozorg-Haddad, Solgi, and Loáiciga 2017). Andrews and Bartlett (2003) apply an evolutionary algorithm to a firewater deluge system, the purpose of this was to determine an optimal system design constrained by available resources. This used a type of evolutionary algorithm known as a Genetic Algorithm (GA) in which the decision vector is encoded into a set of genes known as a chromosome. A schematic representation of how two chromosomes can produce two children is given in Figure 2.13, each gene of a child is randomly copied from one of the parent's genes. This paper evaluates all the objectives as costs such that they can be summed together, thereby creating a single objective problem. Often it is impossible to combine multiple objectives into a single objective as they may be unrelated or require a weighting which is unknown. In a paper by Chambari, Rahmati, Najafi, et al. (2012) two objectives with different units were optimised with a multi-objective evolutionary algorithm, the reliability and cost of a system. Through comparison with a particle swarm approach, the success of the evolutionary algorithm was demonstrated. A multi-objective optimisation of petroleum processing was investigated by Ivanov and Ray (2014), they noted how previous literature had typically been single-objective orientated and found that a multi-objective approach was a well-suited technique for the problem.

In a landmark paper Deb et al. (2002) presented the Non-Dominated Sorting Genetic Algorithm II (NSGA-II) algorithm, this is a multi-objective GA which provides a fast, elite preserving and diversity preserving algorithm. The success of this algorithm is reflected in its wide application (Golchha and Qureshi 2015). An oil and gas production process was modelled by Liu, Gao, and Wang (2015), the optimisation algorithm

was used to simultaneously maximise the oil production, minimise the water production and minimise the energy consumption. Maintenance strategy was optimised in a paper by Wang and Pham (2011), NSGA-II was applied to maximise system availability and minimise the system cost rate through modifying preventive maintenance strategy. Jamshidi and Esfahani (2015) optimised the maintenance policy for a complex system with corrective maintenance, preventive maintenance and different repair levels. The objectives are to minimise the cost and maximise the system's reliability. In this literature NSGA-II was shown to be a successful optimisation technique in determining solutions to AM problems.

An advantage of evolutionary algorithms is that they typically generate a set of solutions that will all have different trade-offs between their objective functions. This allows a user to select the best solution from a selection of solutions that are dominant over all the other solutions (Marler and Arora 2004). Additionally evolutionary algorithms have little requirements on the optimisation problem or shape of the Pareto front and as such are a useful tool for optimisation of a problem with an unknown Pareto front shape. Thus evolutionary algorithms can be successfully applied to a wide range of problems where little is known about optimal solutions. A limitation of the evolutionary algorithms is that in some cases it converges towards a local optimum as opposed to a global optimum as generations become increasingly similar and genetic diversity decreases. However, methods do exist for maintaining diversity such as mutation operators that add random genetic changes, and crowding operators that prefer distant solutions in objective space (Deb et al. 2002). Another limitation of evolutionary algorithms is that they require more calculations of objective functions which correspond to a slower computational speed. Additionally unlike other techniques the solutions cannot be guaranteed to be Pareto optimal, they can only be shown to be dominant of other generated solutions.

2.5.5 Summary of Multi-Objective Optimisation Techniques

In Table 2.5 the main advantages and disadvantages of each multi-objective optimisation technique are summarised.

It is not clear in this work, which objectives are the most important or what weighting should be given between them. For this reason, it was decided to use an evolutionary algorithm to optimise the results. This will present a set of solutions that are near the Pareto front, from these a solution can be selected that balances the

Optimisation Technique	**Advantages**	**Disadvantages**
Weighted Sum Method	• Reduces multi-objective optimisation to single objective optimisation	• Requires preference between objective functions to be selected at the start of the optimisation
Lexicographical Method	• Requires no weighting of objectives	• Can ignore differences in lower priority objectives • Requires objective thresholds to be selected
Goal Programming	• Minimises deviation from goal in each objective	• Requires specification of a goal for each objective
Evolutionary Algorithms	• Does not require any preferences between objectives to be specified • Produces solutions converging to the Pareto front, a solution can be selected at the end of the optimisation	• Can require more computation of objectives than other approaches

Table 2.5: A summary of the advantages and disadvantages of the multi-objective optimisation techniques.

different objectives.

2.6 Summary and Discussion

One of the aims of this thesis is to develop a PN to simulate the degradation and AM tasks of an offshore oil and gas platform. Several different techniques were discussed in Section 2.3 which have all been used extensively in reliability engineering. Each technique showed particular merit in different areas, for instance, FTA provides a method for the qualitative and quantitative analysis of a single system failure mode, BNs are well-suited for modelling systems with uncertainty and MPs can model system state changes. PNs and their extensions were shown to be able to model a wide-range of processes due to their abstract form. In particular, stochastic PNs can simulate the sampling of any distribution to represent a process, this is an advantage over the MP limitation of exponential distributions.

An aim of the thesis was to produce an integrated AM and production model. From a review of the literature it was found that approaches to this typically evaluated the production availability. For example, Meng, Kloul, and Rauzy (2018) performed an analysis of the production availability of a platform through a stochastic simulation of asset failure and repair rates. This methodology demonstrated the effect of varying the asset repair rate on the production availability but was a limited AM model as it only considered assets to be in working or failed states. In a stochastic PN model by Briš (2013) the AM of the production of an offshore oil and gas platform was examined. This contained assets with multiple condition states and simulated the degradation through these and considered preventive and corrective maintenance. This was used to determine a production availability. This thesis aims to go a step further and evaluate production quantities of the oil and gas through the platform's lifecycle dependent on the failures of assets via an integrated model of continuous production fluid flow and discrete degradation and AM actions. This is achieved through the use of a hybrid stochastic PN that is developed for this work.

From discussions with industrial contacts it was identified that one area of interest was to determine the required number of AM teams present on a platform. This was important due to the limited accommodation capacity of a platform, when extra workers are necessary a floatel may be needed which can incur significant costs. The number of maintenance teams was investigated by Marseguerra and Zio (2000), with the use of a GA that optimised the number of teams and in addition maintenance

intervals. Looking again at the stochastic PN model by Briš (2013) the constraint of a single maintenance team was considered but this was not expanded to investigate the effect of different number of teams. This thesis looks to examine the effect on the AM process by varying the number of AM teams on an offshore oil and gas platform.

Although ETA was able to calculate the probability of outcomes of an initiating event, it was seen that the current literature on consequence analyses of loss of containment of oil and gas predominately involved CFD approaches. Typically, CFD simulations are detailed and require many calculations resulting, in high computational requirements. Due to this the number of scenarios that can be modelled are limited. In this thesis a platform's production system is modelled, which involves a large number of vessels containing various fluid quantities. Further, the location of a leak within a vessel can affect the discharge rate of the oil and gas and thus the consequence. Therefore, this thesis required a methodology that could simulate a large number of scenarios, for this reason an analytical model by Lewthwaite et al. (2006) was adapted for use in this work. This model requires fewer calculations than a CFD analysis and is capable of modelling the probability and magnitude of pool fires, jet fires and explosions.

The optimisation of the AM strategy is a problem that has seen the application of many approaches in the literature, Section 2.5 presented an overview of these approaches. The ideal performance of a platform requires the simultaneous optimisation of conflicting objectives, in reality all of the objectives cannot be optimised at the same time and therefore a multi-objective optimisation algorithm is required. It was seen that evolutionary algorithms are well-suited to multi-objective problems as they require no weighting or preference of any objective to be specified. Further, the algorithm produces a set of solutions that are spread across the solution space and approach the Pareto surface. Thus a solution can be selected after the algorithm is completed and the shape of the possible solutions in solution space is known. Furthermore, it was seen that NSGA-II found success in reliability engineering and other areas. This was due to, firstly, its relatively low computational requirements compared to other evolutionary algorithms and secondly, its preservation of the diversity of the solutions in the solution space. For these reasons NSGA-II is applied to optimise the AM strategy in this thesis.

Three techniques have been selected for this thesis. Firstly, a PN has been selected to simulate the degradation, AM and production processes. This degradation and AM will be modelled as discrete processes while the production will be contin-

uous corresponding to the fluid flow of oil and gas through the production assets. Furthermore, some degradation mechanisms of the production assets will result in hydrocarbon leaks, thereby predicting the frequency of leaks through the PN. Secondly, an analytical model was chosen to perform a consequence analysis to calculate the frequency and magnitude of fires and explosions. Thirdly, an evolutionary algorithm was selected to determine the optimal solution to the AM strategy. This is such that a solution set is generated approaching the Pareto front from which a solution can be selected which balances the different objectives.

Chapter 3

System Descriptions

3.1 Introduction

This chapter aims to familiarise the reader with the design of the systems being examined in this thesis. The scope includes three systems: the production system, the power system and the firewater deluge system. These systems are not considered independently but instead have several interdependencies between them, for example, the electric pumps in the firewater deluge system require a constant supply from the power system. Furthermore, due to the fact that the condition of every asset is dependent on the availability of inspection and maintenance teams there is an indirect relationship between them.

The modelled systems aim to accurately represent those on a typical offshore oil and gas platform and the models developed will include the degradation and failure of the assets. To achieve this, a data driven approach is taken in the decisions behind the system designs. There are two significant data sources used to make the system design decisions. Firstly, an extensive reliability engineering database is used, known as Offshore and Onshore Reliability Database (OREDA), this is discussed in detail in Section 3.2. Led by this data source, a number of system features that will be included in the model were identified, these are presented in Section 3.3. The secondary data source was a case study of a platform in the North Sea known as Beryl B, this is selected as it is an oil and gas processing platform that is in its life extension stage. The design of all of the systems are based on the platform's systems' designs, the resulting platform layout is presented in Section 3.4.

The production system, which is discussed in detail in Section 3.5, is a set of assets

that process the incoming well fluids into oil and compressed gas streams. The chosen case study platform has a full production train, meaning that all of the assets involved in taking incoming well-fluids and processing them into oil and gas streams are included in the design. The design of the system is taken directly from the design of the Beryl B platform, including a detailed description of the production system with flow rates and fluid parameters that helped in creating an accurate model of the fluid flow. The failure modes of these assets are discussed with a focus on failure modes that can cause the leakage of hydrocarbons.

Most of the systems on the offshore platform rely on a constant supply of electricity and therefore the failure of this supply can cause issues throughout the platform. It is the importance of the power system that means it is modelled in this thesis, its structure and relationships with other systems are described in detail in Section 3.6. The power system has a high degree of redundancy requiring the failure of multiple components to cause a system failure. Furthermore, there are three levels of function, firstly main power where all systems can run, secondly emergency power where only safety systems are operating and finally no power where all powered systems fail. To understand the relationships between the levels of function a fault tree is presented , in Section 3.7, that relates all of the system's assets to each other.

The final system modelled is the firewater deluge system, which is presented in Section 3.7. The purpose of this system is to respond to an active leak through the dispersal of a large quantity of water into the module where the leak is present. The elements of this system are the detection of a leak and the response of pumps and piping to deliver the deluge to the area. Similar to the power system, the firewater deluge system has a high degree of redundancy to ensure a reliable system. Fault trees are constructed to describe how the assets cause system failure.

For a duty-holder to manage the degradation of assets they must understand the condition of the assets, this is achieved through inspections. Associated with each asset are a set of observables that inspection act on to reveal the progress of degradation mechanisms. Two inspection types are considered, internal and external, these act on a subset of the assets' observables, therefore only allowing the discovery of the effects of some of the degradation mechanisms. Observables and the inspection process are described in Section 3.8.

The main purpose of the construction of a model that can simulate the described system is to analyse the performance of various AM strategies. The AM strategy is

composed of a set of variables that determine how inspections and maintenance are performed. In particular, the strategy gives the interval between inspection actions and the decision as to which revealed states lead to maintenance being scheduled and queued for the asset. It is defined on an asset by asset basis such that the strategy can be tailored according to the degradation and criticality of the asset.

Through the system designs presented in this chapter, the basis for the formulation of a model has been set. The model must be capable of successfully representing all of the system elements that have been discussed, and furthermore, must model their lifecycle and evaluate the platform's performance with respect to varying AM strategies. The production system design is given in Section 3.5 and the other systems will be described through a series of fault trees.

3.2 Data Sources

The primary data source used this research was the Offshore and Onshore Reliability Database (OREDA), which is widely considered a leading reliability data source for the industry (Sandtorv, Hokstad, and Thompson 1996). The document states that one of its primary purposes is to provide a source of reliability data for analyses into decisions in offshore operations, this aligns with the purpose of this work and thus OREDA provides an ideal data source to build this model from. In particular, the data was sourced from the 4^{th} edition of OREDA (OREDA 2002).

The database is formed of a large set of data-sheets, each covering a single type of asset. The assets covered vary from pressure vessels to valves to wellheads with these further divided into sub-categories by their use or dimensions. These data-sheets provide data of recorded failures from all the participating sites and in doing so build up a picture of the failure rates of each asset. In each data-sheet the failures are categorised into three severities, which OREDA define as:

- **Incipient Failure**: *'A failure which does not immediately cause loss of a system's capability of providing its output, but which, if not attended to, could result in a critical or degraded failure in the near future.'*
- **Degraded Failure**: *'A failure which is not critical but which prevents the system from providing its output within specifications. Such a failure would usually, but not necessarily, be gradual or partial, and may develop into a critical failure in time.'*

- **Critical Failure**: *'A failure which causes immediate and complete loss of a system's capability of providing its output.'*

From these definitions it can be derived that an incipient failure accelerates the rate at which degraded and critical failures occur but itself does not impact the asset's output. Additionally it can be seen that both a degraded and critical failure cause the output to be out of specification, this implies that for a system with a visible output that both of these failures would be instantaneously revealed. Therefore, components within the production and power systems should have their degraded and critical failure modes classified as revealed failures and component in the firewater deluge system should have theirs classified as unrevealed. Here, we define a revealed failure to be known to the dutyholder, such that maintenance can be immediately queued, whereas, an unrevealed failure is not known until an inspection is performed on it.

Each failure in the OREDA data-sheets are described by a Mean Time To Failure (MTTF), with the absence of more information about the failure times this implies a constant failure rate. However, it is typically assumed in reliability engineering that the probability of failure is not constant but instead increases with time, as discussed in Section 2.2. In particular, in considering the LE phase of the platform lifecycle, increasing failure rates would be expected, such as can be modelled with an exponential distribution, $f(x) = e^{kx} : k > 0$. Therefore it was decided that failures in this research will instead follow a probability distribution function that increases with time but which have their mean equal to the failure's MTTF from OREDA. The methodology of constructing the probability distribution functions is described in Section 4.7.1.

3.3 Degradation, Inspection and Failure

The assets onboard an offshore oil and gas platform are subject to a variety of degradation mechanisms with causes ranging from internal corrosion, or blockage from sediment build-up to weathering effects from their harsh operating environment. As the assets age their condition is expected to degrade, AM aims to monitor this degradation and respond with inspections and maintenance to ensure a productive and safe platform. Therefore, it is vital that the model must effectively simulate the degradation mechanisms of a platform. Any of the degradation mechanisms might lead to the failure of the asset so a degradation model must model the multiple degradation mechanism pathways that can result in the asset's failure.

The degradation mechanisms act on different aspects of the asset; inspections are performed to monitor the degradation. The progress of a degradation mechanism is measured through an observable that indicates the current condition of a component, it is this observable - not the degradation directly - that an inspection measures. For example, a pressure vessel may be degraded over time by corrosion from the fluids it handles, to measure the progress of the degradation an inspection is performed to measure the vessel wall thickness. These observables can be categorised into a linear series of discrete conditions corresponding to increasing degradation, in this research this will be referred to as a condition chain. The assumption of discrete conditions reflects the detail to which an inspection can reveal, that is to say there is a limit to the condition that can be known. Similar condition chains were seen in the literature review in Section 2.3.3 and Section 2.3.4 by, for instance, Shafahi, Masoudi, and Hakhamaneshi (2008), Dhulipala and Flint (2020), Audley and Andrews (2013) and Briš (2013).

When inspecting an asset, different types of inspections can be performed, broadly these can be divided into two distinct categories: internal and external. An internal inspection requires that the asset is isolated and production is stopped whereas an external inspection does not, this makes external inspections preferable. To reflect the loss of production caused from an internal inspection, they have a greater cost associated with them. Some observables can only be inspected via an internal inspection and others only by external inspections, although these do overlap with the condition of some observables being revealed by both. For instance, in a Separator an internal inspection will reveal the condition of both the *Vessel Wall Thickness* and the *Deposit Size*, while an external inspection will reveal the *Vessel Wall Thickness* and *Structural Wall Thickness*. This behaviour increases the complexity in determining the optimal inspection interval for each inspection type.

In selecting an inspections interval the feasible values range from the inspection duration to beyond the platform's life-time such that an inspection is never performed. This is reduced to a set of possible values for an inspection interval that represent realistic intervals. In the context of the optimisation algorithms this has the benefit of reducing a continuous - and therefore infinite - search space to a discrete and finite search space. This reflects real world inspections, as in practice, inspections are most likely to take place at regular intervals. The discrete set of intervals are weekly with a minimum of one week and a maximum of one week more than the maximum simulation time, this allows for intervals across the search space to be examined. The maximum

interval was set to exceed the simulation time so that the full-range of inspection strategies could be examined, including the case where no inspections are performed throughout the life-cycle, representing a run-to-failure approach. The final month is used to allow the possibility of an interval greater than the simulation time such that the inspection is never performed.

As defined by OREDA, the incipient failure mode accelerates the failure rate of the other failure modes but by itself does not cause the loss of a system's capability of providing its outputs. Therefore for each condition in the condition chain there are two modes, these are with the incipient failure mode present and without. To differentiate between these a *state* is defined as a pair, $S = C \times F_I$, with the observable's condition, $C \in \{1, 2, \ldots, n\}$ for n conditions, and $F_I \in \{True, False\}$ representing whether the incipient failure mode is present or not. Furthermore, these states can be defined for both the actual and revealed conditions and incipient failures, where the actual states represent the current condition and the revealed states represent the condition at the time of the last inspection. Thus for a condition chain with n conditions, there are $2n$ actual states and $2n$ revealed states.

It is assumed that an asset can fail from any condition in its observables, although the probability of failure is not constant but increases as the condition degrades. For example, when an observable with 6 conditions is in the 1^{st} condition the probability of failure is very high but as the subsequent conditions are reached the probability of failure increases. In addition, following the OREDA definition, the incipient failure mode does not cause the asset to fail but instead increases the probability of failure into the degraded or critical failure mode. This is manifested in the model by the probability of failure being dependent on the current state of the observable.

The performance of maintenance on an asset is not assumed to be started as soon as maintenance is queued. On a real platform maintenance is performed during intervals when maintenance teams are available to work. This is simulated in the model by periodic maintenance windows during which maintenance actions can be performed, thereby making maintenance actions grouped. This further has the effect that maintenance tasks accumulate by the start of a window a number of maintenance tasks have accumulated and form a backlog. Hence it is important to investigate the prioritisation of maintenance tasks.

Figure 3.1: Beryl B Platform in the North Sea (Online: Rigadvisor UK 2020).

3.4 Platform Layout

The North Sea platform Beryl B was selected as a case study and provided a detailed description of the production, safety and utility systems (MNSL 1993). Beryl B, shown in Figure 3.1, is a platform that both drills well-fluids and processes them into oil and compressed gas for export. Beryl B began producing in 1984 and is still producing at the time of publication of the thesis, the platform is in its 37^{th} year and thus is firmly in the LE stage of its lifecycle. Therefore, this platform is an apt choice because it is representative of the platforms targeted by this work, given that the platform processes oil and gas and is in its LE stage.

Offshore platforms are constructed from a series of connecting modules with different purposes varying from oil processing to accommodation to helicopter landing pads. The exact layout of these modules are different for every platform dependent on their size, capabilities and environment. A schematic for a typical oil and gas processing platform's modules is given in Figure 3.2. Many different modules are identified here, the scope of this research's analysis is limited to the oil and gas processing modules, power generation module and firewater pumps module. These were discussed in Section 1.6 and were selected as they represent some of the most critical systems for maintaining a safe operating environment. By focusing on a subset of the modules a more detailed analysis of them can be performed.

The oil processing module consists mainly of processes to divide the incoming well-

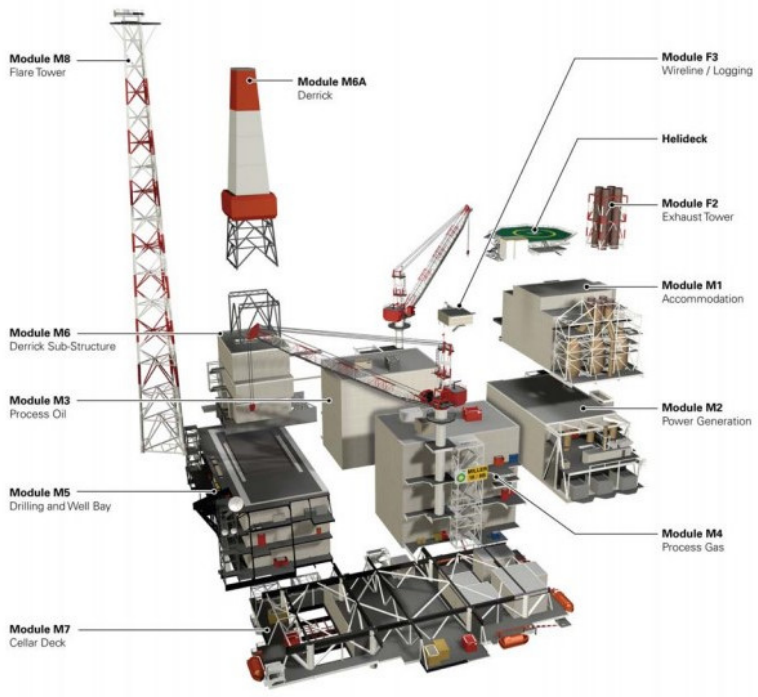

Figure 3.2: A typically platform's module layout (Online: Offshore Energy Today 2020).

Name	**Volume (m^3)**	**Area (m^2)**
Separation	400	100
Compression	800	200
Power Generation	140	75
Firewater Pumps	200	50

Table 3.1: Data on the sizes of the modules analysed in this thesis.

fluids into oil, gas and water streams and is known as the *Separation* module. The gas processing module consists mainly of a series of assets to increase the gas pressure and remove any remaining liquids, this is known as the *Compression* module. The power generation module consists of a series of generators for the main and emergency power. The firewater pump module contains the pumps that provide firewater for the deluge system with electric and diesel powered pumps that allow them to run when the power generation has failed. The volumes and areas of these modules are useful for the consequence analysis discussed in Chapter 6, these values are listed in Table 3.1.

Vessel	Function	Count
Pipe	Transports fluids from an input to an output	23
Separator	Separates an incoming stream to its oil, gas and water components	2
Valve	Controls the flow of fluids between an input and output	4
Scrubber	Removes liquids from a gas stream	6
Contactor	Removes water from a gas stream	2
Compressor	Increases the pressure of a gas stream	4
Heat Exchanger	Increases or decreases the temperature of a stream	4

Table 3.2: Production vessel functions.

3.5 Production System

The purpose of the production system of an offshore oil and gas platform is to process well fluids into oil and compressed gas, which involves several assets to perform various tasks. The system boundaries are defined to be the well-fluid inlet and the water, oil and gas exports. An analysis of Beryl B provided the data for the production system design, from this the production vessels were derived and in addition the fluid quantities and flow rates were specified. A graph of connected modules was constructed from the Beryl B data to represent the flow of fluids of the production process, this is shown in Figure 3.3. These assets are connected through their fluid flows, which can be connected in complex manners, for instance, a flow can loop back to an earlier vessel, or a vessel can have multiple outgoing flows.

In total the production system has 45 assets of 7 types, these are: Pipes, Valves, Scrubbers, Heat Exchangers, Separators, Contactors and Compressors. The purpose and count of each of these assets is given in Table 3.2. In addition, the assets define the resolution of the production system, such that they are considered to be indivisible. However, as discussed in Section 3.3, they can be affected by multiple degradation mechanisms and have several failure modes.

The production system, as specified in the Beryl B design, has no asset redundancy. This means that if any asset fails to operate then the system will fail and there will be a loss of production. The lack of redundancy increases the importance of AM to minimise

Figure 3.3: A modular representation of the production process of the Beryl B platform showing the assets the fluids pass through.

the number of failures and thereby the production downtime. An asset can undergo incipient, degraded and critical failure, each of which can affect its production rates; the incipient failure mode does not affect the asset's performance but does increase its degradation and failure rates to both degraded and critical failure modes. The OREDA definition states that a degraded failure mode should correspond to a reduction in the assets function, this is assumed to be represented by a reduction in the production rate. A critical failure mode is associated with a complete loss of functionality so is represented by halting the production.

A key metric for measuring the performance of a platform simulation is the cumulative lifecycle production of oil and gas. This can be modelled by simulating the fluid flow throughout the lifecycle where the flow rates are dependent on the failure modes of the production assets. By simulating throughout the lifecycle, the relationships between the failures and the loss of production can be accurately quantified.

The fluids carried by the production system are volatile and dangerous. The loss of containment of these fluids can escalate to a fire or explosion in undesirable circumstances. Due to the significant potential consequences of a leak it is important to account for the possibility of this scenario in a modelling framework. Additionally, after a leak has occurred the active safety systems of the platform must respond. In Section 3.7 the firewater deluge system is discussed in relation to its ability to mitigate the potential effects of a leak.

3.6 Power System

The power system is responsible for creating electricity and distributing it across the platform to a wide variety of assets, at any time it can be in one of three states-of-operability: main power, emergency power and total failure. Main power corresponds to the the power system running at full capacity such that all assets on-board are powered. In the emergency power state there is insufficient power for the production systems and therefore they are shut-down, although the emergency power does still provide power to the safety systems. For this model this means the firewater deluge system still receives its supply. Finally total failure causes power supply to be lost to all assets on the platform such that no production or active safety systems are operational.

The power system's design is taken from the Beryl B platform. The main power

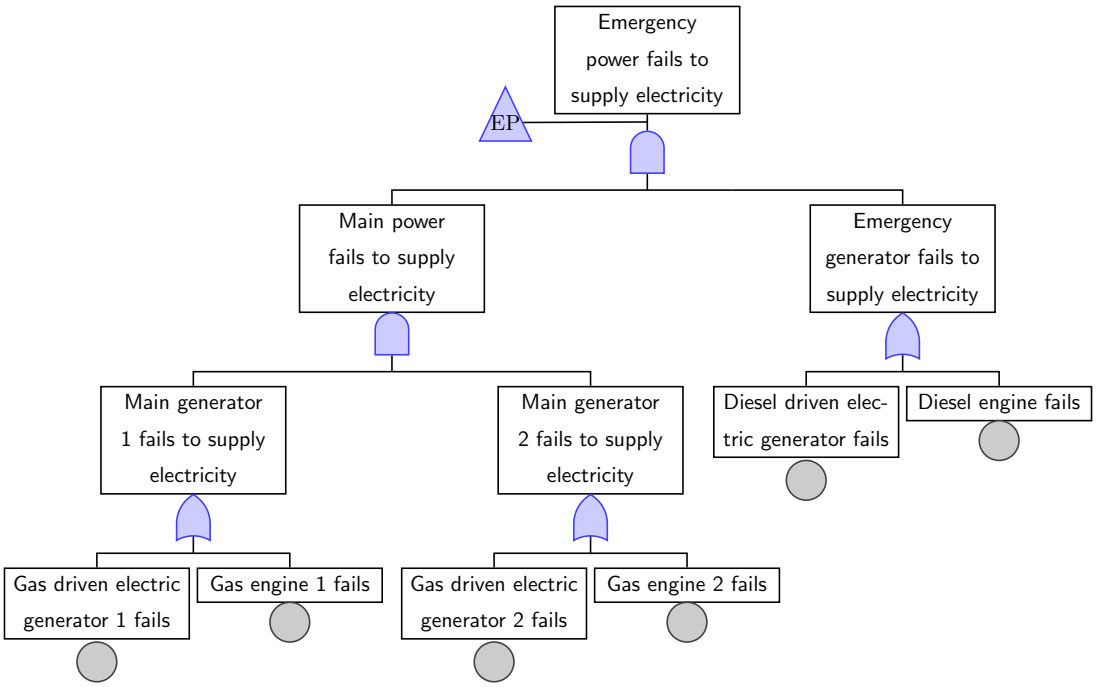

Figure 3.4: A fault tree of the top event 'Emergency power fails to supply electricity' on platform Beryl B.

of the platform is supplied by two gas driven generators that run in parallel, these are redundant such that a single generator is capable of powering the whole platform if necessary, this means that the failure of one does not cause a shut-down of production. The emergency power has a dedicated diesel driven generator that activates when the main power fails. During normal operation the emergency power is taken from the main power supply. Therefore, an outage of the emergency power requires that all three of these generators are simultaneously failed.

The data from OREDA splits the generator into two components, the engine and the electric generator, and thus the modelled systems reflect this structure. The gas-driven and diesel-driven generators are based on different OREDA data sheets for the corresponding generator types. The failure of either of these components will cause the generator to fail. A fault tree of the power system is given in Figure 3.4, this shows how the failure of the assets can lead to a failure of the main power, or the emergency power or both.

Due to the redundancy of the power system, the failure of any asset may not have an effect on the output of the system. For this reason the failure's in this system are considered to fail unrevealed. To construct a model that incorporates the power system it is crucial to simulate not only the lifecycle of the system's components but

also the effects that it has on the availability of the production and firewater deluge system, which is discussed next.

3.7 Firewater Deluge System

The purpose of the firewater deluge system is to mitigate the consequences of an oil or gas leak through the rapid dispersal of large quantities of water into a module. The system maintains a ringmain of water, following the detection of a leak the deluge valves in that module will open and water will be dispersed into the area. This will cause a drop in pressure of the ringmain, which triggers the firewater pumps to maintain the pressure. It is important to note that the system is a standby system with the pumps only activating when the water pressure drops. As a leak can occur at any time the firewater deluge system must aim to always be available to respond to an incident. To help achieve the high levels of availability that this safety system requires, there is a high degree of redundancy to reduce the effects of an asset's failure.

The deluge in each module is fed from the firewater ringmain which is separated by deluge valves that open following a detection event. The valves are grouped together in a skid, which is typically arranged in parallel to provide redundancy on the failure of a valve. In this work it is assumed that there are two deluge valves present in each module's skid. These are designed such that the each valve is capable of providing a full flow rate on its own.

The top-level fault tree for the firewater deluge of a module has been constructed, as shown in Figure 3.5. It takes inputs from the other fault trees in the firewater deluge system.

The water is supplied to the system via a set of firewater pumps. Each firewater pump is composed of two parts, a seawater lift pump that raises seawater to the platform and a booster pump that pumps the water into the firewater ringmain. The seawater lift pumps and booster pumps are composed of a further two assets: a centrifugal pump and a diesel or electric engine. The Beryl B platform has a total of four firewater pumps, two of these are powered by diesel and the other two are electrically powered. The fault tree of a diesel powered pump is given in Figure 3.6, it can be seen that the occurrence of any of the basic events will cause the failure of the pump. The fault tree is given for diesel pump 1, a similar fault tree exists for diesel pump 2. The electric-powered pumps are connected to the emergency power system and therefore

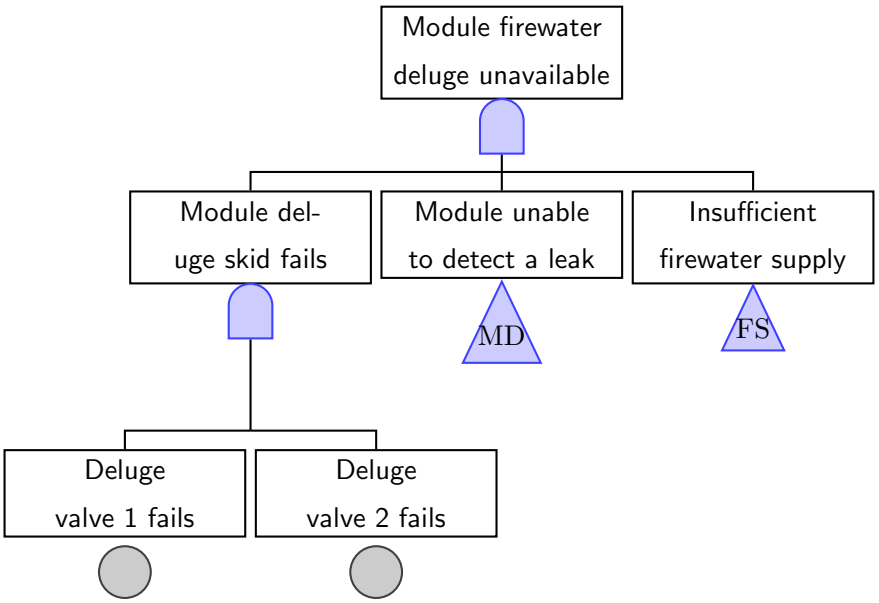

Figure 3.5: A fault tree for the top event 'Module firewater deluge unavailable' in a module

on failure of this these two pumps stop operating. The fault tree for the first electric powered pump can be seen in Figure 3.7, its structure is very similar to the structure of the diesel-powered pump with the addition of an event related to the failure of the emergency power supply. Again, a similar fault tree exists for electric pump 2. The state of the emergency power supply is derived from an event in the power fault tree in Figure 3.4, and so defines an interdependency between the systems.

The pump system has a high degree of redundancy with just two of the four pumps capable of supplying the full firewater requirement in the case of other pump failures. This relationship is represented with a fault tree in Figure 3.8, where the state of each pump is derived through the transfer symbols in their fault trees. It is important to note that both electric pumps rely on the emergency power supply and therefore when this fails both diesel pumps are required to be operational for the firewater supply to meet its requirements.

The firewater deluge system is a safety system that is required to activate on demand, for the majority of its life the system is in standby. In the standby period assets can fail and potentially cause the system to be unavailable, which would not be revealed until an inspection is performed. Therefore, the assets of the firewater deluge system fail unrevealed meaning that an inspection is required to discover their failure.

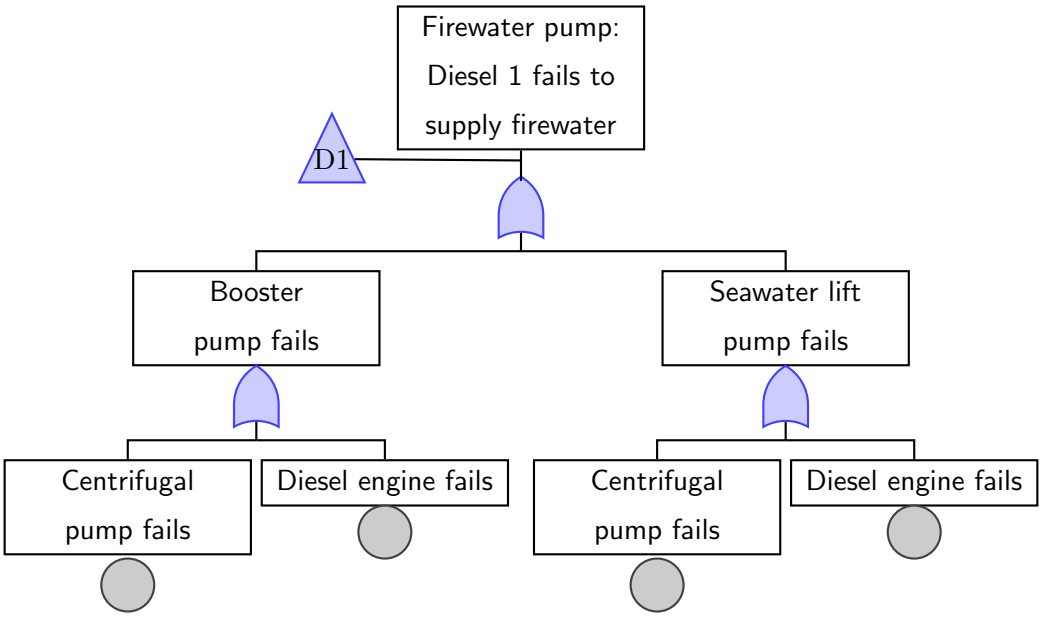

Figure 3.6: A fault tree of top event 'Firewater pump: Diesel 1 fails to supply firewater' on platform Beryl B.

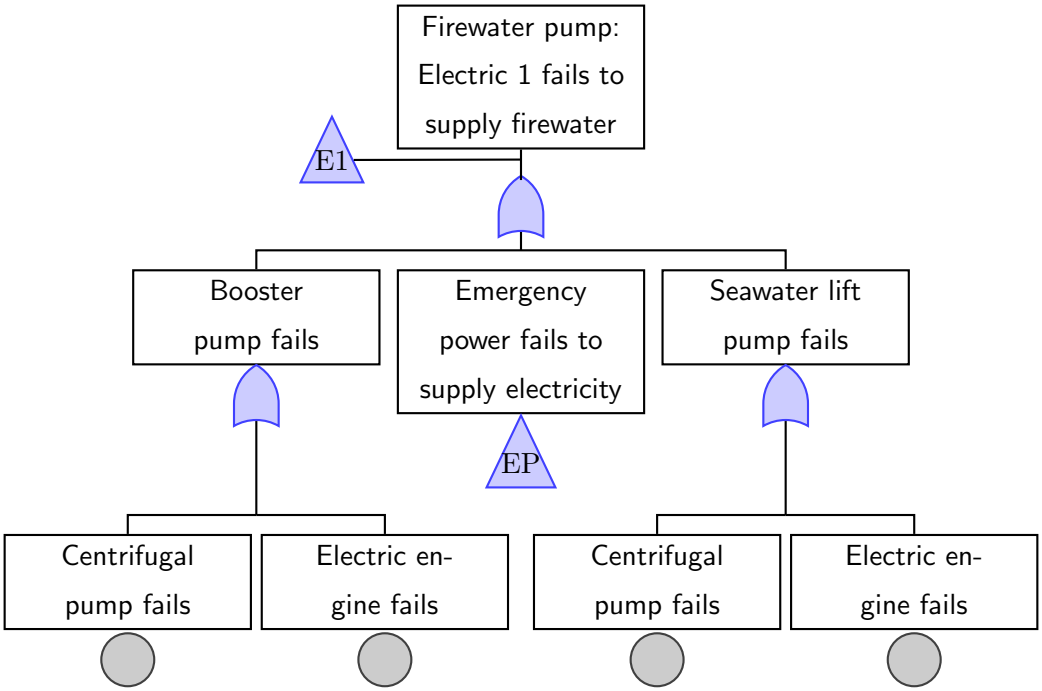

Figure 3.7: A fault tree of top event 'Firewater pump: electric 1 fails to supply firewater' on platform Beryl B.

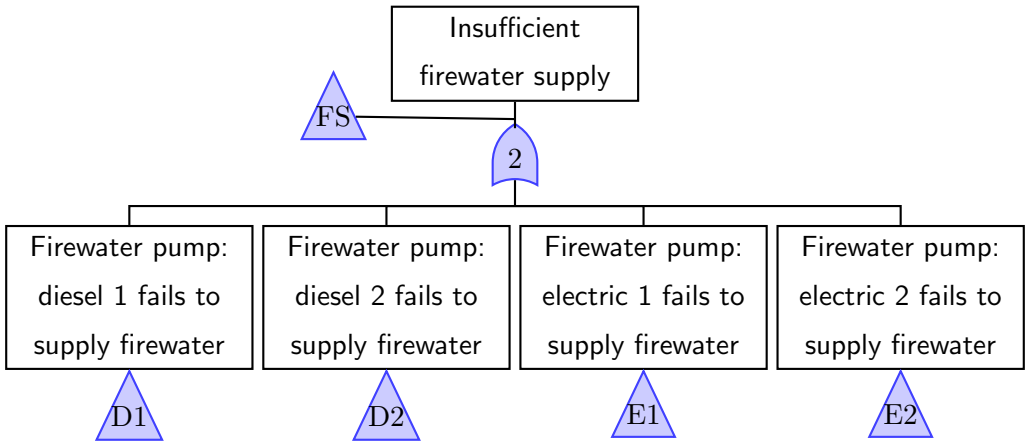

Figure 3.8: A fault tree of for top event 'Insufficient firewater supply' on platform Beryl B.

3.7.1 Detection

For the firewater deluge system to activate in the event of a leak or fire the detection system in the relevant module is required to be available. The detection system is itself divided into modules, within each module there are several detectors that provide a large degree of redundancy. A common spacing for fire and gas detectors is a 5 metre grid (HSE n.d.), therefore a good approximation of the number of detectors in each module can be calculated from its area.

To prevent false alarms the fire and gas logic system only activates the firewater deluge system when two or more detectors report a detection event. It is assumed that detectors, when not failed, will always detect a fire or gas leak in their module. Therefore, to detect a leak 2 detectors in the module must be operational, so the detection system will fail when $N-1$ detectors are failed in a module with N detectors. Furthermore, the detection system also requires a power supply from the emergency power system. These requirements are represented by a fault tree for the failure of a module's detection system to detect a fire or gas leak, as shown in Figure 3.9.

3.8 Observables

To be able to construct a model, the information on the degradation mechanisms and failure modes of the assets must be known. These are found through an analysis of the data from OREDA, data-sheets corresponding to each asset type were examined and the main failure modes were extracted. From these failure modes a corresponding

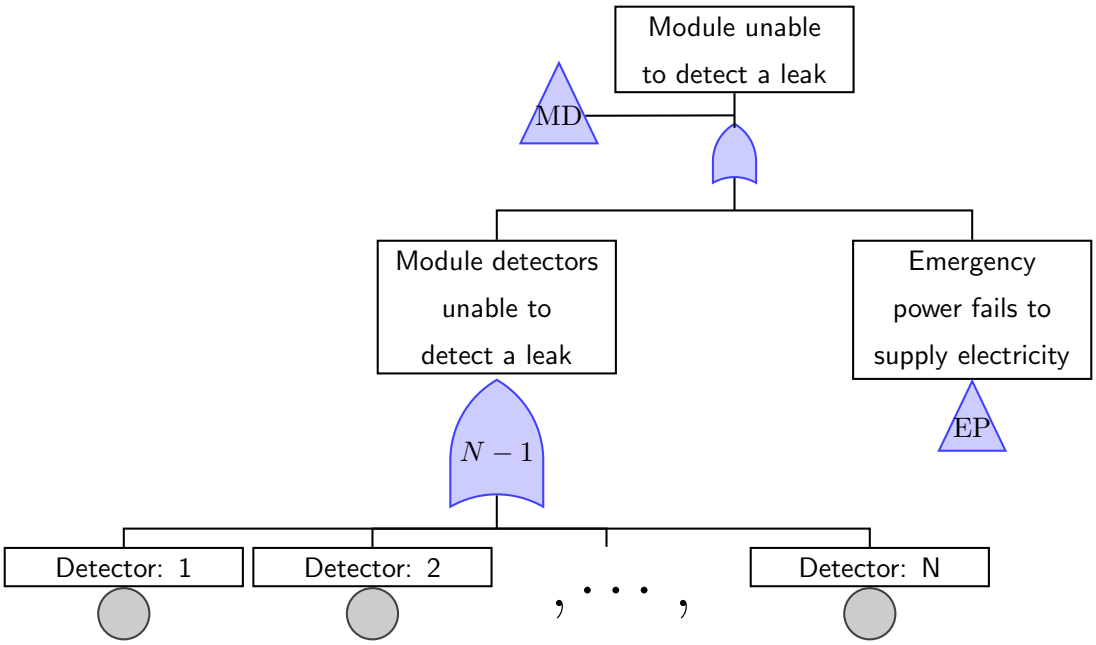

Figure 3.9: A fault tree for a top event 'Module detectors unable to detect a leak' in a module with N detectors.

observable was found that can be inspected to determine the current progress of the degradation that terminates in the failure mode. In some cases a failure mode cannot be associated with a degradation mechanism as the failures occur randomly, an example of this could be an instrument failure.

The production asset observables are listed in Table 3.3, this also gives the observable with a leakage failure mode, additionally the inspection intervals that reveal the current condition of the observables are given. It can be noted that for each production asset, it is assumed that only a single one of the observables has leakage failure modes. Similarly, the firewater deluge system and power system asset observables and their inspections are given in Table 3.4. Here there is no column for leak failure mode as these are non-production assets so a leak will not be of hydrocarbons that could lead to a fire or explosion.

Some of the observables cannot be found at an internal or an external inspection, these represent degradation mechanisms which have sporadically occurring failures, therefore there is no inspection that will reveal information on the condition of the related system. These observables have only a single condition such that they transition to a failure mode with no degradation process. The number of conditions for each assets' observables are given in Appendix B.1.

Asset	Observable	Leak FM	Inspection Type	
			Internal	External
Pipe	Wall Thickness	✓		✓
Separator	Vessel Wall Thickness	✓	✓	✓
	Structural Wall Thickness			✓
	Deposit Size		✓	
	Instrument Failure			
Valve	Wall Thickness	✓		✓
	Closing Times		✓	
Scrubber	Vessel Wall Thickness	✓	✓	✓
	Structural Wall Thickness			✓
	Instrument Failure			
Contactor	Vessel Wall Thickness	✓	✓	✓
	Structural Wall Thickness			✓
	Instrument Failure			
Compressor	Vessel Wall Thickness	✓	✓	✓
	Structural Wall Thickness			✓
	Internal Degradation		✓	
	Instrument Failure			
Heat Exchanger	Vessel Wall Thickness	✓	✓	✓
	Structural Wall Thickness			✓
	Deposit Size		✓	
	Instrument Failure			

Table 3.3: A table of the observables of the production assets and their inspection types and whether their failure results in a hydrocarbon leak.

Asset	Observable	Inspection Type	
		Internal	**External**
Deluge Valve	Wall Thickness		✓
	Closing Times	✓	
Water Firefighting Diesel Engine	Piping Failure	✓	✓
	Starting Unit Failure		✓
Water Firefighting Centrifugal Pump	Seal Failure	✓	✓
	Piping Failure	✓	✓
	Internal Components	✓	
Seawaterlift Electric Motor	Control Unit		✓
	Internal Components	✓	
Seawaterlift Centrifugal Pump	Seal Failure	✓	✓
	Piping Failure	✓	✓
	Internal Components	✓	
Fire/Gas Detector	Detector Head		✓
Main Power Gas Engine	Piping Failure	✓	✓
	Starting Unit Failure		✓
	Internal Components	✓	
Main Power Gas Driven Electric Generator	Piping Failure	✓	✓
	Control Unit		✓
Emergency Power Diesel Engine	Piping Failure	✓	✓
	Internal Components	✓	
Emergency Power Diesel Driven Electric Generator	Internal Components	✓	
	Control Unit		✓

Table 3.4: A table of the observables of the firewater deluge and power generation assets and their inspection types.

Furthermore, the data-sheets from OREDA give the failure rates of the incipient, degraded and critical failure modes. These are given in the form of a MTTF therefore implying a constant failure rate, although typically in reliability modelling failure rates are not constant but instead increase with age (Smith 2017). In reliability engineering a Weibull distribution is often used in stochastic models to simulate the increased failure rate with age (McCool 2012). These distributions are fit such that the probability of failure increases with time and so that the mean is the MTTF from OREDA. The mean, μ, of the Weibull distribution is calculated with the gamma function, Γ, such that,

$$\mu = \lambda\Gamma\left(1 + \frac{1}{k}\right), \tag{3.1}$$

where λ and k are the scale and shape paramaters respectively. For brevity the data of the Weibull distribution parameters are not included here, although they are given in full in Section B.1.

3.9 Asset Management Strategy

A core aim of this work is to evaluate the effectiveness of AM strategies on an offshore oil and gas platform. The AM strategy defines the decisions that are made relating to maintenance and inspections given knowledge on the known condition states of the assets on-board the platform. The strategy is separately defined for every possible maintenance action and inspection in the model, since the rate of degradation, the rate of failures and the consequences of the failures vary for each state in each observable in each asset. Thus an AM strategy decision should depend on the probability of failure in the future and the acceptable level of unavailability of that asset. Furthermore, the severity of the consequence of a failure must be considered, this should be considered in conjunction with the probability of the failure occurring. An effective AM strategy balances two objectives, firstly to minimise the unavailability of the systems and secondly to minimise the AM expenditure. In this research we primarily consider two AM strategy variables, the maintenance decision and the inspection interval.

A maintenance decision is the choice of whether to perform maintenance or not when a given state is revealed by an inspection. There is a maintenance decision associated with every revealed state in an observable, the strategy defines which states are set to queue maintenance when revealed and which are not. The decision should be based on the probability of failure in the future given that it has been inspected to be in that state and also what the effects of the asset failing would be in relation to

system availabilities and consequent events.

An inspection interval is the time between which periodic inspections take place, the strategy defines a unique inspection interval for every asset in the model. As an inspection acts on the entirety of at least one observable the interval should be based on the total failure rate of the observable. Similar to the maintenance decision, the inspection interval should also account for the effects of the observable's failures.

3.9.1 Maintenance Backlog

Through discussions with industrial contacts, it was identified that a pressing issue in LE is that as the platform ages and failure rates increase, the number required maintenance tasks increase. It is often the case that these tasks accumulate more quickly than they can be completed and thus a maintenance backlog is created, methods for prioritising these maintenance tasks are valuable (HSE 2007). Therefore, it is of importance to have a methodology in the model for the prioritisation of maintenance actions from a backlog.

3.9.2 Number of Asset Management Teams

It is important to consider the number of teams required to perform inspection and maintenance tasks. The number of these teams influences the sizing of the accommodation structures and therefore the design of platforms in the future. Thus this model also includes a resource limitation on the number of maintenance and inspection teams such that tasks can only be performed when a team is available.

3.9.3 Asset Management Optimisation

To maximise the performance of a platform it is necessary to optimise the performance of the AM strategy. By tuning the maintenance decisions, inspection intervals and number of teams, an optimisation procedure aims to determine optimal solutions that maximise the platform's performance. The approach taken to perform this optimisation is discussed in detail in Chapter 7.

3.10 Hydrocarbon Leaks

As discussed, every production asset has a leakage failure mode. Due to the flammability of the fluids this can pose a large risk to the platform and the personnel. However, the risk from a leak can vary significantly, depending on which asset is leaking, due to different fluid quantities and pressures. For example, it would be expected that a leak from a scrubber containing high pressure gas would pose a greater risk than a leak from a low pressure pipe. To quantify the possible outcomes of a leak this model framework will also include a consequence analysis which will evaluate leak scenarios. The production process takes an incoming stream from the well-head and through separation and compression produces an oil and gas stream, in doing so pressure vessels containing oil, gas or two-phase are all involved. Therefore the consequence analysis model must be capable of modelling vessels with any of these contents.

The occurrences of the leakage failure modes will define the initial conditions of the consequence analysis through the leaking asset's dimensions and fluid quantities. In Section 3.5, it was discussed that the fluid flows will be modelled throughout the platform's lifecycle, this means that the fluid quantities of every asset is known at all times. Therefore, when a leak occurs the fluid quantities of the leaking asset are taken from this.

There are three major possible escalation events of an oil or gas leak on an offshore platform, these are pool fires, jet fires or explosions (Suardin et al. 2009). An effective consequence analysis must evaluate the probability of each of these events and furthermore must assign a magnitude to the events. It is not necessary for the magnitude of different events to be comparable. It is enough to know that the magnitude of all must be minimised for the optimisation procedures used in this work.

3.11 Summary and Discussion

This chapter has discussed the design of the platform's systems and modelling decisions, the design decisions have been justified through a data-oriented approach with two main sources, namely: OREDA and platform Beryl B. Firstly, OREDA has provided data on the failure modes and failure rates for all of the assets within these systems. The definitions of the incipient, degraded and critical failure modes played a key role in the identification of the failure mechanisms. Secondly, the North Sea

platform Beryl B has been used as a case-study to supply information on the layout and design of the production, power and firewater deluge systems. In addition, it gave information on the fluid flow rates and quantities which made lifecycle fluid flow modelling possible. Together these data sources have allowed for a complex system to be specified that accurately represents a platform and its systems.

3.11.1 Degradation, Inspection and Failure

From an analysis of the reliability data, it was decided that multiple degradation mechanisms must be simulated for each asset type. In addition, it was decided that a linear series of conditions was the best technique for modelling the degradation. This series is known as an observable and inspections can reveal the condition corresponding to the degradation mechanism. Two inspection types are considered, these are internal and external inspections, and they act on different observables of an asset. Following the OREDA definition, an incipient failure mode increases the failure rate of degraded and critical failure modes but does not reduce the operation of the asset. This is reflected in the model by its presence increasing the degradation rate and failure rate of the observable.

When an asset's failure occurs this can either be immediately revealed to the operator or can require an inspection, these are known as revealed failures and unrevealed failures respectively. This was applied to the degraded and critical failure modes, whereas the incipient failure mode always occurs unrevealed, this is because the incipient failure mode does not result in any loss of functionality of the asset but instead increases the degradation rates. As a failure of the production asset results in a loss of production it was assumed that these failures are revealed. Similarly, the loss of power supply is assumed to be immediately apparent to an operator and so the assets of the power system also fail revealed. Conversely, the firewater deluge system is a standby system and so its failure is not known until it is activated so the assets are assumed to fail unrevealed.

3.11.2 Platform Systems

The scope of this thesis includes three systems: the production system, power system and firewater deluge system. The designs of these systems were taken from Beryl B and include interdependencies between assets, both within the systems and between systems. For instance, the production system and parts of the firewater deluge system

were reliant on the emergency supply from the power system. The production system was seen to have no redundancy which contrasted with the power system and firewater deluge system, which each had large degrees of redundancy. This reflects the importance of the systems, where the safety systems require a higher availability than the production system.

3.11.3 Asset Management Strategy

The purpose of the model is to evaluate different AM strategies and ultimately used to provide the decision variables for optimisation algorithms. The AM strategy is composed of maintenance decisions, inspection intervals and the number of inspection and maintenance teams that are stationed on the platform. Every state has a maintenance decision associated with it that defines whether or not maintenance will be performed when an inspection reveals the observable is in that state. Inspections are assumed to be periodic and the inspection interval defines the inspection frequency, in addition, the possible value of the intervals are limited to a discrete set of monthly times. The maintenance decisions and intervals are defined for every state and inspection in the model so the number of parameters in the search spaces of the AM strategy is likely to be large.

3.11.4 Hydrocarbon Leaks

Leaks of hydrocarbons from the production vessels can have dangerous consequences, it was decided that a consequence analysis was needed to evaluate leak scenarios. This is initiated by the occurrence of a leakage failure mode and is based on the fluid quantities of the leaking asset. It must be capable of modelling any production asset, whether it contained oil, gas or two-phase and furthermore, it evaluates three possible escalation events: pool fires, jet fires and explosions. The analysis will calculate the probability density functions for the events and will also evaluate the distribution of magnitudes of the events.

This chapter has presented the specification and design features of the model, the implementation of a model to fit these requirements is discussed in the next two chapters. Firstly, a PN is described in Chapter 4 which models the degradation and AM processes and also simulates the production's fluid flow throughout the platform's lifecycle. It also encodes the relationships between the assets and the interdependencies between systems through a network of nodes and arcs. Secondly, a consequence

analysis, detailed in Chapter 6, evaluates the probability of outcomes following a leak scenario given by production asset failure modes in the PN. These two parts are linked, such that the results of the PN and the consequence analyses it triggers form part of the evaluation of the AM strategy.

Chapter 4

Hybrid Stochastic Petri Net Model

4.1 Introduction

This chapter presents a detailed description of the PN part of the thesis' model. This is achieved through an extension to the traditional PN framework known as a Hybrid Stochastic Petri Net (HSPN) that combines discrete and continuous time elements to form an abstract modelling framework that is capable of simulating complex systems. The HSPN is the main component of the model, it simulates the life-cycle of the platform, this involves the simulation of asset degradation, AM tasks and the production process. Three systems are simulated, these are the power system, production system and firewater deluge system. The degradation and AM of the assets in these systems are modelled by the HSPN.

A Petri net was chosen as the central element of the model for several reasons. It was capable of modelling AM as a discrete processes through timed transitions which could simulate stochastic degradation and failures. Additionally, it can accommodate arbitrary connections between nodes through transitions and arcs, which provides a great deal of flexibility in modelling the interdependencies between the assets. The hybrid extension to the Petri net further increased it's utility by permitting simulation of fluid production flows which can also be made dependent on discrete nodes in the AM part of the net. The HSPN is an excellent model which provides the flexibility required to simulate the complex system detailed in Chapter 3.

The HSPN is composed of a union of a discrete stochastic PN and a continuous PN

which are described in Section 4.2 and Section 4.3 respectively. These provide a basis for the formulation of the HSPN, which is given both intuitively and mathematically in Section 4.4. The complete HSPN model is large with a total of 11020 transitions and places. To aid in constructing this net in a concise manner a technique to modularise the net is applied, this is achieved through the use of substitution transitions, introduced by (Jensen and Kristensen 2009), which are discussed in Section 4.5. These allow for a hierarchical net structure to be constructed that simplifies the appearance of the net without the loss of any functionality.

The structure of the degradation and AM of a generic asset is detailed in Section 4.7. This involves the construction of several substitutions transitions for the simulation of degradation, periodic inspections, preventive maintenance and corrective maintenance. These are then connected together to form a complete asset substitution transition capable of simulating multiple degradation mechanisms that are inspected by internal and external inspections. The AM strategy is encoded into the initial markings of places and the delays of timed transitions.

The first system presented is the power system in Section 4.8, this system provides the electricity to the platform. This can provide electricity at three levels dependent on the failures present in the system, firstly when fully operational this can power all the assets on the platform, secondly is an emergency power supply that operates only the safety systems and finally a total failure of the system that causes no power to be supplied to any system onboard. The electricity supplied from this system is crucial for both the production and firewater deluge system and the dependency between these systems will be discussed in Section 4.9 and Section 4.10 respectively. An unavailability tree of the power system is constructed in the net for the three levels of power supply which is based on the fault tree design seen in Section 3.6.

The HSPN for the production system is presented in Section 4.9. It is in this part of the net that the continuous element of the HSPN is used, it is used to simulate the flow of fluids through the production assets. The rate of the fluid flow through each asset depends on the current failure mode of the asset, which is determined through the AM part of the HSPN. The purpose of the production system's net is to determine the quantities of oil and gas produced so that the effect of various AM strategies on production can be analysed. These quantities are important metrics as they are one of the key performance indicators of the platform because they determine it's income.

The construction of the firewater deluge system's HSPN is presented in Section 4.10.

This system has a significant amount of redundancy in its design, for instance it has four pumps while only two are needed to supply a full capacity. The fault trees seen in Section 3.7 are used to construct equivalent unavailability nets for the firewater supply. The activation of the firewater supply is reliant on the detection of a leak and thus the detection system most be operational. To determine this another unavailability net is constructed for a detection system in a given module.

4.2 Discrete Stochastic Petri Net

A discrete stochastic PN extends the basic framework with the addition of timed transitions, these fire after a delay when enabled by their incoming places (Marsan et al. 1995). The delay can either be a constant time or it can be stochastically sampled from a probability density distribution every time it is enabled. The addition of discrete time greatly improves the modelling capabilities of the PN (Bause and Kritzinger 1996). The graphical representation of each of the nodes in a discrete stochastic PN is given in Figure 4.1. In this model timed transitions are used to simulate the degradation of components, periodic inspections and other timed events.

There are several ways in which places can enable transitions, a selection of nets are examined in Figure 4.2 which are used to explain how all the different interactions between places and transitions work. In Figure 4.2a the transition T_1 has incoming places P_1 and P_2, for the transition to be enabled the markings of each must equal or surpass the weighting of the arcs. The arc from P_1 has no inscription so the weighting is one, whereas the arc from P_2 is inscribed with w where $w \in \mathbb{N}^+$. If the marking of the places are greater than these weights then T_1 can fire. On firing the marking of P_1 and P_2 are reduced by their arc's weights and P_3 is increased by its arc's weight.

Figure 4.2b has a similar structure although in this net the arc from P_2 is an inhibitor arc. This will disable the transition and prevent it from firing whenever its marking exceeds the inhibitor's weight (Reisig and Rozenberg 1998). Additionally when T_1 does fire the marking of P_2 will be unchanged. If the inhibitor arc is replaced

Discrete place | Discrete untimed transition | Discrete timed transition

Figure 4.1: The nodes of a discrete stochastic PN.

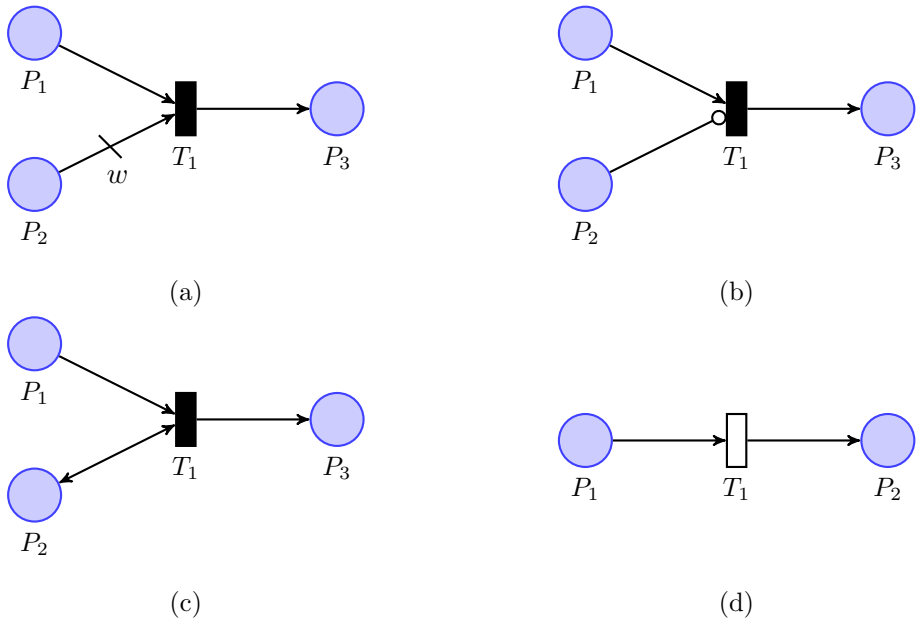

Figure 4.2: Some example nets of a discrete stochastic PN.

with a pair of arcs, one from P_2 to T_1 and one back from T_1 to P_2 then we have the net given in Figure 4.2c. A pair of arcs like this will be referred to as a double arc. With this structure T_1 is enabled when P_1 and P_2 are both marked, but when T_1 fires the marking of P_2 is unchanged as the double arc means that the transition removes and adds the same number of tokens to the place.

Untimed and timed transitions obey the same rules to be enabled to fire. In Figure 4.2d the transition is timed, associated with it is either a constant delay or a probability density distribution. In the case of a constant delay, C, then if P_1 becomes marked at time t it will fire at time $t + C$. Whereas in the case of a distribution then when P_1 becomes marked at t a sample, χ, will stochastically be taken from the distribution and it will fire at $t + \chi$.

4.3 Continuous Petri Net

A continuous PN is an extension to the technique that replaces the discrete events of a PN with continuous processes. This is achieved through replacing the standard places and transitions with continuous places and transitions, which add and remove the places' markings continuously over time. This expands the possible uses of a PN to simulate temporal process and in contrast to the discrete stochastic PN this can model processes that happen over a continuous time period instead of events happening at

Figure 4.3: The nodes of a continuous PN.

discrete times.

In a continuous PN the marking of a place is not an integer but can be any non-negative real number, $\mathbb{R}^+$ (Alla and David 1998a). Alternative nodes are used in the continuous PN that have different behaviours to their discrete counterparts. A continuous transition has a firing rate associated with it, this defines the rate at which tokens are removed from incoming continuous places. In this thesis the continuous nodes will follow standard notation and be represented by a circle or rectangle with a double border as shown in Figure 4.3.

The rules for enabling a transition within a continuous PN differ from the rules for a discrete PN in some scenarios, in Figure 4.4 a set of possible structures are examined. In Figure 4.4a the transition is enabled if P_1 and P_2 both have a marking greater than zero. The transition will decrease the markings of the incoming places at a rate equal to the connecting arc's weight multiplied by the transition's firing rate. Similarly it will increase the marking of outgoing places by the arc's weight multiplied by its firing rate. In a continuous PN the weight of an arc is no longer restricted to an integer but can be any positive values, $w \in \mathbb{R}^+$. An inhibitor arc is present from P_2 to T_1 in Figure 4.4b, this functions in the same way as in a discrete PN in that when the marking of P_2 exceeds the arc's weight the transition will be disabled.

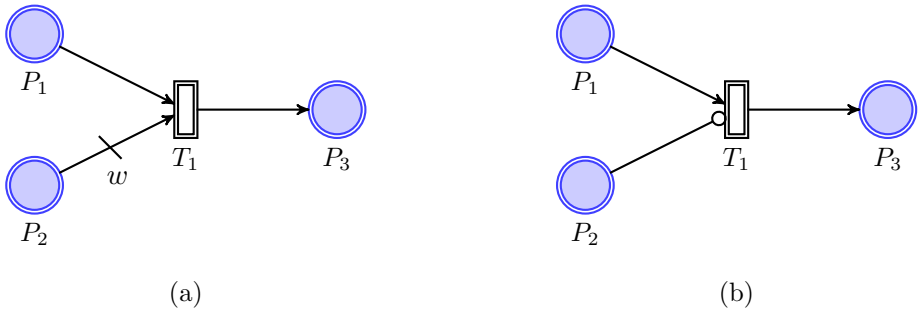

Figure 4.4: Some example nets of a continuous PN.

4.4 Hybrid Stochastic Petri Net

Both the discrete stochastic PN and the continuous PN introduce time to the technique, although each approached this in a different way. The discrete stochastic PN introduced timed transitions that fire at discrete intervals whereas the continuous PN introduced transitions that add and remove tokens from the places continuously. In the design of this model it was seen that both discrete and continuous processes are present. For instance in modelling the life-cycle of an offshore oil and gas platform there are several discrete processes such as inspections and maintenance. Furthermore, in this work degradation is also modelled as a discrete process, this is discussed in detail in Section 4.7.1. Degradation is modelled discretely so that the maintenance decisions can be made based on the discrete condition that each degradation mechanism is in. However, the performance of the platform requires the measurement of the production of oil and gas, which is a continuous process. Therefore for this research it is advantageous to have a framework that is capable of modelling both discrete and continuous processes, for this reason a HSPN framework was developed.

The HSPN is constructed through a union of the discrete stochastic PN and the continuous PN (Ghomri and Alla 2007). Within the discrete and continuous parts of the HSPN the net obeys the same rules as defined in Section 4.2 and Section 4.3. To complete an intuitive description of the HSPN the interface between these two parts must be defined, through the nets presented in Figure 4.5 the interfaces are discussed.

Discrete transition can be connected to continuous places as incoming and outgoing transitions. The case of an outgoing continuous place is given in Figure 4.5a, when enabled the transition fires and increases the marking of P_2 by $w \in \mathbb{R}^+$. An incoming continuous place is shown in Figure 4.5b, here the transition is enabled when the marking of P_1 is greater than or equal to the arc's weight w. When firing the transition will instantaneously decrease the marking by w. Continuous places can also connect to discrete transitions through inhibitor and double arcs, shown in Figure 4.5c and Figure 4.5d respectively. These will disable or enable the transition when the marking of the continuous places is greater than or equal to the arc's weight.

A discrete place cannot be connected to a continuous transition in any way that would imply the transition could change the marking of the place. As such a discrete place incoming to a continuous transition can only be connected via an inhibitor or double arc, as in Figure 4.5e and Figure 4.5f. These behave as they do in the discrete net and will disable or enable the continuous transition dependent on their marking.

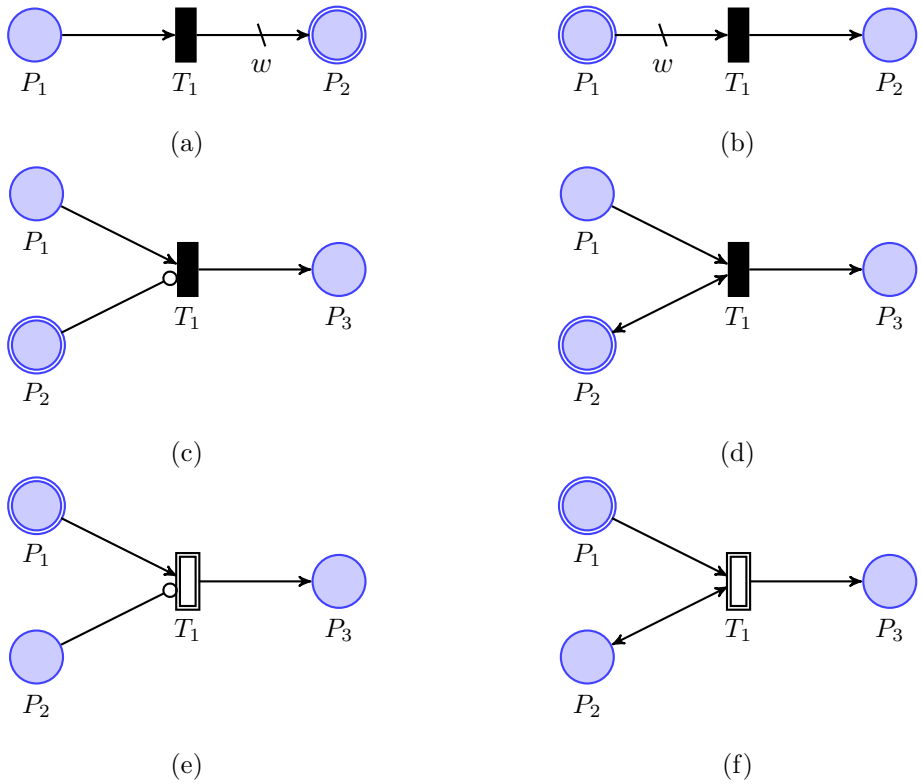

Figure 4.5: Interactions between the discrete and continuous parts of the HSPN.

Transition Priorities

An additional feature in this thesis' HSPN is transition priorities, these are used to prescribe an order to a set of transitions that are all enabled to fire simultaneously (Mahfoudhi et al. 2012). Figure 4.6 provides an example of how the prioritisation is implemented. Transition T_1 has high priority, p_H, and transition T_2 has low priority, p_L, when a transition does not have a priority inscribed it is assumed to have a normal priority. The higher priority transition will always fire first, in this example if P_1 and P_2 are both marked then T_1 will fire, otherwise if P_2 is unmarked then T_2 will fire.

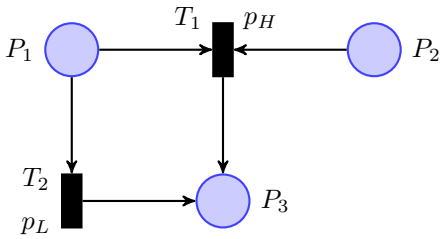

Figure 4.6: An example of transition priorities.

4.4.1 Mathematical Definition

The structure of the HSPN used in this modelling framework is based on a definition by Ghomri and Alla (2007). The definition presented here includes the addition of transition priorities that increase the model's functionality. The structure of the HSPN used in this modelling framework can be mathematically described as a tuple, $\mathbf{HSPN} = \{P, T, \mathbf{Pre}, \mathbf{Post}, h, p, \tau, m_0\}$, where:

- $P = \{P_1, P_2, \dots P_{N_P}\}$ is a finite set of places with discrete places, P^D, and continuous places, P^C, such that $P^D \cup P^C = P$ and $P^D \cap P^C = \emptyset$.
- $T = \{T_1, T_2, \dots T_{N_T}\}$ is a finite set of transitions with discrete transitions, T^D, and continuous transitions, T^C, such that $T^D \cup T^C = T$ and $T^D \cap T^C = \emptyset$.
- $\mathbf{Pre} : \begin{Bmatrix} P_i \times T_j \to \mathbb{N} & : P_i \in P^D \\ P_i \times T_j \to \mathbb{R} & : P_i \in P^C \end{Bmatrix}$ is the pre-incidence mapping.
  These values represent the weights of arcs incoming to transitions from places. A mapping to zero represents no arc connecting the place and transition, whereas a negative value represents an inhibitor arc.
- $\mathbf{Post} : \begin{Bmatrix} P_i \times T_j \to \mathbb{N}_0^+ & : P_i \in P^D \\ P_i \times T_j \to \mathbb{R}_0^+ & : P_i \in P^C \end{Bmatrix}$ is the post-incidence mapping.
  These values represent the weights of arcs outgoing from transitions to places. A mapping to zero represents no arc connecting the transition to the place. Here no negative values are permitted as an inhibitor arc cannot connect a transition to a place.
- $h : P \cup T \to \{D, C\}$ defines if a place is discrete or continuous.
- $\tau : T \to \mathbb{R}_0^+$ associates each transition with a non-negative real number. For a discrete transition this corresponds to a time delay and for a continuous transition this corresponds to a firing rate.
- $p : T \to \mathbb{R}$ is the priority of each transition. If multiple transitions are enabled at the same time then the transition with the greatest priority fires first.
- $m_0 : \begin{Bmatrix} P_i \to \mathbb{N}_0^+ & : P_i \in P^D \\ P_i \to \mathbb{R}_0^+ & : P_i \in P^C \end{Bmatrix}$ is the initial marking of each place.

4.5 Substitution Transitions

To aid in constructing the HSPN in this model, a technique is used to modularise nets and then connect them in a hierarchical manner. These modules are known

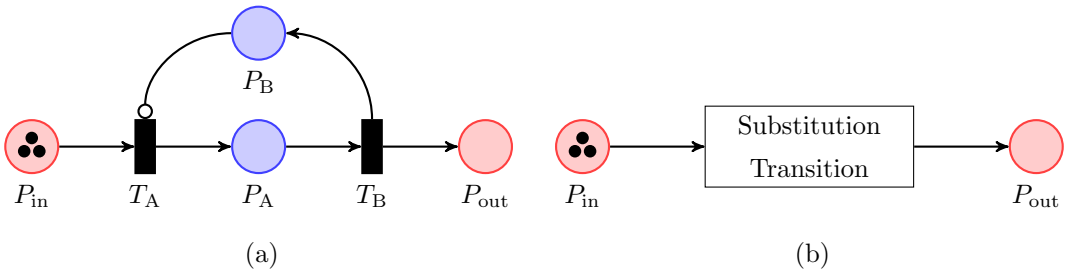

Figure 4.7: An example of a basic substitution transition.

as substitution transitions as they connect to places in the same manner as a regular transition would (Jensen and Kristensen 2009). Substitution transitions contain hidden PNs and function as such, they are an abstraction that reduces the apparent complexity of larger nets (Sheng and Prescott 2017). The net hidden inside the substitution transition functions under the normal rules of the HSPN.

The model contains several substitution transitions that fit together in a hierarchical structure to form the complete system. Each substitution transition has a set of places that connect to the next layer of the net, in this research these places are known as socket places. To differentiate socket places they will be represented by red places, with non-socket places represented by blue places. Figure 4.7 shows a basic substitution transition with socket places P_{in} and P_{out}. The hidden net of P_A, P_B, T_A and T_B function as normal, in this case only allowing one token to pass through the substitution transition from P_{in} to P_{out}.

4.6 Logic Gates

Logic gates are used throughout the HSPN to form a variety of structures. In the literature logic gates are frequently seen to be represented in PN form (Yang, Liu, et al. 1997; Guo et al. 2016; Chew, Dunnett, and Andrews 2008). Typically in the literature the gates have been constructed to activate only once such that they record an activation of the gate in the output place. In this work the gates are designed to update their output dependent on the current state of the inputs. As these gates are repeated throughout the net it is advantageous to define substitution transitions for them.

In Figure 4.8 an OR gate, an AND gate and a k-out-of-N gate are defined. These are all given for four incoming places but can be generalised for an arbitrary number of places. For the OR gate the top place becomes marked with a single token when

any of the base places become marked by the relevant transition $T_{\text{Up},i}$. Additionally the gate is updating, such that when none of the base places are marked the top place is emptied by the T_{Down} transition. Similarly the top place of the AND gate is marked when all of the base places are marked by T_{Up} and will be emptied when at least one of the bases are no longer marked by the relevant $T_{\text{Down},i}$

A k-out-of-N gate requires k of the N incoming places to be marked for the top place to become marked. The k-out-of-N gate's structure is more complex, $P_{\text{Count},i}$ is marked with the number of incoming places that are currently marked. The places $P_{\text{Store},i}$ are marked when the incoming place has been counted and become unmarked when the incoming place is no longer marked and its contribution to the count place is removed. The top place, P_{Top} is marked when P_{Count} is greater than or equal to k and is unmarked when it is less than k.

4.7 Asset Management Model

In this model the AM processes are simulated using the HSPN, for each asset there is a substitution transition that models these processes known as an asset substitution transition. There are three types of AM processes simulated, these are periodic inspection, preventive maintenance and corrective maintenance. In addition to inspection and maintenance the asset substitution transition simulates the degradation process and is capable of modelling multiple degradation mechanisms.

Performing a simulation of the HSPN would simulate a single life-cycle of an offshore oil and gas platform. The outcome of a simulation of the HSPN will be different for every simulation due to the randomness introduced by the many timed transitions that stochastically sample from probability density distributions. Therefore to analyse the life-cycle of the platform it is not enough to examine a single simulation. Instead a Monte Carlo (MC) method is applied, this performs a large number of simulations of the HSPN to produce a large data set of results from which meaningful results can be extracted.

A typical offshore oil and gas platform has a design life of approximately 25 years (Stacey, Birkinshaw, and Sharp 2008) and a significant proportion of these are now operating beyond their design life in LE, in some regions such as the UKCS this is as high as 50% (DECOM 2014). To represent the effect of LE this model simulates the life-cycle of the platform over a 50 year period. Thus at 25 years into a simulation the

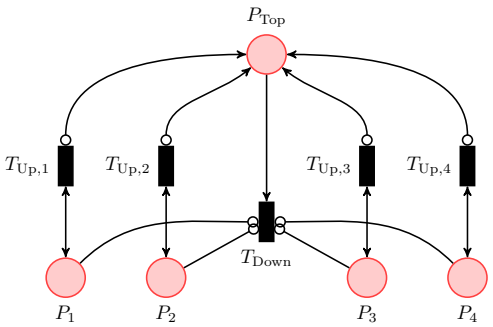

(a) An OR Gate for four places.

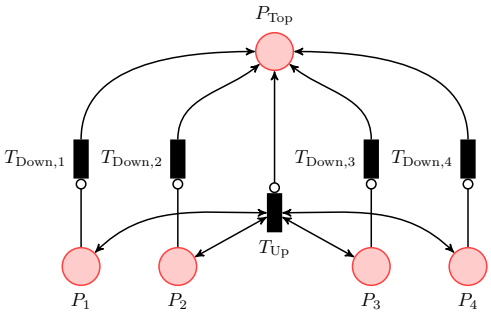

(b) An AND Gate for four places.

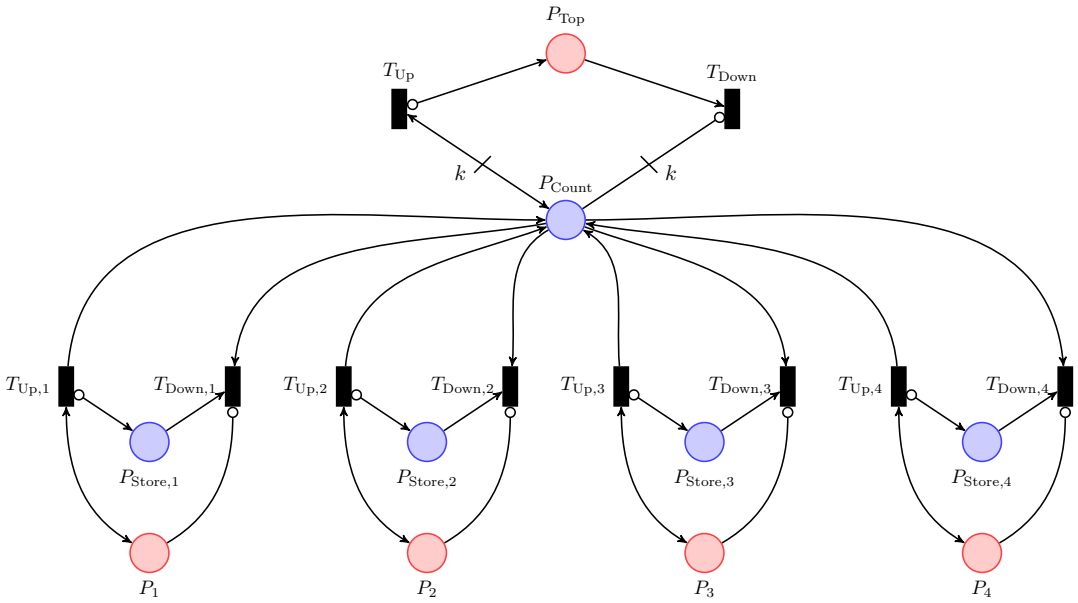

(c) A k-out-of-N OR Gate for four places.

Figure 4.8: Substitution transition of logic gates.

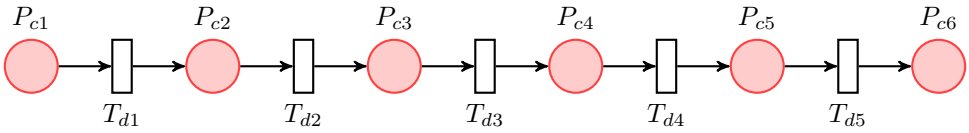

Figure 4.9: The condition degradation substitution transition.

state of the platform will be representative of a platform entering into its LE stage. In addition, the failure rates are not constant throughout the life-cycle but increase with time to simulate the ageing assets.

This section presents a full description of the structure of the AM part of the net, this involves several substitution transitions that each model a different element of the process. The substitution transitions are combined in a hierarchical manner to form a complex asset substitution transition that models the degradation, failure and maintenance for multiple degradation mechanisms and internal and external inspections.

4.7.1 Condition Chain

In this model the condition of an observable is considered to be discrete, in the HSPN these are represented by a series of increasingly degraded places known as a condition chain. This is a linear progression of alternating places and transitions, an example with 6 conditions is shown in Figure 4.9. This kind of chain is frequently seen in modelling the degradation of a component and has proved to be a good technique for simulating degradation using a discrete process (Andrews 2013; Briš 2013; Le and Andrews 2013; Le and Andrews 2015).

The places represent successively more degraded places, starting with P_{c1} which is *Good as new* and ending with P_{c6} which is *Critically Degraded* and is considered as degraded as possible. It is assumed that initially the asset is in a good as new condition. At the beginning of a simulation the first condition place P_{c1} holds a single token while all other places are unmarked. The stochastically timed transitions $T_{\mathrm{d}j} : j \in 1, ..5$ fire to progress the token along the chain, thus the probability density distributions assigned to these transitions define the degradation rate. At any time in the simulation exactly one of the condition places $P_{\mathrm{c}i} : i \in 1, .., 6$ will be marked, where the marked place represents the current condition state of the observable.

An asset can undergo several different degradation mechanisms, these occur at different rates and have different failure modes. Therefore for each degradation mech-

anism associated with an asset there is a corresponding condition chain in the HSPN. This allows for each degradation mechanism to follow their own degradation distributions and furthermore allows the condition to be inspected and maintained independently.

At the end of this section a description of each place in the nets is given in Table 4.6, some places appear in multiple nets, this table summarises in which substitution transition each place appears. The transitions are also described in tables throughout the section, these are not shared between substitution transitions and so are detailed following their figures.

Degradation Distributions

To simulate the degradation of the components the condition chain transitions are stochastically sampled from distributions. In this research it was decided to use the two-parameter Weibull distributions for the transitions. This distribution is frequently used in research to represent degradation and failure rates (Gorjian et al. 2010), this is in part due to its ability to simulate failure behaviours such as infant mortality and wear-out. In relation to LE, wear-out is of particular interest as an increased failure rate is expected in the asset's later life. The Weibull distribution was selected as opposed to other distributions due to the above reasons and as it is parametrised only by two-variables which reduces the information needed from data sources to encode it.

The probability density function of the Weibull distribution is given by,

$$f(x;\lambda,k) = \begin{cases} \frac{k}{\lambda}\left(\frac{x}{\lambda}\right)^{k-1}\exp\left(-(x/\lambda)^k\right) & : \quad x \geq 0, \\ 0 & : \quad x < 0, \end{cases} \tag{4.1}$$

where $\lambda \in (0,\infty)$ is the scale parameter and $k \in (0,\infty)$ is the shape parameter (Rinne 2008). The scale parameter defines how spread out the distribution is with a greater scale parameter corresponding to a wider spread, whereas the shape parameter defines the form of the distribution. Considering the distribution as a failure distribution then $k < 1$ defines a failure rate that decreases over time, $k = 1$ defines a constant failure rate and $k > 1$ defines a failure rate that increases over time. A set of example Weibull distributions are given in Figure 4.10a. The cumulative distribution function can be

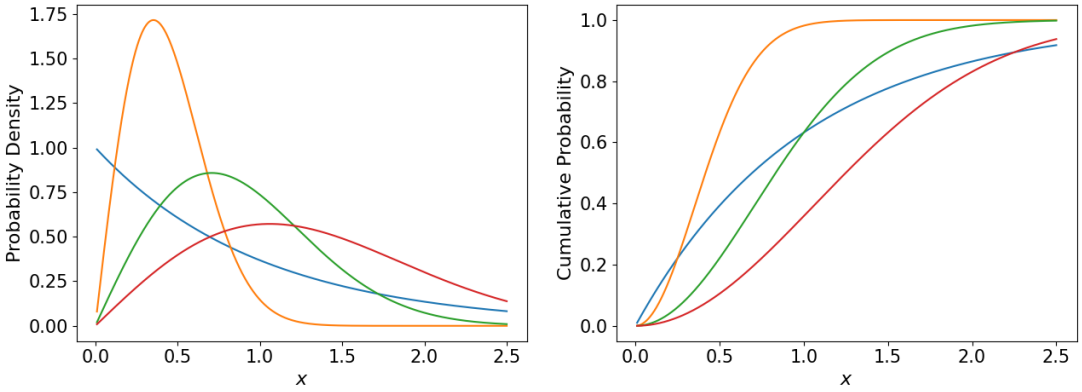

(a) Probability density function.

(b) Cumulative distribution function.

Figure 4.10: Weibull distribution functions. $\lambda = 1$, $k = 1$, $\lambda = 0.5$, $k = 2$, $\lambda = 1$, $k = 2$, $\lambda = 1.5$, $k = 2$.

found through integrating the probability density function, this is given by,

$$F(x;\lambda,k) = \int_{-\infty}^{x} f(t;\lambda,k)dt, \tag{4.2}$$

$$F(x;\lambda,k) = \begin{cases} 1 - \exp\left(-(x/\lambda)^k\right) & : \quad x \geq 0, \\ 0 & : \quad x < 0. \end{cases} \tag{4.3}$$

The corresponding cumulative distribution functions are shown in Figure 4.10b. In this research all Weibull distribution have a shape parameters greater than one, this is to represent the increased probability of degradation as the time in that condition state increases. Specifically, a shape parameter, $k = 1.2$ is assumed for all degradation transitions. This was chosen as a reasonable value for an increasing degradation rate. However, if a dutyholder had access to data pertaining to the rate of increase then the shape parameter could be modified to more accurately represent the degradation.

To retrieve a sample from the Weibull distribution a random number, χ, is generated in the range $\chi \in (0, 1)$. This is then equated to the cumulative distribution $F(x;\lambda,k)$ and rearranged for x. Therefore a sample of the Weibull distribution is given by,

$$x = \lambda\left\{-\ln(\chi)\right\}^{1/k} \quad : \quad \chi \in (0,1). \tag{4.4}$$

In the context of using this distribution for a stochastically timed transition then the sample defines the time of firing, such that if the transition is enabled at time, t, it will fire at time $t + x$.

The OREDA data (OREDA 2016) gives MTTF for the failure modes, this is then

adapted to the fit the Weibull distributions of the observable's condition chain and failure transitions. As the shape paramter is known, the scale paramater can be calculated through Equation 3.1, such that,

$$\lambda = \frac{\mu}{\Gamma\left(1 + \frac{1}{k}\right)}. \tag{4.5}$$

4.7.2 Failure Modes

An observable's failure modes can be reached from every condition in a condition degradation substitution transition. As discussed in Section 3.2 each condition chain has three failure modes associated with it: *Incipient*, *Degraded* and *Critical*. According to the OREDA definition the failure mode *Incipient* does not cause the asset to fail but does cause the failure rate to the *Degraded* and *Critical* failure modes to increase.

There is one path present to mark the *Incipient* failure mode place P_{fI}, from condition place P_{ci} through timed transition T_{fI}. Associated with T_{fI} is a probability density function such that the probability of it firing can vary with the duration of time the P_{ci} is marked. For instance, the distribution can be selected such that the probability of firing increases with the time marked. The condition can also reach the *Degraded* and *Critical* failure mode places P_{fD} and P_{fC} respectively. For each of these there are a pair of transitions, one enabled by the *Incipient* place, P_{fI}, through a double arc, $T_{\mathrm{fD,wI}}$, and one disabled through an inhibitor arc, $T_{\mathrm{fD,nI}}$, for the degraded failure mode. These two transitions allow the failure rates to be specified for with or without an *Incipient* failure present. Again a probability density function is used for these transitions, the probability density function is selected so that the $T_{\mathrm{fD,wI}}$ is more probable to fire than $T_{\mathrm{fD,nI}}$ corresponding to an increased failure rate. The exact values used in this research can be found in Appendix B, in Section B.2.

An asset can fail from any of the conditions in a condition chain, therefore a failures net for a condition chain can be constructed through the composition of the condition failure substitution transitions, this is given in Figure 4.12. This higher level substitution transition will aid in the construction of more complex nets.

4.7.3 Inspection

There are several inspections that can be performed on an asset, each of these reveal the states of a subset of the asset's observables. For each inspection an inspection clock substitution transition is constructed in the net as shown in Figure 4.13. The inspection

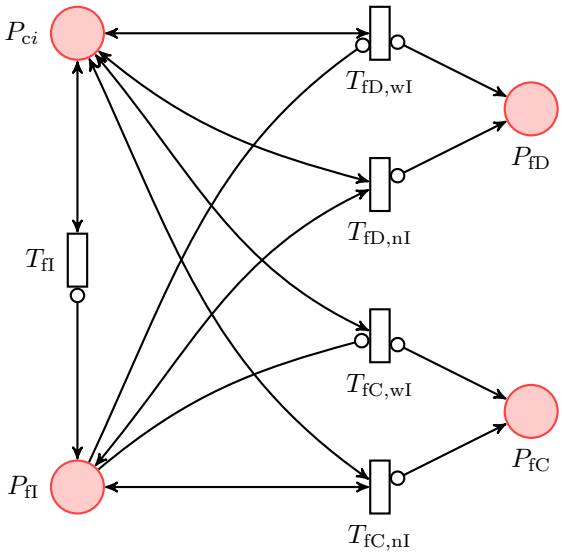

Figure 4.11: A condition failure substitution transition.

Transitions	**Description**
T_{fI}	Transition to cause an incipient failure from condition i
$T_{\mathrm{fD,wI}}, T_{\mathrm{fC,wI}}$	Transition to cause a degraded or critical failure respectively when an incipient failure mode is present
$T_{\mathrm{fD,nI}}, T_{\mathrm{fC,nI}}$	Transition to cause a degraded or critical failure respectively when an incipient failure mode is not present

Table 4.1: Description of transitions for the condition failure substitution transition given in Figure 4.11.

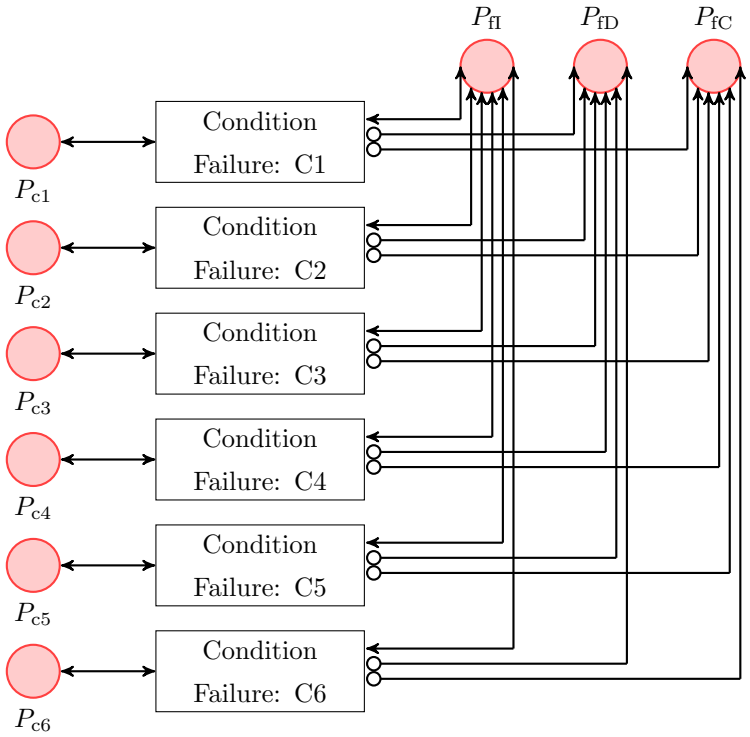

Figure 4.12: Chain failures substitution transition.

clock models the interval between inspections and then, subject to the availability of an inspection team, performs the inspection. The inspection clock is constructed such that P_{iAct} is marked periodically at the sum of the inspection interval and duration times. This inspection may be delayed if no inspection teams are available after the inspection interval has surpassed, if this is the case the inspection is performed when the next team is available. The number of inspection teams are represented by the marking of socket place P_{iT} which is shared by all inspection clocks. At initialisation of the simulation P_{rClock1} is marked with one token, this starts the clock. The place P_{rCounter} is used to hold a count of the number of inspections performed in its marking. This is used to determine the cost of the inspection activities.

In addition to the inspection clock there is an inspection action substitution transition that performs the action of an inspection to reveal the current condition of the observable and any failure modes present. This net exists in two types: fail unrevealed and fail revealed, shown in Figure 4.14a and Figure 4.14b respectively. The socket place P_{iRev} is marked when an inspection is in progress. This place is connected to the inspection clock's action place P_{iAct} in the higher level asset substitution transition which will be detailed in Subsection 4.7.6. This inspection will fire the relevant transi-

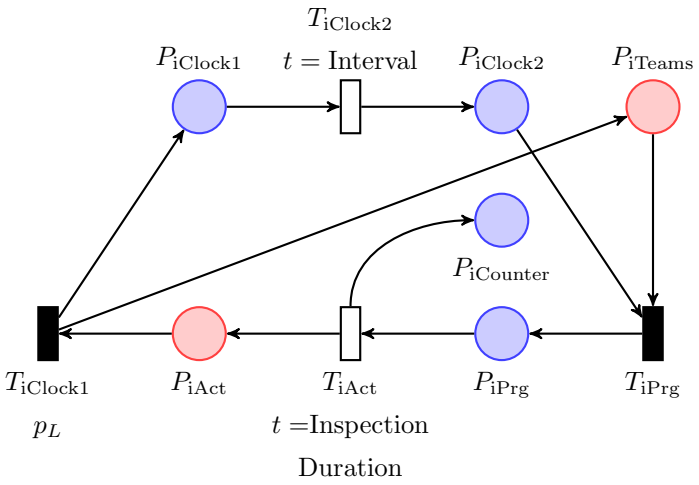

Figure 4.13: The inspection clock substitution transition. This net determines the time at which an inspection is performed.

Transitions	**Description**
T_{iClock1}	Transition to complete the inspection and return the inspection team
T_{iClock2}	Transition with constant delay to represent the interval between transitions
T_{iPrg}	Transition to check their is sufficient inspection teams
T_{iAct}	Transition to perform the inspection and iterate the inspection counter

Table 4.2: Description of transitions for the inspection clock substitution transition given in Figure 4.13.

tion marking the revealed condition for the currently marked condition. For instance if P_{c3} is marked then T_{i3} will fire marking P_{rC3}, assuming that P_{rC3} is not already marked. Similarly any failure modes will be revealed via transitions T_{ifI}, T_{ifD} and T_{ifC}. For the case of failure revealed then T_{ifD} and T_{ifC} instantaneously fire when the relevant failure mode are marked without the need of an inspection. The reason that the incipient failure mode still requires an inspection is because the OREDA definition states that it does not cause any reduction of the system capabilities and therefore it's failure is not immediately apparent.

An inspection reveals the condition of an observable, in the case that previously a condition has already been revealed and now an inspection reveals a later condition then two of the revealed conditions' places will be marked. Only the most recently revealed place should be marked, this will always be the more degraded condition. To remove the token from the previously revealed place a set of transitions are connected to each revealed condition place to remove the marking from the less degraded condition when a more degraded condition becomes marked. This structure is given in Figure 4.15.

4.7.4 Maintenance

The maintenance actions in this research are divided into two types, these are preventive and corrective. Preventive maintenance is performed on an observable that has not failed, note that this includes the incipient failure mode as the asset's operation is unaffected in this state, as per the OREDA definition. Corrective maintenance is performed once an observable reaches a failure mode and acts to restore the condition of the observable.

The first element of the maintenance net is known as the maintenance queue substitution transition. The purpose of this is to queue a maintenance event when in a state where the maintenance decision is enabled. Figure 4.16a and Figure 4.16b show the nets for the maintenance queue with the preventive maintenance action. It can be seen that to mark the queue place, P_{mQueue}, the correct revealed condition, $P_{rc\mathit{i}}$, must be marked and the revealed incipient failure mode, P_{rfI} must be marked or unmarked respectively. In addition $P_{mDecision}$ must be marked, this encodes the maintenance strategy decision by enabling or disabling maintenance from the state, by changing the marking of this place different maintenance strategy decisions for each state can be implemented. The corrective maintenance queue is shown in Figure 4.16c, this net

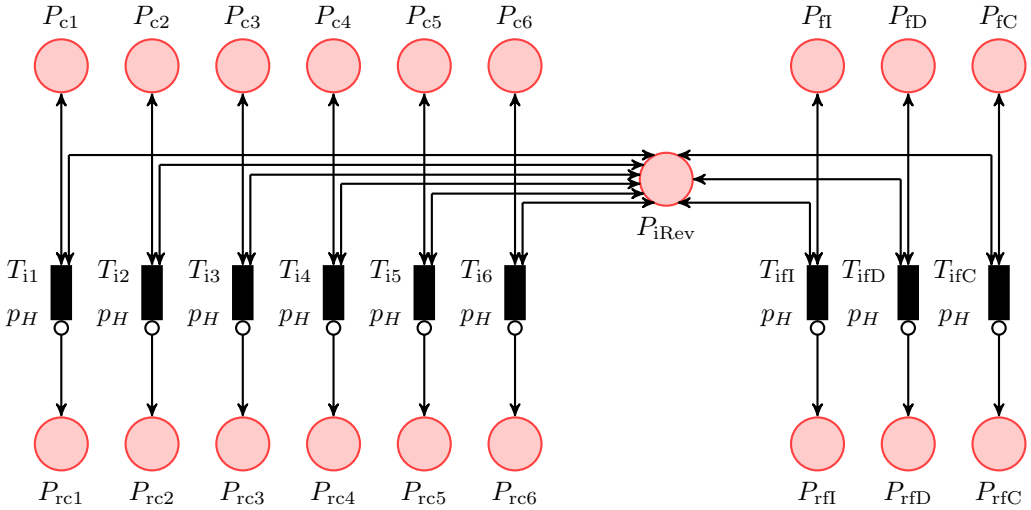

(a) Fail revealed.

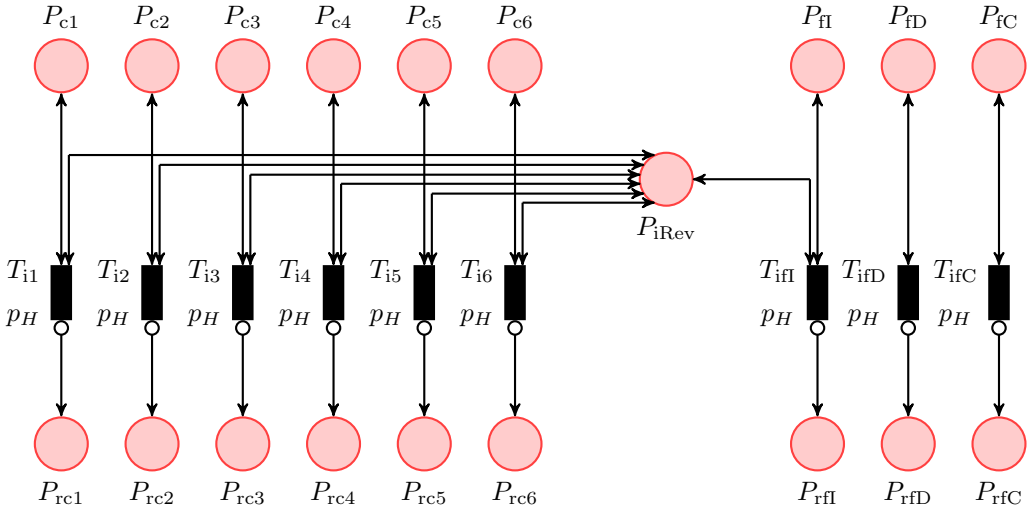

(b) Fail unrevealed.

Figure 4.14: The inspection action substitution transition for conditions and failure modes.

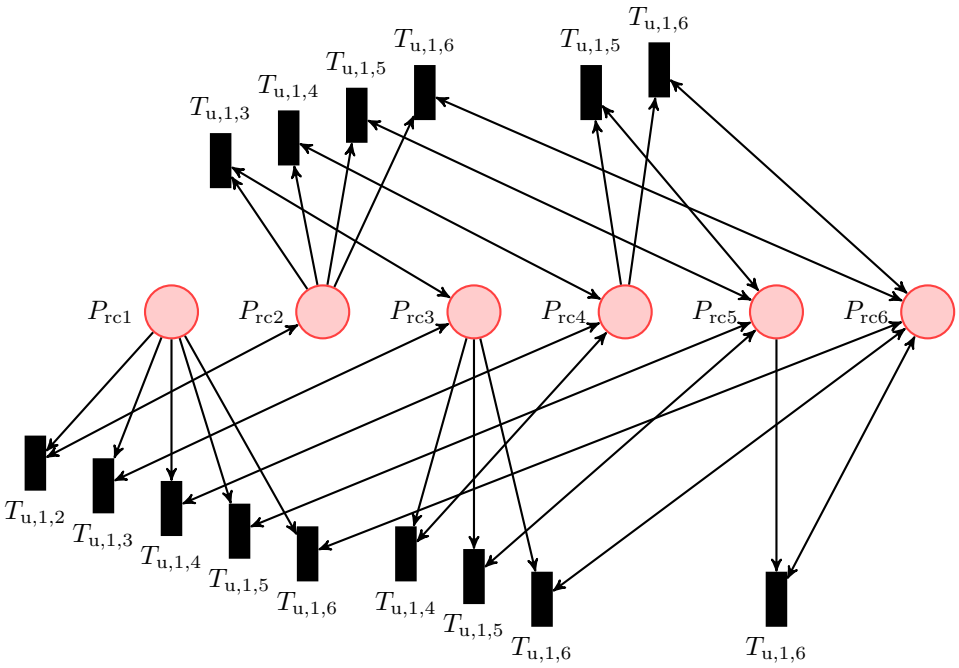

Figure 4.15: The updater substitution transition.

is valid for a revealed degraded or critical failure and will queue maintenance immediately because a failed system will always need repair, therefore there is no maintenance strategy decision place present.

In some situations it may be beneficial for opportunistic maintenance to be performed. The purpose of opportunistic maintenance is to group maintenance actions on similar components with the aim of reducing the expenditure. Opportunistic maintenance is included in this model through a substitution transition, which is given in Figure 4.17. In this figure the opportunistic maintenance is shown for three actions, however this can be generalised to an arbitrary number of actions. The place, P_{mOpp}, represents a decision with it's marking defined by the AM strategy, such that being marked corresponds to enabling opportunistic maintenance. In the case that opportunistic maintenance is enabled and P_{mOpp} is marked, then when the 1$^{\text{st}}$ queue becomes marked, $P_{\text{mQueue},1}$, the other queues should also be marked. This is achieved through the firing of $T_{\text{mOpp},1,2}$ and $T_{\text{mOpp},1,3}$ which will mark the queue places $P_{\text{mQueue},2}$ and $P_{\text{mQueue},3}$ respectively. Note that these also have an inhibitor arc incident on the transitions which prevent the transitions firing if the places are already marked. The same logic applies for all the maintenance queues, such that when any becomes marked, the transitions will fire to mark the other unmarked maintenance queues.

Opportunistic maintenance may be performed when assets are nearby or when the

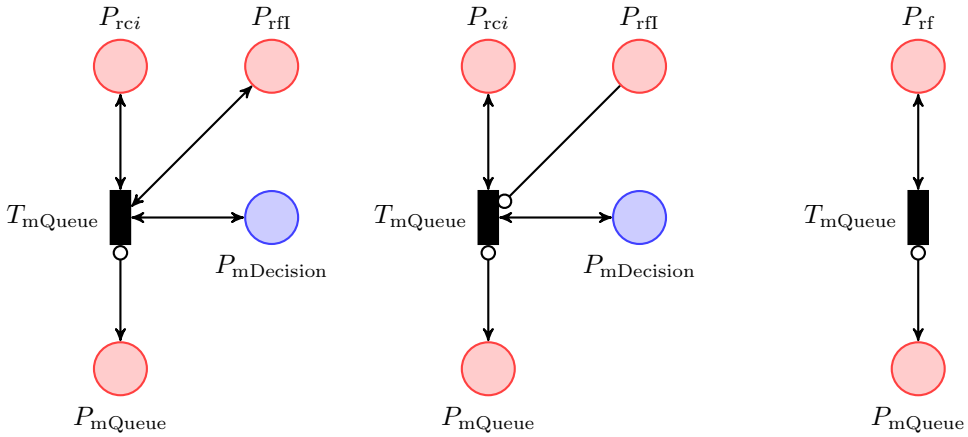

(a) Preventive maintenance for states with an incipient failure.

(b) Preventive maintenance for states without an incipient failure.

(c) Corrective maintenance for a degraded or critical failure.

Figure 4.16: Maintenance queue substitution transition.

repair process is similar. In this work opportunistic maintenance is performed between the observables of an assets. Thereby, if any maintenance action is queued for an asset then, if enabled, opportunistic maintenance will be queued for all of the asset's observables. Opportunistic maintenance results in a cost reduction on each observable repaired. Despite the cost reduction of each maintenance action, the total maintenance cost may be greater due to more maintenance actions being performed. Enabling opportunistic maintenance for an asset may improve the average condition across the observables, however it could also result in excessive maintenance of observable with relatively slow degradation mechanisms.

The next element of the maintenance net is known as the maintenance action substitution transition, this is shown in Figure 4.18. The purpose of this is to simulate the performance of maintenance once it has been queued, this substitution transition is connected to the preventive and corrective maintenance queue substitution transitions. Before the maintenance is performed two checks must be passed, firstly we must be in a maintenance window and secondly there must be at least one maintenance team available. Transition T_{mChecks} can only fire once both of these conditions are passed, these are checked through the markings of socket places P_{mWindow} and P_{mTeams}. The maintenance window marks P_{mWindow} during each window, this is achieved through the clock net Figure 4.19, at the start of a simulation one token is present in P_{mWait}, the firings of T_{mWait} and T_{mWindow} define the interval and duration of the windows. The maintenance teams socket place P_{mTeams} is marked with the number of available

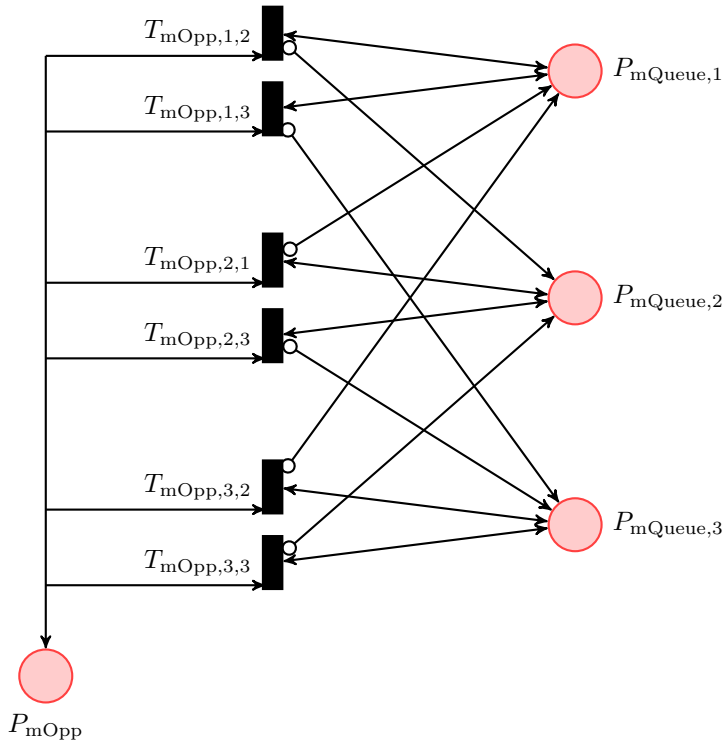

Figure 4.17: Opportunistic maintenance substitution transition, shown for three queues.

teams which are removed for the duration of the maintenance. This simulates the limited capacity of maintenance teams on an offshore platform. Finally the timed transition, $T_{\text{mDuration}}$, simulates the duration of the action, the firing of this adds a token to P_{mCounter} which records the number of maintenance actions. Additionally it marks P_{mReset} which resets the asset's condition, this will be discussed in greater detail later in this section.

The maintenance check transitions, T_{mChecks}, has a dynamic priority associated

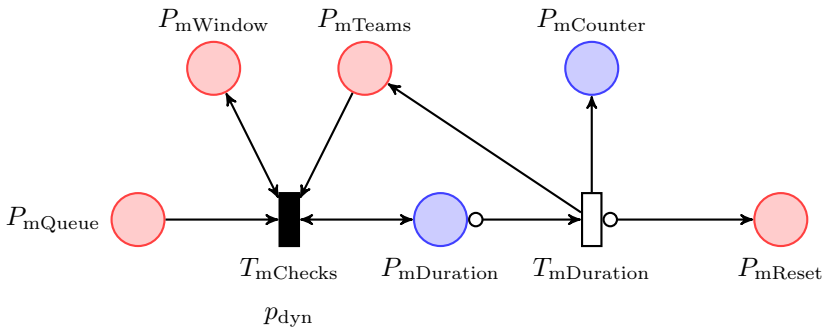

Figure 4.18: Maintenance action substitution transition.

Transitions	Description
T_{mChecks}	Transition to check their is sufficient maintenance teams and the maintenance window is open before maintenance begins
$T_{\text{mDuration}}$	Transition with constant delay to represent the time taken to perform the maintenance.

Table 4.3: Description of transitions for the maintenance action substitution transition given in Figure 4.18.

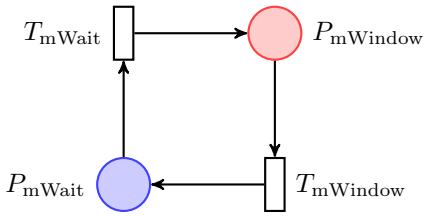

Figure 4.19: Maintenance window clock substitution transition.

with it, denoted by p_{dyn}. This priority can be updated throughout the simulation period dependent on the current state of the HSPN. The purpose of this is to be able to apply a method that tackles the maintenance backlog problem by prioritising the most important maintenance tasks first. A maintenance backlog situation is represented in the net by multiple assets maintenance queue place, P_{mQueue}, being simultaneously marked. An analysis of the relationship between the maintenance queue size and the number of AM teams will be performed in Subsection 5.3.5. To perform a maintenance action, T_{mChecks} must fire which will only fire during a maintenance window, therefore during a maintenance window all of the asset's T_{mChecks} are eligible to fire until all of the maintenance teams are allocated to a task. The order that the maintenance backlog tasks are performed are defined through the relative prioritisations of T_{mChecks}. A prioritised maintenance check transition, T_{mChecks}, exists for all possible maintenance actions for all asset observables. The value of p_{dyn} is defined as a variable of the optimisation algorithm. This approach is discussed in Subsection 7.4.4.

The maintenance queue and maintenance action substitution transitions are connected in the next level of the hierarchy through two substitution transitions, one for the preventive maintenance and one for the corrective maintenance in Figure 4.20 and Figure 4.21 respectively. The preventive maintenance substitution transition combines

Transitions	Description
T_{mWait}	Transition with constant delay, when fired the maintenance window opens
T_{mWindow}	Transition with constant delay, when fired the maintenance window closes

Table 4.4: Description of transitions for the maintenance window clock substitution transition given in Figure 4.19.

both the maintenance with and without an incipient failure mode present, whereas, the corrective maintenance substitution transition combines the corrective maintenance for the degraded and critical failure modes. These nets simplify the construction of a substitution transition that includes maintenance for all conditions and failure modes.

The complete substitution transition for the maintenance process for a single component is shown in Figure 4.22, known as the component maintenance substitution transition. The preventive maintenance for each condition state and failure mode is combined in this substitution transition.

A reset net is shown in Figure 4.23, this is used after a maintenance action to reset the observables to the *Good as new* condition and remove any tokens from the failure mode places. This is constructed of a series of transitions for each place that a token may be in and removes any tokens to empty the entire net. After this process is completed one token is deposited in P_{c1} and one in P_{rc1} to represent the renewed condition of the asset.

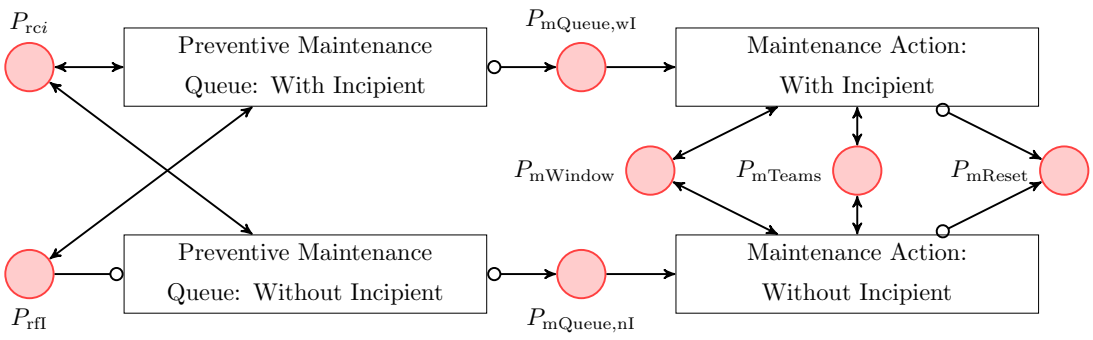

Figure 4.20: Preventive maintenance substitution transition.

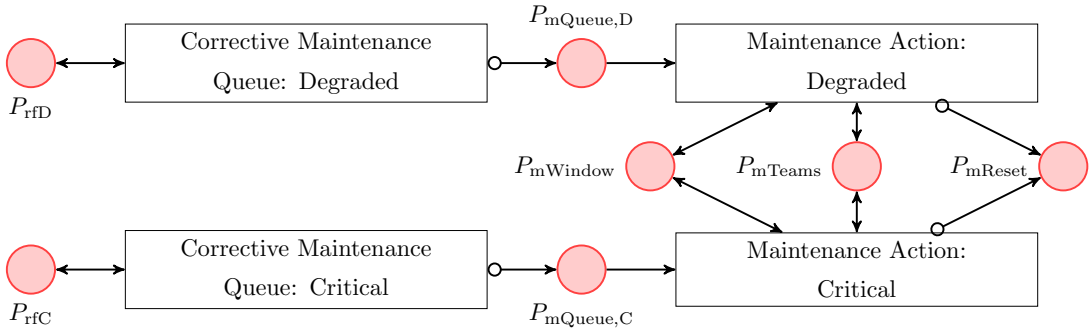

Figure 4.21: Corrective maintenance substitution transition.

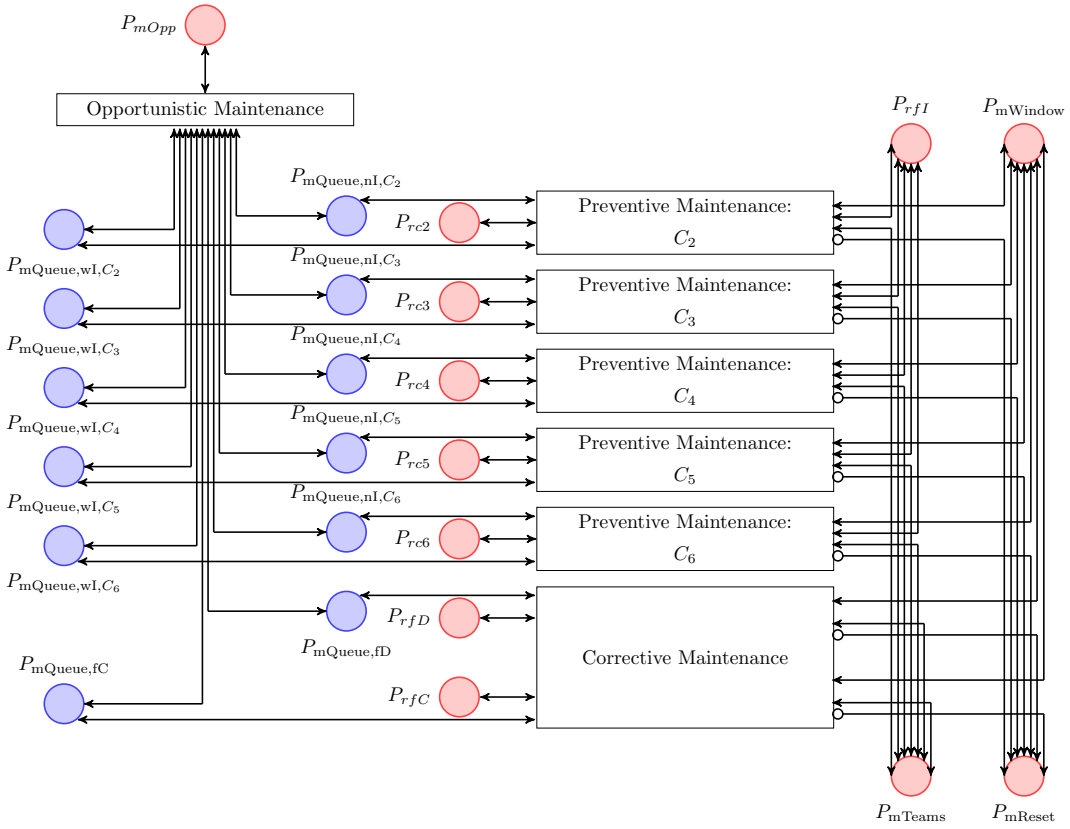

Figure 4.22: Component maintenance substitution transition.

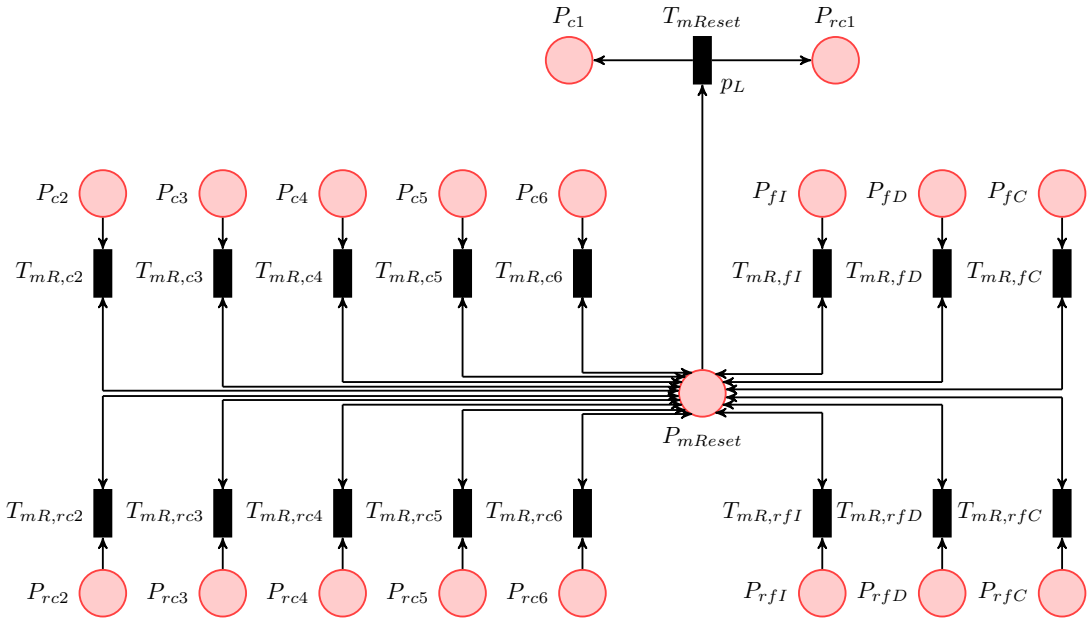

Figure 4.23: Reset substitution transition.

Transitions	Description
$T_{\text{mR},ci}$	Transitions to remove any tokens from condition state for $i \in \{2, n\}$ for n states
$T_{\text{mR,rc}i}$	Transitions to remove any tokens from revealed condition state for $i \in \{2, n\}$ for n states
T_{mReset}	Transitions to reset the condition 1 and revealed condition 1

Table 4.5: Description of transitions for the reset substitution transition given in Figure 4.23.

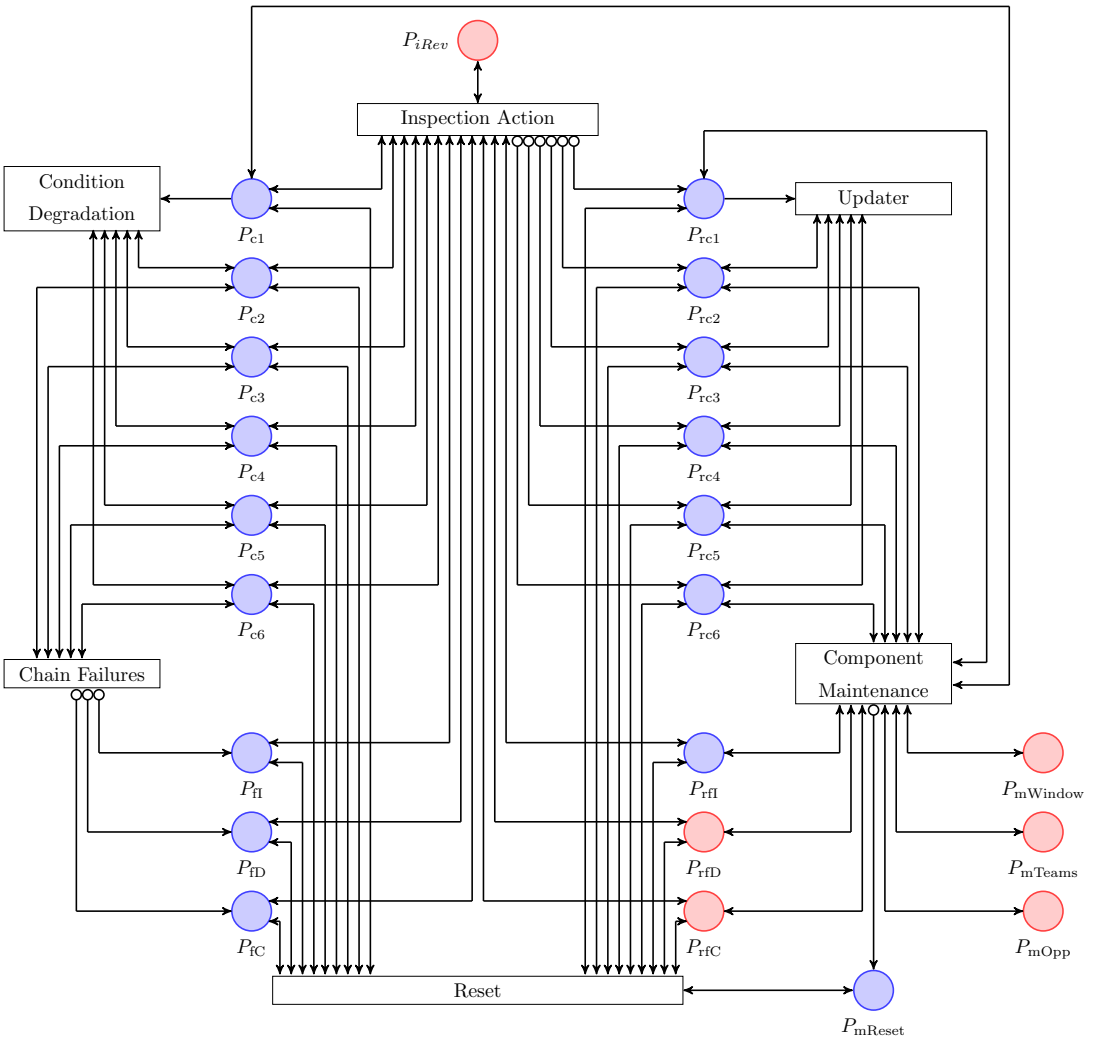

Figure 4.24: Observable substitution transition.

4.7.5 Observable Net

The net that connects together all of the elements of an observable's AM is shown in Figure 4.24, this is known as the observable substitution transition. This can be considered as the master net for all of the processes that the observable can go through including degradation, failure, inspection and maintenance. It is important to note that this net does not include an inspection clock substitution transition, only an inspection substitution transition, thus no inspections will be performed. The inspection clock is connected to P_{iRev} on a higher level in the asset substitution transition which will be discussed in the next section.

4.7.6 Asset Management Net

As this research considers multiple degradation chains and both internal and external inspections it is not sufficient to represent an asset with a single observable. An asset is considered to have multiple observables corresponding to each degradation mechanism. Therefore an asset substitution transition is constructed that is composed of several observable substitution transitions, in addition, to represent the inspection types it also contains an internal and external inspection clock.

Figure 4.25 gives the substitution transition for the AM of a separator, here it can be seen that four observables are modelled: *vessel wall thickness*, *structural wall thickness*, *deposit size* and *instrument failure*. The action of the internal and external inspections are represented by the transitions, $T_{i,i}$ and $T_{i,e}$ respectively. The arcs connecting these to the places associated with each observable ($P_{iRev,vwt}$, $P_{iRev,swt}$, $P_{iRev,if}$ and $P_{iRev,ds}$) define which inspections act on each observable. For instance, the external inspection can be seen to act on the *vessel wall thickness* and the *structural wall thickness*, while the internal inspection acts on the *vessel wall thickness* and *deposit size*. Note here that both inspections act on the *vessel wall thickness* and neither inspection acts on the *instrument failure*. The *instrument failure* is a revealed failure and thus will simply operate until failure with no inspections or preventive maintenance. These different elements are indirectly connected through inspections and maintenance. The inspections create a connection between the sets of observables they act on as they are inspected with the same interval. As maintenance is performed in specific windows there is a connection between all the observables defining when they can be maintained. Further, the finite number of teams imposes a shared restriction on all maintenance and inspection actions and therefore the observables.

For every asset in this model an asset substitution transition has been constructed, these are similar in architecture with their differences being defined by their observables and inspections. The asset substitution transitions for all of the assets are given in Appendix A.

4.8 Power System

A supply of power is required to support both the production system and the firewater deluge system, although these require different levels of supply, main power and emergency power respectively. The HSPN of the power system must determine the level of

Place	Description	Figures
P_{ci}	Condition state for $i \in \{1, n\}$ for n states	4.9, 4.11, 4.12, 4.14, 4.22, 4.23, 4.24
P_{rci}	Revealed condition state for $i \in \{1, n\}$ for n states	4.14, 4.15, 4.22, 4.23
P_{fI}, P_{fD}, P_{fC}	Incipient, degraded and critical failure mode	4.11, 4.12, 4.14, 4.23, 4.24
P_{rfI}, P_{rfD}, P_{rfC}	Incipient, degraded and critical revealed failure mode	4.11, 4.12, 4.14, 4.16, 4.20, 4.21, 4.22, 4.23, 4.24
P_{iTeams}, P_{mTeams}	Inspection and maintenance teams	4.13, 4.18, 4.20, 4.21, 4.22, 4.24
P_{iAct}	Inspection clock active	4.13
$P_{iClock1}$	Marked between inspections	4.13
$P_{iClock2}$	Marked while waiting for an inspection team	4.13
P_{iPrg}	Marked while performing the inspection	4.13
$P_{iCounter}$	Marking equals the number of inspections performed	4.13
P_{iRev}	Inspection of condition in progress	4.14, 4.24
$P_{mDecision}$	Encodes the maintenance decision, when marked maintenance can be performed from the condition state	4.16
P_{mQueue}	Queued for maintenance	4.16, 4.18
$P_{mWindow}$	Marked when maintenance window open	4.18, 4.19, 4.20, 4.21, 4.22, 4.24
P_{mWait}	Marked between maintenance windows	4.19
P_{mReset}	Resetting the observable's conditions and failure modes	4.18, 4.19, 4.20, 4.21, 4.22, 4.23, 4.24
P_{mOpp}	Encodes the opportunistic maintenance decision	4.17

Table 4.6: Description of places and the net figures they are present in.

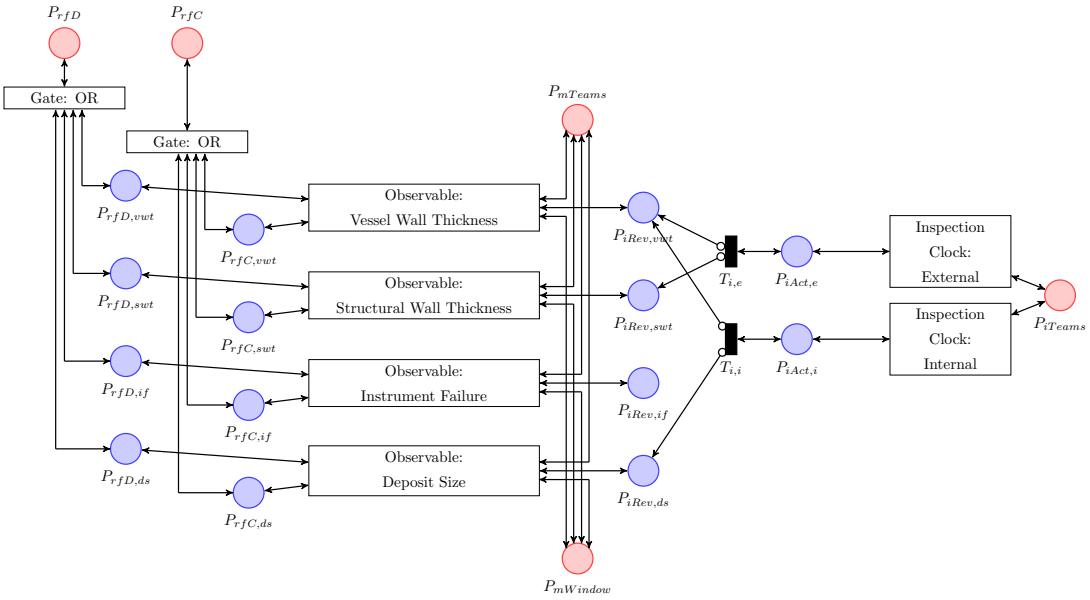

Figure 4.25: Asset net for a separator.

supply at all times throughout the simulation dependent on the current failure modes of the system's assets.

To determine the level of supply an unavailability tree of the power system was constructed, this was based on a fault tree of the system that was presented in Section 3.6. This was used to create an equivalent unavailability tree in the net using the logic gates detailed in Section 4.6, the unavailability tree is given in Figure 4.26. In this net there are two socket places $P_{\text{MainPower}}$ and $P_{\text{EmergencyPower}}$, when marked these represent that the relevant level of supply has failed. These socket places are present in the production and firewater deluge systems to determine their functionality. The details of this are discussed in their sections, Section 4.9 and Section 4.10.

At the base of the unavailability tree socket places for each asset can be seen, these are the socket places from the relevant asset substitution transitions. These follow the structure defined in Section 4.7, where the substitution transitions for each asset are given in Appendix Section A.3. A description of the socket places in the power system unavailability net are given in Table 4.7.

4.9 Production System

The design of the production system was discussed in Section 3.5, this system is arranged in a single train where the critical failure of any asset in the train will result

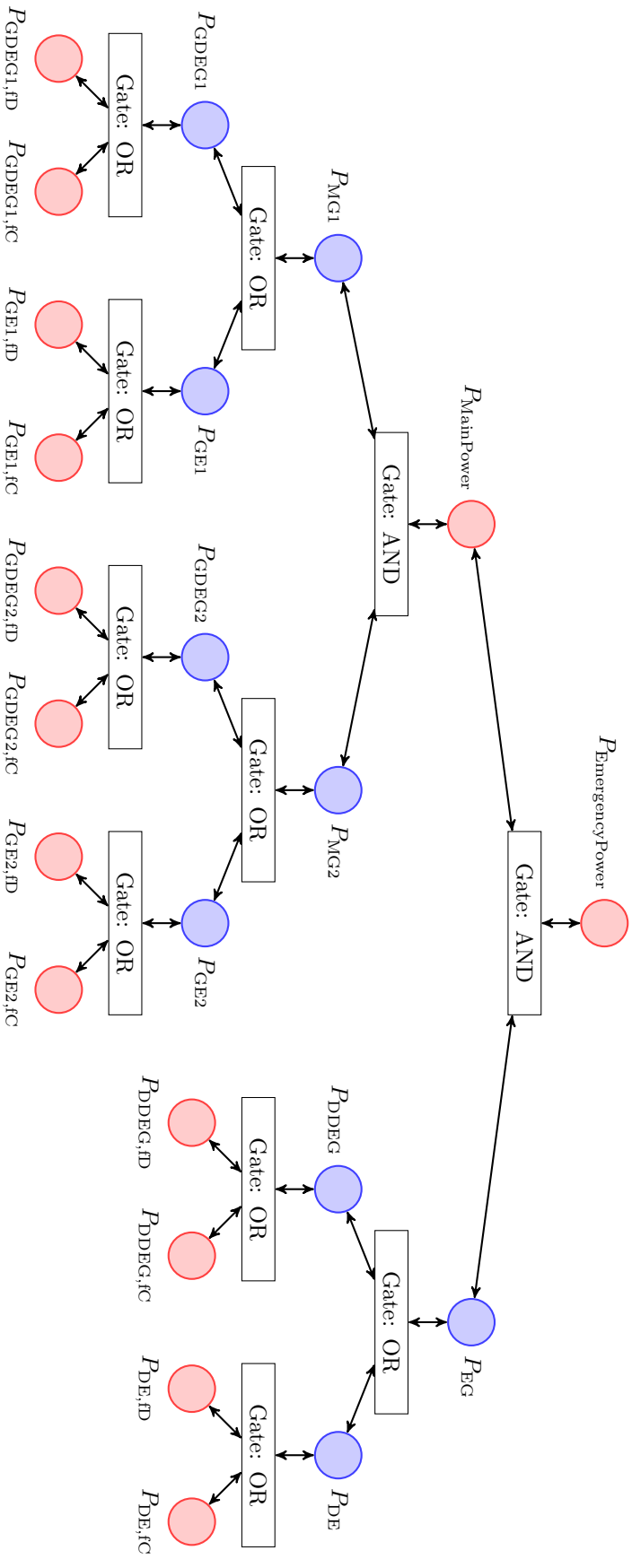

Figure 4.26: The power system unavailability tree.

Place	Description
$P_{\text{GDEG}i,\text{fD}}$	Gas driven electric generator degraded failure modes for $i \in [1, 2]$
$P_{\text{GDEG}i,\text{fC}}$	Gas driven electric generator critical failure modes for $i \in [1, 2]$
$P_{\text{GE}i,\text{fD}}$	Gas engine degraded failure modes for $i \in [1, 2]$
$P_{\text{GE}i,\text{fC}}$	Gas engine critical failure modes for $i \in [1, 2]$
$P_{\text{DDEG,fD}}$	Diesel driven electric generator degraded failure mode.
$P_{\text{DDEG,fC}}$	Diesel driven electric generator critical failure mode.
$P_{\text{MainPower}}$	Failure mode for the main power generation.
$P_{\text{MainPower}}$	Failure mode for the emergency power generation.

Table 4.7: Socket places in the power system unavailability tree. A marked place represents that the place's failure mode is present in the system.

in a loss of production. The availability of the production system is determined in the net throughout the simulation, this is achieved through an OR gate, as detailed in Section 4.6, with the base places being the failure modes the assets in the production system. There exist two of these OR gates, one for the degraded failure mode and one for the critical failure mode. This allows for the evaluation of the production availability in both a reduced functionality and a complete failure of functionality for the degraded and critical failure modes respectively. Within the net there exists an asset substitution transition for every instance of every asset, these simulate the conditions and failures of the asset subject to degradation and AM tasks.

So far it has been seen that the AM substitution transitions have been entirely discrete, the continuous part of the HSPN is used for the modelling of the production processes in simulating the flow of fluids. It is also here that the discrete and continuous parts of the net interact. The purpose of this part of the net is to simulate the flow of fluid's through the production train including the effect of any asset failure modes.

Figure 4.27 gives the production substitution transition for an asset, the flow is simulated through the decrease of marking from continuous place P_{in} and the simultaneous increase in marking at continuous place P_{out}. There are two continuous transitions that could fire dependent on the failure modes, assuming a constant supply of main power. Firstly T_{Full}, this represents the full operation of the asset and is enabled when the asset is neither degraded nor has a critical failure mode present as defined by the socket places P_{fD} and P_{fC}. When in full operation the rate of removal of tokens in

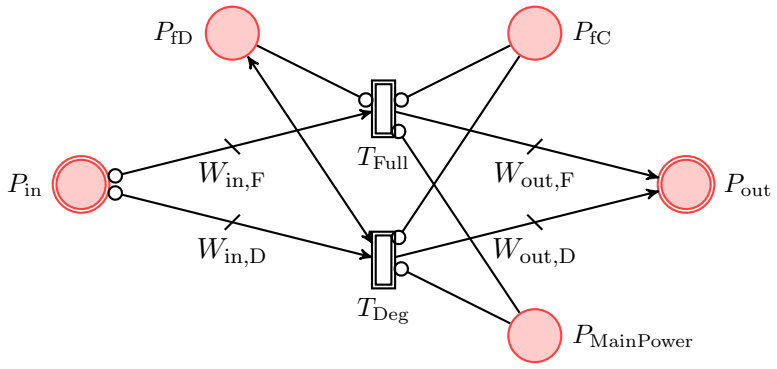

Figure 4.27: The production substitution transition for a generic asset.

P_{in} is determined by $W_{\text{in,F}}$ and the rate of deposit of tokens in P_{out} is determined by $W_{\text{out,F}}$. Secondly T_{Deg} represents the degraded operation of the asset, this is enabled when in the degraded failure mode only and is associated with a reduced production rate. This is implemented in the net by $W_{\text{in,D}}$ and $W_{\text{out,D}}$ which are constrained to be less than the equivalent full operation weights, that is to say $W_{\text{in,D}} < W_{\text{in,F}}$ and $W_{\text{out,D}} < W_{\text{out,C}}$. In this work it is assumed that in the degraded operation the production rate is halved such that $W_{\text{in,D}} = W_{\text{in,F}}/2$ and $W_{\text{out,D}} = W_{\text{out,F}}/2$. However, if a user wished to then they are free to set these weights to any values representing to the flow into and out of the asset. The unit of the weightings represent the mass flow rate into and out of the asset.

The production process is also dependent on a constant supply from the power system. The production assets require a supply of the main power to function. This requirement is implemented into the HSPN through the socket place $P_{\text{MainPower}}$ which inhibits both of the continuous transitions, T_{Deg} and T_{Full} when marked, and therefore stops the asset's production when the supply fails.

The failure of a production asset can lead to a leakage of hydrocarbons in certain situations. This is modelled by one of the asset's observable's failure modes causing a leak. For instance a separator's observable *vessel wall thickness* will cause a leak when the failure mode is reached. A full list of the observables that correspond to a leak failure mode was given in Table 3.3. In the HSPN the occurrence of these leak failure modes are represented by the marking of the observable's failure modes in the asset substitution transition, in this case these are $P_{\text{rfD,vwt}}$ and $P_{\text{rfC,vwt}}$ in Figure 4.25.

These production substitution transitions are chained together to form the production train on the platform. As the entire production chain is quite large the whole platform production net is not presented here, instead a small subset of the produc-

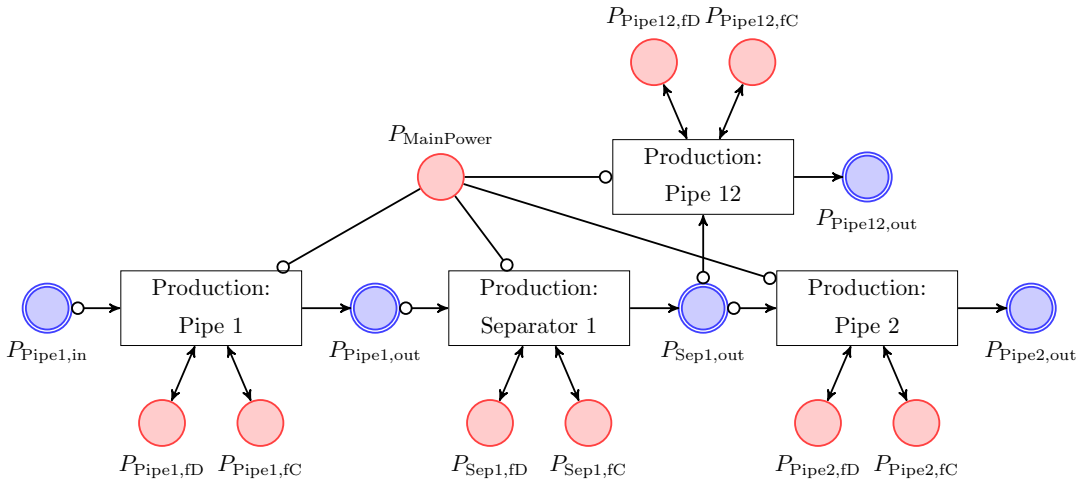

Figure 4.28: Production net for a section of the production train.

tion net is presented such that the concept of connecting the production substitution transitions can be understood. In Figure 4.28 a section of the production net can be seen that includes the assets *Pipe 1*, *Separator 1*, *Pipe 2* and *Pipe 12*. It can be noted that the outgoing continuous place of an asset's production substitution transition is the incoming continuous place of the next asset's production substitution transition. Further it can be seen that at a junction in the production net that multiple production nets share the previous production net's outgoing continuous place. This can be seen in *Pipe 2* and *Pipe 12* which share outgoing continuous place $P_{\text{Sep1,out}}$ as their incoming continuous place. In this case, the flow rate into each pipe is defined by the weights $W_{\text{in,F}}$ or $W_{\text{in,D}}$, dependent on the asset's failure mode, in each pipe's production net shown in Figure 4.27. A description of the socket places in Figure 4.28 are given in Table 4.8. The full production chain follows a similar design, it is given in a series of nets shown in Appendix A in Section A.4.

The rest of the platform production net is constructed following the same design principles. This net allows for the production process to be simulated taking account of the effects of failures and the AM strategy. The production system contains 45 assets with a total of 67 inspections, the optimisation of the AM strategy requires each of these to be optimised separately. Therefore the search space for inspection intervals is very large and effectively impossible to directly search all of the possible combinations, which is why an optimisation algorithm will be used. The optimisation is discussed in detail in Chapter 7.

Place	Description
P_{in}	Continuous place with marking representing the flow into the asset.
P_{fD}	Degraded failure mode for the asset.
P_{fC}	Critical failure mode for the asset.
P_{out}	Continuous place with marking representing the flow out of the asset.
$P_{\text{MainPower}}$	Failure mode for the main power generation.

Table 4.8: Socket places in the production substitution transitions in Figure 4.28. A marked place represents that the place's unavailability failure mode is present in the system.

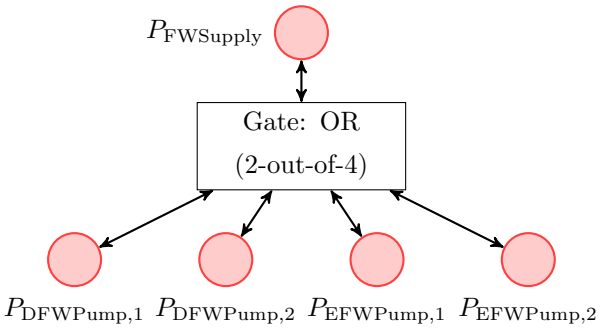

Figure 4.29: The firewater unavailability tree.

4.10 Firewater Deluge Systems

The firewater deluge system is designed to release large quantities of water into a module of the platform with an active leak. A leak may occur at any time in the platform's life-cycle and the firewater deluge system must be ready to respond and thus the system demands a high availability. The system is designed with a high degree of redundancy in it, thus it is resilient to the failure of many of its assets. In particular the firewater is supplied by four pumps in parallel although only two of the four pumps are required to be operational to provide a full supply. This relationship can be represented with an unavailability tree using a k-out-of-N gate, as given in Figure 4.29. The socket place P_{FWSupply} gives the current state of the firewater supply, such that when marked the supply has failed.

To determine the unavailability of the firewater supply the unavailability of the component firewater pumps must be evaluated, this is achieved through the construc-

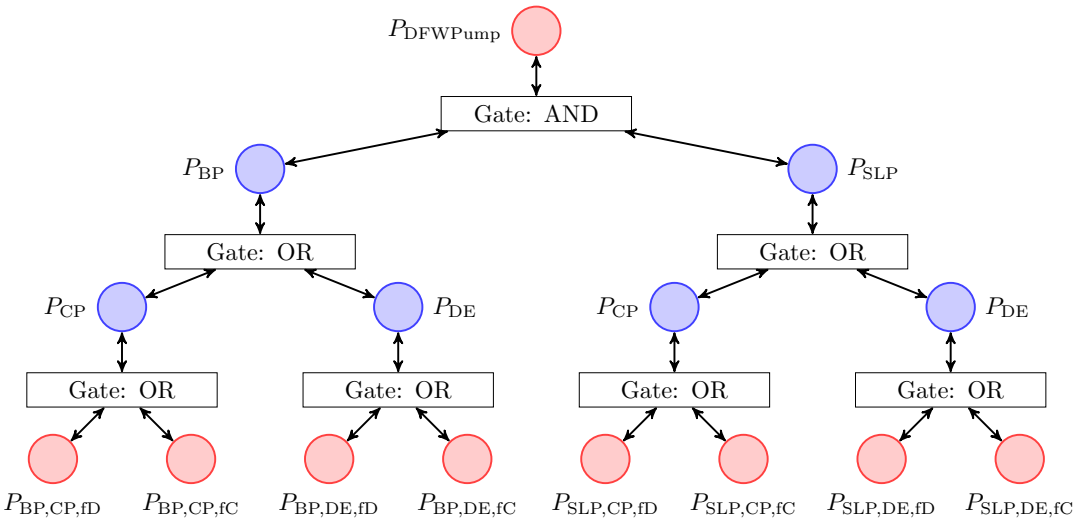

Figure 4.30: The unavailability tree of the diesel firewater pump.

tion of their own unavailability trees. There are four instances of firewater pumps of two types: two diesel firewater pumps and two electric firewater pumps. The unavailability trees of these are similar, although it is important to note that the two electric pumps are reliant on the emergency power. The unavailability trees of both are based on their fault trees that were discussed in Section 3.7.

The firewater pumps requires the operation of a booster pump and a seawater lift pump, which in turn both require a centrifugal pump and either a diesel or electric engine. Additionally an electric firewater pump requires a supply from the emergency power, this is given by the socket place $P_{\text{EmergencyPower}}$ from the power system. The unavailability trees constructed from these designs are given in Figure 4.30 and Figure 4.31 for the diesel and electric firewater pumps respectively. A description of the socket places in the firewater deluge system nets are given in Table 4.9.

So far only the firewater supply has been examined, this is capable of providing a sufficient firewater supply, although to be a successful safety system it must also be able to detect a hydrocarbon leak. This is achieved through the detection system, which was discussed in Subsection 3.7.1. In this system design there is a detection system for each module and a leak in a module will only be detected if the corresponding detection system is functional. The functioning of a module's detection system requires a minimum of 2 detectors to be operational and additionally requires a supply from the emergency power. From this design the fault tree and hence the unavailability tree of a module's detection system is constructed which is given in Figure 4.32.

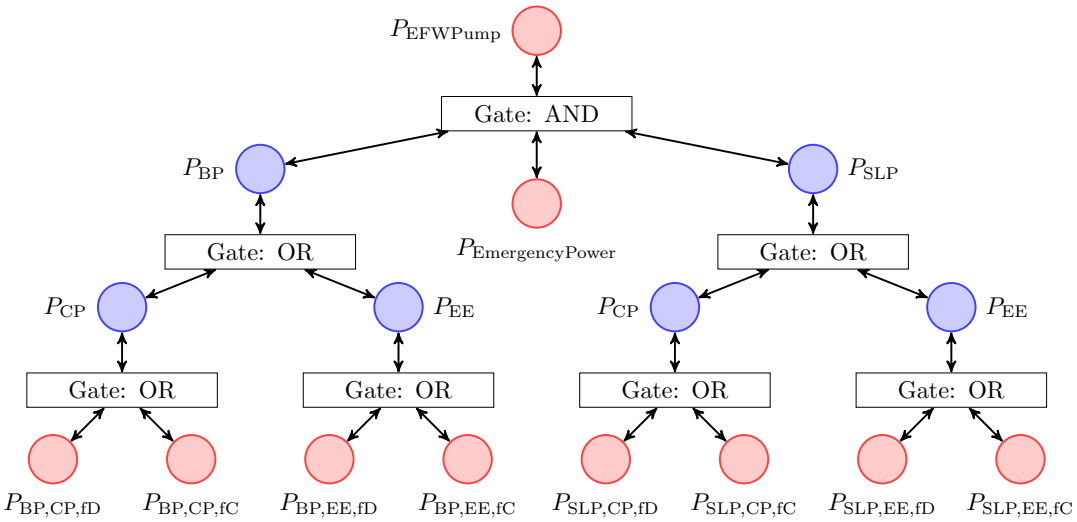

Figure 4.31: The The unavailability tree of the electric firewater pump.

Place	Description
P_{FWSupply}	Failure mode of the firewater supply.
$P_{\text{DFWPump},i}$	Failure mode of the diesel firewater pump for $i \in [1, 2]$.
$P_{\text{EFWPump},i}$	The failure mode of the electric firewater pump for $i \in [1, 2]$.
$P_{\text{BP,CP,fD}}$	The degraded failure mode of the centrifugal pump of the booster pump.
$P_{\text{BP,CP,fC}}$	The critical failure mode of the centrifugal pump of the booster pump.
$P_{\text{SLP,CP,fD}}$	The degraded failure mode of the centrifugal pump of the seawater lift pump.
$P_{\text{SLP,CP,fC}}$	The critical failure mode of the centrifugal pump of the seawater lift pump.
$P_{\text{EE,CP,fD}}$	The degraded failure mode of the centrifugal pump of the electrical engine.
$P_{\text{EE,CP,fC}}$	The critical failure mode of the centrifugal pump of the electrical engine.
$P_{\text{EmergencyPower}}$	The failure mode of the emergency power.

Table 4.9: Socket places in the firewater deluge system nets. A marked place represents that the place's unavailability failure mode is present in the system.

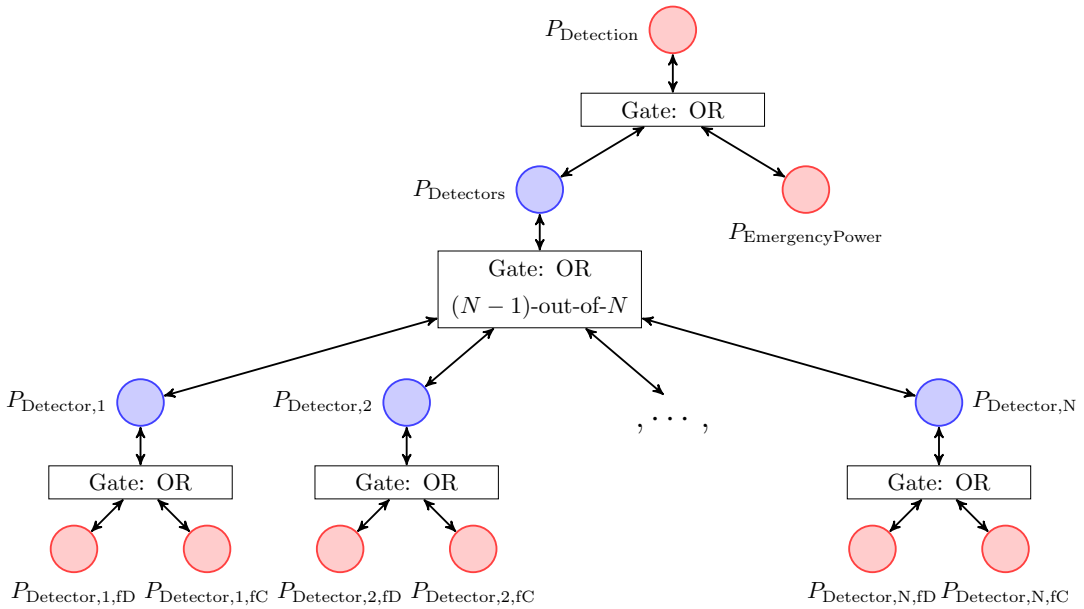

Figure 4.32: The detection unavailability tree for a module with N detectors.

To determine the availability of the firewater system in a particular module, the results of the unavailability trees of Figure 4.29 and Figure 4.32 must be combined with the state of the deluge valves. The corresponding fault tree was given in Figure 3.5. The top place, P_{ModuleFW}, is marked when the firewater deluge system is unavailable in that module. This is used as an input to the consequence analyses, this will be discussed in detail in Section 6.7. A description of the socket places in the detection and module deluge system net are given in Table 4.10.

The assets in the firewater deluge system are expected to operate on demand while at all other times they are in standby. When in standby the assets could have failed but the failure of the system will only be discovered on demand, as such the assets are considered to fail unrevealed so that their failures are only identified following an inspection.

The firewater deluge system's purpose is to reduce the probability of an explosion and to minimise the size of a fire following a leak. The HSPN model simulates the failures of the assets and through that the availability of the firewater supply and detection system. When a consequence analysis is triggered by a leakage failure mode the current availability of the firewater deluge system is passed to the consequence analysis. This allows the effects of the deluge to be included in the analysis.

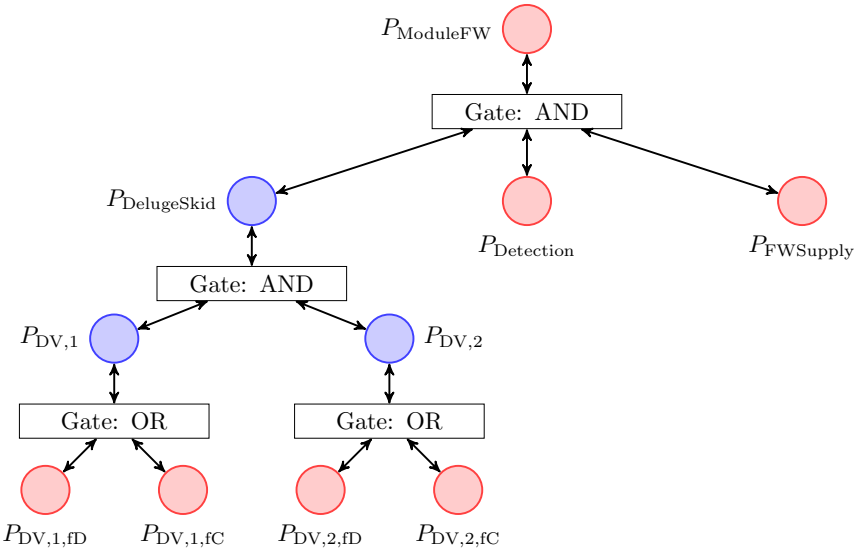

Figure 4.33: The module firewater deluge unavailability tree.

Place	Description
$P_{\text{Detection}}$	Failure mode of the detection system .
$P_{\text{EmergencyPower}}$	Failure mode of the emergency power system.
$P_{\text{Detector},i,\text{fD}}$	The degraded failure mode of detector $i \in [1, N]$.
$P_{\text{Detector},i,\text{fC}}$	The critical failure mode of detector $i \in [1, N]$.
$P_{\text{DV},i,\text{fD}}$	The degraded failure mode of deluge valve $i \in [1, 2]$.
$P_{\text{DV},i,\text{fC}}$	The critical failure mode of deluge valve $i \in [1, 2]$.
P_{ModuleFW}	The unavailability of the module's firewater deluge system.

Table 4.10: Socket places in the detection unavailability net and the module firewater deluge system unavailability net. A marked place represents that the place's unavailability failure mode is present in the system.

4.11 System Interdependencies

As discussed in Chapter 3, the systems are not modelled independently but are linked. Failures in a system can effect the performance of another system. For example, the electric firewater pumps are reliant on the emergency power generation, if the emergency power generation was to fail then so would the electric firewater pumps. In Figure 4.34 all of the interdependencies between the systems modelled in this thesis are displayed.

Central to the interdependencies is AM, this is as the state of each system depends on the failure modes of its components which is modelled by the AM. The HSPN described in this chapter allows for all of these systems to be modelled together in a single coherent model, with the interdependencies being represented through socket places.

The interdependencies between the systems are detailed as follows,

- **Main power supply**: The main power supply is dependent only on the AM of its assets.
- **Production**: The production is dependent on the AM of the production assets and the supply of mains power.
- **Emergency power supply**: When the main power supply is working the emergency power is also supplied but when this fails it relies on the AM of the emergency generation assets.
- **Firewater pump (Diesel)**: The diesel firewater pump is only dependent on the AM of its assets.
- **Firewater pump (Electric)**: The electric firewater pump is dependent on both the AM of its assets and an electricity supply from the emergency power.
- **Firewater supply**: The firewater supply is dependent only on the two firewater pumps.
- **Compression/Separation module detection**: The detection systems in each model are dependent on the AM of their assets and an electricity supply from the emergency power system.
- **Compression/Separation module firewater deluge**: The modules' deluge is dependent on the AM of their assets, the firewater supply and their module's detection system.

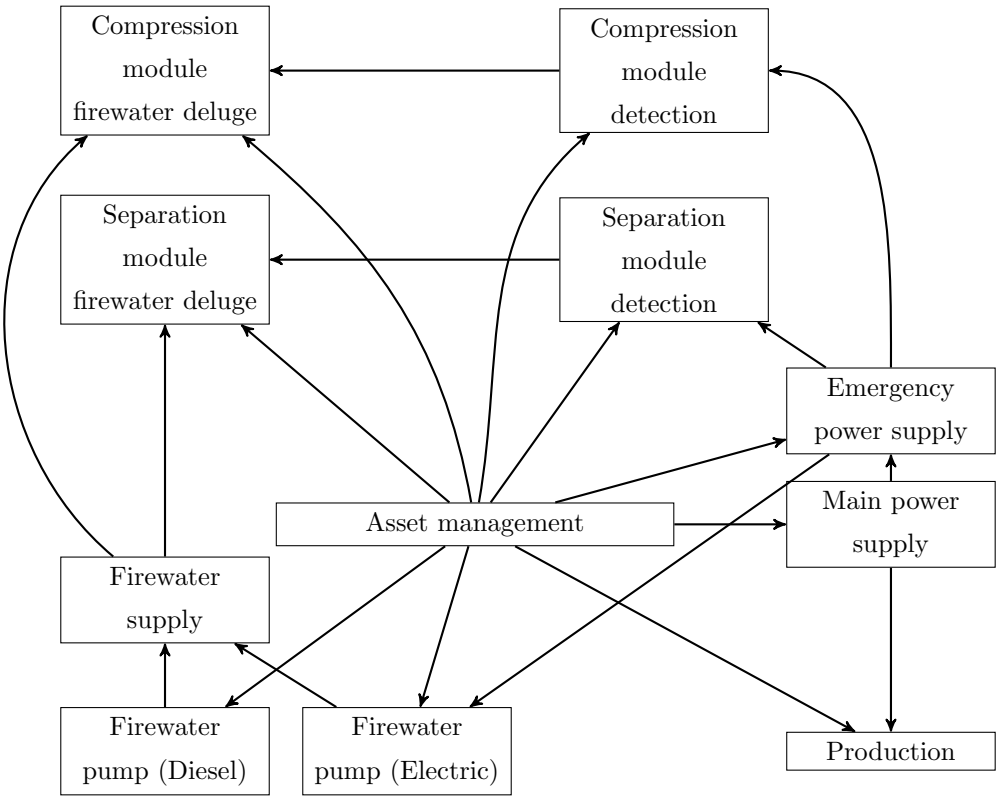

Figure 4.34: A diagram of the interdependencies between the modelled systems.

4.12 Summary and Discussion

Through the union of a discrete stochastic PN and a continuous PN a HSPN formulation was presented. This is capable of modelling instantaneous, constant, stochastically sampled and continuous transitions, which paves the way for the construction of a detailed model. In this chapter a detailed description of the HSPN model of an offshore oil and gas platform was presented.

In total there were 24803 nodes of which 16583 were transition and the remaining 8220 were places. To aid in constructing and understanding the model, the concept of substitution transitions was introduced, these allowed for parts of the net to be hidden inside transitions without changing the behaviour of the net. Through this a detailed and hierarchical HSPN was constructed for the modelling of an offshore oil and gas platform.

This model has a wide scope, it covers three interconnected systems on an offshore oil and gas platform: the power system, the production system and the firewater deluge system. These systems are composed of sets of assets which have their degradation

and AM processes modelled by the HSPN.

The continuous part of the HSPN is applied to the production process of the platform, by continually adding and removing markings from places a fluid flow can be simulated. This flow represents the quantity of fluid flowing in and out of an asset, at the end of the flows the markings accumulated throughout the platform's life represent the total production of oil and gas.

In the following chapter, simulations of the HSPN are performed for a selection of AM strategies. The results of the simulations are analysed to compare strategies through several different metrics.

Chapter 5

Asset Management Analysis

5.1 Introduction

The HSPN presented in the previous chapter is capable of simulating the life-cycle of a platform where an AM strategy can be defined in the net's initial conditions. Through the simulation of the HSPN a variety of results can be found to evaluate the performance of each strategy. In this chapter AM strategies will be compared through the results of HSPN simulations.

To perform simulations of the net and to gather results it is necessary to use a computational model, for this work software was developed to simulate a HSPN. Section 5.2 gives an overview of the software, which is seen to be written to be highly performant such that it can perform many simulations in a reasonable time-frame.

This results section will examine the outputs that are produced through simulations of the Petri net and demonstrate how these can be used to compare AM strategies. The effects of varying the inspection intervals and maintenance decisions on the probability of being in a condition with respect to the platform age will be seen. Between inspections degradation can take place, the time between a condition degrading and an inspection revealing it is known as it's exposure, the relationship between the exposure and the inspection interval will be examined. In addition, the effect of the number of inspection and maintenance teams on the size of the maintenance backlog will be examined. The production quantities are defined by the continuous part of the net but are linked to the discrete AM net, the relationship between inspection intervals and the production quantities is investigated.

5.2 Software Overview

To be able to produce results from the HSPN model, software was written to simulate the net following the mathematical definition given in Subsection 4.4.1. There were several advantages to creating custom software for this research, these included:

- There was no restriction imposed by the software on the mathematical definition chosen for the net.
- The software could be optimised for both the mathematical definition and the specific system model used in this thesis.
- The software could be written to directly integrate with other elements, such as the consequence analysis and genetic algorithm, which will be discussed in detail in Chapter 6 and Chapter 7 respectively.
- Custom data structures could be implemented that allowed a wide range of results to be collected efficiently.

The system is represented by 24,803 with 16,583 transitions, thus to ensure that the computation was timely it was imperative that the software would have a high performance and could rapidly simulate platform lifecycles. To achieve the desired performance the programming language C++ was chosen due to it's high code execution speed and additionally, as an object-orientated language, it is excellent for representing the objects of the HSPN, such as places, transitions, arcs and tokens. An overview of the software's main structure is given in the following connected flowcharts. Figure 5.1 and Figure 5.2 define the logic for determining which transitions need firing in the discrete and continuous net respectively and Figure 5.3 defines how a lifecycle simulation is implemented.

The simulation of the HSPN is performed through a series of steps with unequal timesteps until the simulation time is elapsed. The duration of each timestep is defined by either the time at which the next discrete transition is due to fire or the time at which the next continuous transition will become either enabled or disabled. Looking first at the discrete part of the net, Figure 5.1 breaks down the steps taken to update the firing list, $\mathbf{F}$, which defines the discrete transitions that are queued to fire and the time they are due to fire at. The flowchart takes as an input $\mathbf{T}_D$, which is a set of discrete transitions to be checked. It will be seen that these are transitions which have income arcs from places whose markings have changed in the last step. The logic is to check if each transition, $T \in \mathbf{T}_D$, if T is enabled and not in F then it's firing time will be sampled and added to $\mathbf{F}$, or if T is not enabled and in $\mathbf{F}$ then it will be removed

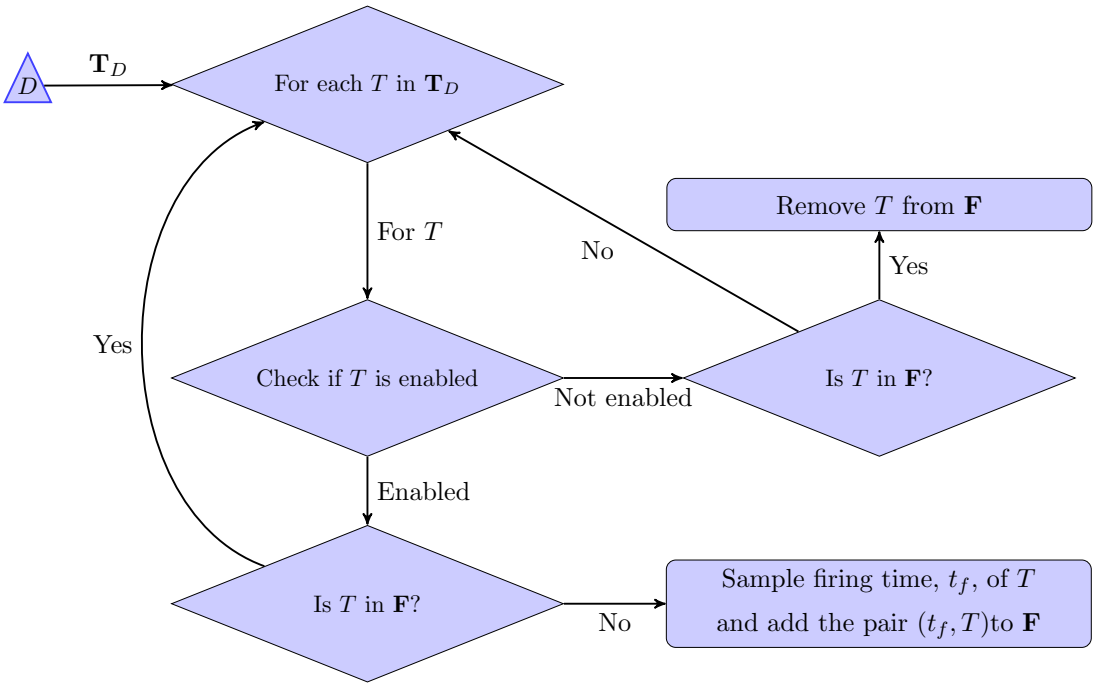

Figure 5.1: An overview flow chart for the structure of discrete logic for the HSPN.

from $\mathbf{F}$, otherwise no change will be made. Thereby, the firing list will be updated with respect to the changes relating to $\mathbf{T}_D$.

The continuous part of the net was also simulated to use uneven timesteps as opposed to small iterative steps, so as to produce a performant simulation. To achieve this, logic was implemented to calculate the soonest time in which a continuous transition would switch from enabled to disabled or the reverse. In Figure 5.2 the logic for determining this time and the corresponding transition is given, this takes an input of a set of continuous transitions, $\mathbf{T}_C$. Briefly, the logic is to find the set of all places outgoing, $\mathbf{P}_{\text{out}}$ from every transition, $T \in \mathbf{T}_C$. Next the rate of change of marking for each P due to the transitions $\mathbf{T}_C$ is calculated. The set of transitions out, $\mathbf{T}_{\text{out}}(P)$ from P is then checked to determine the time, t, at which the transition will switch from enabled to disabled or the reverse. These times are then collected for all $\mathbf{T}_{\text{out}}(P)$ for all P, the smallest of these times and the corresponding transitions are then set at (t_C, T_C). The time represent the earliest time in which a continuous transition will switch between enabled and disabled and therefore, is the latest time which a timestep can be taken over.

The overall logic to perform a simulation of the HSPN is given in Figure 5.3. Here it can be seen that first the initial conditions are set, that is to load the net design and to set the initial markings. Next, the discrete logic is performed with all discrete

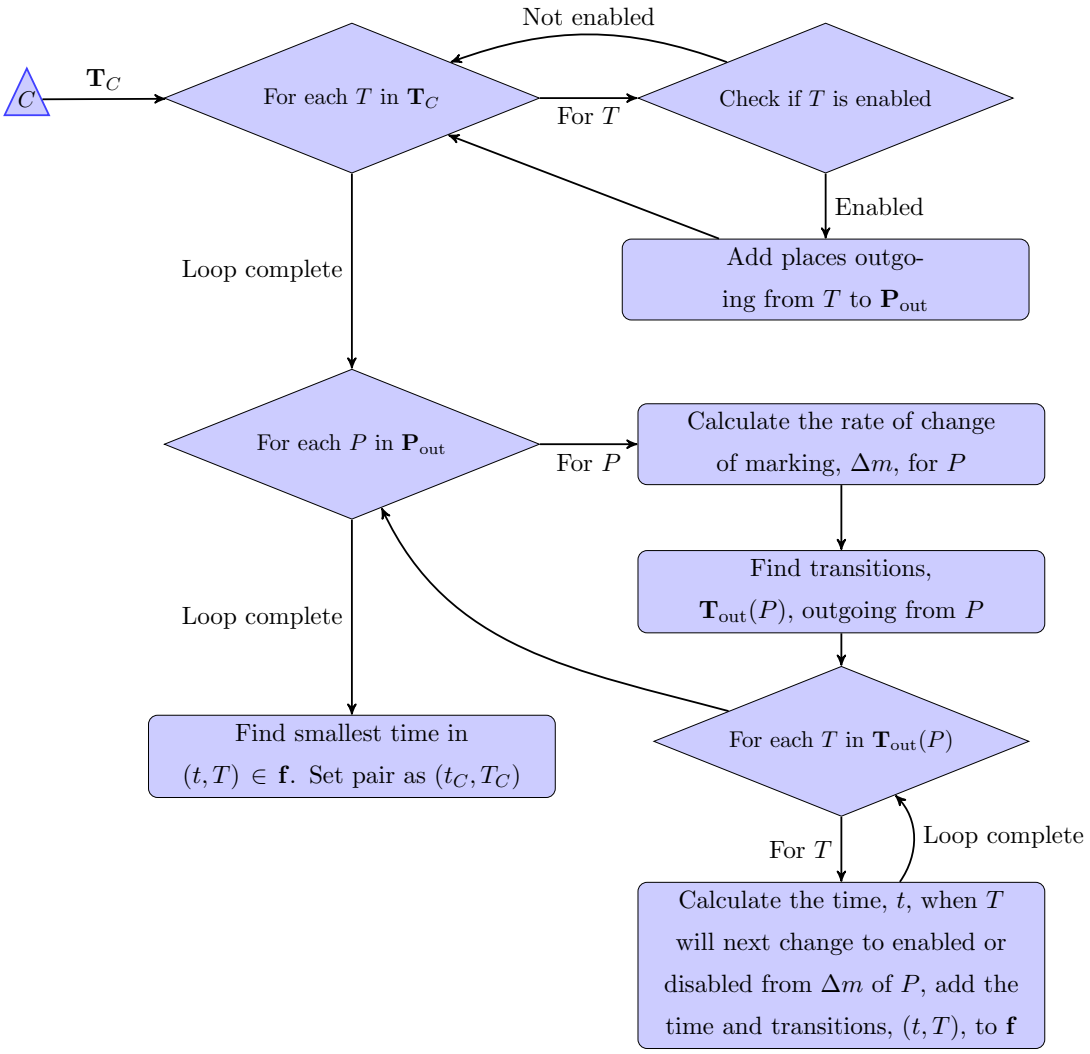

Figure 5.2: An overview flow chart for the structure of continuous logic for the HSPN.

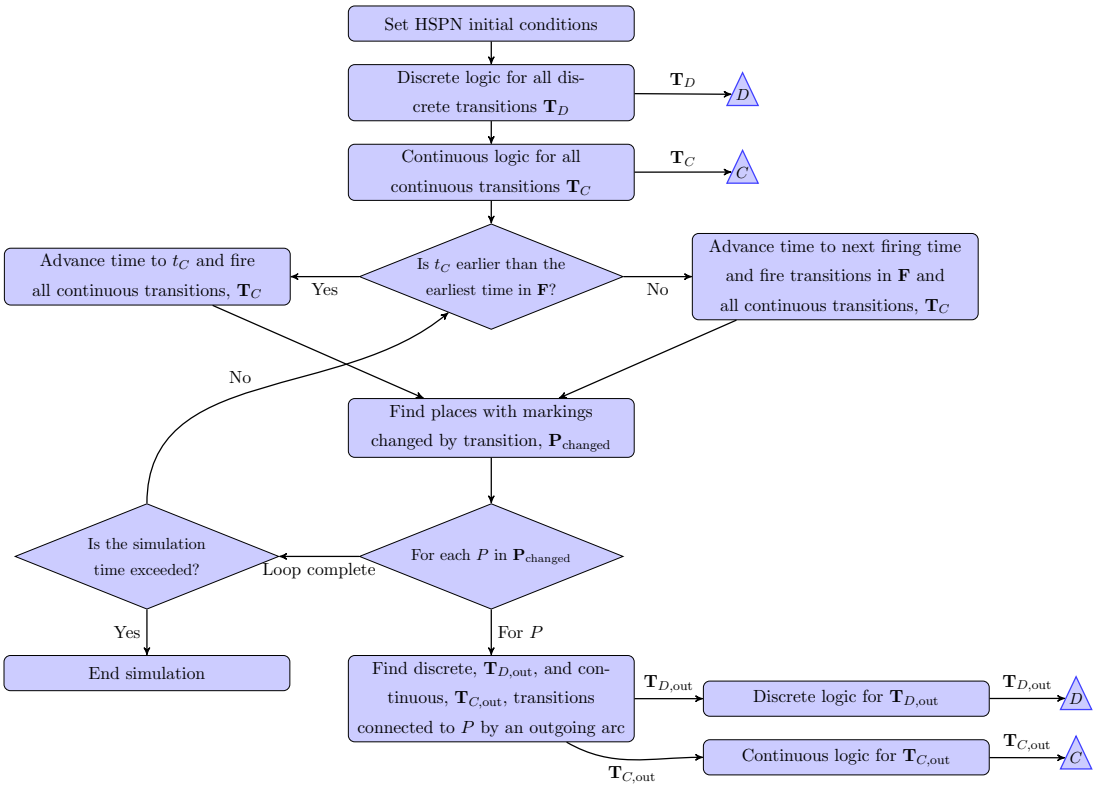

Figure 5.3: An overview flow chart for the structure of the HSPN code.

transitions as input through Figure 5.1 to form a firing list, $\mathbf{F}$. This is followed by the continuous logic, which is performed for all continuous transitions through Figure 5.2 to find (t_c, T_C). After this, the main simulation loop is entered, at each the time is advanced either to t_C or the earliest time in $\mathbf{F}$, whichever is earlier. If the time from $\mathbf{F}$ is earlier, then the corresponding discrete transition is fired. In both cases all of the continuous transitions are fired such that their outgoing places are changed dependent on the arc weights and the time passed. Following this, the set of places whose markings have changed are collected and the discrete and continuous logics are performed on the outgoing transitions from each of those places. Crucially, the transitions checked in each step are only a small subset of all the transitions in the net, by only checking these the simulation time is greatly improved. This loop is then continued until the simulation time is exceeded.

To further improve the performance of the code, other optimisations were implemented. When performing a MC simulation, the HSPN is repeatedly simulated with the same initial conditions, thus the transitions that are initially enabled will be unchanged. Therefore, the set of initially enabled transitions is only calculated on the first HSPN simulation and cached, such that the following can use this set instead

of rechecking the transitions. Another improvement was made by determining and caching the transitions which would need to be checked after a transitions is fired, as opposed to finding the transitions required after each firing. The development of this software allowed for performant simulations, which meant that results could be obtained for a variety of AM strategies and, in addition, provided a platform that will be used to integrate with other model elements, such as the consequence analysis and the optimisation.

5.3 Asset Management Strategy

Throughout the simulation period the degradation of an observable is simulated by the stepping through of the observable's discrete conditions. This degradation process is countered by AM tasks that aim to decrease the failure rate of the observable by increasing the time spent in the less degraded conditions. The decisions behind the performance of maintenance and inspections are defined by the AM strategy which sets the intervals of periodic inspections and from which revealed states' maintenance is queued. The decisions of the AM strategy will ultimately determine the probability of the observable being in a given state at a given time.

In this section the effects of varying the AM strategy will be investigated. Initially these analyses will examine the pipe asset, this is selected as it has only one observable and one inspection. By first examining this simple asset the effects of varying the AM strategy can be clearly understood, this provides a good basis for understanding the effects on more complex assets and systems.

The model requires a number of inputs, these are given in full in Appendix B. The AM strategy parameters are defined for the whole system, here only the parameters relevant to the pipe are used. The inputs required to simulate this model of a pipe are:

- Distribution parameters for the degradation parameters $T_{\mathrm{d}i}$ for $i \in [1, 5]$ in Figure 4.9. Defined in Table B.21.
- Distribution parameters for failure transitions: T_{fI}, $T_{\mathrm{fD,wI}}$, $T_{\mathrm{fD,nI}}$, $T_{\mathrm{fC,wI}}$ and $T_{\mathrm{fD,nI}}$ in Figure 4.11. Defined in Table B.62.
- Constant delays on $T_{\mathrm{mDuration}}$ in Figure 4.20 and Figure 4.21 defining the preventive and corrective maintenance durations respectively. Defined in Table B.91.
- Constant delay on the inspection clock, T_{iClock1} and T_{iClock2} in Figure 4.13 defin-

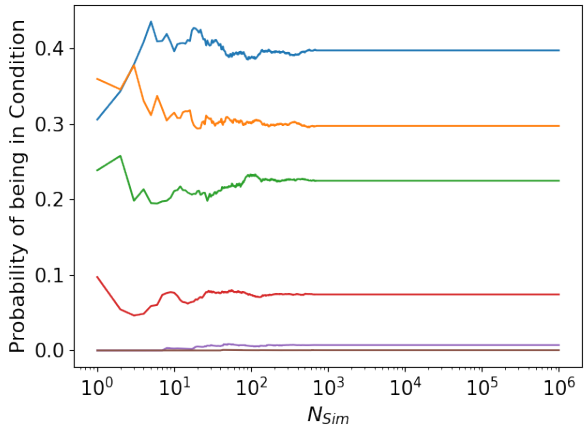

Figure 5.4: Convergence test showing the average probability of being in each condition for an inspection interval of 5 years and maintenance performed for C_3 and the more degraded conditions for a simulation period of 50 years. C_1, C_2, C_3, C_4, C_5, C_6.

ing the inspection duration and interval respectively. Defined in Table B.91.

- The number of maintenance teams, this defines the initial marking of P_{mTeams} in Figure 4.18. Defined in Table B.95
- The number of inspection teams, this defines the initial marking of P_{iTeams} in Figure 4.13. Defined in Table B.95

The probability of being in each condition as a function of the simulation time is given for a selection of example AM strategies in Figure 5.5. This is a set of three AM strategies, denoted A, B and C which will be used through this thesis as example strategies. Broadly, strategy A can be thought of as a reasonable strategy to benchmark the model. Strategy B is a more proactive strategy with shorter inspection intervals and preventative maintenance from less degraded conditions. Strategy C is a less proactive strategy which has longer inspection intervals and preventative maintenance is performed from more degraded conditions. The strategies parameters are detailed in full in Appendix B, in Section B.4.

The results in Figure 5.5 were obtained using a MC method of $N_{\text{Sim}} = 10^6$ simulations and calculating the proportion of simulations in each condition as a function of the simulation time. To ensure that this is a sufficient number of simulations a convergence test was performed. In Figure 5.4 the results of this test can be seen. This shows how the average probability of being in each condition converges as N_{Sim} increases, with converged results at 10^6.

It can be noted that across all the AM strategies there is a continual increase in the probability of being in more degraded conditions and a corresponding decreased probability for the less degraded conditions. This demonstrates the effect of ageing, with the asset's expected condition becoming more degraded across the platform's life-cycle.

Comparing the results of the strategies, it can be noted that the probability of being in more degraded conditions is greater for the less proactive strategy C, with the reverse being true for B. This is due to two effects, firstly an earlier maintenance decision will result in the condition being renewed to *Good as new* more often, as can be seen in B. Secondly, more frequent inspections will increase the knowledge of the actual condition of the asset. As the maintenance is only performed on the revealed condition, both the inspection interval and maintenance decision must be well selected for an effective improvement in the condition.

From these results, it appears that AM strategy B is the best, however, this analysis does not account for the expenditure of the increased inspections and maintenance. This will be examined later in this thesis in the optimisation in Chapter 7.

It is clearly evident that modification of the AM strategy has a large effect on the time spent in the conditions and states of an observable. When considering many assets, each with multiple observables and inspections, the search space of inspection intervals and maintenance decisions becomes very large. Thus a direct analysis of all possible strategies is effectively impossible.

At the beginning of the simulation period the observable is in C_1, as the simulation progresses the probability of being in the more degraded conditions increases. Therefore when entering the LE stage at 25 years the condition of the observable is likely to be in a degraded condition. This reflects how a real-world pipe would begin its LE stage with its assets in degraded conditions.

5.3.1 Periodic Inspections

In Figure 5.6 the effect of varying the inspection intervals on the mean time in each condition can be seen. This is shown for the actual conditions and the revealed conditions in Figure 5.6a and Figure 5.6b respectively. In this example maintenance is performed whenever the condition is inspected and found to be in C_3 or worse, such that C_1 and C_2 are known as the unmaintained conditions and C_3, C_4, C_5 and C_6 are known as the maintained conditions. These figures demonstrate how a decrease in

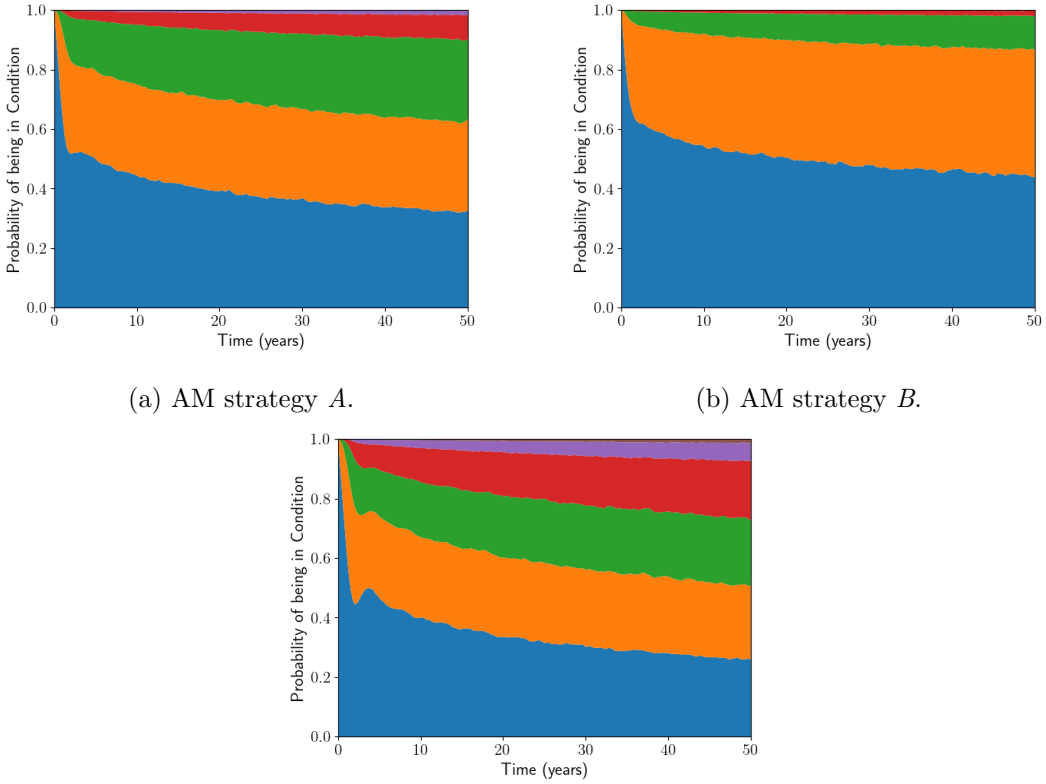

(a) AM strategy A.

(b) AM strategy B.

(c) AM strategy C.

Figure 5.5: The probability of being in each condition through a simulation period of 50 years for various AM strategies. For the observable *Wall Thickness* of *Pipe 1*. C_1, C_2, C_3, C_4, C_5, C_6.

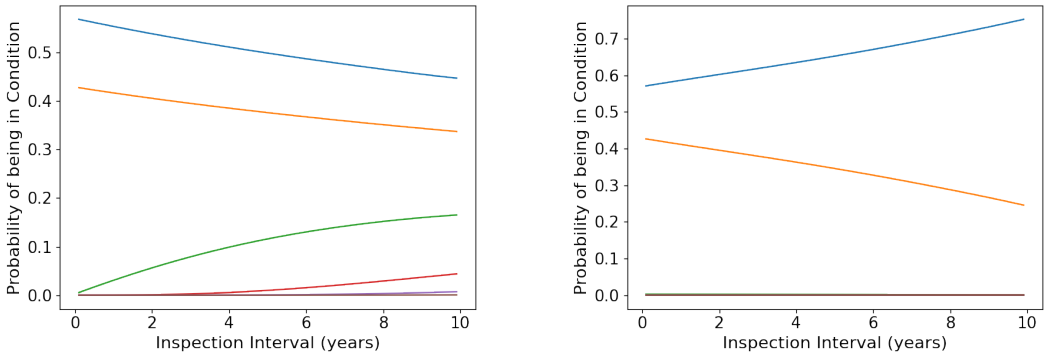

(a) Actual condition states.

(b) Revealed condition states.

Figure 5.6: The probability of being in each condition for different inspection interval. C_1, C_2, C_3, C_4, C_5, C_6.

the inspection interval increases the amount of time spent in the unmaintained actual conditions while decreasing the time spent in the maintained actual conditions. In addition it can be seen that as the inspection interval is decreased the time spent in the revealed conditions converge to the time spent in the actual conditions, demonstrating the improved knowledge of condition as more inspections are performed. Additionally the maintained revealed states can be noted to have near-zero times, this is as the time spent in these states is only the time between them being entered and maintenance being performed.

The effects of the varying inspection interval on the probability of being in each state can also be found, these are given in Figure 5.7. These are split into four figures by actual and revealed states and by whether an incipient failure mode is present or not. Examining first the actual states in Figure 5.7a and Figure 5.7b, it can be noted that a reduction in the inspection interval can be seen to correspond to a decrease in probability of being in the state for the maintained states and an increase in probability for the unmaintained states. This is caused by more frequent inspections decreasing the delay before maintenance is queued for the maintained states which results in more maintenance and therefore an increase in the probability of being in the unmaintained states. Secondly, examining the revealed states in Figure 5.7d and Figure 5.7c, it can be seen that only the unmaintained states have significant amounts of probability of being in the states, this is as the maintained states' probabilities are only the duration before maintenance is performed. Additionally, it can be noted that the probability of being in the state is much greater without an incipient mode, this is as the probability of failing to an incipient mode from the first few states is very low. The absolute difference

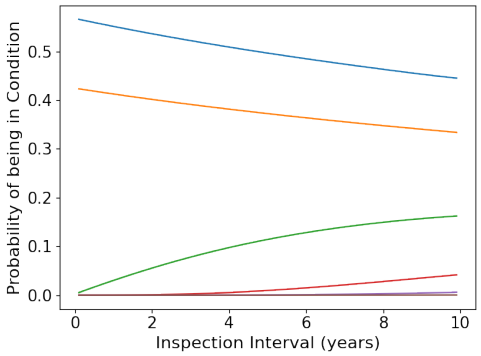

(a) Actual state without an incipient failure mode present.

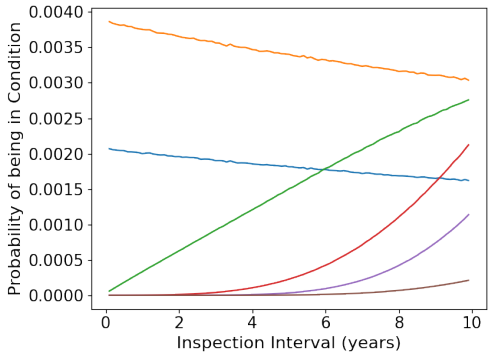

(b) Actual state with an incipient failure mode present.

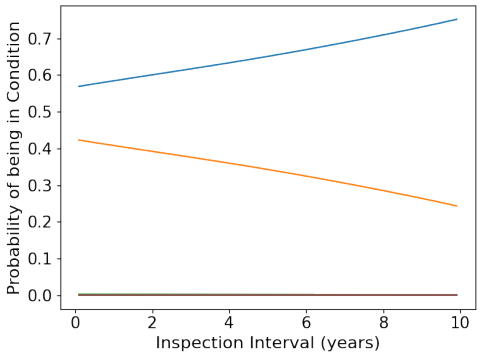

(c) Revealed state without an incipient failure mode present.

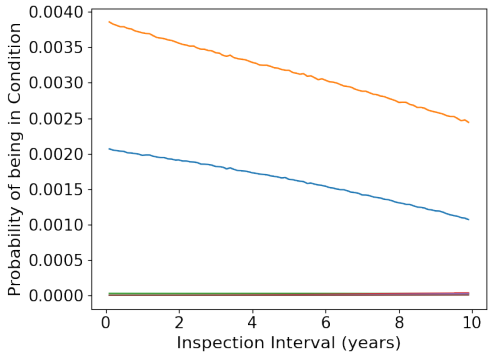

(d) Revealed state with an incipient failure mode present.

Figure 5.7: The probability of being in each state for different inspection interval where maintenance is performed for states $S_i \; \forall \; i \geq 3$. S_1, S_2, S_3, S_4, S_5, S_6.

between the time in each in revealed state and the time in the corresponding actual state decreases with more frequent inspections reflecting the increased knowledge of the state of the pipe. This difference is known as the exposure and is discussed in the following section.

5.3.2 Exposure

The exposure time is the duration between a state being entered and an inspection revealing that state. This indicates the delay in the knowledge of an observable's state and a good AM strategy will produce small exposure times. Figure 5.8 gives a representation of a state degradation and inspection timeline that gives the exposure time. An actual state S_i is entered at time $t_{S,i}$, which then later degrades into the next

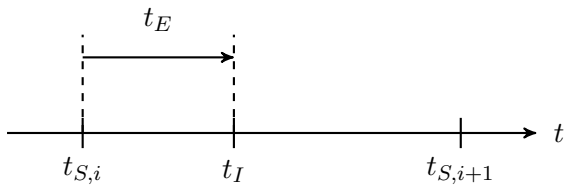

Figure 5.8: Timeline demonstrating the exposure time of a state.

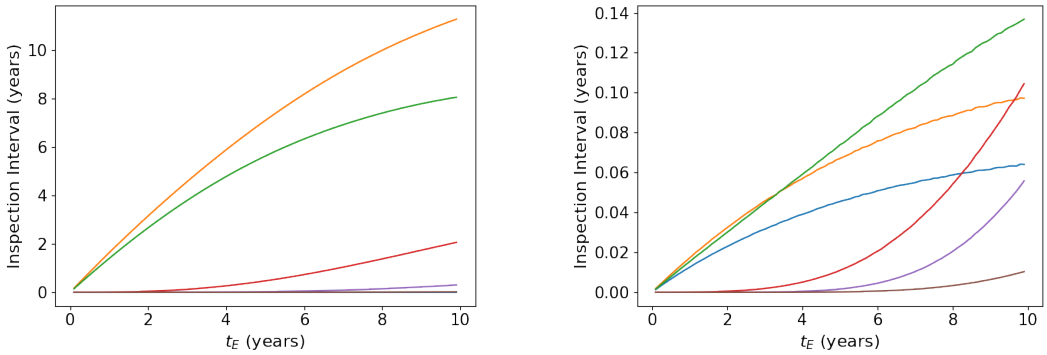

(a) Exposure without an incipient failure mode present.

(b) Exposure with an incipient failure mode present.

Figure 5.9: Total time of exposure for each state for varying inspection intervals. S_1, S_2, S_3, S_4, S_5, S_6.

state, S_{i+1}, at time $t_{S,i+1}$. Suppose that in between these times an inspection takes place at t_I then the exposure time is given by $t_E = t_I - t_{S,i}$.

The relationship between the inspection interval and the total exposure times for each state is given in Figure 5.9. The effect of changing the inspection interval is clear here, reducing the exposure times for all states as the interval decreases. This represents the increase in knowledge of the system's current state. For an effective AM strategy it is important to minimise the exposure time as maintenance decisions should be based on the current state of the observable. A strategy that results in high exposure times corresponds to an increased probability that the observable's revealed state is not the same as the actual state. As failure rates increase from the more degraded states, a longer exposure corresponds to a higher risk of failure.

5.3.3 Failure Rates from States

The failure of an asset can result in its unavailability and possibly the unavailability of a system it is part of. Some failure modes of pressurised vessels can result in a risk

of fire and explosion, which will be covered in Chapter 6. Therefore, it is important to understand the failure rate of assets. The failure rate from a state gives the mean number of failures per unit time, in this case a failure is counted as a degraded or critical failure mode since an incipient failure does not affect an asset's functionality. Two failure rates can be defined for each state with respect to the simulation time, λ_{sim}, and the time in the state, λ_{state}. These are such that λ_{sim} represents the failure rate from a state across the entire simulation, where λ_{state} gives the failure rate while in that state. For a simulation with N_F failures from the state, these are given by,

$$\lambda_{sim} = \frac{N_F}{t_{sim}}, \tag{5.1}$$

$$\lambda_{state} = \frac{N_F}{t_{state}}, \tag{5.2}$$

where t_{sim} is the duration of the simulation and t_{state} is the time spent in the state, such that $t_{state} \leq t_{sim}$ and therefore $\lambda_{sim} \geq \lambda_{state}$.

The condition failure substitution transition was presented in Figure 4.11 and was designed to implement the OREDA definition of an incipient failure mode to increase the failure rates to the degraded and critical failure modes when an incipient failure mode was present. By comparing Figure 5.10a and Figure 5.10b this behaviour can be seen where the failure rates from states with an incipient failure mode present are greater than the states without. In this example maintenance is set to be performed for S_3 and more degraded states. The failure rates decrease for these states as the inspection interval decreases, the cause of this is in the shape of the Weibull distribution. This is such that the probability of failure is not constant but increases with time spent in the state, therefore shorter times spent in the state correlate with a decreased failure rate. The unmaintained states S_1 and S_2 have a small increase in λ_{state} as the inspection interval decreases, this is due to the same effect but the time in the states increases so λ_{state} increases.

Although the state failure rate, λ_{state}, was greater for the incipient failure mode, by comparing Figure 5.11a and Figure 5.11b it can be seen that the λ_{sim} is greater for the states without an incipient failure mode. This is because the time spent in the states with an incipient failure mode present is significantly less than without and this effect outweighs the increased failure rate in the states. As in Figure 5.10, the failure rates decrease for the S_3 and more degraded states and increase for S_1 and S_2. This is again due to an increased time in the first two states and a decreased time in the later states. The sum of the simulation failure rates, $S_\Sigma = \sum S_i$, measures the effectiveness of the AM strategy on the observable as a whole. As would be expected it can be seen

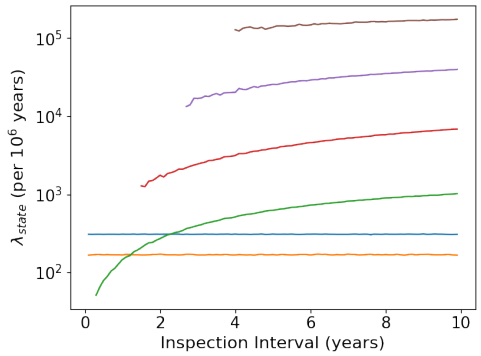

(a) States without an incipient failure mode.

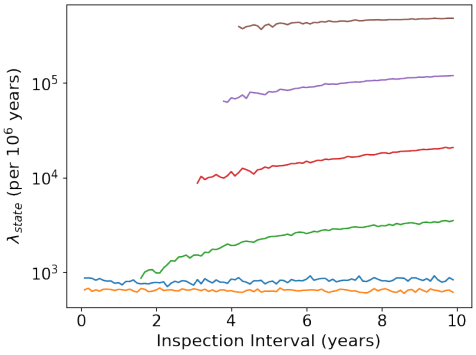

(b) States with an incipient failure mode.

Figure 5.10: State failure rates, λ_{state}, plotted against inspection intervals. S_1, S_2, S_3, S_4, S_5, S_6.

that the sum of the failure rates decreases as the inspection interval decreases.

5.3.4 Inspection Types

The system design is such that there are internal and external inspections for most assets, these act on different sets of the asset's observables. So far the pipe asset has been examined, this only has an external inspection, so to compare the two inspection types a more complex asset must be chosen. Here, a separator is examined as it has four observables and both internal and external inspections. The internal inspection reveals the condition of the *Vessel Wall Thickness* and the *Deposit Size* observables, whereas the external inspection reveals the condition of the *Vessel Wall Thickness* and the *Structural Wall Thickness*. Therefore, both inspections are required to determine the condition of all the observables. The results of varying the internal and external inspection intervals on the unavailability of a separator is given in Figure 5.12.

The unavailability of the separator is decreased through a reduction in the inspection interval for both inspection types with the unavailability's minimum being approached as the inspection intervals approach zero. It is important to note that the relation is asymmetric between the inspection types, this is as the inspection types can only decrease the contribution of unavailability from the observables it acts on. It can be seen that change in the internal inspection interval has a greater effect, thus the unavailability contribution from the observables it inspects is greater than the observables the external inspection acts on.

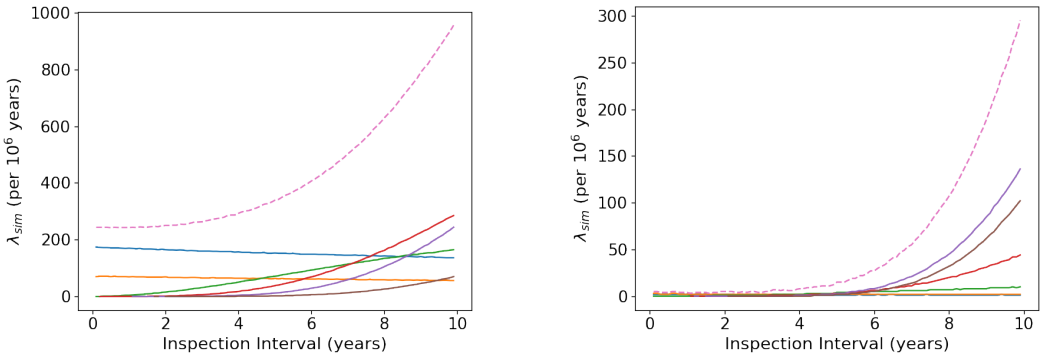

(a) States without an incipient failure mode.

(b) States with an incipient failure mode.

Figure 5.11: Simulation failure rates, λ_{sim}, plotted against inspection intervals. S_1, S_2, S_3, S_4, S_5, S_6, S_Σ.

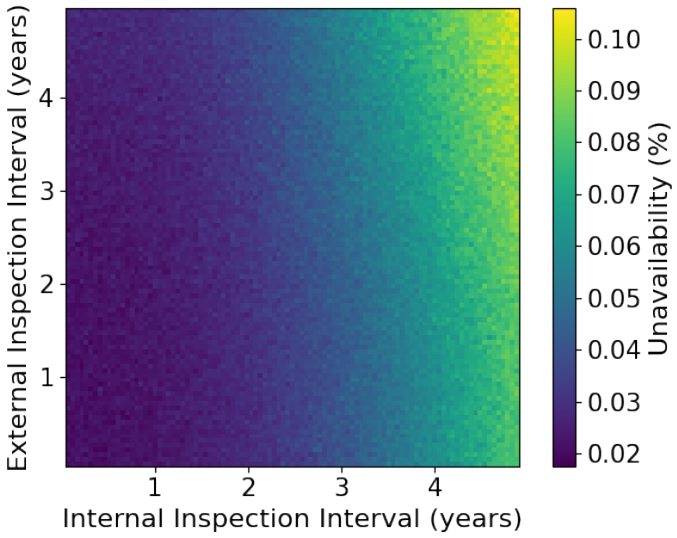

Figure 5.12: The unavailability of a separator under different intervals for internal and external inspections.

5.3.5 Maintenance Backlog

A maintenance backlog is formed when the number of maintenance tasks required consistently outstrips the rate at which maintenance can be performed resulting in a queue of maintenance tasks forming. When an inspection reveals a sufficiently degraded observable, maintenance is queued. However, maintenance actions are constrained to only be performed during the maintenance window, as introduced in Subsection 4.7.4, thus the queue depth will increase only between these windows. As discussed in Section 1.9, a maintenance backlog is an issue of particular importance to platforms in and approaching LE due to the ageing assets requiring more maintenance. A maintenance queue depth, $M_Q(t)$, can be defined as the number of maintenance tasks queued at time, t. This can be calculated through the HSPN, by summing the number of marked maintenance queue places, p_{mQueue}, in the maintenance action substitution transition, seen in Figure 4.18, at any given time.

The sizing of the maintenance and inspection teams is of critical importance to the maintenance queue depth. By increasing the number of maintenance teams, T_M, more maintenance tasks can be completed simultaneously. Whereas, an increase in the number of inspections teams, T_I, increases the size of the backlog, this is as more inspections will cause more maintenance actions to be added to the backlog.

In Figure 5.13, the maintenance queue depth through the platform's lifecycle is shown for AM strategy A, given in Subsection B.4.1, with varying numbers of maintenance and inspection teams. The model evaluates the maintenance queue depth for given number of teams, through this figure the expected pay-off for varying the number of teams can be seen. It can be noted that the maintenance queue depth increases with the platform age, this reflects the build up of a maintenance backlog as the platform ages that duty-holders report.

The best case maintenance queue is given for $T_M = \infty$ and $T_I = \infty$, where no restriction is given by the availability of teams. A queue still exists as maintenance is only performed in a maintenance window. The queue depth is almost equal for $T_M = T_I = 4$ throughout the platform's lifecycle, thus increasing the number of teams further would not be of value. Although, this result is valid subject to AM strategy A, as the strategies parameters are varied the optimal number of teams will change. This is investigated as part of an optimisation algorithm later in the thesis, in Subsection 7.4.3.

In Figure 5.13, only equal number of maintenance and inspections teams were

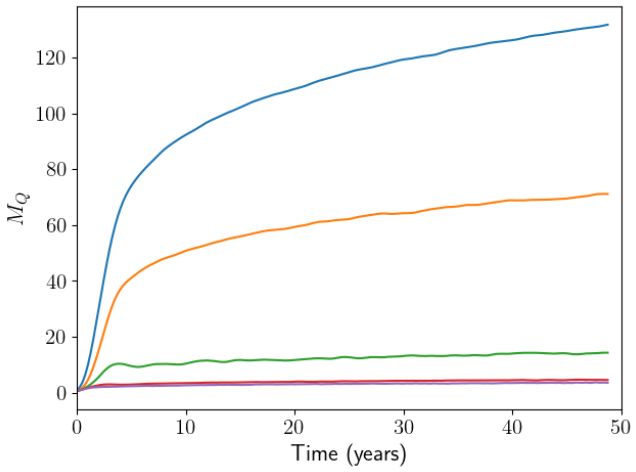

Figure 5.13: The maintenance queue depth through the platform's lifecycle for different number of maintenance teams, T_M, and inspection teams, T_I. $T_M = T_I = 1$, $T_M = T_I = 2$, $T_M = T_I = 3$, $T_M = T_I = 4$, $T_M = T_I = \infty$.

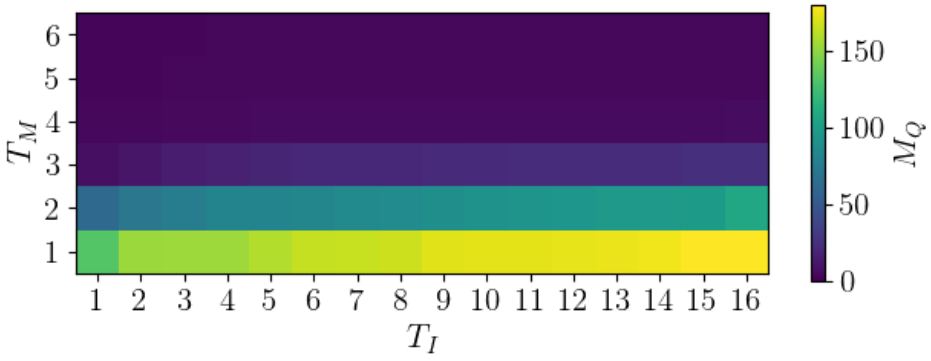

Figure 5.14: The maintenance queue depth at the end of the platform lifecycle as a function of maintenance teams, T_M, and inspection teams, T_I.

plotted. Although, the model is capable of simulating arbitrary numbers of both teams. The final maintenance queue depth at the end of LE can be compared when varying the number of teams. A heat-map of the final maintenance queue depth can be seen in Figure 5.14, again this was simulated using AM strategy A and varying the number of teams.

This heat-map shows the relationship between increasing the number of maintenance teams and a decrease in the backlog size, where it can be noted that there are diminishing returns as the number of teams increases. Interestingly, it can be seen that as the number of inspection teams increases for a constant number of maintenance teams the maintenance queue depth also increases. By increasing the number of

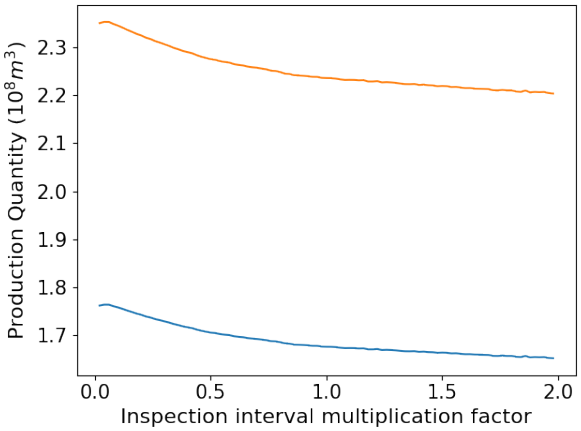

Figure 5.15: The production quantities for a global multiplication factor on the default inspection intervals for a 50 year lifecycle. Oil, Gas.

inspection teams, the exposure of a degraded condition is reduced and therefore maintenance is queued earlier. Thereby, the maintenance backlog is increased but only as the knowledge of the actual condition of the assets is increased.

5.3.6 Production Modelling

In Figure 5.15 the total oil and gas production quantities for the platform's lifetime are presented for globally changing inspection intervals. Here global changes are examined that are applied to all of the inspections to demonstrate the effect changing inspection intervals has on the production. All of the inspection intervals are changed through a multiplication factor applied to the inspection intervals defined by AM strategy A given in Appendix B, in Subsection B.4.1. It can be seen that the production quantities decrease as the inspection intervals increase. This demonstrates that the availability of the production assets increases, resulting in greater production quantities.

When a production asset in the oil or gas production chain is in a degraded failure mode then the production rate is reduced and when it is in a critical failure mode the production of oil or gas is halted. In Figure 5.18 the time that at least one of the production assets in the oil or gas processes are in a degraded or critical failure mode are plotted. This demonstrates how the time spent in these failure modes correlates with a decrease in the oil and gas production quantities.

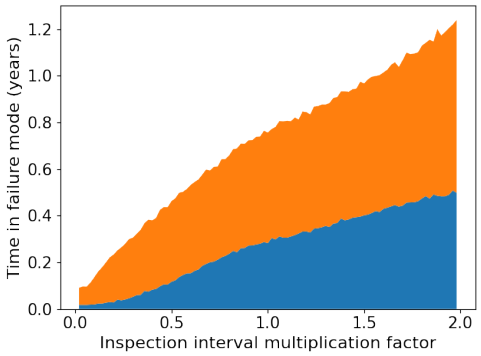

Figure 5.16: Time spent in oil production failure modes.

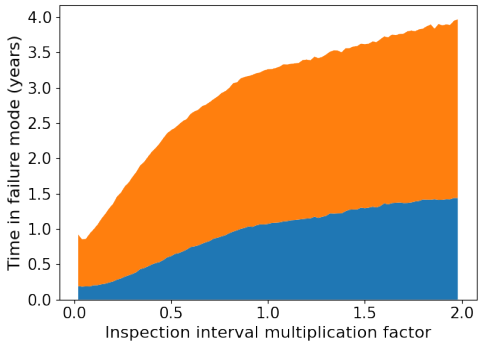

Figure 5.17: Time spent in gas production failure modes.

Figure 5.18: Time spent in the production critical and degraded failure modes for a 50 year life-cycle. Degraded, Critical.

5.4 Summary and Discussion

Software was developed specifically for the HSPN model using C++. By developing custom software: there was no constraint on the mathematical definition of the net and the software could be integrated with other elements such as the consequence analysis and optimisation. Due to the scale of the model and the large number of simulations required there was a focus on producing performant code. The majority of the code execution time was taken in checking if transitions were enabled, to optimise the code, it was written so that only the minimum number of transitions would need to be checked with each step.

The AM strategy is encoded into the HSPN and can be varied independently for every maintenance decision and inspection. The search space of possible strategies is very large and thus cannot be practically searched, this is one of the reasons for the use of the optimisation algorithm in Chapter 7. In this chapter the effects of varying the AM strategy on smaller example assets and systems were presented. This demonstrated the capabilities of the model to produce a wide variety of results for measuring the performance of an asset or system.

It was seen that the HSPN model can be used to evaluate several performance metrics, which can be used to compare the effect of varying aspects of the AM strategy. Specifically, the effect of varying the inspection interval on the exposure, the time spent in a more degraded state than last inspected, was discussed. While exposed,

the asset is at a greater probability of failure than known, therefore it is important to minimise this time. Further, the failure rate from each state was analysed, showing the relationship between decreasing the inspection interval resulted and a decreased failure rate for each state. Of interest to duty-holders is the accumulation of a maintenance backlog throughout the platform life-cycle, the effect of varying the number of teams on this was examined which revealed a critical number of maintenance teams. Additionally, the unavailabilities of the systems can be calculated throughout the simulation time through fault tree analogous structures. The unavailabilities of the power system were connected to the production and firewater deluge systems to represent their dependencies. The production rate of each asset was seen to be dependent on the current failure mode of the asset, with a degraded failure associated with a decreased rate.

The HSPN simulates the failures of the production assets, including leak failure modes. Thus the occurrence of leaks from each asset is found through the HSPN, although this does not determine the possible escalation events following the leak. To achieve this a consequence analysis must be performed that can be attached to the HSPN model. Chapter 6 presents a detailed description of the consequence analysis used in this research.

Chapter 6

Consequence Analysis

6.1 Introduction

The production vessels of an offshore oil and gas platform contain volatile fluids which, following a leak, can pose a threat to the platform and its workforce. Some of the possible consequences were discussed in Section 1.7, where some of the worst accidents in the industry were discussed, demonstrating the dangers that are associated with a loss of containment. It is due to the severity of the possible consequences that a consequence analysis technique is included in this model, this produces quantifiable results relating to the frequency and magnitude of fires and explosions. The consequence analysis is connected to the HSPN and can be used to evaluate the consequences' probability density functions for a given AM strategy.

In this chapter the consequences of a leak are analysed using a numerical simulation technique, that calculates the change of fluid quantity in the vessel and the surrounding module. The time-evolution of a leak is analysed to determine both the frequency and magnitude of the consequent events for a leak scenario, given by the failure of a production asset. In this analysis, there are four possible outcomes that are considered, these are an explosion, a jet fire, a pool fire and no escalation. The consequence analysis is linked with the HSPN presented in the previous chapter, it is used to evaluate leak scenarios triggered by particular production asset failure modes. Thereby, the consequences associated with each leakage failure mode of a production asset can be evaluated.

Some of the initial conditions of the consequence analysis are taken from the HSPN model such that the results reflect the system's current state, these include the dimen-

sions of the leaking vessel, the quantities of oil and gas and the initial pressure inside the vessel. In addition, the analysis is based on two stochastically sampled variables relating to the leak size and location. Due to these stochastic variables the time-evolution of a leak is not constant and thus to obtain results that accurately represent the possible time-evolutions of a leak a MC approach is taken. This is applied to each leak scenario, which produces a distribution of results such that probability density functions for the various outcomes can be determined.

The integration of the HSPN and consequence analysis is used to calculate risk profiles for a given AM strategy. This is used to analyse the risk associated with a single asset and from the whole platform. The risk profiles will be given both as functions of platform age and of consequence magnitude. Three AM strategies are compared and used to demonstrate the change in risk from more and less proactive strategies.

The consequence analysis is based on a technique originally developed by Andrews, Smith, and Gregory (1994) and further developed by Foster and Andrews (1999) and Lewthwaite (2006). This was specifically developed for simulating leak scenarios on offshore oil and gas platforms. The primary advantage of the technique is that it is far less computationally demanding than traditional CFD techniques, which typically model dispersion in 3-dimensional space. While this may produce less detailed results, it allows for more scenarios to be considered which provides a good basis for analysing the probability distribution functions of multiple escalation events.

6.2 Initial Conditions

The analysis is dependent on a number of initial conditions relating to the vessel, the module, the fluid quantities and the firewater deluge system. There are two sources of the initial conditions, these are:

- **The HSPN**: This gives parameters defining the vessel and module dimensions and availability of the firewater deluge system. These are dependent on which asset triggered the analysis and the current state of the system at that time. The details of this are discussed in Subsection 6.2.1.
- **Stochastically Sampled**: Parameters relating to the height of the leak and the diameter of the hole are stochastically sampled at the start of the simulation. The details of this are discussed in Subsection 6.2.2.

Vessel Type	Index	Module	Volume (m^3)	Height (m)	Gas Pressure (bar)	Oil (%)	Gas (%)
Valve	1	Separation	14.5	0.5	13.0	0.0	100.0
	2	Compression	9.8	0.5	49.0	28.57	71.43
	3	Separation	37.5	0.5	186.0	30.67	69.33
	4	Compression	5.8	0.5	1780.0	0.0	100.0
Separator	1	Separation	166	10	20.7	53.01	46.99
	2	Separation	109	10	1.6	52.29	47.71

Table 6.1: Data on some of the production vessels used by the consequence analysis. The completed tables for all of the assets are given in Appendix C in Table C.3 and Table C.4.

6.2.1 Initial Conditions from the HSPN

During the simulation of the HSPN if the place of a leak failure mode of a production asset becomes marked then a consequence analysis is triggered. Many of the initial conditions of the analysis are determined by which asset is leaking and the current marking of its production place. The production asset failure which triggered the consequence analysis determines several initial conditions based on the physical dimensions and fluid quantities of the leaking asset. These values are unique for every production asset, in Table 6.1 the initial conditions for a subset of the production assets are given, for brevity the remaining production assets are given in Appendix C. The values given in the table define the physical parameters of the oil and gas as well as the vessel, these will be used in calculations to determine the discharge rates of the oil and gas. These values were taken from fluid flow diagrams of the production process of Beryl B. The time-evolution is not only dependent on the vessel but also on its surroundings, each production asset is either in the *Separation* or *Compression* module, these also define the initial conditions of the module's dimensions and the ventilation rate.

Furthermore, the consequence analysis is also dependent on the availability of the firewater deluge system as this can reduce the magnitude of an overpressure caused by an explosion. The availability is given by the marking of two of the places in the HSPN, these were detailed in Section 4.10. Firstly, if the firewater supply place, P_{FWSupply} from Figure 4.29, representing the availability of the firewater pumps to supply water,

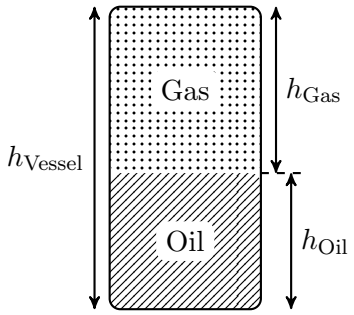

Figure 6.1: Heights of oil and gas in a two-phase asset.

if marked then the supply is unavailable. Secondly, the detectors must be operational for the module that the leak is in, this requires $P_{\text{Detection}}$ from Figure 4.32 to be unmarked for the relevant module. For the firewater deluge system to be operational both of these places must be unmarked at the time the leak occurs.

6.2.2 Initial Conditions of the Leak

The initial conditions from the HSPN give data on the vessel, module and firewater deluge system but do not give data on the leak position or size. These are instead given by stochastically sampling probability distribution functions. In particular two variables are stochastically sampled, these are the leak height, h_{Leak}, and the leak hole radius r_{Leak}.

The leak height is uniformly sampled from the height of the vessel such that $h_{\text{Leak}} \in [0, h_{\text{Vessel}}]$. Some assets of the production system are two-phase and contain both oil and gas, these are assumed to be vertically separated with a geometry given by Figure 6.1. It is assumed that a leak where $h_{\text{Leak}} < h_{\text{Oil}}$ will discharge only oil until the oil height has been reduced such that $h_{\text{Leak}} > h_{\text{Oil}}$ whereupon the oil discharge will cease and the gas will begin leaking.

The leak hole radius is also stochastically sampled, which is taken from an exponential probability density function, although, this does have a dependence on the HSPN. The observables in the HSPN with leak failure modes have two levels of failure, degraded and critical. These both trigger a consequence analysis but a critical failure mode is considered to result in a more dangerous situation. This is represented in the consequence analysis by corresponding to greater rates in the radii exponential probability distributions, these values are given in Table 6.2. Therefore, the leak radius is determined through the following equation,

Symbol	Failure Mode	Value (m)
R_{Leak}	Degraded	0.05
	Critical	0.1

Table 6.2: The leak hole radius exponential distribution rates for degraded and critical failure modes.

$$r_{\text{Leak}} = -R_{\text{Leak}} \ln(\chi), \tag{6.1}$$

where χ is a stochastically sampled number in the domain $(0, 1)$. Thus the leak area, A_{Leak}, is given by,

$$A_{\text{Leak}} = \pi r_{\text{Leak}}^2. \tag{6.2}$$

6.3 Oil Discharge

An oil containing vessel will leak oil so long as the leak hole height, h_{Leak}, is less than the oil height, h_o. As the outflow of oil will decrease the oil height over time, thus eventually the oil height will be less than the leak height. The rate at which oil leaks from the vessel is given by the mass discharge rate, this defines the mass of oil leaving the vessel per unit time. The oil mass flow rate is given by the equation (Lewthwaite 2006),

$$W_o = \left[2{A_{\text{Leak}}}^2 \rho_o \left(p_o - p_{\text{atmo}} + g\rho_o \left(h_o - h_{\text{Leak}}\right)\right)\right]^{1/2}. \tag{6.3}$$

Here A_{Leak} is the area of the leak hole, p_o is the oil pressure in the vessel, p_{atmo} is the atmospheric pressure, ρ_o is the density of the oil and g is gravitational acceleration. The exact values of the constants used here and throughout this chapter are given in a series of tables in Appendix C.

Therefore, the rate of change of the volume of oil in the vessel is given by,

$$\frac{dV_o}{dt} = -\frac{W_o(t)}{\rho_o}. \tag{6.4}$$

Thus, the oil in the vessel at a time t is given by the integral,

$$V_o = V_{o,0} - \frac{1}{\rho_o} \int_0^t W_o(\tau)\, d\tau, \tag{6.5}$$

where $V_{o,0}$ is the volume of oil in the vessel at time $t = 0$. The outflow of oil is assumed to accumulate in a pool on the decking of the module with a fixed depth, the oil pool

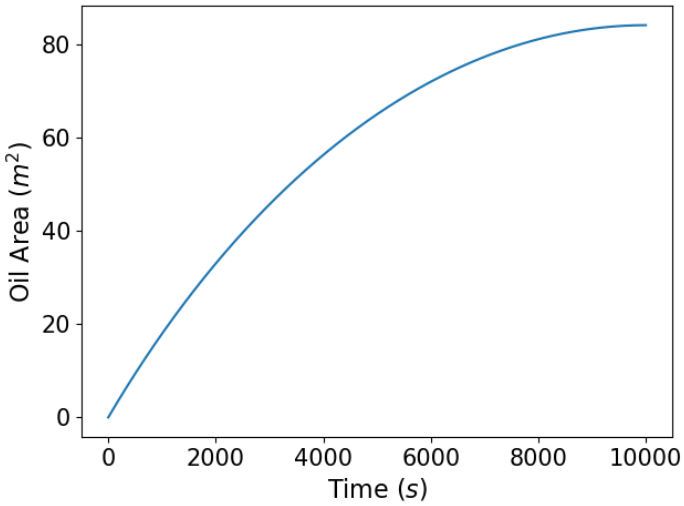

Figure 6.2: An example of the oil pool area's time-evolution following an oil leak from a separator.

area, A_o, at time t is therefore given by,

$$A_o = \frac{1}{\rho_o D_o} \int_0^t W_o(\tau) d\tau, \tag{6.6}$$

where D_o is the depth of the oil pool.

The oil pool area is bounded by the area of the module, any excess oil is assumed to escape the module and is not considered further by this analysis. The area of each module was given in Table 3.1. An example of the build-up of an oil pool can be seen in Figure 6.2, where the oil pool area can be seen to increase throughout the simulation. The rate of increase declines with time, since the oil mass discharge rate decreases as the difference between the oil height and the leak height decreases.

6.4 Gas Discharge

The gas in the vessel is assumed to fill the space that is not taken by the oil, therefore the gas can only leak when the leak height, h_{Leak}, exceeds the oil height, h_o. When the gas flow through the leak hole reaches the speed of sound the flow is known as choked, when it is below the speed it is unchoked. The flow is unchoked if,

$$\frac{p_g}{p_{\text{atmo}}} < \left(\frac{\gamma+1}{2}\right)^{\frac{\gamma}{\gamma-1}}, \tag{6.7}$$

where γ is the ratio of specific heat of the gas at constant pressure and at constant volume and p_g is the gas pressure in the vessel.

For an unchoked gas flow the gas mass flow rate is given by,

$$W_g = \left(2{L_A}^2 \left(\frac{\gamma}{\gamma - 1} \right) K^{\frac{-1}{\gamma}} {p_{\text{atmo}}}^{\frac{1+\gamma}{\gamma}} \left[\left(\frac{p_{\text{atmo}}}{p_g} \right)^{\frac{1-\gamma}{\gamma}} - 1 \right] \right)^{1/2}, \tag{6.8}$$

where $K = p_g / (\rho_g{}^{\gamma})$ and ρ_g is the gas density. For a choked flow the gas mass flow rate is given by,

$$W_g = L_A \left[p_g \rho_g \gamma \left(\frac{2}{1+\gamma} \right)^{\frac{1+\gamma}{\gamma-1}} \right]^{1/2}. \tag{6.9}$$

The outflow of gas into the module is assumed to immediately and perfectly mix with the air in the module. This assumption is a key difference with more complex CFD models, where the gas concentration will vary with position in the module and change with time. By assuming this the computational requirements are significantly decreased.

The change in gas density in the vessel is given by,

$$\frac{d\rho_g}{dt} = -\frac{W_g}{V_g}. \tag{6.10}$$

Here V_g is the volume of gas in the vessel, defined as $V_{\text{Vessel}} - V_o$.

The gas discharge into a module accumulates to create a gas cloud, this can be measured by the concentration of flammable gas in the module, $C_g \in [0, 1]$, which is given by,

$$C_g = \frac{V_{\text{module,g}}}{V_{\text{module}}}, \tag{6.11}$$

where $V_{\text{module,g}}$ is the volume of flammable gas in the module and V_{module} is the volume of the module. The volume of each module was given in Table 3.1. It is assumed that the volume of flammable gas is limited to the volume of the module, such that $C_g \leq 1$.

Assuming that the module is ventilated then a ventilation rate, M_v , can be defined that determines the rate at which the flammable gas is removed. The change in the gas concentration is given by,

$$\frac{dC_g}{dt} = \frac{1}{V_{\text{module}}} \left[W_g - C_g \left(W_g + M_v \right) \right] \tag{6.12}$$

The time-evolution of the gas concentration for a typical gas leak from a vessel is given in Figure 6.3 for a scrubber in the compression module. It can be seen that initially the concentration rapidly increases as the pressure differential is large, the concentration then exponentially decays as the ventilation rate exceeds the gas discharge rate.

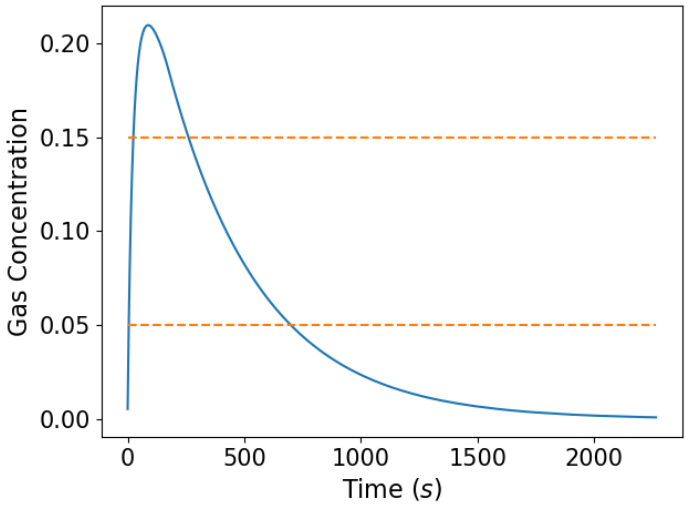

Figure 6.3: An example of the gas concentration in the compression module for a gas leak from a scrubber.

The two horizontal lines shown in Figure 6.3 represent the Lower Flammable Limit (LFL), and the Upper Flammable Limit (UFL). These limits define the range of concentrations at which the flammable gases can be ignited. Thus an explosion can only occur when the gas concentration is in the range $C_{\text{LFL}} \leq C_g \leq C_{\text{UFL}}$.

Figure 6.4 demonstrates a simulation that included both an oil and a gas leak. In this situation the oil height initially surpassed the leak height and so oil was discharged into the module, this had the effect that the gas expanded in the vessel and thus the density decreased. A discontinuity can be seen in the result corresponding to when the oil height reduced to below the leak height and thus a gas leak began as the oil leak ended. The discharge of gas then further reduced the density at a greater rate than previously.

6.5 Consequent Events

The discharge of oil or gas into a module is the first step towards a fire or explosion. The consequence analysis considered four possible consequence events of a leak, these are: an explosion, a jet fire, a pool fire and no escalation. Each of these is caused by the ignition of a different aspect of the leak: an explosion is caused by the ignition of an accumulation of gas in the module, a jet fire is caused by the ignition of the gas leak at the hole's location and a pool fire is caused by the ignition of an oil pool on the module's floor.

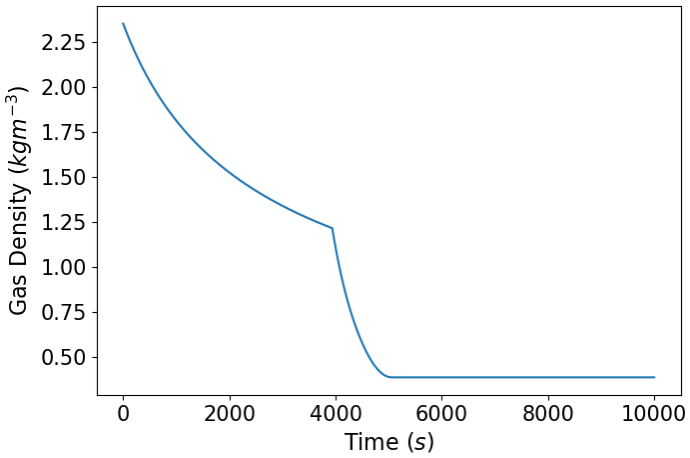

Figure 6.4: The time-evolution of the gas density of a leak from a separator that begins as an oil leak until the oil height reduces to below the leak height and gas begins leaking.

The magnitudes of each event are measured through different quantities that cannot be directly compared, an explosion is measured by its overpressure and jet fires and pool fires are measured by their flame lengths. Although both of the fires measure their magnitude through the flame lengths, these still cannot be compared as the heat flux from the flames will be different for flames of the same length. Therefore, the consequence analysis provides the magnitude of these events but does not provide a method to compare them. However, when comparing results of analyses the magnitudes can be compared within each event and furthermore, the total number of events can be compared.

A leak will escalate to an explosion or fire when an ignition source is present. An assumption of this analysis is that ignition sources have a constant probability of occurrence such that for each unit time there is a fixed probability that an ignition source is present. The probabilities of ignition for each consequent event are given in Appendix C in Table C.2.

6.5.1 Explosion

An explosion is caused by the ignition of a gas accumulation in a module, as mentioned previously the gas concentration must be between the LFL and the UFL to cause an ignition. The magnitude of an explosion is measured by the pressure wave it creates, this is known as the overpressure. The equation for an overpressure is given

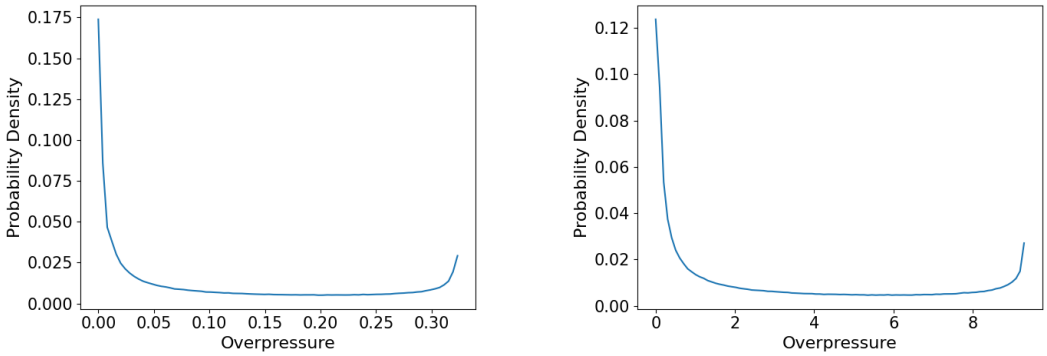

(a) Firewater deluge available.

(b) Firewater deluge unavailable.

Figure 6.5: Probability density functions for the overpressures for *Separator 1* deluge system availability and unavailability.

by (Lewthwaite et al. 2006),

$$O = O_{\max} \exp\left\{A\left(\frac{C_g}{C_s} - 2B + 1\right)\left(\frac{C_g}{C_s} - 1\right)\right\} \quad : \quad C_{\text{LFL}} \leq C_g \leq C_{\text{UFL}}. \tag{6.13}$$

Where $O_{\max}$ is the maximum overpressure, C_s is the stoichiometric concentration and A, B are constants. The constants $O_{\max}$, A and B are dependent on whether the firewater deluge system is currently available or not, thereby representing the effect of the deluge. These are such that the overpressure is significantly large for a scenario where the system is unavailable. These constants are given in Table C.1.

The distribution of overpressures from *Separator 1* can be seen in Figure 6.5a and Figure 6.5b as a probability density function for a leak with or without the firewater deluge system respectively. It can be noted that the probability density generally decreases as the overpressure increases, this is as the overpressure is proportional to the gas concentration at the time of ignition. The gas concentration must increase from zero to the LFL before decaying, thus the time spent in lower concentrations is greater. The overpressure can be seen to peak at $O_{\max}$, this corresponds to ignition at the UFL. This is more probable than nearby magnitudes as simulations where the gas concentration exceeds UFL must cross the boundary twice increasing the time spent and thereby the probability of ignition near the UFL.

The shape of both figures are identical but differs by a scale factor of the overpressure magnitude. This is expected as the mass discharge rates and ignition probabilities are invariant to the firewater deluge system availability. Although the overpressure is dependent on the deluge's availability resulting in the overpressure being significantly

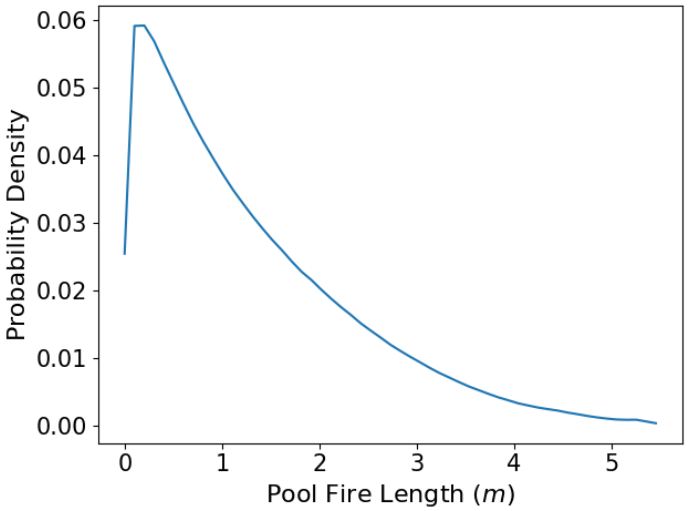

Figure 6.6: A probability density function of pool fire lengths for *Separator 1*.

greater for an unavailable deluge system. Therefore, a high availability for the firewater deluge system is desirable for significantly reducing the overpressure in the case of an explosion.

6.5.2 Pool Fire

A pool fire is caused by the ignition in a module of an oil pool that has accumulated over time by the discharge of oil into the module. The magnitude of the fire is measured via the length of its flame, L_p, this is given by a formula derived by Moorhouse (1982) such that,

$$L_p = 6.2u^{-0.044}D_p\left(\frac{R_B}{\rho_{\mathrm{o,atmo}}\left(gD_p\right)^{1/2}}\right)^{0.254}. \tag{6.14}$$

Here u is the wind speed, D_p is the pool diameter, R_B is the mass burn rate and $\rho_{\mathrm{o,atmo}}$ is the atmospheric oil density.

In Figure 6.6, the probability density function of the flame lengths can be seen, this is obtained by performing a MC simulation on a leak from *Separator 1*. It can be noted that the maximum probability is obtained for a relative short flame length, as the flame length is proportional to the pool area this implies that most of the ignitions occur at early times before a large pool has had time to accumulate. Further, the probability of flame length follows an exponential decay after the peak, this corresponds to a decreased probability of ignition of larger pool areas.

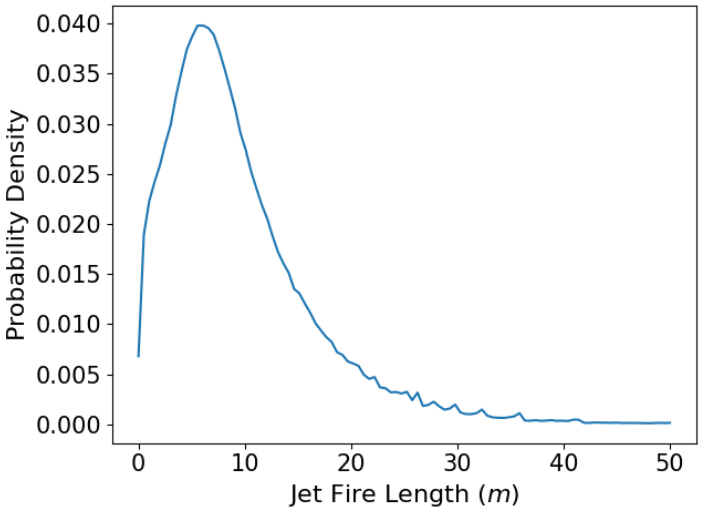

Figure 6.7: A probability density function of jet fire lengths for *Separator 1*.

6.5.3 Jet Fire

In addition to an explosion, a gas leak can also lead to a jet fire. This is caused by the ignition of the gas at the location of the leak. Due to the high pressure of the gas at the leak location an ignition can produce a particularly large flame. In general, a jet fire flame length will be much longer than a pool fire's but these are not comparable as the duration and heat flux of the flames will differ for the same lengths.

The magnitude of a jet fire is given by the length of its flame, which is proportional to the gas mass discharge rate and is given by,

$$L_j = 15\,(W_g)^{0.41}\,. \tag{6.15}$$

This relationship was derived by Thomas (1963).

The probability density function for the flame lengths for *Separator 1* are given in Figure 6.7. It can be noted that the maximum probability jet fire length is near $10m$ with the probability decreasing for both shorter and longer flame lengths. Due to the proportional relation of the jet fire length, this figure is similar to the probability density function of the gas mass discharge rate.

6.6 Simulation of the Consequence Analysis

A simulation of the consequence analysis is performed through evaluating various equations at small iterative time-steps. This calculates the change of oil and gas quantities

in the vessel and the module at each time-step. Through this, the time-evolution of a hydrocarbon leak can be simulated. Furthermore, there is a probability of an ignition source being present at each time-step which can escalate to an explosion, jet fire or pool fire if enough oil or gas is present in the correct location. The initial conditions to the analysis are taken from the HSPN and from data on the physical parameters of the vessel; these were detailed in Section 6.2.

Explicitly a time-step of a consequence analysis simulation follows these steps:

1. Calculate oil and gas mass flow rates with Equation 6.3 and Equation 6.7 respectively.
2. Update the oil pool area and gas concentration in the module with Equation 6.6 and Equation 6.12 respectively.
3. Update the oil volume and gas density in the vessel with Equation 6.4 and Equation 6.10 respectively.
4. Evaluate the probability of ignition source to determine if an ignition source in present. If present then determine if any escalation events can occur and calculate their magnitude:

    - Explosion: Can escalate if the gas concentration C_g is between the lower and upper flammable limits, C_{LFL} and C_{UFL} respectively. Overpressure given by Equation 6.13.
    - Pool Fire: Can escalate if there is a oil pool are greater than zero. Pool fire length given by Equation 6.14.
    - Jet Fire: Can escalate if there is a gas mass flow rate greater than zero. Jet fire length given by Equation 6.15.

The time-steps are repeated until either an escalation event occurs or the oil mass flow rate, gas mass flow rate and gas concentration reach zero.

The analysis contains several stochastic elements, such as the leak height, leak area and sampling of the ignition source probability, thus the results are non-deterministic. Therefore, to fully understand the possibly consequences of a leak event, it is not enough to perform a single consequence analysis, as this gives just a single possible sequence of events. Instead a MC method was applied to perform a set of consequence analysis simulations, and from these probability density functions of their results are created. An example of these probability density functions for the consequent event magnitudes were seen previously in Figure 6.5, Figure 6.6 and Figure 6.7.

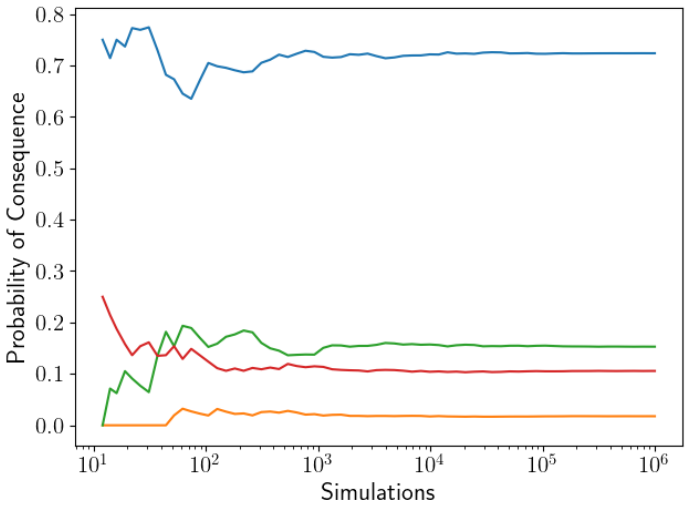

Figure 6.8: Convergence of the probability of each consequence for *Valve 3*. None, Explosion, Jet fire, Pool fire.

6.6.1 Convergence Test

It is important that the number of consequence analysis simulations that are performed in each set are enough to produce reliable results. To decide the number of simulations required a convergence test was performed. In Figure 6.8, the convergence of the probabilities of the consequence events for a leak from *Valve 3* can be seen, this asset was used as it contains a mix of oil and gas and so can result in any consequence. Here it can be seen that by 10^6 simulations the probabilities have converged. Therefore, it was decided that it would be sufficient for each consequence analysis to be performed as a MC simulation with 10^6 simulations.

6.6.2 Event Probabilities

A leak scenario can end in any of the escalation events discussed above or no escalation, the probability of each of these events depends on a variety of factors such as the gas concentration, oil pool area and gas discharge rate. To evaluate the probability of each of these events a MC method is used to repeatedly simulate the time-evolution with the stochastically sampled initial conditions. In Figure 6.9, the resulting probability of the escalation events can be seen for the two separators and their two failure modes. The separators are arranged in series with the liquid outflow of the first leading into the second, thereby the quantity of oil in the first is greater in *Separator 1* and similarly the quantity of gas is greater in *Separator 2*.

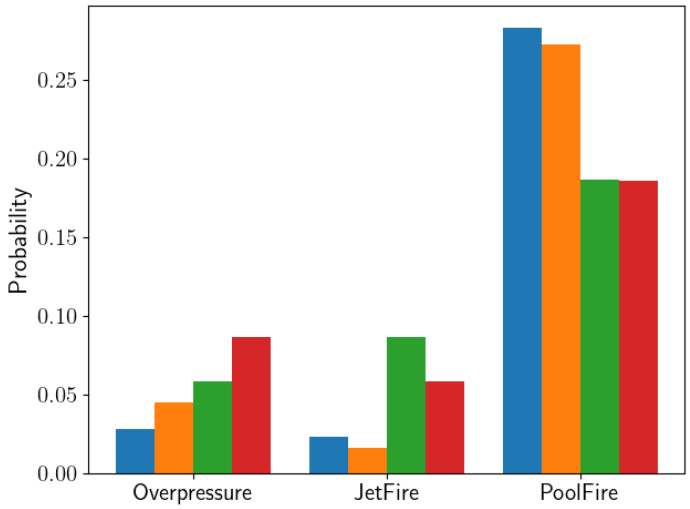

Figure 6.9: The probability of the escalation events for the two separators for the two failure modes. Separator 1 (Degraded), Separator 1 (Critical), Separator 2 (Degraded), Separator 2 (Critical).

A vessel with a high quantity of oil correlates with an increased probability of an oil leak as the probability that the leak height will be below the oil height is greater. This can be seen to be reflected in the results as *Separator 1* has a much higher probability of escalating to a pool fire. A similar effect can be seen for *Separator 2* where the greater quantity of gas results in a higher probability of a gas leak and therefore greater probability of explosions and jet fires.

In addition, the failure modes of the separators alter the resulting probability of the consequent events. Recall that the critical failure mode corresponds to a greater leak hole radius in comparison to a degraded failure mode. It can be noted that this has the effect of increasing the probability of an overpressure which corresponds to a decrease in the probability of jet and pool fires.

6.7 Integration with the HSPN

The consequence analysis has been seen to be capable of determining the frequency and probability density functions of the magnitudes of each consequent event. This analysis is used in conjunction with the HSPN to determine the consequences of leaks from the production assets and the frequency of the leaks. When a leak failure mode is entered in the HSPN it will correspond to a set of inputs to the consequence analysis

and thereby a set of results. Therefore, through the MC simulation of the HSPN the probability of particular consequence analyses being triggered can be determined.

For each production asset there are two failure modes associated with a leak, these are the degraded and critical failure modes. Each of these corresponds to a different exponential distribution of leak hole radii in the consequence analysis, as discussed in Subsection 6.2.2. Furthermore, the consequence analysis is dependent on the availability of the firewater deluge system and produces different results for when the system is available and unavailable. Therefore, for each production asset four consequence analyses are performed, for two failure modes each with the firewater deluge system available or unavailable.

The connections between the HSPN and consequence analysis are given in Figure 6.10. It can be seen that the inputs from the HSPN are the failure modes, the vessel and module and the module's firewater deluge system availability. A consequence analysis is triggered by a production asset entering a failure mode from a leak causing condition chain. Production assets can have multiple condition chains, corresponding to different observables. It is assumed in this model, that for each asset, only a failure from one of the condition chains will cause a hydrocarbon leak. In Table 3.3, the condition chains from which a failure will trigger a leak were given. In the HSPN when either the degraded failure mode place, P_{fD} or the critical failure mode place, P_{fC}, becomes marked the consequence analysis is started; these places were first seen in Figure 4.11. The leak hole radius rate, R_{Leak}, is defined dependent on the failure mode through Table 6.2. The oil volume and gas pressure are given through a look-up table based on which asset the leak failure modes belong to, this table is given in Table C.3 and Table C.4. Similarly, the module volume is found through another look-up table depending on the module the asset is located in, this table was given in Table 6.1. Finally, as the overpressure caused by an explosion is dependent on the presence of deluge, the module's firewater deluge system availability state is given by the marking of P_{ModuleFW}, from unavailability tree given in Figure 4.33. The places P_{fD}, P_{fC} and P_{ModuleFW} are socket places from the HSPN. Through the HSPN they are dependent on the AM of several assets, for beverity here only the socket places are shown.

Figure 6.10 also shows the relationships between the inputs from the HSPN to the consequence analysis simulations. A consequence analysis of a leak event is composed of a series of simulation performed via the MC method. This is done as the simulation is non-deterministic due to its stochastically sampled inputs, thus by collating the results of the MC method the possible consequences can be better understood. Some

of the inputs from the HSPN go directly into the simulation, these are the oil volume, gas pressure, module volume and module firewater deluge system availability. These are seen to be outside of the *Monte Carlo Method* box, there are two more inputs that are inside the box, these are stochastically sampled for each iteration of MC. Firstly, the leak hole radius, this is sampled from an exponential distribution with rate, R_{Leak}, defined by the failure mode. Secondly, the leak hole height, this is sampled from $[0, h_{\text{Vessel}}]$, where h_{Vessel} is defined by the vessel data.

A simulation will produce either no consequent event or an explosion, jet fire or pool fire and will calculate the magnitude of the event. As a consequence analysis is composed of a set of simulations, by combining the results of the simulations the probable consequences can be determined. Specifically, the probability of each consequent event from the leak can be calculated. In addition, the magnitude of each consequent event can be collated into a probability density function. Thereby, providing metrics for the consequences of a leak event, such that different leak events can be compared.

Each assets' consequence analyses are performed separately to the HSPN analysis such that high quality results can be determined by performing the consequence analysis MC method with many simulations, specifically 10^6 simulations were performed for each scenario. The results of each scenario are then stored and when the HSPN is simulated and a leak occurs the corresponding result for the asset failure mode and current module's firewater deluge system availability is found, this result can then included when analysing the results of the HSPN. Through the separation of the consequence analysis and the HSPN the computational demands can be drastically decreased, without compromising on the quality of results, which increases the power of the method. This reduced a single simulation run-time from approximately 30 seconds to 0.06 seconds.

The production vessels on the platform each contain different volumes of oil and gas and additionally the pressure and density of the gas varies. This has a large effect on the probability of the different consequent events for each production vessel. By performing the consequence analysis for each production asset the probability of each consequent event can be determined. The probabilities of each consequent event following a leak can be seen for all of the production assets in Figure 6.11, these results are for the critical failure; the corresponding results for the degraded failure mode are given in Appendix C in Figure C.1.

The production process first separates the oil and then processes the gas stream,

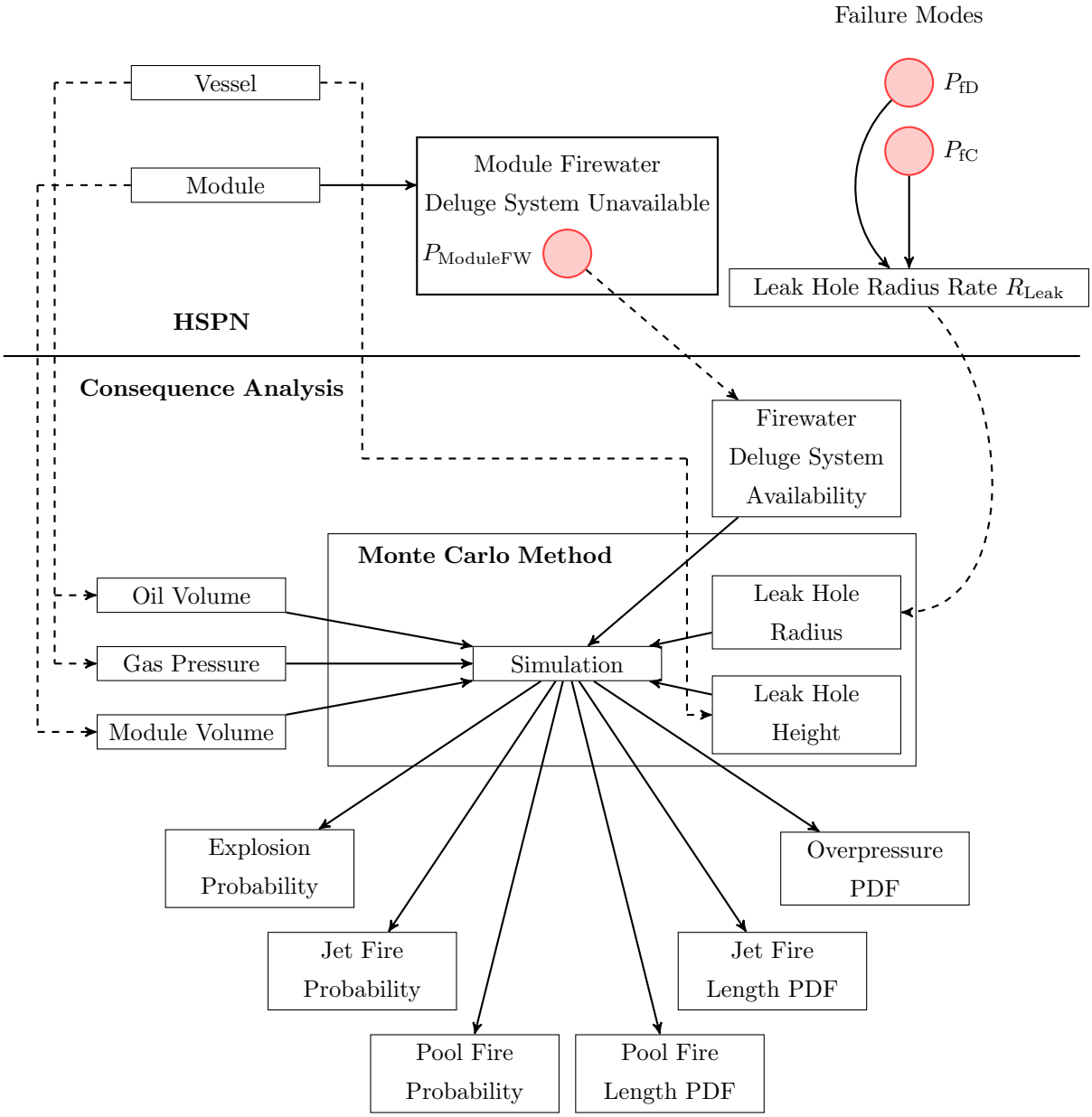

Figure 6.10: The relationships between the HSPN and the consequence analysis.

thus many of the assets later in the production chain do not contain any oil and therefore their probability of a pool fire is zero. The compression stage of the process increases the pressure of the gas, this will discharge at a higher rate following a leak. The effects of this can be seen in the results by examining the assets with higher indices. The exact position of the assets can be seen by referring back to Figure 3.3. In general the probability of explosion increases while the probabilities of jet fire and no escalation are decreased, it is thought that this is due to an increased pressure correlating with an increased probability of the gas concentration being between the flammable limits.

One of the observables of a production asset will have a leakage failure mode. It is the degradation rate and the effects of the AM tasks on this observable that will determine the mean time for a leak to occur. As each type of production asset is subject to different degradation mechanisms and AM strategies it is to be expected that the mean frequency of leaks varies between assets. Through a MC simulation of the HSPN the mean frequency of leaks for each type of production asset was found, the results are given in Figure 6.12. These results were generated through simulating the HSPN with AM strategy A, defined in Appendix B in Subsection B.4.1.

These results are useful for identifying the outcomes of various AM strategies. For instance, the high frequency of leaks from valves may imply that a more proactive AM strategy is required whereas the low frequency of leaks from the scrubbers could imply that inspection intervals could be increased. Nevertheless, this figure alone does not account for the risk posed by a leak, for instance, even so the leak frequency of a valve is high, in Figure 6.11 it can be seen that the probability of the escalation events varies greatly between the four valves in the model. This is as the volume of oil and gas in each valve is different, therefore the probability of each escalation event varies. The same effect can be seen in the pipes, with step changes when the volume of oil and gas carried by each pipe changes. This change is caused by a production asset such as a separator or a scrubber. Therefore, in reflection to this information the AM strategies should be unique for each production asset, even within the same type. This helps justify the choice on the work for the AM strategy to be assigned individually for each asset.

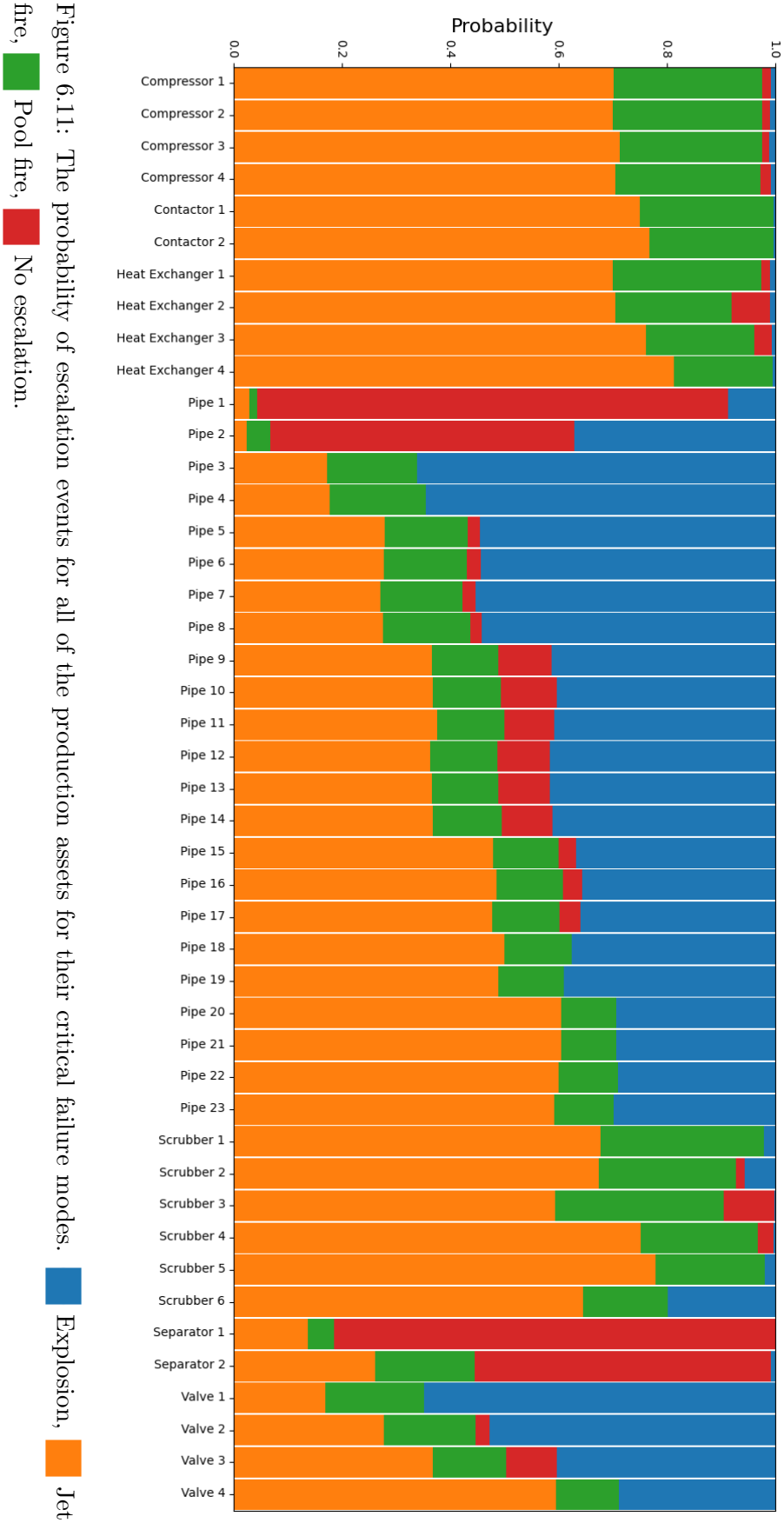

Figure 6.11: The probability of escalation events for all of the production assets for their critical failure modes.

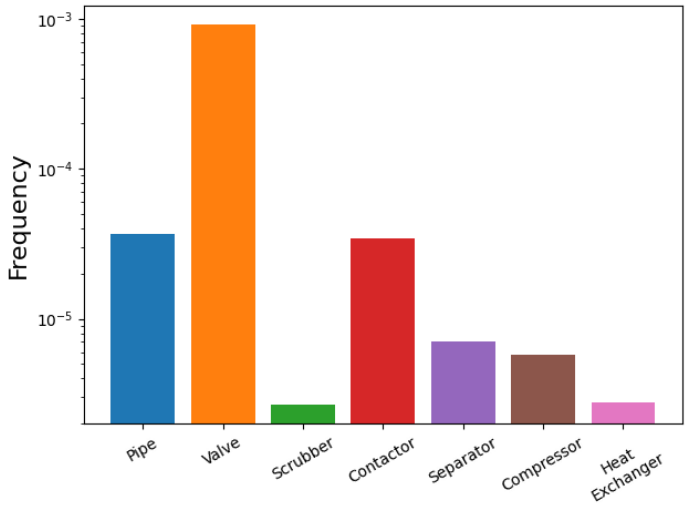

Figure 6.12: The mean frequency of leaks from each production asset type.

6.8 Consequent Events and Platform Age

Through the integration between the HSPN and consequence analysis, risk profiles resultant from a given AM strategy can be evaluated. It would be expected that the frequency of leaks increases with platform age as assets degrade and failures become more probable. Here, the relationships between the platform age and the consequent events are examined. To perform this analysis, we examine the asset *Valve 3*, this was chosen as it contains a mixture of oil and gas, so a leak has the potential to end in any of the three consequent events. To determine the probability of the valve's failure mode as a function of the platform's life-cycle a MC simulation is performed of the HSPN, which is simulated with AM strategy A.

A leak can be triggered by either a degraded or critical failure mode, in Figure 6.13 the probability of the different failure modes is given as a function of the platform age. This is further categorised into failure modes when the firewater deluge system is available and unavailable. This is relevant as an explosion's overpressure is dependent on the firewater deluge system. Combined, this presents four distinct consequence analyses for each asset. The probability of failure increases with the platform age as the assets degrade until reaching a constant value that AM actions maintain.

The failure modes with the firewater deluge system unavailable increases as the platform ages, at a rate faster than the total failure probability, this can be seen more clearly as a percentage of the total failure probability, in Figure 6.14. Thus,

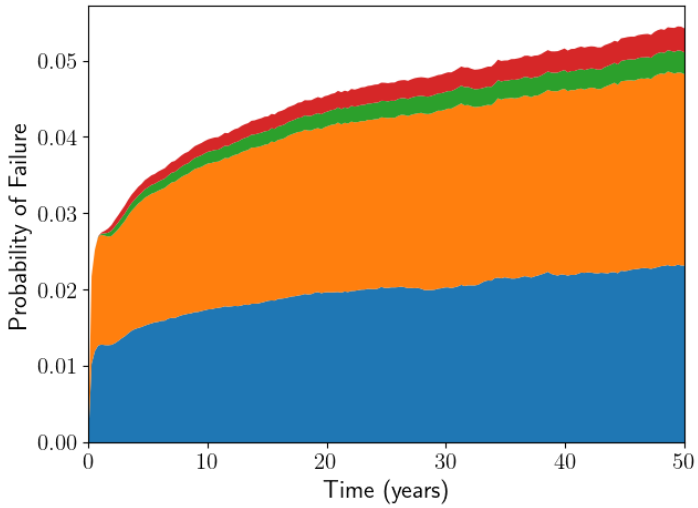

Figure 6.13: The probability of different failure modes for *Valve 3* as a function of the platform age from the different failure modes with and without the firewater deluge system available. Degraded with the firewater deluge system available, Critical with the firewater deluge system available, Degraded with the firewater deluge system unavailable, Critical with the firewater deluge system unavailable.

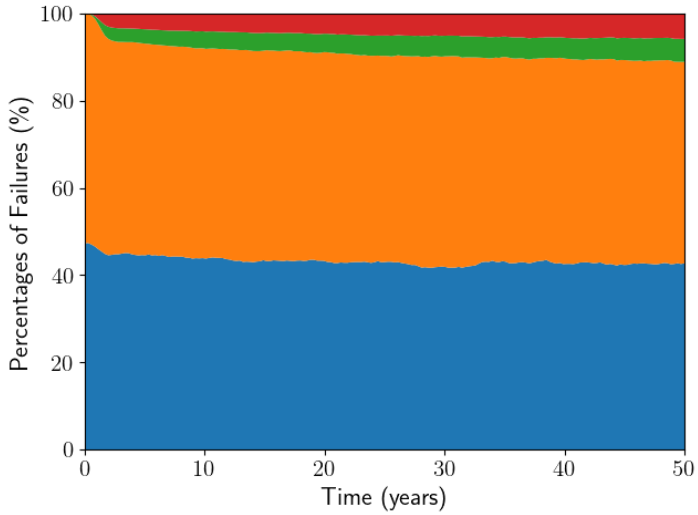

Figure 6.14: The percentage of failures for *Valve 3* as a function of the platform age from the different failure modes with and without the firewater deluge system available. Degraded with the firewater deluge system available, Critical with the firewater deluge system available, Degraded with the firewater deluge system unavailable, Critical with the firewater deluge system unavailable.

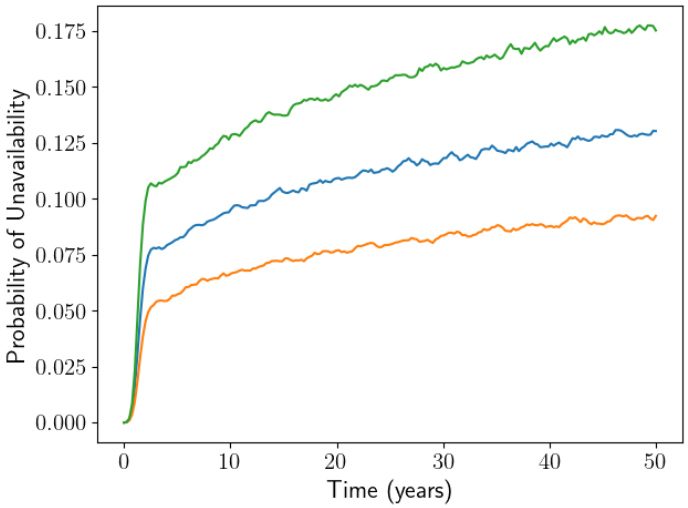

Figure 6.15: The probability of the separation module's firewater deluge system being unavailable for different AM strategy. *Strategy A*, *Strategy B*, *Strategy C*.

it can be inferred that the probability of failure of the firewater deluge system must also increases. This is confirmed by Figure 6.15 which shows the unavailability of the firewater deluge system increase in both modules through the platform's life-cycle. Here, strategies A, B and C are plotted, where strategies B and C will be examined later in this chapter.

As the HSPN calculates the probability of failure and the consequence analysis determines the magnitude of that failure, a risk can be evaluated for each consequent event. The probability of failure is a function of platform age, t, thus the risk can also be calculated to also be a function of platform age. The risk profile for a consequence event, C, is given by,

$$R_C(t) = \sum_{F\in\{Deg,Cri\}} \sum_{D\in\{Av,Un\}} P_{F,D}(t) P_{F,D}(C) \mathbb{E}[P(M_{F,D})] \tag{6.16}$$

Where, $P_{F,D}(t)$, is the probability of failure mode F with the firewater deluge system in state D at time, t, $P_{F,D}(C)$ is the probability of consequence C. $\mathbb{E}[P(M_{F,D})]$ is the expectation value of the magnitude's probability density function. To account for all scenarios that could cause the consequence, the risk is summed over the four possible inputs defined by the two failure modes and the two availabilities of the firewater deluge system.

As the three consequent events measure different types of event and are in different units they should not be directly compared. Thus, their risk is calculated separately, denoted as $R_{\mathrm{C,Ovp}}$, $R_{\mathrm{C,JFL}}$ and $R_{\mathrm{C,PFL}}$ for overpressure, jet fire length and pool fire

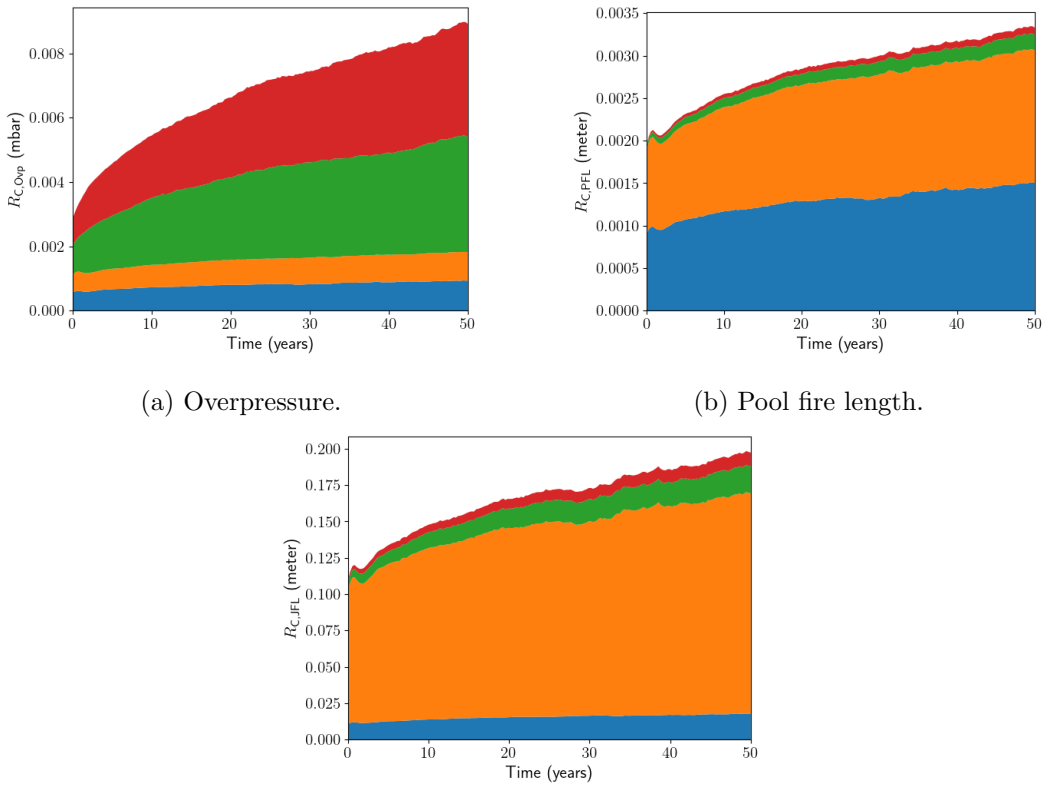

(a) Overpressure.

(b) Pool fire length.

(c) Jet fire length.

Figure 6.16: The risk profile of each consequence caused by Valve 3, categorised into risk contribution from each failure mode. Degraded with the firewater deluge system available, Critical with the firewater deluge system available, Degraded with the firewater deluge system unavailable, Critical with the firewater deluge system unavailable.

length respectively. These risk profiles are given in Figure 6.16, categorised into the contributions from each failure mode and firewater deluge system availability.

All of the risk profiles increase with platform age, which reflects the increasing probability of failure. However, the rate at which the risk of overpressure increases exceeds the corresponding rates in the pool and jet fire lengths. This is a result of the failure probability of the firewater deluge system increasing with the platform age, which can be seen in the contribution from the failure modes where the unavailable firewater deluge system are greater than the failure modes with it available. This corresponds to an increase as overpressures are greater when the firewater deluge system is unavailable, defined by $O_{\max}$, A and B in Equation 6.13. The pool fire length has a similar profile to the risk, this indicates that the magnitude of the degraded and critical

failure modes must be similar. Conversely, the jet fire length has significantly greater magnitudes from the critical failure modes compared to the degraded, which demonstrates the increased risk from the critical failure mode. The risk from the different consequences incentives an effective AM strategy which will provide a high firewater deluge availability and reduce failure rates, in particular of critical failure modes.

6.9 Asset Management Strategy Comparison

The risk profile for a consequence event was given in Equation 6.16, this was defined for the expectation value of the magnitude's probability density function. The risk profile can be generalised to be a function of both platform age, t, and magnitude M, through the equation,

$$R_C(t, M) = \sum_{F \in \{Deg, Cri\}} \sum_{D \in \{Av, Un\}} P_{F,D}(t) P_{F,D}(C) P(M_{F,D}). \tag{6.17}$$

Thus, the risk profile can be plotted as a two-dimensional heat-map with respect to platform age and consequence magnitude. As before, the risk profile between the consequences cannot be compared, however, the risk profile can be used to compare the performance of different AM strategies.

Risk profile heat-maps are plotted for three AM strategies in Figure 6.17. The three AM strategy are given explicitly in Appendix B in Section B.4, these are denoted A, B, C.

It can be noted that the risk of greater magnitudes increases with platform age for all of the strategies and consequences. This is as the probability of failure increases with platform age due to the degradation, thus more leaks will occur and thereby will increase the risk across all magnitudes. It can be seen that the more proactive AM strategies, such as strategy B, have lower overall probabilities in comparison to the less proactive AM strategies, such as C, this would be expected as the probability of a failure decreases with well-maintained assets.

The effect on the overpressure is prominent as the overpressure is significantly increased when the firewater deluge system is unavailable, as discussed in Subsection 6.5.1. In strategy C's overpressure heat-map, it can be seen that the probability of larger overpressures is increased. This implies that the AM strategy is inadequate for controlling risk and specifically that the probability of the firewater deluge system being unavailable is too high. This is confirmed by Figure 6.15, where the probability

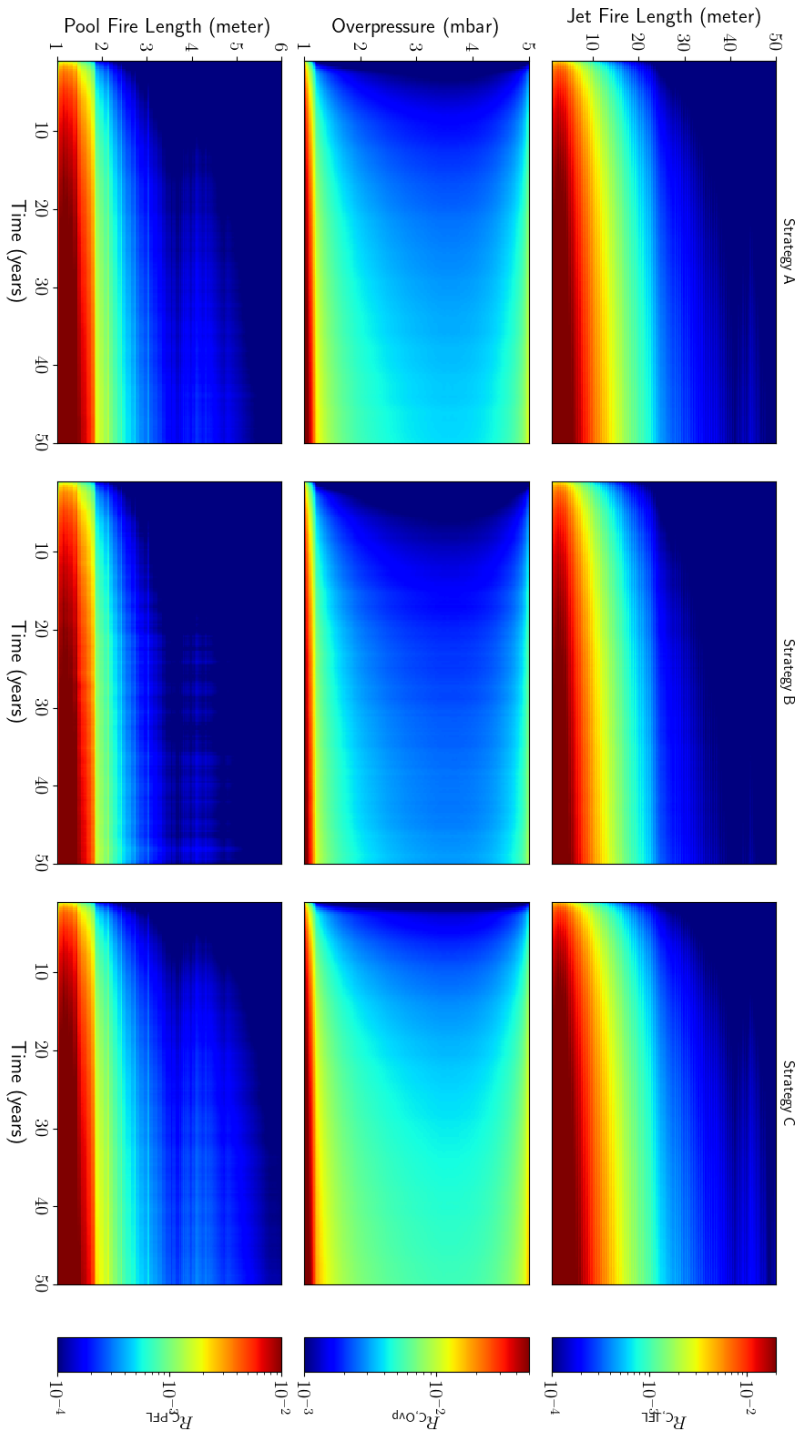

Figure 6.17: The total probability density of the consequences' magnitudes throughout the platform life-cycle for AM strategy *A*, *B* and *C*.

of the separation module's firewater deluge system for the three strategies is given. The probability of unavailability increases for all the strategies through the platform lifecycle, demonstrating the increased challenges of LE. In contrast strategy B, has a relatively low probability of a high overpressure at any platform age. Although, the probability of a smaller overpressure is still likely, visible as a thick line from 0 mbar to approximately 0.35 mbar, at all platform ages. This corresponds to an explosion when the firewater deluge is available which suppresses the explosion and reduces the overpressure, as discussed in Subsection 6.5.1.

In strategies A and C, the probability density can be seen to increase with platform age across all magnitudes. This demonstrates the increased risk that the platform is exposed to as it ages and enters into a LE stage. Strategy B demonstrates that the risk can be controlled and to not increase as the platform ages with sufficient maintenance and inspections. However, this strategy is not necessarily efficient, maintenance and inspections may be performed that do not meaningfully contribute to controlling the risk and thereby unnecessarily increase the AM expenditure. The process of finding efficient strategies that are effective in controlling risk and maximising production is tackled in Chapter 7 using an optimisation algorithm.

6.10 Summary and Discussion

This chapter has presented a consequence analysis technique for a hydrocarbon leak from a production vessel, triggered by failure modes in the HSPN model. The purpose of this analysis was to determine both the probability of escalation events and their magnitude's for a leak from an arbitrary vessel. Unique analyses were performed for every production asset and failure mode with all possible states of the safety systems. Thereby, providing a useful metric for investigating the consequences associated with platform simulations.

The analysis was centred on the evaluation of small iterative time-steps of 0.1 seconds that calculated the rate of oil or gas leakage and the changing quantities inside the vessel and in the surrounding module. In comparison to other CFD techniques this made more assumptions but this allowed for numerous simulations to be quickly performed. From the quantities of oil and gas in the module three escalation events were considered, pool fires, jet fires and explosions. The probability of occurrence of each of these events and of no escalation was determined through the use of a MC method to stochastically sample the scenario's initial conditions. In addition

probability density functions for the magnitudes of the possible consequent events were constructed.

Separate analyses were performed for every production asset and their leak failure modes. These were pre-processed to provide a high degree of detail to the HSPN without incurring a high computational footprint. It is reasonable to assume that this approach could be taken for an application to real vessels, as it only requires initial conditions on the vessel's dimensions and the fluids contained. This functioned such that whenever a failure of the appropriate observable occurs in the a HSPN, a look-up table retrieves the corresponding consequence analysis result and adds it to the simulation's total consequence analysis results.

The integration of the HSPN and consequence analysis provided a good methodology for evaluating the risk associated with a given AM strategy. The HSPN calculates the probability of leak failure modes which was combined with the consequence analysis to produce the risk associated possible consequence events. The contribution to the risk was seen to not be equal from each failure mode. For explosions, the overpressure risk contribution was greatest from the failure mode with the firewater deluge system unavailable. Whereas, for jet fires, the risk was dominated by critical failure modes.

The risk profile was expanded to be a function of both platform age and of magnitude, which allowed a comprehensive understanding of the time-evolution of the risk. Applied to all of the assets in the platform, the risk profile could be used to evaluate the effectivity of a given AM strategy with respect to the risk from leaks. Three example AM strategies were compared, which demonstrated the change in risk when enacting a more or less proactive strategy. Although, it can evaluate the effectivity of a strategy it does not consider the expenditure. This is addressed in the following chapter through the use of an optimisation algorithm.

Chapter 7

Optimisation

7.1 Introduction

Together the HSPN and consequence analysis form an integrated model for simulating a production platform's life-cycle, accounting for the degradation, AM and the consequences of leak events. It can be configured with various AM strategies through the initial marking and transition delays in the HSPN, then can be used to determine several metrics, including the mean number of inspection and maintenance actions performed, the frequency and magnitude of leak events and the oil and gas production quantities. Thereby, the model can be used to evaluate the performance of various AM strategies. Although, the AM strategy has many variables, as will be discussed in Section 7.4, so it is difficult to manually find the optimal strategy. This is the motivation behind creating a technique for exploring the AM strategy search space and finding optimal solutions. In this chapter, an optimisation technique will be presented to determine a set of optimal AM strategies using the HSPN and consequence analysis to evaluate the performance of each strategy.

There are different objectives to measure the performance of the platform with, that often conflict with each other. For example, the production will want to be maximised whereas the number of maintenance tasks will be wanted to be minimised for a smaller expenditure, although, more maintenance will ensure a high production availability. It is important to be able to consider the different objectives of the platform's performance simultaneously and thus a multi-objective optimisation technique was chosen.

There are several approaches to optimise a multi-objective problem, some of which

were discussed in Section 2.5. A multi-objective optimisation technique aims to determine solutions that simultaneously optimise multiple criteria. It is advantageous to use a technique that does not require any weighting or preference of the objectives, as it does not require any assumptions on the importance of the objectives. Instead an algorithm is used that produces a set of solutions that span the Pareto surface, this allows a user to select a strategy based on the optimal solutions with different pay-offs between objectives.

First introduced by John Holland in 1960 and extended by David Goldberg in 1989, a genetic algorithm is an optimisation technique that is inspired by the process of evolutionary biology (Tsoukalas and Uhrig 1997; Sadeghi, Sadeghi, and Niaki 2014). It mimics the evolution of a genetic code through the comparisons of the fitness of solutions and a breeding process that passes genetic code through generations. A genetic algorithm is a general purpose technique that is frequently used to generate solutions to a wide variety of problems. In this work a genetic algorithm is applied to the model to determine a set of optimal solutions to the AM strategy. Some variants of a genetic algorithm are capable of optimisation with multiple objectives, as discussed in Section 2.5. In particular, a variant known as the Non-Dominated Sorting Genetic Algorithm II (NSGA-II) was selected to be applied to this model.

This technique had a few attributes that led to it being chosen, these included:

- The algorithm is computationally fast, with a complexity of $O(MN^2)$, where M is the number of objectives and N is the population size (Verma, Pant, and Snasel 2021).
- It is elite preserving meaning that the non-dominated solutions transfer between generations without alteration. This helps retain the optimal solutions.
- A crowding distance is calculated to preference solutions that are distant in solutions space, which helps produce a solution set that is diverse.

The details of these attributes are discussed in detail in Section 7.3.

7.2 Objective Selection

To be able to compare the relative success of each AM strategy in the model, an objective vector must be defined that can be evaluated by the model. The optimisation aims to minimise or maximise each value in the objective vector. Typically, the solutions are conflicting and it is impossible for all of them to be optimised by a solution. In-

stead NSGA-II produces a set of solution that each are a pay-off between the different objective values.

The search ability of multi-objective evolutionary algorithm significantly decreases as the number of objectives increases. There are two main reasons, firstly, the number of non-dominated solutions increases and secondly, there is an exponential increase in the number of solutions required to approximate the Pareto surface (Purshouse and Fleming 2003; Khare, Yao, and Deb 2003; Ishibuchi, Tsukamoto, and Nojima 2008). Generally, multi-objective evolutionary algorithms are considered effective up to 3 objectives, which is in alignment with the objective vector used in this work.

The objectives are chosen to measure disparate aspects of the system's performance, to provide an overall view of the platform from multiple perspectives. In many cases, to improve one of the objectives will correspond to a negative effect in the other, through use of a multi-objective algorithm there is no requirement to specify any preference or weighting between the objectives. Specifically the following three objectives were selected,

1. **Production**: The total production quantities oil and gas through the platform's lifetime, given as a fraction of the maximum possible production. The algorithm aims to maximise this.
2. **AM expenditure**: The total expenditure on inspection and maintenance actions. The algorithm aims to minimise this.
3. **Escalation events**: The total number of escalation events caused by the leakage failure mode of the production assets. The algorithm aims to minimise this. The magnitudes were not used as objectives because they can cannot be directly compared and therefore three additionally objectives would be required, which would be much more difficult to successfully optimise.

Each solution is evaluated through many simulations of the model with the given AM strategy, the objective values are the mean results from the simulations. This is as the model has stochastic elements and therefore many simulations are required to gain an accurate result. The exact definitions of these three objectives vectors are detailed in the following sections.

7.2.1 Production

This objective measure the total oil and gas production of the platform, and the optimisation technique will aim to maximise the value. These are given by the final

marking of two continuous places, corresponding to the *Oil Export* and *Gas Export* in Figure 3.3. These places accumulate marking throughout the platform's life-cycle, at any time the flow is dependent on the failure modes of the assets in the production chain. Recall from Section 3.5, that the flow rate is reduced for an asset in a degraded failure mode and is zero for an asset in a critical failure mode. Furthermore, the production system is reliant on the main power system, thus a failure of this will cause production to cease. Thus to ensure that there is a high production, an effective AM strategy is required to maximise the availability.

The production objective is calculated as a normalised value from the total production of the oil and gas, such that,

$$P = \frac{P_{\mathrm{o}}}{2P_{\mathrm{o,max}}} + \frac{P_{\mathrm{g}}}{2P_{\mathrm{g,max}}} : P \in [0, 1]. \tag{7.1}$$

Where, P_{o} is the total oil production, $P_{\mathrm{o,max}}$ is the maximum possible oil production, P_{g} is the total gas production and $P_{\mathrm{g,max}}$ is the maximum possible gas production.

7.2.2 Asset Management Expenditure

Maintenance and inspections have associated costs, for economical running a duty-holder would want to minimise the expenditure spent on these, while ensuring a productive and safe platform. Within the HSPN, each maintenance and inspection substitution transition has a place, initially unmarked and iterated every time an action is performed, that is used to count the number of actions. P_{mCounter} in Figure 4.18 stores the number of maintenance actions performed on that condition chain. For inspections, in Figure 4.13 P_{iCounter} stores the number of inspections actions performed, either internal or external, on the asset.

It would be expected that, maintenance on different assets and condition chains would have different costs associated with them. Similarly, the cost of an inspection would vary with both the asset being inspected and whether it is an internal or external inspection. To account for this the cost of each maintenance actions and inspections is individually defined for each condition chain and inspection type on every asset. The exact values are given in Section B.3, as no precise maintenance and inspections values could be found these are intended to be just indicative. It is reasonable to assume that a duty-holder would have approximate expenditures for the various maintenance and inspections actions that could be applied to this model.

To calculate the AM expenditure, E_{AM}, the sum must be taken of the product of

the maintenance or inspection and their cost. Additionally, the cost of the maintenance and inspections teams must be included, this incentives the strategy to minimise the crew size. Explicitly,

$$E_{\text{AM}} = \left(\sum_{i=1}^{N_M} C_{i,M} E_{i,M}\right) + \left(\sum_{i=1}^{N_I} C_{i,I} E_{i,I}\right) + N_{\text{M,Teams}} E_{\text{M,Teams}} + N_{\text{I,Teams}} E_{\text{I,Teams}}, \tag{7.2}$$

where N_M and N_I are the number of maintenance and inspection actions and $E_{i,M}$ and $E_{i,I}$ are the i^{th} maintenance and inspection expenditures. $C_{i,M}$ and $C_{i,I}$ are the i^{th} final markings of maintenance and inspections counters, P_{mCounter} and P_{iCounter}, respectively. $N_{\text{M,Teams}}$ and $N_{\text{I,Teams}}$ are the number of maintenance and inspection teams and $E_{\text{M,Teams}}$ and $E_{\text{I,Teams}}$ are the costs per team.

7.2.3 Escalation Events

When a production asset enters into a leak failure mode it corresponds to an input to the consequence analysis based on the current state of the HSPN, as discussed in Section 6.7. The consequence analysis' results give the probability of the three escalation events and of no escalation, these vary between the production asset, failure mode and the availability of the module's firewater deluge system. The probabilities are denoted here as, $Pr(E_i)$, for $i \in \mathbf{I}$, where $\mathbf{I}$ is the set of possible escalation events, $\mathbf{I} = \{\text{Explosion}, \text{Jet Fire}, \text{Pool Fire}\}$ Through the Monte Carlo simulation of the HSPN the probability of each consequence analysis input can be determined, $Pr(I)$. This can be used to determined the total number of escalation events, N_E, given by,

$$N_E = Pr(I) \sum_{i \in \mathbf{E}} Pr(E_i). \tag{7.3}$$

7.3 Non-Dominated Sorting Genetic Algorithm II

The algorithm was initially introduced in by Deb (1999) and was later developed further into its second iteration (Deb et al. 2002). It has been a popular technique with a literature review of multi-objective optimisation in maintenance by Syan and Ramsoobag (2019) finding that NSGA-II was the most commonly used multi-objective technique, accounting for 32% of the literature surveyed. The most notable part of NSGA-II, is its fast-non-dominated-sorting algorithm which ranks the solutions, this has been central to its success (Hamdani et al. 2007). Verma, Pant, and Snasel (2021)

note how the computational run time of the algorithm is fairly low, with a time complexity of $O(MN^2)$, where M is the size of the objective vector and N is the size of the population in each generation.

At the core of NSGA-II is a Pareto-based ranking process, the purpose of this is to create an ordered list of solutions according to their dominance over other solutions. As previously discussed, a solution is said to dominate another solution if and only if all of its objectives are more optimal or equal to the other's objectives with at least one objective being more optimal. This was discussed in detail in subsubsection 2.5. For each solution a ranking can be defined, which is the count of how many solutions dominate it. There will always be at least one solution with a ranking of zero, meaning that no solutions dominate it. The set of solutions with a ranking of zero are known as the non-dominated front and define the optimal solutions, through the generations the algorithm aims to minimise the distance between these solutions and the Pareto surface. Therefore this algorithm is ideal as it produces a diverse set of solutions that showcase the effects of an AM strategy.

Another key element of NSGA-II is that it is elite preserving, this means that the best solutions from one generation are carried into the next generation. This ensures that the best solutions remain in the population throughout the process. Research by Zitzler, Deb, and Thiele (2000) determined that elitism improves the convergence rate of an optimisation algorithm. One disadvantage of NSGA-II, and any GA technique, is that it is not guaranteed to converge to the global optimal solution but can be stuck in a local optima (Wang 1997). However, the diversity mechanisms of NSGA-II help to reduce the probability of becoming stuck in a local optima.

NSGA-II's breeding process is composed of a series of algorithms and operators that are combined to take a population of solutions and create a new population based on their objective vectors. The algorithms and operators are first introduced here individually, where their purpose and mechanisms are explained. Once these are described, the breeding process is detailed which utilises all of these algorithms and operators within a loop to iterate through generations and converge on an optimal set of solutions.

7.3.1 Binary Tournament Selection

A binary tournament selection is a method that creates a new population by performing many tournaments between randomly selected solutions. To perform binary

tournament selection two solutions are randomly selected from the population (Sivaraj and Ravichandran 2011). A tournament is performed between these two in which the fittest solution is selected. This process is then repeated until a new population of the desired size is created. This process is biased towards selecting the best solutions but will preserve genetic variety across the population. Thus the fitness of the new population is increased as the fittest solutions tend to be repeated in the new population.

In a single-objective optimisation the fittest solution is obvious but in a multi-objective optimisation this is not the case as one objective may be more optimal whereas another objective is not. In the case of NSGA-II the fittest solution is determined by the solution that is dominated by the fewest other solutions. This is known as the solution's rank and will be used in the *Fast-Non-Dominated-Sorting Algorithm*, discussed in Subsection 7.3.4.

It is important to note that although the most fit solution will be selected for any tournament, the selection process does not guarantee the fittest solutions will continue to the next generation. As the solutions are randomly selected from the population then relatively unfit solutions can still be selected for the next generation when two unfit solutions are selected for the tournament. This randomness prevents the solutions converging too fast and thus prevents niche's from forming which can lead to local optima being found instead of the global optima.

7.3.2 Crossover Operator

The crossover operator combines the chromosomes of two parents to generate offspring. It is based on biological reproduction to simulate the mixing of two parent's genes. There are several different types of crossover operators that produce their offspring with different methodologies (Umbarkar and Sheth 2015). Furthermore the different encodings of the genes may necessitate different techniques.

In this work each gene in the chromosome is encoded as a binary bit, that is the gene can either be a 0 or 1. In this thesis' work there are several decision variables that cannot be encoded as a 0 or 1, for example the inspection interval is taken from a selection of discrete timings. To encode this the discrete set of intervals are indexed and several bits are used to form a binary number that is equal to the interval's index.

A uniform crossover operator is used in this research. An offspring's binary gene is chosen by randomly selecting one of the two parents and taking the gene's value

from that parent. This is repeated for each gene until an offspring's chromosome is formed. An example of the transferring of the genetic code of two parents to produce an offspring is given in Figure 7.1.

Parent 1	0	1	1	0	1	1	1	0	0	1	1	0
Parent 2	1	1	0	1	0	0	0	1	1	0	1	1
Offspring	1	1	1	0	0	1	0	1	1	0	1	0

Figure 7.1: The breeding of two parent's genetic code to produce an offspring. The genes carried over from the parents to the offspring are shown in boxes.

7.3.3 Mutation Operator

To introduce randomness into a solution's genetic code the mutation operator is used. The benefit of having randomness in the genetic code is two-fold, firstly, to create novel solutions that would not be found through breeding and secondly, to aid in avoiding solutions becoming stuck in local optima.

The mutation operator acts on the genes of an individual after selection and crossover to introduce randomness into the genes (Koenig 2002). Associated with the mutation operator is a probability, $M_P \in [0, 1]$, for every binary gene a random number, χ, is stochastically sampled from a uniform distribution on the domain $[0, 1]$, if $\chi < M_P$ then the binary gene is flipped.

7.3.4 Fast-Non-Dominated-Sorting Algorithm

The fast-non-dominated-sorting algorithm produces a series of *fronts*, these are sets of solutions with equal domination counts. This is such that each solution in a front is dominated by an equal number of solutions in the population. The first front is the set of solutions with a domination count of zero, therefore these solutions are non-dominated by any solution in the population. The algorithm is constructed to minimise the comparisons between solutions required such that the computational time is minimal.

The algorithm begins by considering each solution in the population, $x \in P$, these are compared through the domination operator against every other solution, $y \in P$. This determines, firstly, a set of solution that x dominates such that $X_a = \{y | x \prec y\}$ and, secondly, the number of solutions that dominate y given by $m_a = |\{y | x \not\prec y\}|$.

The first front is found by identifying the non-dominated solutions, this is given by $F_1 = \{x | d_x = 0\}$. Next the solutions of the first front are iterated through, $x \in F_1$, and all of the solutions in it's set of dominated solution $y \in X_a$ have their domination counter, m_b reduced by one. If any of these now equal zero then they are added to the second front. This is repeated through each front until all of the fronts are identified.

7.3.5 Crowding Distance Assignment

The crowding distance assignment is used to increase the diversity of the population. It represents the distance between solutions in objective space. Constructing the next generation's population is done in order of fronts, when a front is reached that if added in its entirety would make the new population too large, then the crowding distance is calculated to select which of the solutions will be passed to the next generation. The solutions are selected in order of decreasing crowding distance such that the distance between the solutions is maximised.

Considering a single front F_k, for each solution, i, a crowding distance, $d(i)$, is calculated, this is the sum of crowding distance contributions $d(j;i)$ for all the objectives $\mathbf{o}(i) = \{o_1(i), o_2(i), \ldots, o_n(i)\}$ When calculating an objective's crowding distance, the objectives for all the solutions are sorted, such that $o_j(i) \leq o_j(i+1) : \forall i \in F_k$. A contribution for objective j is given by,

$$d(j;i) = \begin{cases} \left(o_j(i+1) - o_j(i-1)\right) / \left(o_{j,\max} - o_{j,\min}\right) & : \quad 1 < i < n \\ \infty & : \quad i \in \{1, n\} \end{cases}, \tag{7.4}$$

where $o_{j,\max}$ and $o_{j,\min}$ are the maximum and minimum values of the objective function. Note that the first and final objective values are assigned infinity, due to the sorting these are the most extreme in the front for objective j. Thus they are considered the most diverse solutions and so are assigned infinity.

Finally the crowding distance for solution i is given by the sum of $d(j;i)$ for $j \in \{1, 2, \ldots, n\}$, such that

$$d(i) = \sum_{j=1}^{n} d(j;i). \tag{7.5}$$

Through this a crowding distance is defined for each solutions, this is used as part of the breeding process.

7.3.6 Breeding Process

The breeding process connects the operators and algorithms described in the above subsections to form the complete NSGA-II. The process is constructed through a number of steps that are summarised in the flow chart shown in Figure 7.2. The purpose of the breeding process is to create a new generation of solutions based on the domination and diversity of the solutions in the current generation.

The main body of the flow chart is a loop that defines the breeding of the next generation. Broadly, the objective functions are calculated for each solution in the population, these are then ranked based on their domination of other solutions. A new generation is then created through breeding the solutions with the binary tournament selection

The process is initialised by creating a randomised population, which the process will breed and mutate into fitter solutions. A population, P_0, is constructed of N solutions, where the binary genes of each solution are randomly sampled such that the population is at a maximum entropy. Additionally, the generation counter, i, is initiated at zero, this will keep track of which generation is currently being evaluated.

The main loop of the algorithm begins with a population, P_i, of solutions, the first step is to evaluate the objective functions of each solution and then determine the non-dominated rank of each solution. An offspring population, O_i, is generated by a series of binary tournament selections from P_i with the victorious solution having the lesser rank. The offspring solutions are created through the crossover operator on the two parent solutions from the tournament. To complete the offspring population the mutation operator is applied to the solutions causing random mutation in the genes, which aids in avoiding solutions become stuck in local optima. Finally the objective functions of the solutions in the offspring populations are calculated, these will be used in the next step.

Next, a combined population, C_i, is constructed as the union of the parent population, P_i, and the offspring population, O_i, such that $C_i = P_i \bigcup O_i$. The fast non-dominated sorting algorithm is then applied to the combined population, this ranks the solutions by the number of solutions they are dominated by. The solutions are sorted into sets of equal rank, known as fronts, such that the front, F_3, consists of solutions that are dominated by three other solutions. Therefore, the front F_0 represents the most optimal solutions in the population as they form the non-dominated front, as the algorithm progresses this aims to approach the Pareto surface. It is important

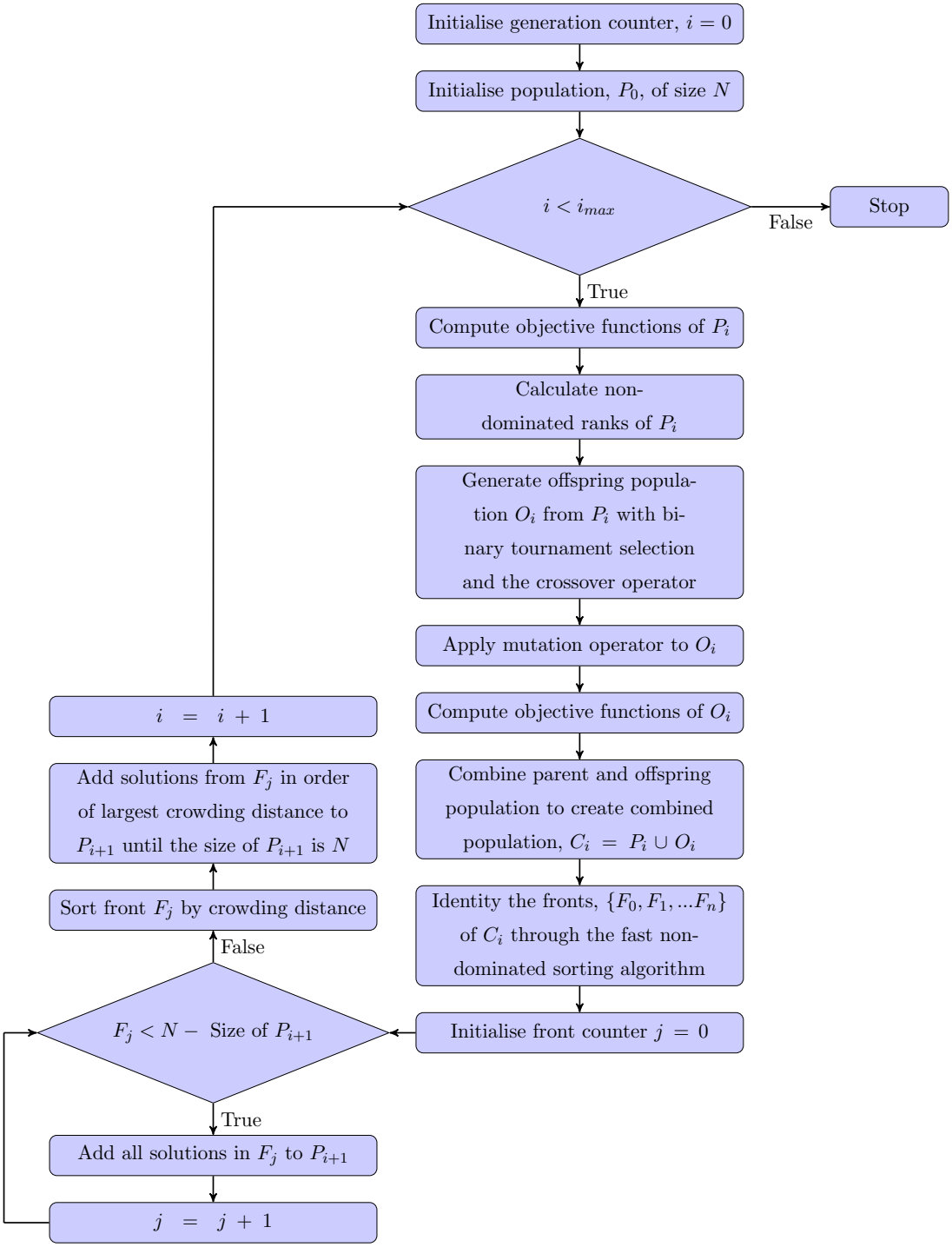

Figure 7.2: Flow chart of the NSGA-II algorithm.

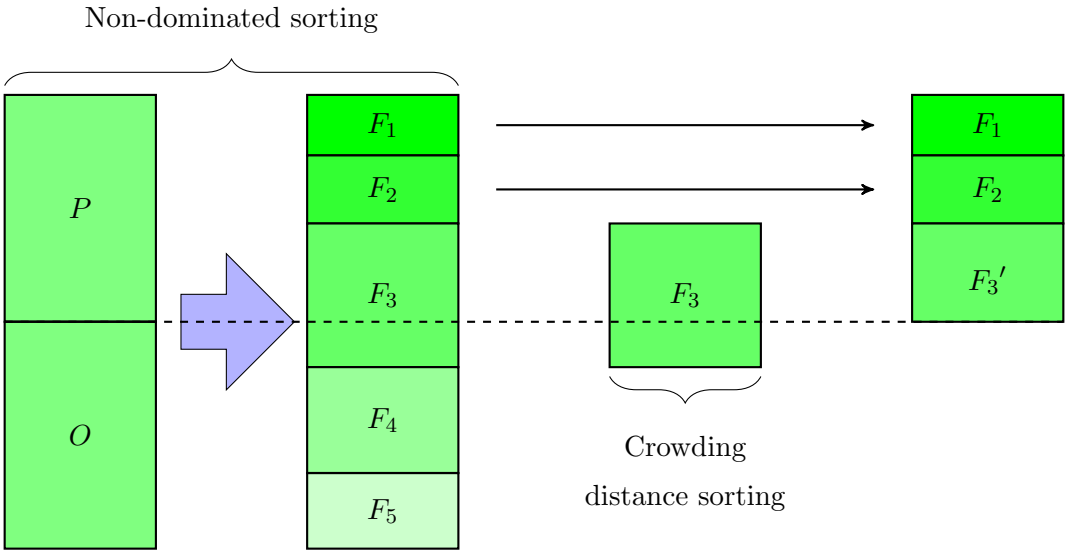

Figure 7.3: NSGA-II Algorithm.

to note that this ensures elitism, since the non-dominated front from both the parent and offspring populations is preserved into the next generation.

The next generation's population, P_{i+1}, is constructed by considering the fronts in sequence, beginning with front F_0 and continuing until P_{i+1} contains N solutions. Considering a front F_j containing M solutions then all of the solutions in F_j are added to P_{i+1} if and only if $L + M \leq N$, where L is the number of solutions in P_{i+1}. Otherwise, if $L + M > N$, then the solutions will not all fit in P_{i+1}, in this case, crowding distance assignment is used on the front to sort the solutions by their proximity to other solutions in the front. These solutions are then added in decreasing order of crowding distance to P_{i+1} until it contains N solutions. This concludes the construction of the next generation's population, the final step is to increment the generation counter, i. The loop is then repeated until $i > i_{\max}$, where $i_{\max}$ is the predefined maximum number of generations. Visually the breeding of the combined population to the next generation's population can be seem in Figure 7.3.

7.4 Application to the Model

So far, the NSGA-II has been described as a general purpose technique, in this section the algorithm is applied to the HSPN model. As discussed in Section 7.2, the AM strategy is optimised to maximise production, and minimise the number of escalation events and AM expenditure. Changes in the AM strategy are represented by changes

in the initial conditions of the HSPN which in turn affect the performance of the simulated platform.

The decision variables of NSGA-II represent the AM strategy and are stored in the genetic code of the solution. Each decision variable defines an initial condition in the HSPN, which can be a place's initial marking, the constant delay associated with a timed transition or the priority associated with a transition. There are five variable types that define the AM strategy which were first discussed in Section 3.9. A further description of the variables and how they are defined are given in Subsection 7.4.2, Subsection 7.4.1, Subsection 7.4.3 and Subsection 7.4.4. The decision vector is composed of many instances of these variable types, totalling 1255 decision variables.

The genetic code is composed of a series of binary genes, thus each gene can encode only two values. Many of the AM strategy variables are not boolean valued and therefore cannot be encoded by a single gene, instead they are encoded in binary by a series of genes. For instance, the possible values of the inspection interval cover all of the weeks in the simulation time which is 2600 values. The number of binary values needed to encode this range is given by,

$$N_G = \lceil \log_2(R) \rceil, \tag{7.6}$$

where $\lceil \cdot \rceil$ is the ceiling function. This is such that the binary representation can exceed the variable's range when $\log_2(R)$ is not an integer. When decoding the genes and applying them to the HSPN the variables are limited to the maximum of the range. This will create a bias towards the maximum value of the gene, although this effect is not apparent in the results. For decision variables where the range can be selected freely, they are selected such that $\log_2(R) \in \mathbb{N}$, so as to remove any maximum bias. The range and number of genes for each AM strategy variable are given in Table 7.1, in addition the number of instances of each gene in the model are given. It can be seen that in total there are 13970 genes, nevertheless it will be seen that the algorithm is successful with such a large decision space.

In the case of this model the evaluation of the objective functions corresponds to performing a MC simulation of the HSPN with initial conditions defined by the solution's genes. The results of the MC simulation include the values for each objective and in doing so define the performance of the solution. Due to the stochastic elements in the HSPN, a MC simulation is required to reduce the uncertainty of the objective functions. Nevertheless, the number of simulations are limited by computational power and time and a balance must be struck between a sufficient number of simulations

Variable Type	**Range**	**Binary Genes**	**Instances**	**Total Binary Genes**
Inspection interval (weeks)	$[1, 2600]$	12	97	1164
Maintenance decision	$[2, N_C - 2]$	$\lceil \log_2(N_C) \rceil$	218	654
Opportunistic maintenance decision	$[0, 1]$	1	32	32
Inspection teams	$[1, 64]$	6	1	12
Maintenance teams	$[1, 64]$	6	1	12
Maintenance priority	$[0, 511]$	9	1344	12096
		Totals	1693	13970

Table 7.1: AM strategy variable types, their value range, the number of genes required to encode this and the number of instances of the gene in the model. Here, N_C is the number of conditions in the observable associated with the maintenance decision.

and acceptable computational demands. Fortunately, genetic algorithms are resilient to noisy objective functions with high degrees of uncertainty (Friedrich et al. 2016; Goh and Tan 2007). It was decided that the objective function would evaluate each solution with 100 simulations of the HSPN. This was chosen as a balance between the computational requirements and the convergence of the model's results. Through experimentation of different number of simulations it was decided that each objective function will be evaluated through 1000 simulations of the HSPN, this was found to result in a good balance. In Section 5.3, it was seen that by 1000 simulations the results were showing a good convergence. The optimisation was performed over 1000 generations with a population of 100 solutions and the mutation probability was set to 0.05. This was found to give a good results set.

7.4.1 Inspection Intervals

The inspection interval variables define the minimum time interval between inspections being performed. The actual time between inspections can be greater as inspections can only be performed when at least one inspection team is available, thus insufficient teams can lead to delays in the inspection being performed. The interval is defined individually for each inspection in the model, in total this comes to 103 variables. The variable defines a constant time delay associated with timed transition, T_{iClock2}, in the inspection clock substitution transition shown in Figure 4.13. As the gene is encoded by binary only a discrete set of time intervals can be defined, in this work increments of one week were used. The gene allowed the algorithm to have the freedom to select any interval over the whole simulation time, to the resolution of a week. This large range allows for the optimisation to select the inspection interval to be longer than the platform's lifecycle, in effect defining a run-to-failure strategy.

7.4.2 Maintenance Decision

A maintenance decision variables defines the first condition from which preventive maintenance is performed. For instance, if an observable had a maintenance decision of 3 then maintenance will be queued when an inspection reveals the observable to be in condition 3 or worse. The maintenance decision is defined individually for every assets' observables, thus giving the optimisation complete control over the maintenance strategy. The minimum value of the variable is 2 as preventive maintenance cannot be performed on the first state as this represents the good-as-new condition. As the

number of condition states in an observable can vary the range of the variable is $[2, N_C - 2]$, where N_C is the number of conditions in the observable.

The variable defines the decision places, $P_{\text{mDecision}}$, in Figure 5.13. For a given observable there are two $P_{\text{mDecision}}$ places per condition, one for a state with an incipient failure and one without. Therefore, an observable has two maintenance decision variables for with and without the incipient failure mode, both corresponding to a set of N_C decision places. For example, a maintenance decision of 3 will correspond to the 2^{nd} condition's decision place being unmarked, with the remaining, more degraded, conditions' decision places being marked. Thereby, allowing preventative maintenance for the 3^{rd} and more degraded revealed conditions. The prioritisation of the maintenance backlog is discussed in Subsection 7.4.4.

7.4.3 Asset Management Teams

The AM team variables define the number of inspection and maintenance teams available on the platform. Unlike the other variables, the inspection and maintenance teams have only one instance of each in the model. The inspection teams variable defines the initial marking of P_{iTeams}, seen first in Figure 4.13. Similarly, the maintenance teams variable defines the initial marking of P_{mTeams}, seen first in Figure 4.18. As the teams are shared between all assets they can be seen in every asset net, shown in Appendix A. Insufficient teams can result in failures not being spotted, which can result in asset unavailability. The unavailability of a safety asset can increase the risk during a leak event, while the unavailability of a production asset can result in lower production quantities. These are both measured by objectives and thus the optimisation while aim to minimise production asset unavailability.

It was seen in Subsection 5.3.5 that the maintenance queue depth is related to the number of AM teams. It was demonstrated that the critical number of teams was 3 for AM strategy A. As the optimisation can define a wide range of strategies the critical number of teams has the potential to greatly vary and far exceed 3. Therefore, the range of the decision variable was set to $[1, 64]$.

7.4.4 Maintenance Prioritisation

The maintenance prioritisation is implemented in the NSGA-II by associating each transition with a priority given through the corresponding genes. The priority is asso-

ciated with transition, T_{mChecks}, seen in the maintenance action substitution transition, shown in Figure 4.18. When there is a maintenance backlog, multiple of these transitions will be simultaneously enabled. The order in which these transitions fire is determined by their relative priorities. The maintenance priority's genes have a range of $[0, 511]$, which is defined such that the priority corresponding to 0 as the minimum and 511 as the maximum, the transitions with the lowest value will fire first.

7.4.5 Opportunistic Maintenance Decision

An opportunistic maintenance decision variable defines if maintenance will be queued for all of an asset's observables when maintenance has been queued for one of the observables. If an inspection reveals an observable is degraded such that the maintenance decision qualifies it to be queued for maintenance, then, if enabled, the opportunistic maintenance decision will queue maintenance for all of the asset's observables. The HSPN implementation of this was given in Figure 4.17 such that a binary gene corresponds to the initial marking of P_{mOpp}. Thereby, each opportunistic maintenance decision requires only one binary gene to define P_{mOpp} as marked or unmarked, which does not change throughout the HSPN simulation as it is only connected to transitions through double arcs. One opportunistic maintenance decision is shared between the observables in an asset, such that the total count of genes equals the number of assets with the exception of pipes because they only have one observable and therefore opportunistic maintenance is not applied.

7.5 Objectives' Optimisation

The aim of a multi-objective optimisation algorithm is to minimise or maximise each objective. In a genetic algorithm the optimal values of these objectives are approached through successive generations that aim to improve upon the last. It is important to understand that NSGA-II does not attempt to converge on a single solution but instead to produce a range of diverse solutions near the Pareto surface. Therefore, it would be expected for the optimisation to produce a variety of solutions for each objective that satisfy each objective to a different degree.

7.5.1 Pareto Surface

To better understand the evolution of the solution set, the position of the solutions in objective space must be examined. To achieve this, two figures are presented that give the solutions between pairs of solutions, these are given for solutions of individual generations, selected to demonstrate the evolution of the solution set. The production and AM expenditure are shown in Figure 7.4 and the AM expenditure and number of escalation events are given in Figure 7.5. The points represent individual solutions where their colour corresponds to the number of solutions they are dominated by, for clarity only the first three fronts are plotted. The first front represents the non-dominated solutions, these will not always appear on the edge of the dominated area in these figures as the Pareto surface is three dimensional. Note that the generations shown are not equally spaced, this is to show the optimisation process because most of the optimisation happens in the first few generations.

In Figure 7.5 some of solutions are not close to the non-dominated front in the 2D projection. Although, in Figure 7.4 the solutions are closer to the front. This implies that it was easier to optimise the production and AM strategy than the number of escalation events. However, it can be noted that the average value of the number of escalation events is improved through the optimisation being significantly decreased.

It can be seen that as the generation increases the solutions form fronts that span the objective space. Initially the AM strategies are poor and can be seen to be clustered in small regions of the objective space, this is as the initial decision vectors are randomised and produce ineffective strategies. As the algorithm progresses through generations the solutions spread out and approach the Pareto front.

7.5.2 Production

The evolution of the production objective can be seen in Figure 7.6, where the mean production of each generation and the standard deviation are plotted. The production can be seen to quickly increase in the first few generations, then continue to gradually increase throughout the optimisation. This suggests that continued improvements to the AM strategy are made throughout the optimisation, albeit at a slower rate than the improvement from the initial random population. The AM strategy changes for the initial increase can be though of as large changes such as setting an inspection interval to be a reasonable value. Whereas the improvements seen throughout the optimisation

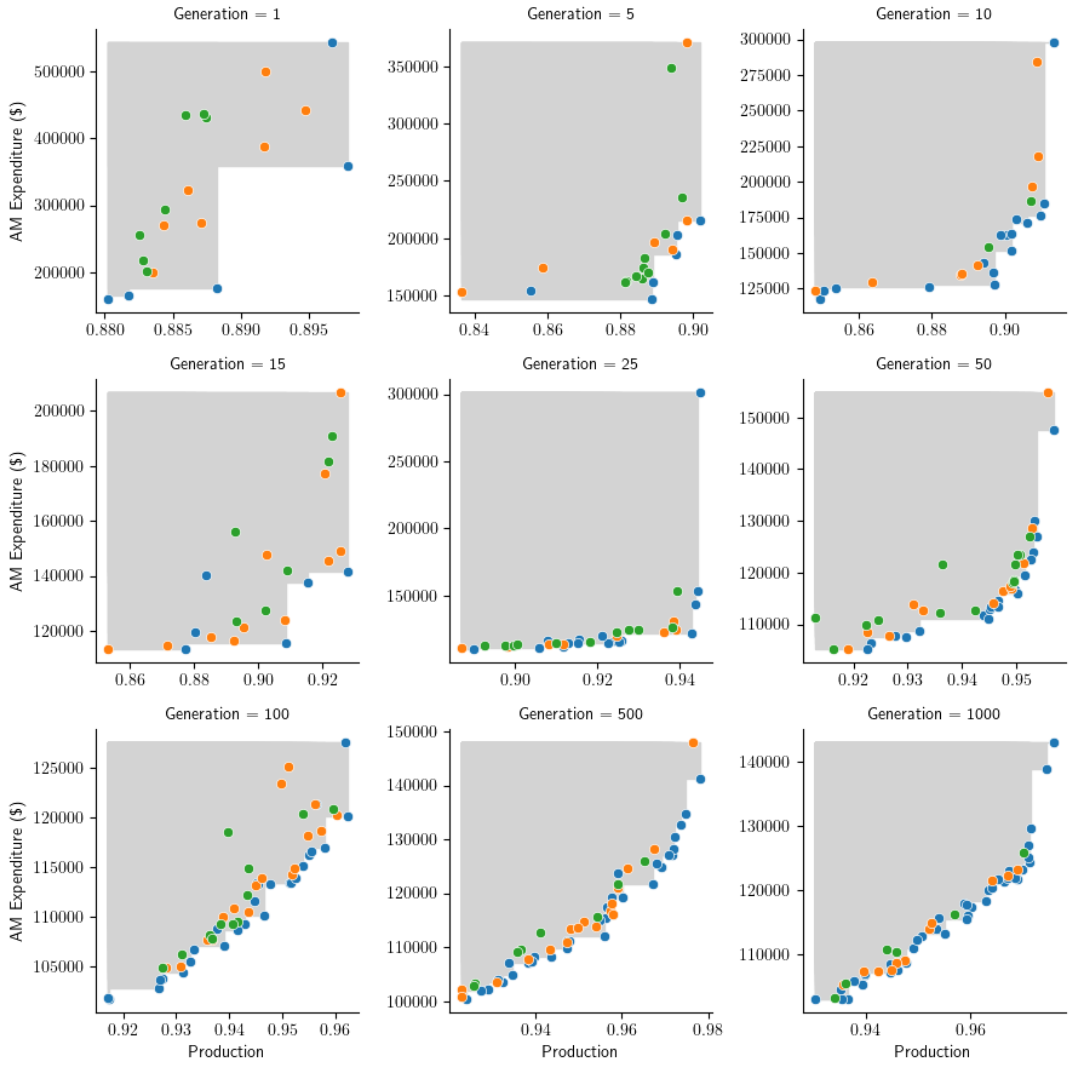

Figure 7.4: The solutions of the first three front in the production and AM expenditure objectives. Front 1, Front 2, Front 3, Dominated Area.

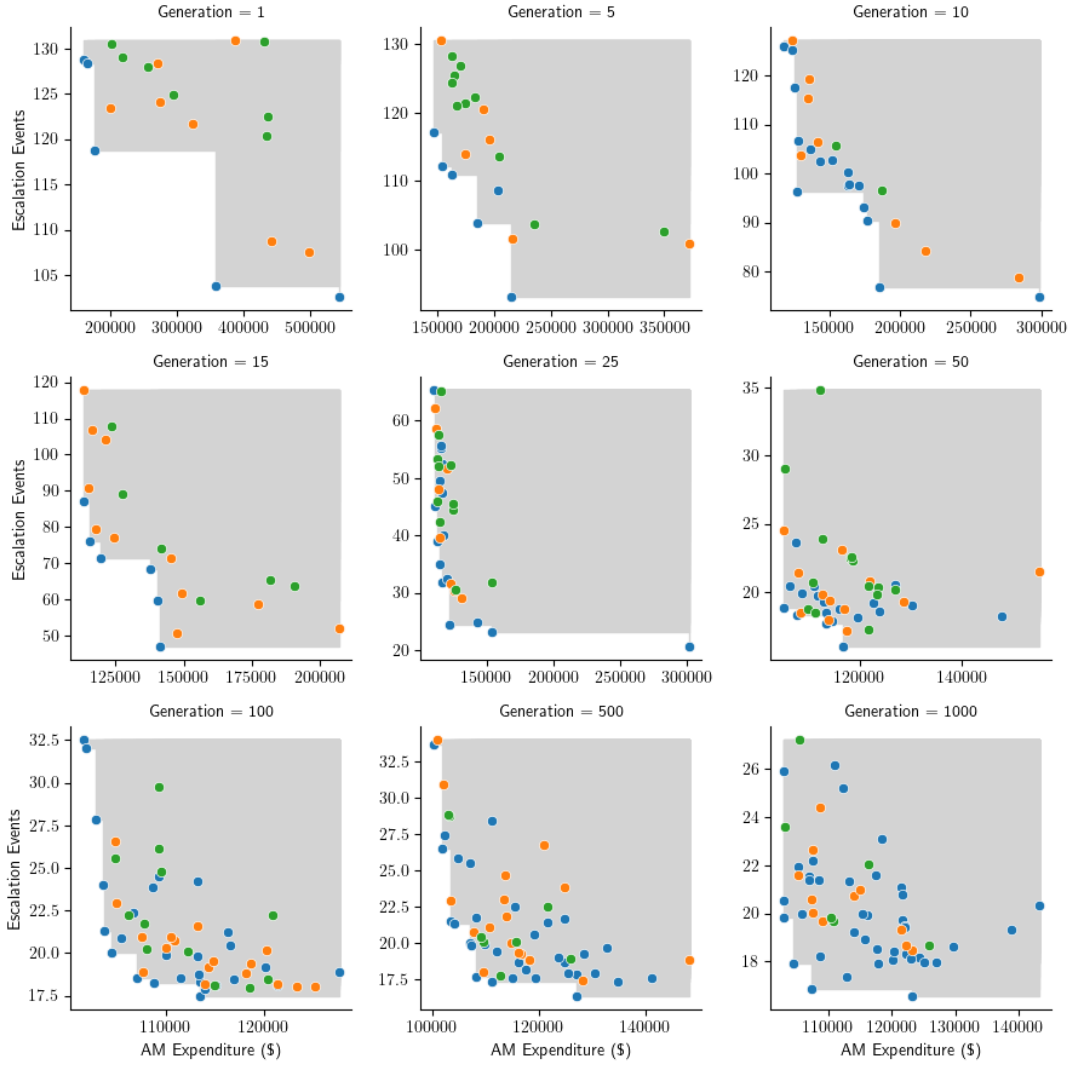

Figure 7.5: The solutions of the first three fronts in the AM expenditure and number of escalation events objectives. Front 1, Front 2, Front 3, Dominated Area.

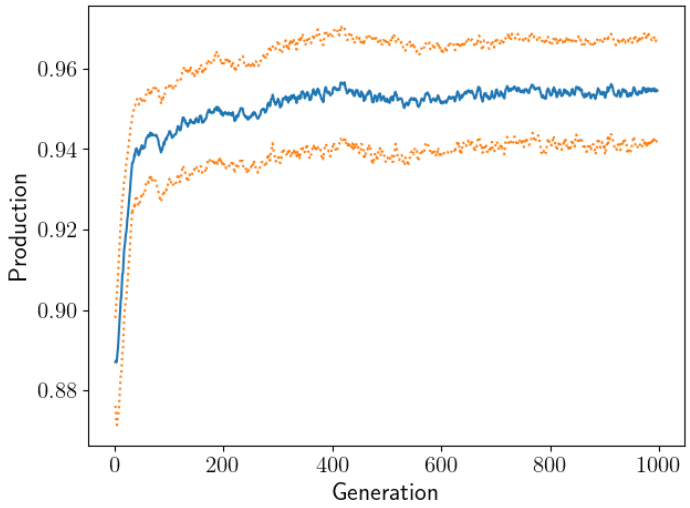

Figure 7.6: Mean production for each generation. Average, --- Standard Deviation.

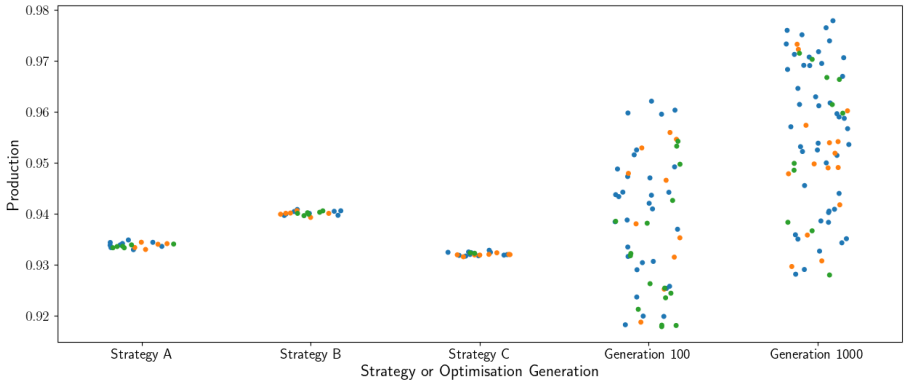

Figure 7.7: Comparison of example AM strategies with optimisation generations for the production objective. Front 1, Front 2, Front 3.

are fine-tuning where the optimal decision variables are being found. The standard deviation can be seen to remain relatively large throughout the optimisation, this is as the solutions span the Pareto surface, as seen in Figure 7.4. This result demonstrates that the model and optimisation have the ability to find AM strategies which achieve a high production availability without compromising on AM expenditure or the number of escalation events.

The results of the optimisation can be compared with three example AM strategies, first introduced in Section 5.3, where A is considered a reasonable strategy, B is more proactive and C is less proactive. Each strategy was evaluated and compared with the solutions of the 100^{th} and 1000^{th} generation of the optimisation for the production

availability in Figure 7.7. First examining the strategies, it can be noted that the highest production availability is achieved by strategy B, followed by A and C. This corresponds to the proactivity of the strategies and demonstrates, as expected, more frequent inspections and performing preventative maintenance earlier resulted in a higher production.

The solutions from the 100^{th} and 1000^{th} generations, can be seen to include a range of objective values, some being worse than any of the three strategies, but the majority achieving a higher availability. Between the two generations the entire set of solutions can be seen to shift towards higher availability, demonstrating that the increased fitness through the optimisation. The majority of the final optimised solutions are shown to outperform the three example strategies for the production availability objective.

7.5.3 Asset Management Expenditure

The AM strategy expenditure is the summation of the maintenance costs, the inspections costs and the cost for the teams. The optimisation algorithm aims to minimise the total expenditure but this does not necessarily mean that each expenditure component will be minimised. This is as an increase in one expenditure may result in a greater decrease in another expenditure, resulting in an overall decrease. In Figure 7.8a, the total AM expenditure can be seen to be successfully optimised. However, the standard deviation is fairly large thus the optimisation produces a variety of options to the duty-holder for the expense. A duty-holder can compare the expense with the production and escalation events through Figure 7.4 and Figure 7.5.

By decomposing the total expenditure the optimisation of the strategy can be observed. The maintenance expenditure, shown in Figure 7.8b, can be seen to decrease. This is caused by fewer corrective maintenance actions being performed as corrective maintenance is more expensive than preventative maintenance. Through performing preventative maintenance at suitable times the asset will fail less frequently and therefore, corrective maintenance will be required less frequently.

For preventative maintenance to be performed successfully, it is important to have good knowledge of the actual condition of the platform's assets which is achieved through a successful inspection routine. In Figure 7.8c, it can be seen that the inspection expenditure increases throughout the optimisation. This demonstrates that the optimisation found that the expenditure caused by more frequent inspections resulted in an overall decrease through reduced corrective maintenance. However, the

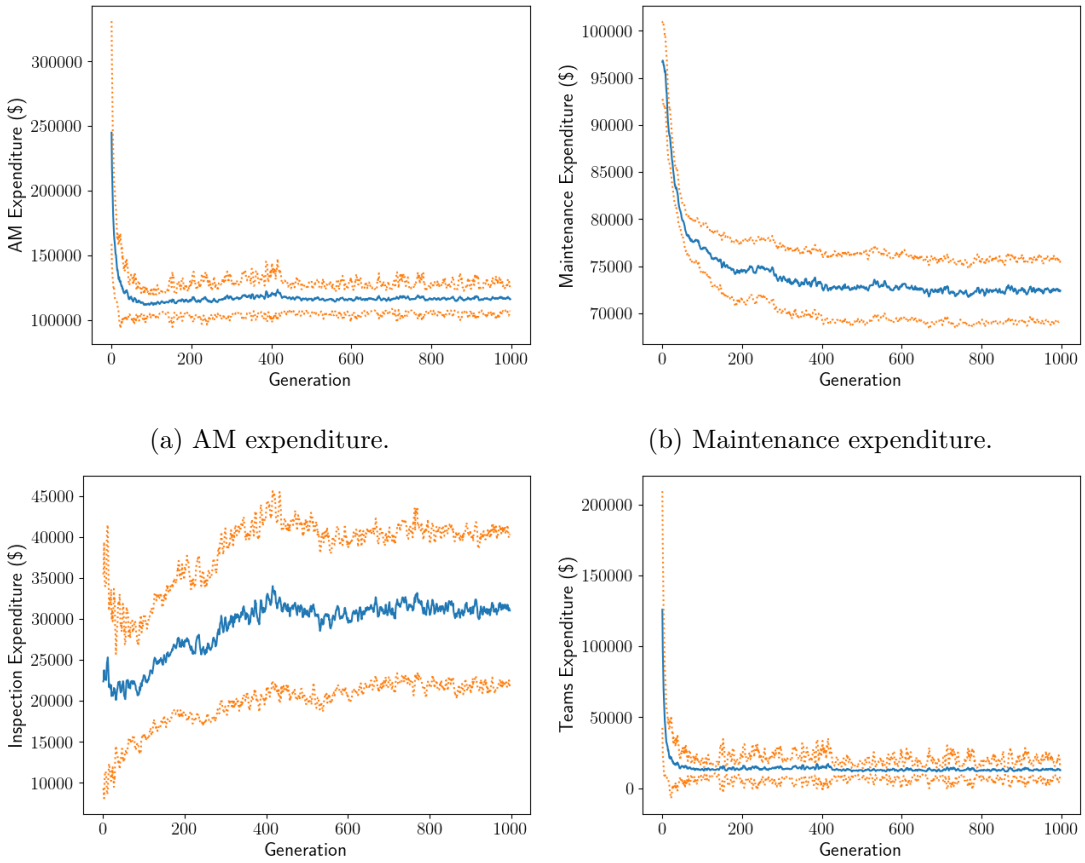

(a) AM expenditure.

(b) Maintenance expenditure.

(c) Inspection expenditure.

(d) Team expenditure.

Figure 7.8: The mean AM expenditures for each generation. ▬ Average, --- Standard Deviation.

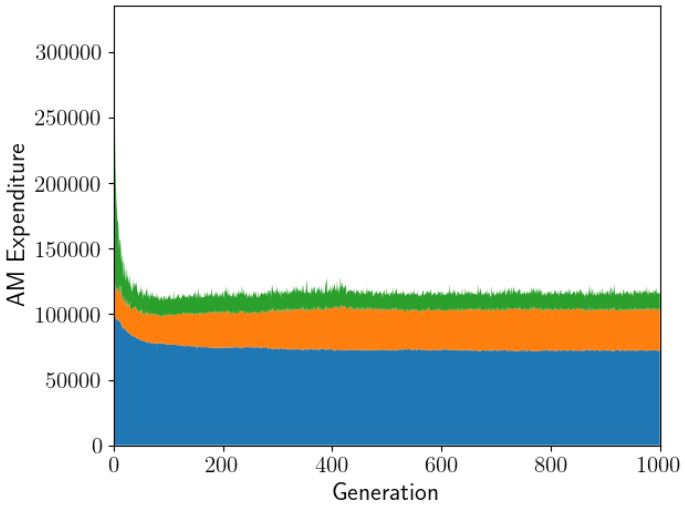

Figure 7.9: Breakdown of AM expenditure contributions Maintenance Expenditure, Inspection Expenditure, Teams Expenditure.

standard deviation of the solutions can be seen to be significant which means that non-dominated solutions were found for a wide range of inspection intervals.

The final component of the AM expenditure is the expenditure of the maintenance and inspections teams. The resulting expenditure can be seen in Figure 7.8d, which is related to Figure 7.16a and Figure 7.16b through a weighted sum. This can be seen to reduce from the initial value and converge as the optimisation progresses.

The relative contributions of these element is given in Figure 7.9. The maintenance expenditure can be seen to have the largest expenditure, although it reduces throughout the optimisation whereas the inspection expenditure increases. The demonstrates that the optimisation found that increasing the inspection frequency corresponded with a decrease in the maintenance expenditure.

A comparison of the objective values between the three example strategies and the solutions from the 100^{th} and 1000^{th} generations are given in Figure 7.10 for the AM expenditure. A significant difference can be seen between the strategies, with increased expenditures corresponding to the proactivity of the strategies, such that more AM tasks increased the expenditure. The optimisation solutions can be seen to produce a variety of solutions across the objective space, including solutions more expensive than strategy B, but also many solutions which are less expensive than any of the strategies. These solutions also have higher production availabilities, as seen in Figure 7.7, which demonstrates that the optimisation has found a more efficient way to allocate the AM

Figure 7.10: Comparison of example AM strategies with optimisation generations for the AM expenditure objective. Front 1, Front 2, Front 3.

resources which is both cheaper and results in a higher production availability than the example strategies. Between generations 100 and 1000 the solutions can be seen to produce lower expenditures, with a significant proportion of them being cheaper than the three example strategies.

7.5.4 Escalation Events

Figure 7.11 shows the evolution of the escalation events through the optimisation procedure. There is a relatively quick reduction in the mean number of escalation events from the initial population which then remains in a steady state throughout the optimisation. This indicates that significant improvements could not be made, this could be due to failures from the *Good as New* condition which cannot be avoided by preventative maintenance.

Through the consequence analysis, risk profiles can be evaluated for the three consequent events. These are evaluated for each solution as described in Section 6.9, using the HSPN and consequence analysis results. The risk was calculated in Equation 6.17 as a function of both platform age and the magnitude. By integrating over the platform age the risk of each solution can be found as a function of magnitude, such that,

$$R_C(M) = \int_0^{t_{\text{sim}}} R_C(t, M)dt. \tag{7.7}$$

Where t_{sim} is simulation time, here set at 50 years. This was evaluated for each solution in a generation and the average was taken, next this was calculated for each generation. The results of this are plotted as a generational risk densities for each consequence in

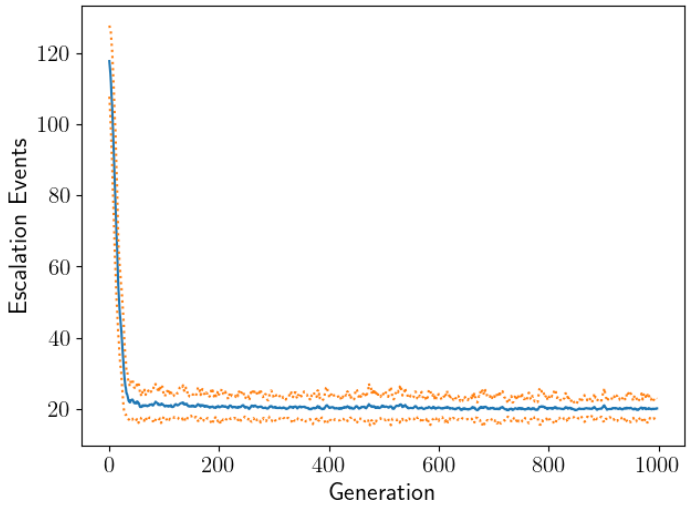

Figure 7.11: Mean escalations events for each generation. ▬ Average, --- Standard Deviation.

Figure 7.12.

The risk densities can be seen to significantly reduce early in the optimisation and reach a steady risk throughout the remaining optimisation. This reflects the evolution of the escalation events through the optimisation as the total risk will decrease with fewer escalation events. The magnitudes' distributions follow similar profiles throughout the optimisation with the risk decreasing approximately equal throughout the magnitudes. It is clear from these plots that the optimisation results in a decreased risk across all of the consequences.

Figure 7.13 shows the number of escalation events for the example AM strategies and the optimisation solutions at generation 100 and 1000. Comparing the AM strategies, it can be seen that the number of escalation events is most successfully minimised by strategy B, followed by A then C. This corresponds to the proactivity of the AM strategies, and as seen in Figure 7.10, the minimisation of the escalation events is reflected in an increased AM expenditure. The solutions of generation 100 approximately are comparable with the example strategies in this objective. Although, by generation 1000 the number of escalation events can be seen to have been reduced and outperform the example strategies.

Considering together the comparisons between the strategies and optimisation generations given in Figure 7.7, 7.10 and 7.13, it can be noted that the optimisation outperforms the three example strategies in all of the objectives simultaneously. The

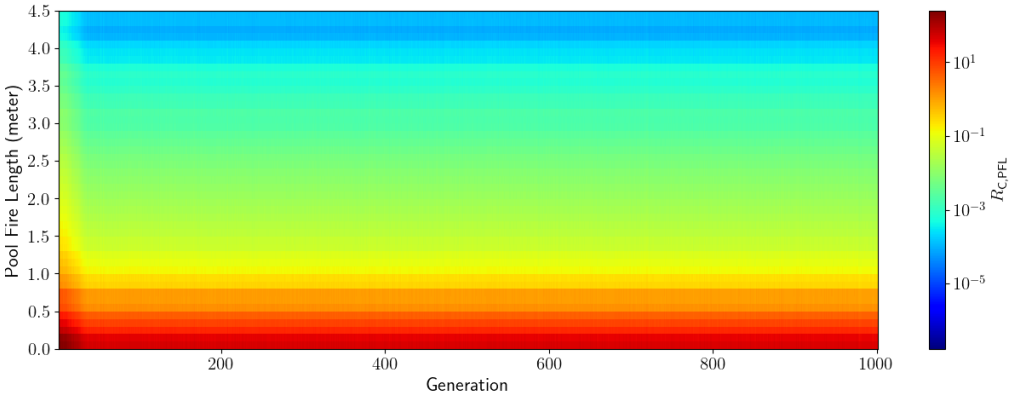

(a) Pool fire.

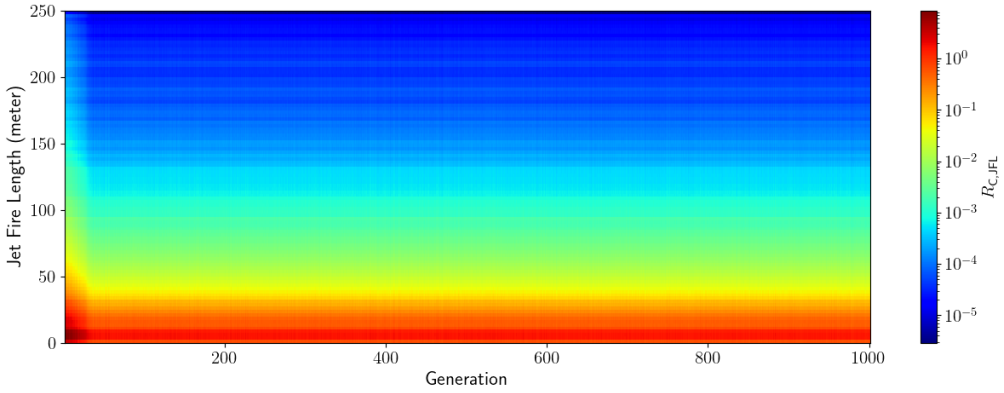

(b) Jet fire.

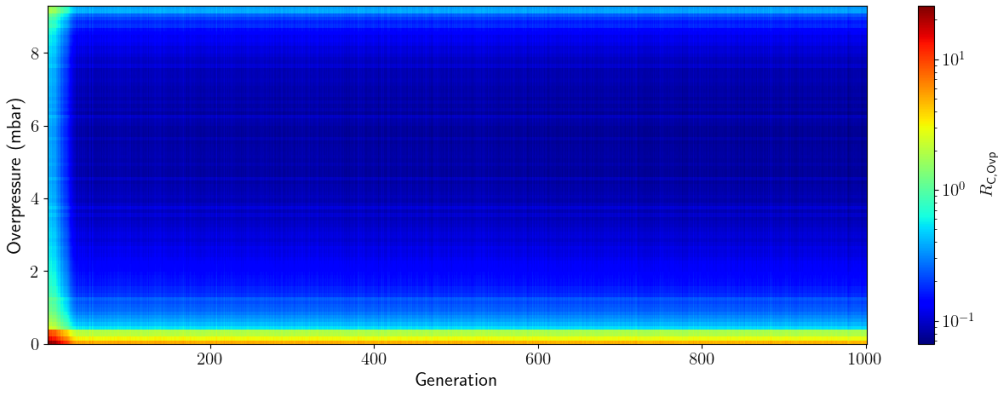

(c) Explosion.

Figure 7.12: The density of risk as a function of the consequence's magnitude and generation.

Figure 7.13: Comparison of example AM strategies with optimisation generations for the number of escalation events objective. Front 1, Front 2, Front 3.

example strategies had an increase in production availability or decrease in escalation events correspond to an increase in AM expenditure. Whereas, the optimisation algorithm was able to produce solutions which more efficiently used AM resources such that the expenditure was minimised while still increasing production availability and reducing the number of escalation events.

7.6 Decision Variable Results

The optimisation procedure is based on the values of the objectives vectors, which are set as metrics of the platform's whole-life performance, whereas the decision variables define the AM strategy. A duty-holder can select a solution from its position in objective space and be able to see the corresponding decision variables, thereby selecting an AM strategy based on the simulated platform's performance. The decision variables were detailed in Section 7.4, with a total of 1693 variables for each solutions which makes plotting or tabling the entire decision vectors impractical so subsets of the decision results will be examined here.

7.6.1 Inspection Intervals

The frequency of inspections will determine the knowledge of the condition of the assets. Infrequent inspections will lead to longer exposures, being in a more degraded condition than was found at the last inspection. This will lead to delays in maintenance being performed as the maintenance decision is based on the last inspected condition.

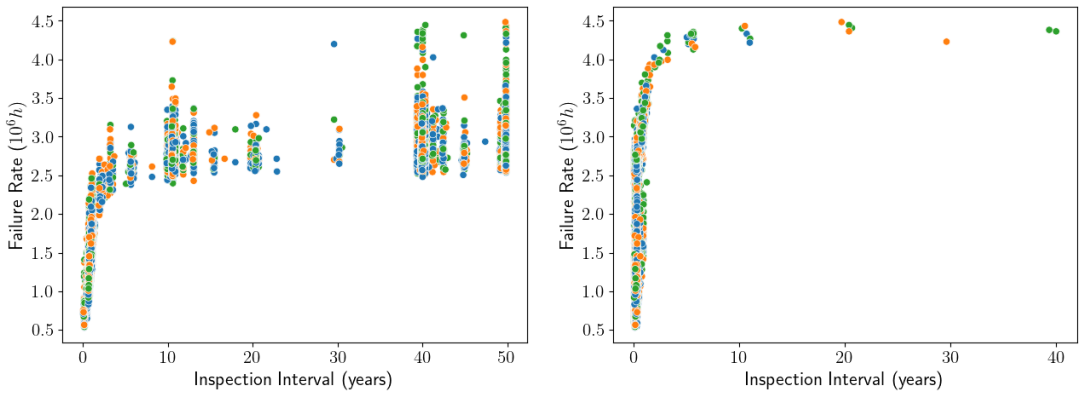

(a) Internal Inspection.

(b) External Inspection.

Figure 7.14: The relationship between the inspection interval and the failure rate of *Valve 1* for solutions of the optimisation. Front 1, Front 2, Front 3.

On the other hand, too frequent inspections incur greater expenditure and can require excess inspection teams, further increasing the expenditure. Therefore, the inspection interval is a pay-off between condition knowledge and AM expenditure, which the optimisation algorithm aims to solve.

Preventative maintenance will reduce the failure rate of an asset as the probability of failure is greater for more degraded conditions. To ensure preventative maintenance is carried out effectively it relies on knowledge of the asset's conditions, which requires appropriate inspection intervals. The relationship between the inspection interval and asset's failure rate for *Valve 1* is given for internal and external inspections in Figure 7.14 where each point in the figures is a solution of the optimisation.

The failure rate of the asset is not entirely determined by the inspection intervals, this results in differences in the relationship between the different solutions. There are several other decision parameters that will effect the asset's failure rate. For instance, the maintenance decisions of the asset's observables will change when preventative maintenance is performed in response to the condition revealed by the inspection. In addition, the number of inspection teams will determine the delay before inspections are performed after their interval is elapsed. Further, the inspection intervals and maintenance decisions of other assets will indirectly effect the failure rate of this through their use of the AM teams. Finally, both the number of maintenance teams and the prioritisation of maintenance actions across the system will influence the delay before maintenance actions are carried out.

Both inspections show that for the majority of the inspection intervals are insuf-

ficient at reducing the failure rate, only at short inspection intervals is a significant reduction in the failure rate seen. This demonstrates that the critical region of inspection interval for *Valve 1* for both internal and external is a between 0 and 2 years. For external inspections there are few solutions with inspection intervals greater than 10 years, demonstrating that there are few Pareto optimal solutions with long external inspections. Conversely, the internal inspection intervals can be seen to be spread throughout the inspection intervals, thus Pareto optimal solutions must exist across all possible intervals.

7.6.2 Maintenance Decisions

The maintenance decision defines the revealed conditions from which preventative maintenance is queued to be performed at. The purpose of performing preventative maintenance is to reduce the probability of failures and therefore reduce unavailability, leaks and expensive corrective maintenance. Although, if the preventative maintenance is too proactive it can be overly expensive. This balance is captured by the three objectives of the optimisation.

The solutions' maintenance decisions can be compared with the failure rate of their asset to understand their dependency. This relationship is given in Figure 7.15, where the mean maintenance decision and mean failure rate for the four valves in the production chain are plotted. It would be expected that the relationship between the maintenance decision and failure rate are similar across the four valves as they have the same degradation and failure rates. An asset's maintenance decision is discretised by the number of states, by taking the mean of four valves the mean decision is not limited to this which helps in seeing the relationship between the decision and failure rate. The maintenance decisions are denoted by C_i+ for $i \in [2, N_O]$ for an observable with N_O conditions, meaning that when inspected maintenance will be queued for condition i and greater.

The mean maintenance decision for every solution was seen to be between C_{2+} and C_{4+}, with the majority being C_{2+} and C_{3+}. This does not indicate that their were no condition chains with maintenance decisions of C_{4+} or C_{5+} as each solution is the mean across four valves. Although, it does indicate that the optimisation found that earlier maintenance decisions were preferable for all solutions, and therefore that run-to-failure operation was not considered a viable solution.

As would be expected, the failure rate is decreased for a more proactive maintenance

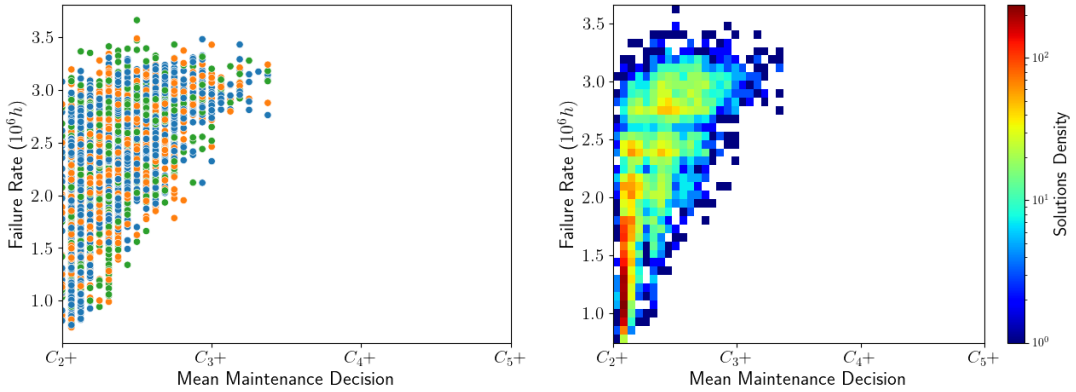

(a) Solutions by front. ● Front 1, ● Front 2, ● Front 3.

(b) Density of solutions.

Figure 7.15: The mean maintenance decision and mean failure rate for each solution across the four valves in the system.

decision as the asset will be more likely to be in a less degraded condition and therefore have a lower probability of failure. However, the relationship has a large variance which is caused by other decision variables in each solution, such as the inspection intervals, maintenance prioritisations and AM team sizing. This demonstrates that the asset's failure rate is not only dependent on the maintenance decision, there are other factors affecting its value. For instance, the relationship between the inspection intervals and the failure rate was seen to be much stronger.

The solutions from all the generations are plotted, this is to better show the relationship and, further, in Figure 7.15b, the density of the solutions are given, note the solution density's logarithmic scale. The underlying data of these two figures is the same, with Figure 7.15a the density of solutions cannot be clearly seen, so Figure 7.15b is plotted for clarity. The density increases for more proactive decisions with the greatest density near C_2+, the first condition from which preventative maintenance is possible. This indicates that the optimisation favoured the more proactive maintenance decisions when considering all the objectives. The concentration of solution near C_2+ shows that in most case the optimisation procedure finds these solutions to be worth the expenditure of preventative maintenance. This may be as, although the preventative maintenance expenditure is increased it corresponds to a greater decrease in corrective maintenance expenditure.

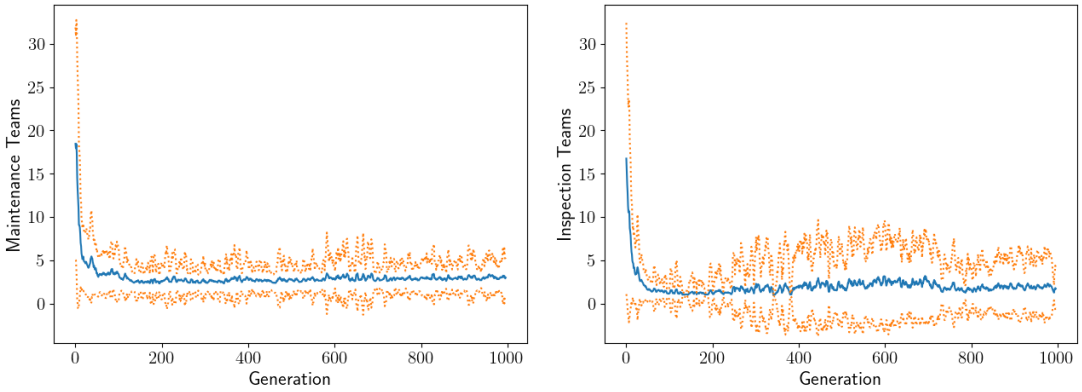

(a) Maintenance teams.

(b) Inspection teams.

Figure 7.16: The mean number of AM teams in each generation. ▬ Average, --- Standard Deviation.

7.6.3 Asset Management Teams

In Figure 7.16a and Figure 7.16b, the mean number of maintenance and inspection teams in each generation are given. Both can be seen to be minimised within approximately 100 generations from the initial population and remained in a steady state for the remainder of the optimisation. Specifically, at the end of the optimisation the mean number of teams was 3.02 ± 2.03 and 1.94 ± 3.29 for the maintenance and inspection teams respectively. Therefore, the optimisation found that for that most solutions more maintenance teams were required than inspection teams. The standard deviation of the inspection teams is large, which is because the solutions spanned a wide range of inspection intervals, as seen in the inspection expenditure in Figure 7.8c. Therefore they require a range of inspection teams to be able to effectively implement each solution's strategy.

Directly proportional to the sum of the maintenance and inspection teams is the teams expenditure, given in Figure 7.8d which contributes to the AM expenditure. Therefore, the optimisation is incentivised to minimise the number of teams, however, enough teams must remain to efficiently perform maintenance and inspections. Crucially, the optimisation is successful in minimising the AM teams while maintaining an effective strategy.

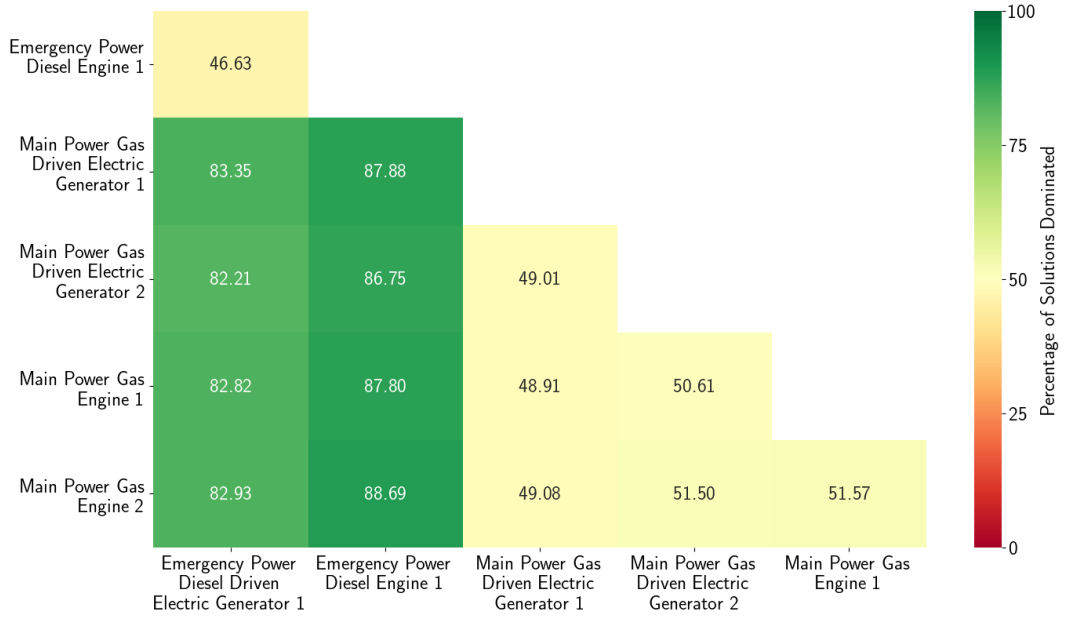

Figure 7.17: The percentage of solutions where the x-axis priority dominates the y-axis priority for the critical corrective maintenance transition of the assets of the power system.

7.6.4 Maintenance Prioritisation

Associated with each preventative and corrective maintenance action is a check transition, T_{mChecks}, seen in Figure 4.18, that has a priority assigned to it. When a maintenance backlog is present in the system then multiple transitions, T_{mChecks}, will be enabled for each maintenance action in the backlog. The order in which these maintenance actions are performed is defined by the relative priority of each transition. Thus, the absolute value of each priority is not of importance, only the relative difference between the priorities.

The priority of each transition is set by the optimisation algorithm, therefore, in the initial population the priorities will be randomly assigned and so the preference of one maintenance action over another will be random. As the algorithm optimises these priorities, you would expect more critical component's maintenance to be prioritised over less critical components.

Considering two maintenance transition, if one transition is prioritised over the other, this can be said to dominate the other transition. For a set of solutions, the percentage of solutions dominated between two maintenance actions can be calculated, here known as the domination percentage. In Figure 7.17, these domination percent-

ages are given for the critical corrective maintenance transition between the assets of the power system. These percentages are given over an average of the solutions of the final 10 generations of the optimisation to represent the converged solutions. The value of a maintenance priority is not meaningful in itself, it is only relevant when compared to another maintenance priorities as the dominant priority will be performed first when both are queued. Therefore, instead of examining the values of the priorities, Figure 7.17 presents the percentage of solutions with transition priorities dominated between different assets. Thereby, this quantifies the relative priorities between maintenance that was found by the optimisation algorithm.

The power system unavailability fault tree, given in Figure 3.4, shows that there is greater redundancy for the main power system than the emergency power system. Therefore, the emergency power maintenance will be prioritised over the main power, which can be seen to be confirmed by the figure, with emergency power maintenance being prioritised by the majority of solutions.

In contrast, the domination percentage between the main power gas driven electric generators and their gas engines are seen to be near 50%, this shows that the solutions have not converged to one maintenance dominating the other. This is as the main power generators requires both of these to be running so there is no preference of maintenance between them, thus no priority is dominant. The same is true for the emergency power diesel engine and the emergency power diesel driven electric generator.

7.6.5 Maintenance Backlog

The maintenance backlog was examined previously in Subsection 5.3.5 in the context of varying the number of maintenance and inspection teams. This was only evaluating the effect of changing two variables, in contrast, within the optimisation the maintenance backlog can be affected by varying any of the decision variables. The optimisation algorithm does not explicitly aim to minimise the backlog's size but does optimise production availability so it is indirectly incentivised to minimise downtime of the assets.

The size of the maintenance backlog is represented by the maintenance queue depth, this is how many maintenance actions are queued at any time. The average maintenance queue depth through the optimisation is shown in Figure 7.18. The maintenance queue depth can be seen to reduce through the optimisation, converging to an average

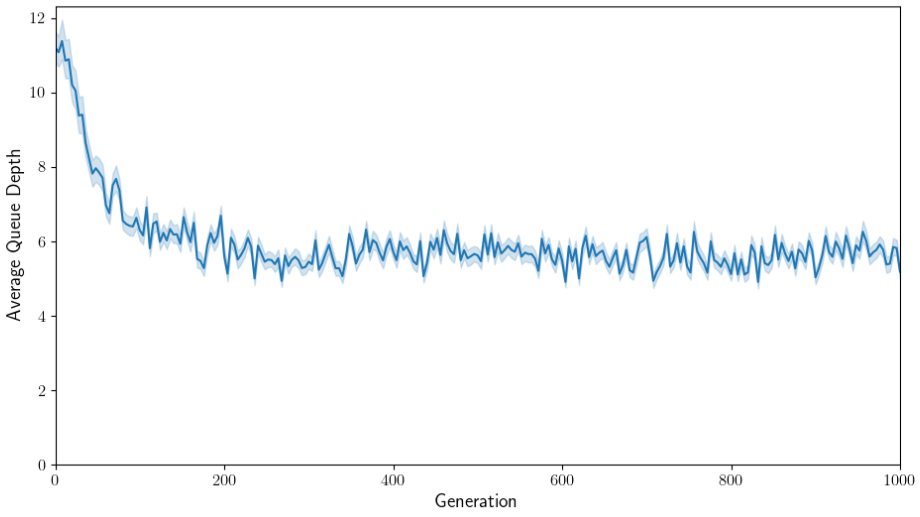

Figure 7.18: The maintenance queue depth through the optimisation shown with a 95% confidence interval.

queue depth of approximately 6.

The main driver of the reduction of the queue depth is the maintenance decisions for the preventative maintenance which define the conditions from which maintenance will be queued when the condition is revealed by an inspection. When the strategy sets these decisions early, maintenance is performed when the asset is only slightly degraded which can result in excessive maintenance being queued and thereby increasing the backlog. In these situations it would be advantageous for the maintenance to be postponed till the asset has degraded further to conserve the maintenance resources. On the other hand, when the decisions are set too late, not only is the risk of failure increased, but corrective maintenance is more probable to be required. As corrective maintenance has longer durations than the preventative maintenance this can also increase the backlog size. The average queue depth can be seen to reduce through the optimisation which demonstrates that the optimisation is successful at determining appropriate maintenance decisions.

7.6.6 Opportunistic Maintenance

The optimisation of the opportunistic maintenance decision is given in Figure 7.19 for each production asset type, where 1 is opportunistic maintenance enabled and 0 is disabled. The pipe asset type is omitted here as it only has one observable and therefore

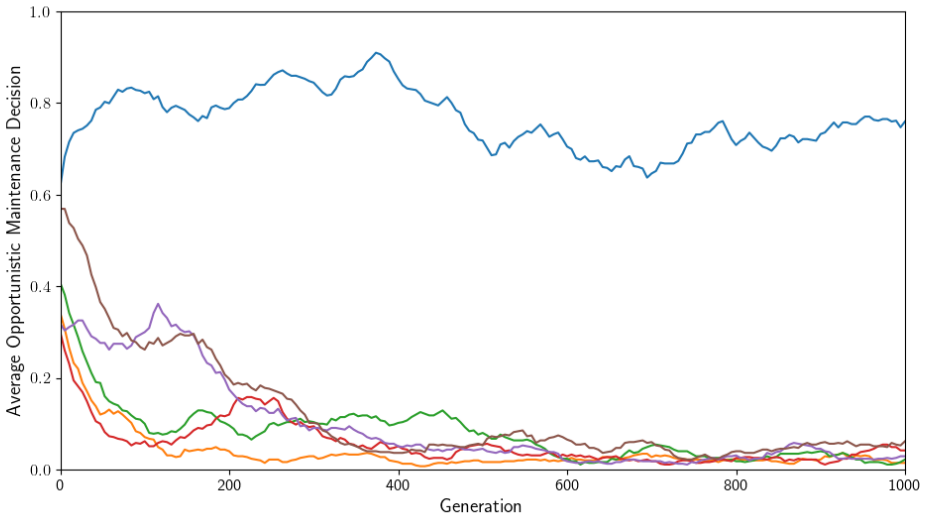

Figure 7.19: Optimisation of the opportunistic maintenance decision for each asset type. Valve, Separator, Scrubber, Contactor, Heat Exchanger, Compressor.

opportunistic maintenance is not applicable. It can be seen that for most assets the optimisation converges on disabling opportunistic maintenance for the majority of solutions, whereas, approximately 80% of the valve's solution enable opportunistic maintenance.

In the model, internal and external inspections reveal multiple observables on an asset and thus from one inspection it can be known whether multiple observables require maintenance. Consider an inspection that reveals two observables A and B, in the case that A is significantly degraded and B is not, an inspection will queue maintenance on A. If opportunistic maintenance is enabled then maintenance will also be queued on B, despite it not being degraded enough to warrant maintenance, which will result in excessive maintenance expenditures. This could be the reason that the majority of the assets converge to disable opportunistic maintenance. Notably the valve has two observables, each inspected separately by the internal and external inspections, thus not being affected by the affected described above.

7.7 Two-step optimisation

The optimisation algorithm discussed so far is capable of producing AM strategy solutions considering three objectives. However, the AM strategy is the same throughout the lifecycle despite the platform operating beyond it's design life. In this section, an extension to the optimisation will be detailed that produces solutions that contain two AM strategies, one for design life and one for the LE stage. By including two AM strategies the algorithm will be able to optimise them to be specific to each lifecycle stage. In this thesis, this extension will be referred to as the two-step optimisation.

To extend the optimisation each gene is copied such that each AM parameter has one design life gene and one LE gene. This results in the number of genes doubling, which greatly increasing the decision space over which the optimisation acts. In the one step optimisation a maintenance strategy gene would define the initial marking of a particular place, which in turn determined whether maintenance was performed given a particular state. Whereas, in the two-step optimisation, the first gene still defines the initial marking but the second gene defines the marking of the place after the design life is elapsed. When the simulation reaches the end of the design life, the place corresponding to the gene will have it's marking updated to equal to gene's value. A similar action is performed for the inspection intervals in changing particular transitions' delays after the design life is elapsed.

Through this method the AM strategies can be completely changed when entering into LE, resulting in significant changes in the platform's performance in each stage. It is important to note that the state of the platform at the end of the design life is dependent on the AM strategy and therefore the LE strategy is dependent on the design life's strategy. An alternative approach could have been to optimise the design life and the LE separately, basing the LE optimisation of a representative degraded start point. This approach was not taken as it would not simulate the interplay between the two AM strategies.

The optimisation process, is unchanged, NSGA-II is still used in the same way, with the difference being it is acting over a larger chromosome. The new genes are included into the chromosome, doubling it's length. Then the optimisation algorithm acts as before breeding all the genes in the chromosomes to produce a solution set.

As the two-step optimisation apply different AM strategies for each stage of the platform's life, it would be expected that probably of being in each condition is changed

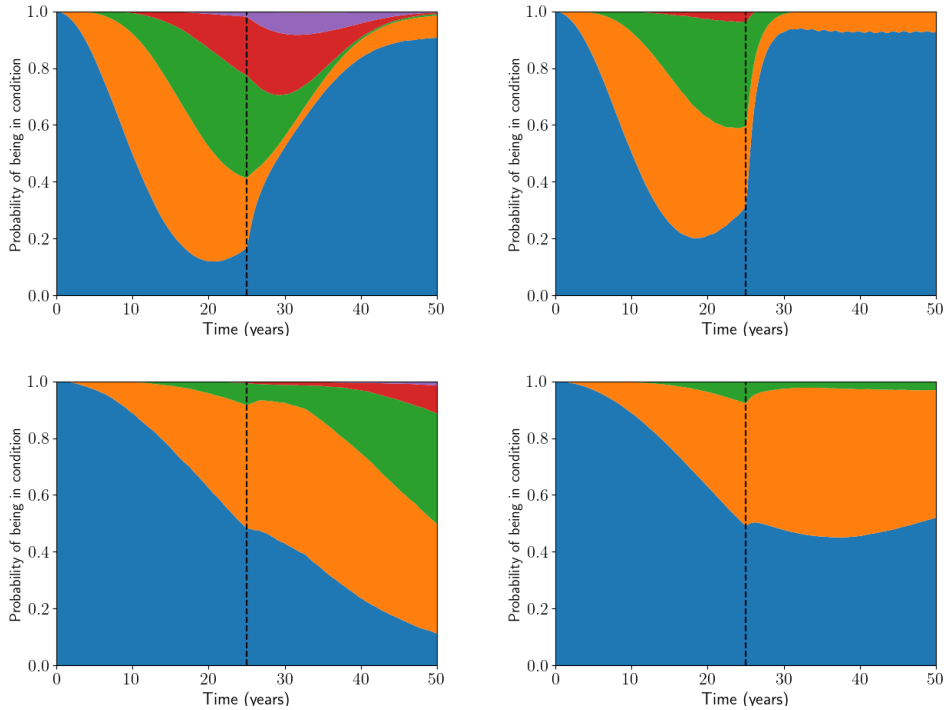

Figure 7.20: Examples of the probability of being in each condition through a simulation period for a selection of solutions in a two-step optimisation. For the observable *Wall Thickness* of *Pipe 1*. C_1, C_2, C_3, C_4, C_5, C_6.

after the design life is surpassed. In Figure 7.20, the resulting probability of being in each condition from a selection of randomly generated chromosomes are shown for the *Wall Thickness* of *Pipe 1*. The examples demonstrate how the probability of being in each condition can be significantly modified through the lifecycle by the two AM strategies. These particular examples are not chosen to represent good optimisations solutions, but only to demonstrate how changing the AM strategy mid-life can result in significant changes in assets' conditions. Thereby, through modifying the strategy when the LE stage is entered the optimisation could generate a solution that implements a more proactive strategy to improve the condition of assets that have deteriorated over the design life.

It has been seen that the two-step optimisation produces AM strategies that are distinct for the platform stage. The changes in the genes will affect how the simulated AM strategies are performed in the two lifecycle stages, which will corresponds to changes in the objective values. Through the objective values the effectiveness of the two-step optimisation compared to the one step optimisation can be compared. In Figure 7.21a a comparison of the non-dominated front and dominated area for the two-step optimisation and the one step optimisation is shown, specifically a projection of the Pareto surface onto the AM expenditure and production availability is given. The non-dominated solutions from the final generation for the two optimisation are plotted with the area which they dominate shown. A similar plot for the projection of the Pareto surface onto the AM expenditure and number of escalation events can be seen in Figure 7.21b.

It is evident that the two-step optimisation produces a superior set of solutions in all objectives when compared to the one-step optimisation. This can be understood by considering that the options available to the optimisation are doubled in the two-step optimisation, which allows for more efficient and successful AM strategies to be found. Thereby, this demonstrates that through altering the AM strategy between design life and life extension, a platform would be expected to show more optimal performance.

Despite the two-step optimisation producing a fitter solution set it does have a disadvantage in comparison to the one-step optimisation. Early in the optimisation, at low generation numbers the one-step optimisation produces better solutions than the two-step, although as the algorithm continues the two-step begins to produce solutions that better satisfy the objectives. Snapshots at different generation numbers for both types of optimisation are given in Figure 7.22, the non-dominated solutions of each generation and the fronts they form are plotted. It can be seen that at generation

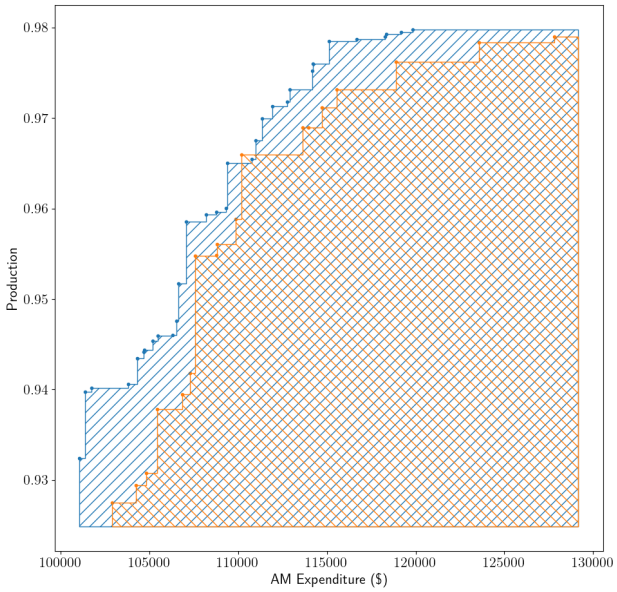

(a) The dominated areas for the production and AM expenditure.

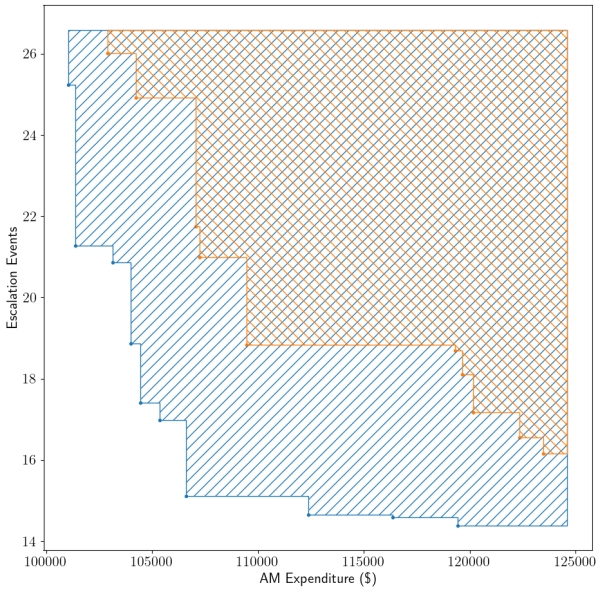

(b) The dominated areas for the number of escalation events frequency and AM expenditure.

Figure 7.21: The dominated areas compared between the one step optimisation and the two-step optimisation. Two-step optimisation, one step optimisation.

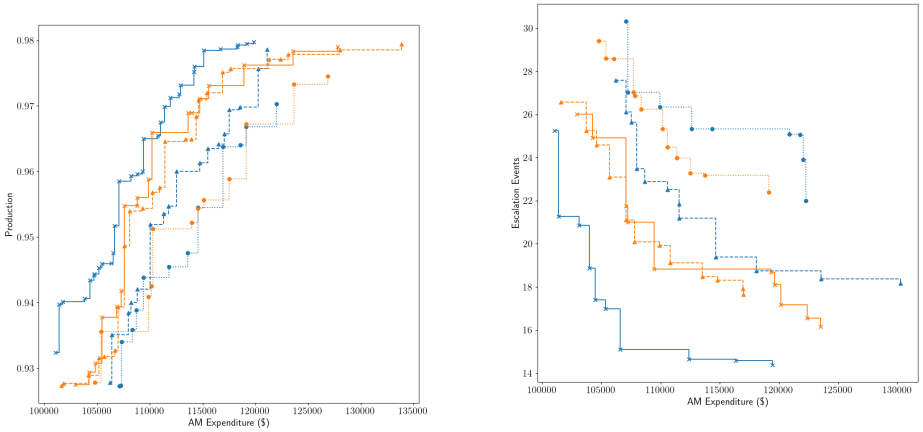

(a) The non-dominated fronts for the production and AM expenditure.

(b) The non-dominated fronts for the number of escalation events and AM expenditure.

Figure 7.22: The non-dominated fronts at three generation snapshots compared between the one-step optimisation and the two-step optimisation. Two-step optimisation at generation 50, two-step optimisation at generation 100, two-step optimisation at generation 1000, one-step optimisation at generation 50, one-step optimisation at generation 100, one-step optimisation at generation 1000.

50 and 100 the one-step optimisation produces a solution set that is superior to the two-step, but by 1000 generations the two-step optimisation has the superior solution set. This demonstrates a trade-off between the two optimisations, with the one-step optimisation being faster but the two-step being able to produce more optimal solutions given enough generations. This slower optimisation of the two-step is due to the increased number of genes which corresponds to a larger decision search space.

Through the two-step optimisation it is clear that to get the best performance out of a platform the AM strategy should be different for the design life and LE. This can be understood by considering that the average observable's condition, early in the lifecycle it's probable that little degradation has taken place which corresponds to a lower probability of failure. As the platform ages, degradation will take place, although AM strategies will act to renew the conditions. Therefore, in LE the platform is expected to be in a different state to as it was during design life and thus a distinct AM strategy for each stage is appropriate. However, it can also be noted that the two AM strategies must be considered together, as the proactivity of a LE strategy is dependent on the design life strategy. Through this optimisation procedure the two strategies are considered together in one model.

7.8 Summary and Discussion

In this chapter an optimisation algorithm has been successfully applied to the model to determine optimal AM strategies. NSGA-II was selected as the optimisation technique as it is a powerful multi-objective general purpose technique. It required that no prior preference needed to be made between the objectives, with the solutions describing the pay-off between the objectives.

The performance of the AM strategy was measured with three different objectives, namely production, escalation events and AM expenditures. Three objectives were selected to form the multi-objective problem, these were the production, the AM expenditure and the number of escalation events. Although the algorithm is capable of having an arbitrary number of objectives, the speed of the evolution decreases as the number of objectives increases. For this reason, only these key objectives were selected.

As NSGA-II was a multi-objective algorithm it was well-suited for attempting to determining the optima in all of the objectives simultaneously. No weighting or

preference was given to any of the solutions in the optimisation specification, the algorithm evolved solutions to cover the optimal surface in objective space. It was seen that the resulting solutions provided a user with a selection of solutions to pick from which each satisfy the objectives to varying degrees. The diversity of the solutions were seen to be good, in Figure 7.4 and Figure 7.5 the Pareto surface can be clearly identified with the solutions spread across it.

The production availability was seen to increase throughout the optimisation, first quickly then gradually, indicating that applying NSGA-II to the model is capable of determining optimal solutions. A decrease was also seen in the AM expenditure, although in examining the contributions it was found that the inspection expenditure increases but was offset by a greater decrease in the maintenance expenditure. Increased inspections will result in more preventative maintenance but less corrective maintenance, as corrective maintenance is more expensive this results in a decrease in maintenance expenditure. The number of escalation events decreased at the start of the optimisation before reaching a steady state. Risk density profiles were calculated, which showed how the risk decreased for each consequence through the optimisation, demonstrating an effective AM strategy.

The decision variables resulting from the optimisation were analysed, as there were a total of 1693 variables only a subset were examined here. The inspection intervals and maintenance decisions of the solutions were shown to have the highest density in the regions were the asset's failure rate was most significantly reduced. The AM teams were seen to be reduced to a steady state, however, the solutions were found to have a range that allowed for a diverse selection of strategies. The maintenance priorities of the power system was investigated, where the emergency power generation assets were shown to be prioritised over the main power generation assets by the majority of solutions, which is due to the redundancy of the main power system.

The application of NSGA-II to the model produced a set of near Pareto optimal solutions to a three objective problem. Thereby, extending the HSPN and consequence analysis further to create a methodology that can not only simulate a platform with a given AM strategy, but can evaluate optimal strategies. The majority of solutions to the optimisation were shown to exceed the example AM strategies in all three objectives simultaneously.

To address the differences of operation in design life and LE a two-step optimisation was applied, this doubled the number of genes to describe two distinct AM

strategies for each lifecycle stage. Thus the optimisation algorithm could create solutions which performed inspection and maintenance differently after entering LE, when the assets were typically in a more degraded state. The increase in possible AM strategies available to the two-step optimisation resulted in more optimal solutions being produced, thereby demonstrating the possible improvement through varying AM strategies through lifecycle stages.

Chapter 8

Conclusion

8.1 Introduction

In the offshore oil and gas industry the majority of large and accessible fields have already had platforms established that are extracting the fluids. Expansion to smaller or less accessible fields is costly, whereas, typically, continuing to extract from the existing platform is more economical. Although, in many cases the existing platforms have been operating for many years and are approaching or have surpassed their design life and have entered into a LE stage. The continuation of asset degradation in this stage is expected to bring new AM challenges to duty-holders.

The work of this thesis aimed to model the assets of a representative platform throughout the platform's design life and its LE stage. The model simulated the degradation, inspection and maintenance of the assets with a HSPN, which was used to investigate the effects of various AM strategies on the platform's performance.

The handling of hydrocarbons can pose a risk of fire or explosion in the case of a leak from one of the production assets. The HSPN was used to determine the probability of a leak from each asset and the condition of the firewater deluge system at the time of the leak. This was then used as an input into a consequence analysis, which evaluated the risk of three different possible consequences to each possible leak. Together the HSPN and consequence analysis formed an integrated model for evaluating the performance and risk of a given strategy.

An optimisation algorithm was then applied to the model to determine a set of optimal AM strategies that satisfied three objectives: production availability, AM expenditure and the number of escalation events. Together, the work formed a useful tool

for determining optimal AM strategies for offshore oil and gas platforms considering distinct aspects of its performance.

The purpose of this chapter is to reflect and critically review the work presented in this thesis. This includes a discussion on the system design and the reasoning behind the major decisions that determined the scope and system structures. In addition, a comprehensive review of the modelling techniques used in this work are examined, namely, the HSPN, the consequence analysis and the application of the NSGA-II. Furthermore, the main data sources are analysed and the effected they had on the model design and results are discussed. Finally, the successes and short-comings of these different areas are examined and from this areas for future research are identified.

8.2 Novelty

A hybrid Petri net modelling approach was taken in this work. The novelty of this was to use the continuous part to model fluid flow through the production assets, while modelling the AM of the production assets with the discrete part. The hybrid approach allowed for these parts to be connected such that the fluid flow rates were dependent on the assets' conditions at all times. Through code developed to simulate the HSPN platform lifecycles could be quickly simulated and used to evaluate the performance of a candidate AM strategy.

A similar previous paper by Briš (2013) modelled the AM of an offshore oil and gas platform's using a stochastic coloured PN, which was previously discussed in Subsection 2.3.4. Comparing the paper to this work it can be noted that in the paper a discrete PN was used and so no fluid production was modelled. In addition, the system covered by this work was more extensive with multiple degradation mechanisms, a larger production system and including the power generation and firewater deluge systems.

Another novel element of this model was the integration of the HSPN and consequence analysis. The consequence analysis was integrated into the HSPN simulation through the failures of the production assets, specifically particular failure modes resulted in a hydrocarbon leak that would trigger a consequence analysis. The initial conditions of the analysis were taken from the state of the HSPN when the leak was triggered, these included the availability of the firewater deluge system in the module and the failure mode type. This integration expanded the capability of the model to

evaluate the platform's performance such that the total risk across the lifecycle could be calculated.

An optimisation algorithm was applied to the model with respect to the AM strategy. This was a large scale optimisation with over 1000 decision variables, which defined the strategy individually for every asset condition and inspection. In addition to maintenance decision and inspection intervals, the optimisation also included some novel decision variables, such as maintenance priority and number of maintenance and inspection teams. Furthermore, a novel two-step optimisation was detailed, this defined two distinct AM strategies for design life and LE. This was shown to produce solution which, in comparison to the normal optimisation, were more optimal across all objectives.

8.3 Assumptions

Throughout this thesis assumptions were made in order to create an effective model. These assumptions are listed below and their effects and limitations are discussed:

- The observables were categorised into a series of discrete conditions. This reflected the limit to which any condition can be measured. Nevertheless, as each condition corresponds to a decision to perform preventative maintenance an increase in the number of conditions would provide more maintenance opportunities. Although, to effectively model these reliable data would be required for each transition.
- Transition timings simulating degradation and failures are sampled from Weibull distributions. This distribution was chosen as it can simulate both infant mortality and wear-out, which is particularly relevant for increased failure rates possible in LE. Nevertheless, there are numerous distributions that could be selected and if data was available that favoured another distribution, which could easily be applied to this work.
- Maintenance actions were assumed to always renew the condition to the first condition state. This assumption ignored the possibility that the maintenance may fail to fully renew the condition, or even degrade it further.
- Every production vessel was assumed to contain a mix of oil and gas only which were vertically stacked. This did not consider the possibility of other fluids being present in the vessel or a more complex mix of the two fluids.
- The leak height was uniformly sampled from the vessels height. In practice due

to different degradation mechanisms a leak may be more likely in particular areas which would change the probability and magnitude of the consequences calculated by the analysis.

- The gas leaking from a vessel is assumed to instantaneously and perfectly mix with the gas in the module. This assumption was made to enable a computationally efficient simulation of a gas leak, although it results in a less accurate simulation of a leak. A CFD approach could more accurately simulate this mixing at the cost of increased computation requirements.
- An oil leak was assumed to accumulate as a pool with a fixed depth onto the module floor until the module was full, excess oil was not considered by the analysis. This assumes a simple accumulation of oil and neglects the effects of excess oil to other parts of the platform.

8.4 System Review

A description of the design of the various systems examined in this work was presented in Chapter 3. The system design included three major systems, the production system, the power generation system and the firewater deluge system. These were selected as the research aimed to evaluate the production and risk of fire or explosion and these systems were considered to be the most critical for this evaluation. Nevertheless, the addition of more systems could be included in further work, which would increase the coverage of the model and therefore more accurately represent an offshore platform. The model was designed to be general such that a user could add any arbitrary system given the necessary information, thus the addition of more system would require no change to the fundamental structure of the model. For instance, the other safety systems discussed in Section 1.5 could be added. Of particular interest would be the HVAC system as the availability of this could affect the accumulation of gas in the consequence analysis.

A simulation of the platform's life spanned 50 years, this represented the initial 25 years of design life followed by an additional 25 years in the LE stage. When entering the LE stage the assets have already been undergoing degradation and AM, therefore, the condition of the assets at the start of LE were representative of expected conditions at the end of design life under the given AM strategy. Simulating for this extended period evaluated an AM strategy over both the design life and LE stage.

The degradation of assets were simulation through a series of observables, with

each observable being associated with a unique degradation mechanism and failure mode. This allowed for the different rates at which the degradation occur be specified separately for each degradation mechanism. The discretisation of the observable was important for the specifying the maintenance strategy because it allowed for preventative maintenance to be queued based on the observable's current condition. The transition times between the conditions and to the failure modes were sampled from Weibull distributions, which were selected as they can simulate increasing failure rate later in the asset's life. Nevertheless, real systems often undergo gradual degradation that would be better simulated with a continuous process. It would be interesting to investigate the application of continuous degradation, possibly through continuous transitions in the HSPN.

Inspection actions revealed the current states of a subset of an asset's observables and failure modes. It is important to note that inspections can be defined to act on multiple observables of an asset, this increased the complexity of the relationships between an asset's inspections and observables. For instance, if a duty-holder wanted to increase their knowledge of a particular observable which was acted on by two inspections, then it would not be immediately apparent which inspection's interval should be decreased. Within the model only periodic inspections were implemented, although, on a real platform there would also be risk based inspections, live condition monitoring and more. In further work, more types of inspections could be added which could improve the accuracy of the model in representing real inspection regimes.

When a production asset is in a degraded failure mode the flow rate is halved and when it is a critical failure mode the flow is halted. Although, there are other activities that can take place that will require production to be stopped. For instance, an internal inspection can require the asset's production to be stopped and some maintenance actions will also require the asset to be taken out of surface for the duration of the task. In future research this behaviour could be added to the system design and the effects on the loss of production could be analysed.

8.5 HSPN Review

The main technique used in this thesis was a PN extension, that was created for this work, known as an HSPN which was described in detail in Chapter 4. The hybrid technique combined the modelling of both discrete and continuous process within a single technique. The discrete part simulated events that changed from one state to

another instantaneously, although these could occur after constant delays or stochastically sampled delays. Degradation, inspection and maintenance were simulated using the discrete part, stochastic sampling of Weibull distributions defined the degradation delays and failures, constant delays were used to simulate periodic inspections and the duration of maintenance actions. In addition to these processes, the model also simulated the production of oil and gas throughout the platform's life, as this is a fluid flow it didn't make sense to model it as a discrete process. This was the motivation behind creating a hybrid net, such that the AM and fluid flow could be simulated within a single technique. Furthermore, by combining the discrete and continuous components interactions and dependencies between the AM and production could be trivially added through simple HSPN structures. In particular, the production rate of an asset was determined by the failure modes of it's observables.

Hybrid PN techniques have previously been constructed and used in research, for instance by Lu et al.; Ghasemieh, Remke, and Haverkort; Khilwani, Tiwari, and Sabuncuoglu (2016; 2013; 2011). Although, this research is the only known use of a hybrid or continuous PN in reliability engineering in the oil and gas industry. As the HSPN was created specifically for this research it could be designed to fit the model's requirements. For example, a priority was assigned to each transition to control the order they fire in, which was used in the optimisation to prioritise maintenance actions.

The degradation of a observable was simulated through a series of stochastic transitions that sample from probability density functions. Thereby, the HSPN is non-deterministic and thus repeating the simulation with the same initial conditions will produce different results. So to evaluate the results of the HSPN a large number of simulation must be performed and analysed for each set of initial conditions, this is achieved through the application of the MC method. In comparison to a non-deterministic approach this is computationally expensive but also accurately represents the stochastic nature of degradation and failures in a real system.

The HSPN is a versatile technique capable of modelling diverse system structures and interdependencies between them. This is of note when considering the power generation and firewater deluge systems, these have a high degree of redundancy to reduce their unavailability. Typically the relationships between the failure of the system's assets are given by fault trees, it was seen that these could be represented within the HSPN, such that system failures were always known subject to the failures of their assets. Furthermore, interdependencies between the systems were included, for example, the electric firewater deluge pumps were dependent on the supply of emergency

power from the generation system. This dependency was easily added by connecting the emergency power system failure place with the electric pump system failure place through a transition. It is considered that this ease of representing and connecting systems was one of the main advantages of the technique, allowing complex systems and interdependencies to be constructed in the net.

The structure of a PN lends itself to a clear graphical representation, which is useful for representing the complex systems seen in this work. Despite this, the scale of the net was too large to display in a single figure, with 24803 nodes, of which 16583 were transitions and 8220 were places. Many of the structures within the net were repeated, these were represented by substitution transitions and inserted into higher level nets to build a hierarchical structure. Through this approach the apparent complexity of the net could be drastically reduced such that it could be understood.

Due to the stochastic elements of the model a MC method was used to determine the results, this was successful in arriving at reliable results but does put a limit on the size of the model. As the model size increases the number of stochastic events also increase and therefore to obtain convergence of results a greater number of simulations would be required to be performed. Thereby, the size of a model in this framework is limited by the computational power available to the modeller. To obtain reliable results from this approximately 10^6 simulations were required. This took approximately 17 hours to complete with a Intel i7-9850H processor and 16GB of RAM.

It was shown how the HSPN model can be used to analyse several aspects of a platform's performance subject to varying AM strategy parameters. For instance, the probability of an asset being in each condition as a function of the platform age could be calculated and used to compare various inspection interval and maintenance decision combinations. The inspection interval could be further examined and used to evaluate the difference between the actual and revealed condition, known as the exposure. As more degraded conditions have greater failure rates, the exposure correlates with an increases probability of failure.

The maintenance backlog is a build-up of maintenance actions through the platform's life-cycle. To keep the backlog controlled, the number of maintenance and inspection teams can be increased, however, this can be expensive as it requires increased accommodation on the platform. The relationship between the maintenance backlog depth and the platform age was simulated for varying number of AM teams. In addition, the continuous net simulated the production quantities, the dependency

on the discrete net was demonstrated through the relationship between varying the inspection interval and the life-cycle production.

8.6 Consequence Analysis Review

The volatility of the fluids present in the production assets poses a risk to the platform on loss of containment in structural damage, economical loss and threat to life. It was therefore consider essential for the model to account for the possibility of a leak and to evaluate the risk of the possible consequences. While the HSPN simulated the occurrences of leaks caused by specific failure modes, it did not analysis the possible consequences of these leaks. A leak could occur from any of the production assets within the model and as the dimensions and fluid quantities are unique for each asset it follows that the probability and severity of the possible consequences will vary by asset. A consequence analysis, detailed in Chapter 6, was created to be able to evaluate the consequences of a leak characterised by initial conditions relating to the asset and the leak size. This was integrated with the HSPN such that an asset's leak failure modes triggered a consequence analysis, which allowed for the performance of AM strategies to be examined accounting for the risk posed by the leaks.

There was a wide range of possible techniques available to perform a consequence analysis of a leak. Examining the literature it was seen that detailed CFD were the dominant technique, these typically were focused on producing highly detailed results. In general, CFD techniques involved dividing a three-dimensional space into small regions and simulating the movement of fluids through these regions using the equations of fluid mechanics. The computational requirements of these are dependent on the level of detail of the simulation although they tend to be significant. Instead a relatively simplistic numerical simulation technique was chosen that did not simulate the three-dimensional space, this had much smaller computational requirements and thus could simulate numerous iterations of many scenarios, which allowed for probability density distributions of each consequence to be calculated for every production asset.

The technique was based on work by Andrews, Smith, and Gregory; Foster and Andrews; Lewthwaite (1994; 1999; 2006), which was designed specifically for the analysis of hydrocarbon leaks on an offshore oil and gas platform. By simulating the discharge of oil or gas from the leaking vessel over iterative time-steps the time-evolution of the leak was calculated, this determined the concentration of gas in the module and the oil pool area which were used to evaluate the severity of a fire or explosion. As the

simulation relied on some stochastic initial conditions relating to the leak position and size it required a MC method to produce a distribution of results. For each production asset four consequence analysis were performed for the degraded and critical leak failure modes with and without the module's firewater deluge system available. Nevertheless, the assumption made to reduce the techniques complexity would also decrease the realism of the simulation, with sufficient computational resources the technique could be replaced with a more detailed three-dimensional CFD approach. This would account for more complex elements such as the physical layout of the platform and the compounding risks posed by nearby assets to a fire or explosion which could also ignite.

The consequence analysis was capable of producing probability density functions of the consequences for leak scenarios from every production asset subject to failure modes and safety system availabilities. By combining results from the HSPN and consequence analysis risk profiles were calculated for the escalation events from each leak. The risks could be calculated as a function of the platform age, where increasing risk was seen throughout the life-cycle. Furthermore, the risk profile could be evaluated as a function of both platform age and escalation magnitude. These risk profiles were then used to compare three example AM strategies, demonstrating the success of the integration of the HSPN and consequence analysis to analyse the risk of the potential consequences.

8.7 Optimisation Review

The combination of the HSPN model and the consequence analysis created a methodology for evaluating the performance and risk of various AM strategies. An optimisation algorithm was applied to the model to produce a technique for determining optimal AM strategies. As the performance can be measured through multiple metrics a multi-objective optimisation technique was used known as the NSGA-II. Chapter 7 provides a detailed description of the optimisation technique and its results. This was shown to be successful in producing a set of solutions that covered the Pareto surface.

An evolutionary algorithm was selected as the optimiser as it does not require a user to specify a particular action for improving the objective values. It instead acts like an evolutionary process, breeding the fittest solutions from each generation, gradually increasing the population's fitness. As genetic algorithms do not have any explicitly defined approach to minimising or maximising the objectives it can find niche and

unexpected solutions that might otherwise be missed.

The optimisation aimed to optimise three objectives of the platform's performance, specifically these were the production availability, AM expenditure and the number of escalation events. These were selected to measure distinct and important aspects of the platform's performance. The optimisation of the objectives would be conflicting, for instance, the optimal AM strategy for minimising the AM expenditure may be non-optimal for the maximising the production availability. An advantage of the NSGA-II was that it required no weighting or preference of any objective, instead it produced a set of results that approached the Pareto surface in the three-dimensions of the three objectives. Thereby, this provided a duty-holder a selection of solutions that satisfied the different objectives to various degrees but were all near the Pareto surface. This meant that the pay-off between the objectives could be seen before a decision had to be made.

The AM strategy was encoded in a decision vector for the NSGA-II, this consisted predominately of maintenance decisions and inspection intervals which were boolean and integer values respectively. To encode these they were both converted into binary and these were represented as strings of binary genes. In total the decision vector was composed of 13970 binary genes, the breakdown of which was seen in Table 7.1. Despite the large size of the decision vector, it was seen that the algorithm successfully produced a set of solutions that were near the Pareto surface.

The solutions generated by the NSGA-II were found to be both diverse and to be near the Pareto front, this was demonstrated by the arcs shown between pairs of the objectives in Subsection 7.5.1. Furthermore, the objective variables were seen to be successfully minimised and maximised. The production availability at first rapidly increased and continued to undergo gradual and steady improvement throughout the generations. The AM expenditure also was decreased by the optimisation, although in examining its contributing parts, it was found that the inspection expenditure increased but this resulted in a reduction in the maintenance expenditure as less expensive corrective maintenance was required. A decrease was also seen in the escalation events early in the optimisation, this was examined further to produce risk profile densities through the optimisation, which showed how the risk was decreased.

The effects of the optimisation on the decision variables was also analysed. It was shown that the solution's inspection intervals and maintenance decisions were concentrated in ranges that had the greatest impact on their asset's failure rates. Both

the maintenance and inspection teams were seen to converge to approximately 3 and 2 teams respectively. Although, the standard deviation of the number of inspection teams was quite large, reflecting the variety of inspection requirements in the solutions. This result is critical for the effective sizing of the accommodation on the platform, it demonstrates that the number of teams required is dependent on the solution a duty holder chooses. In addition, the prioritisation of maintenance actions was examined in respect to the power system. It was seen that the optimisation prioritised the emergency power assets over the main power assets in most solutions, this was a result of the higher criticality of the emergency power assets.

8.8 Data Review

The primary source of data was OREDA which provided the reliability data for the AM modelling. This was composed of data-sheets that were categorised by asset. The coverage of the assets was excellent, with data available for every asset in the model. Although, the cumulative running hours and the number of failure for each asset could vary significantly and thereby the uncertainty of the failure rates would also vary. The confidence in the data could always be improved by the addition of more recorded hours and failures.

The data-sheets recorded the occurrences of various failure modes in three levels of severity which were categorised into *incipient*, *degraded* and *critical*. This provided a good basis for constructing degradation and failure mode based off of real failure rates. Although, the data only gave the failure rates and so the degradation rates of the associated observable had to be estimated. As the inspections of an asset would reveal the condition of an observable it is reasonable to assume that a duty-holder would have data available that could be used to calculate the degradation rates. If data of this type could be sourced and included then the accuracy of the model's results could be improved.

One area in which this research was benefit from would be expenditure data for AM tasks. The expenditures used were estimated with the purpose of being indicative of the inspection and maintenance costs. This was sufficient for constructing a hierarchy of costs where larger assets corresponding with increased costs and corrective maintenance was more expensive than preventative. Nevertheless, if a data source of accurate expected inspection and maintenance expenditures could be found then the expenditures forecast would be more accurate.

8.9 Key Findings

The key findings of this thesis include:

- **Construction of a novel PN technique.** A novel PN technique was formulated specifically to address the needs of this model, known as the HSPN. It was designed to be a hybrid technique with the addition of prioritised transitions. This combined the simulation of discrete and continuous events within a single PN framework which greatly increased the capability of the technique.
- **Application of the HSPN for analysing the performance of an offshore oil and gas platform.** North Sea platform Beryl B was simulated through its life to determine performance metrics based on the results of the HSPN. The net simulated degradation, inspections and maintenance as discrete events while simultaneously modelling production as a continuously process. Through this the performance of the platform was analysed with metrics relating to the expenditure from the AM tasks and the production quantities for the platform's life.
- **Application of a consequence analysis of hydrocarbon leaks.** An approach for simulating the time-evolution of a hydrocarbon leak from a two-phase vessel was constructed. This was a powerful technique that could be applied to a vessel containing a mix of oil and gas at arbitrary volumes and pressures. The stochastic simulations determined a consequent event that could be a jet fire, pool fire, explosion or no escalation. In addition, the magnitude of each of these events could be determined as a flame length or the overpressure resulting from an explosion. This analysis was selected as the computational requirements of a single simulation were low, therefore, through the application of a MC method probability density functions were determined for each consequent event for a given leak.
- **Integration of the HSPN with the consequence analysis.** The consequence analysis was integrated alongside the HSPN such that when particular places in the HSPN became marked, which represented the leak failure modes of the hydrocarbon containing vessels, the consequence analysis is triggered. By combining these techniques into a single framework it increased the aptitude of the framework to provide an effective tool for evaluating the performance of the platform accounting for multiple metrics including the AM expenditures and production quantities and the risk from the consequent events.

- **The multi-objective optimisation of the AM strategy of an offshore oil and gas platform.** The integration of the HSPN and consequence analysis created a model for the evaluation of the performance of a platform throughout its life-cycle under a given AM strategy. To expand the utility of this work an optimisation technique was applied to find optimal strategies. The performance metrics from the HSPN and consequence analysis were not directly comparable as they did not have a common unit or easy conversion method, therefore it was decided that a multi-objective algorithm would be most appropriate. A comprehensive review of the literature found the NSGA-II was a successful optimisation technique for solving multi-objective problems and so this was selected for this work. Furthermore, as an evolutionary algorithm it did not require any specification of procedure for improving the objective values and instead relied on the evolution of fit solution. It was seen the the results of the algorithm were successful in producing a solution set that approached the Pareto surface, which a duty-holder could select an AM strategy from.
- **The analysis of a platform through design life and LE**. The technique simulated the platform for a period of 50 years, composed of an initial 25 years of design life and an additional 25 years of LE. Thus the performance of the AM strategies were evaluated with respect to LE and the associated ageing effects this brings with it. For instance, the condition of the assets at the start of the LE stage can be degraded and furthermore, the conditions may now be more degraded than the last inspection had revealed. The proper sizing of maintenance and inspection teams is crucial for the design of the accommodation and so carries a large cost. The model incorporated the simulation of these teams and the optimisation went further to determine the optimal amount for each solution. Additionally, the prioritisation of maintenance tasks was addressed through the optimisation, demonstrating the prioritisation of assets with high criticality to their systems. The optimisation of the objectives was compared to three reasonable example AM strategies and shown to produce superior solutions in all three objectives simultaneously.
- **Separate optimisation of the design life and LE strategies.** An extension to the model's optimisation was presented which contained two distinct AM strategies, one for design life and one for LE known as the two-step optimisation. To implement this the number of genes were doubled and the HSPN was modified after the design life was elapsed to represent the LE strategy. The produced solution set was shown to be superior to the normal optimisation in objective

space. However, it was also noted that the normal optimisation outpaced the two-step and at lower generation numbers the normal optimisation produced better solutions. Although, given more generations the two-step could arrive at more optimal solutions than the normal optimisation could achieve. This demonstrates that for optimal performance the AM strategy should be changed for the LE stage of the platform's lifecycle. The AM strategy of LE cannot be considered in isolation as it depends on the effectivity of the design life strategy. The two-step approaches optimises both strategies together, thus considering the interdependencies between them.

8.10 Future Research

A number of areas it would be advantageous for future research to focus on were identified in this chapter. These suggestions aim to help researchers understand the key areas that this work could be improved to increase the accuracy and scope of the work. These include:

- **Continuous degradation with the HSPN.** The degradation was simulated as a discrete process through the discrete part of the net. However, research could take advantage of the continuous part of the net to simulate the degradation as a continuous process. This would require new interactions with the inspections, maintenance and failures.
- **More types of inspection.** In this work, periodic inspections were the only type of inspection that were considered. Future research could implement the other types of inspections such as risk-based inspections and live condition monitoring. The inclusion of these would more accurately represent inspection actions on a modern platform and therefore improve the model's results.
- **Production unavailability from maintenance and inspections.** This work considered asset failures to be the cause of all production unavailability. However, other actions can impact the unavailability, for instance internal inspections and maintenance can require an asset to be removed from service. It would be interest for further work to model this and investigate the effect on the production availability.
- **A CFD approach to the consequence analysis.** The consequence analysis used in this research was relatively simple in comparison to other available techniques. This was selected due to the ability to perform a large number of sim-

ulation on each leak event and determine the distributions of the consequences. Nevertheless, given more computational resources a more complex analysis could be performed. This could be a CFD approach that models the dispersion of gas through the platform and further, considers the interaction between fire and explosions and other nearby vessels. With this the accuracy of the consequence analysis results could be greatly improved.

- **Improved data sources.** The primary source of data in this work was OREDA, while it had excellent coverage of the systems' assets, it only considered failure rates and so degradation rates had to be estimated. To improve the quality of the results, data sources relating to the degradation or failure rates would be valuable. In addition, the maintenance and inspection expenditures were also estimated, however, it is reasonable to expect that a duty-holder would have good estimates of these values from experience.

8.11 Summary and Discussion

The main aim of this research was to devise a methodology for analysing AM strategies applied to a producing offshore oil and gas platform throughout its design life and a subsequent LE period. To analyse the performance of the platform, the aim was to evaluate the production and risk from leaks. Furthermore, an aim was to create an optimisation technique for determining the best AM strategies for whole life platform performance.

Following a comprehensive literature review it was decided that a novel PN technique would be developed as the core technique for modelling the platform's AM and production life-cycle. This was enhanced with the addition of a consequence analysis for determining the risk profiles of fires and explosions following a hydrocarbon leak. Together these formed a successful integrated methodology for analysis the effectivity of a given AM strategy. Although, the methodology went further with a genetic algorithm that encapsulated the HSPN and consequence analysis to create an optimisation procedure for determining a set of optimal AM strategies. Ultimately, the work provides a user with a set of strategies for a given platform design that optimally satisfy various objectives along the Pareto front.

References

Abaei, Mohammad Mahdi, Rouzbeh Abbassi, Vikram Garaniya, Shuhong Chai, and Faisal Khan (2018). *"Reliability assessment of marine floating structures using Bayesian network"*. In: *Applied Ocean Research* 76, pp. 51–60.

Abraham, Ajith and Lakhmi Jain (2005). *"Evolutionary multiobjective optimization"*. In: *Evolutionary Multiobjective Optimization*. Springer, pp. 1–6.

Alileche, Nassim, Damien Olivier, Lionel Estel, and Valerio Cozzani (2017). *"Analysis of domino effect in the process industry using the event tree method"*. In: *Safety science* 97, pp. 10–19.

Alla, Hassane and René David (1998a). *"A modelling and analysis tool for discrete events systems: continuous Petri net"*. In: *Performance Evaluation* 33.3, pp. 175–199.

— (1998b). *"Continuous and hybrid Petri nets"*. In: *Journal of Circuits, Systems, and Computers* 8.01, pp. 159–188.

Amin, Md Tanjin, Faisal Khan, and Syed Imtiaz (2018). *"Dynamic availability assessment of safety critical systems using a dynamic Bayesian network"*. In: *Reliability Engineering & System Safety* 178, pp. 108–117.

Andersson, Bengt, Ronnie Andersson, Love Håkansson, Mikael Mortensen, Rahman Sudiyo, and Berend Van Wachem (2011). *Computational fluid dynamics for engineers*. Cambridge University Press.

Andrews, J (2002). *"Fault Tree Analysis–Common Misconceptions"*. In: *Proceedings of the 20th International System Safety Conference*, pp. 401–410.

Andrews, J, Roger Smith, and J Gregory (1994). *"Procedure to calculate the explosion frequency for a module on an offshore platform"*. In: *Process safety and environmental protection* 72.2, pp. 69–82.

Andrews, JD and LM Bartlett (2003). *"Genetic algorithm optimization of a firewater deluge system"*. In: *Quality and reliability engineering international* 19.1, pp. 39–52.

Andrews, John D and Sally Beeson (2003). *"Birnbaum's measure of component importance for noncoherent systems"*. In: *IEEE Transactions on Reliability* 52.2, pp. 213–219.

Andrews, John D and Thomas Robert Moss (2002). *Reliability and risk assessment*. Wiley-Blackwell.

Andrews, John (2013). *"A modelling approach to railway track asset management"*. In: *Proceedings of the Institution of Mechanical Engineers, Part F: Journal of Rail and Rapid Transit* 227.1, pp. 56–73.

Arnold, Ken and Maurice Stewart (1999). *Surface Production Operations, Design of Gas-Handling Systems and Facilities*. Vol. 2. Gulf Professional Publishing.

Audley, Matthew and John Andrews (2013). *"A Petri-net modelling approach to rail track geometry maintenance and inspection"*. In: *Advances in Risk and Reliability Technology Symposium*. Citeseer, pp. 230–243.

Baig, Ahmed Ali, Risza Ruzli, and Azizul B Buang (2013). *"Reliability analysis using fault tree analysis: a review"*. In: *International Journal of Chemical Engineering and Applications* 4.3, p. 169.

Barton, DN, T Saloranta, SJ Moe, HO Eggestad, and S Kuikka (2008). *"Bayesian belief networks as a meta-modelling tool in integrated river basin management—Pros and cons in evaluating nutrient abatement decisions under uncertainty in a Norwegian river basin"*. In: *Ecological economics* 66.1, pp. 91–104.

Bause, Falko and Peter Kritzinger (1996). *"Stochastic Petri Nets"*. In: *Verlag Vieweg, Wiesbaden* 26.

Berk, Joseph (2009). *Systems failure analysis*. ASM International.

Bhandari, Jyoti, Ehsan Arzaghi, Rouzbeh Abbassi, Vikram Garaniya, and Faisal Khan (2016). *"Dynamic risk-based maintenance for offshore processing facility"*. In: *Process Safety Progress* 35.4, pp. 399–406.

Bhattacharyya, SK and AS Cheliyan (2019). *"Optimization of a subsea production system for cost and reliability using its fault tree model"*. In: *Reliability Engineering & System Safety* 185, pp. 213–219.

Bly, Mark (2011). *Deepwater horizon accident investigation report*. Diane Publishing.

Borg, Audun, Bjarne Paulsen Husted, and Ove Njå (2014). *"The concept of validation of numerical models for consequence analysis"*. In: *Reliability Engineering & System Safety* 125, pp. 36–45.

Boudali, Hichem, Pepijn Crouzen, and Mariëlle Stoelinga (2009). *"A rigorous, compositional, and extensible framework for dynamic fault tree analysis"*. In: *IEEE Transactions on Dependable and Secure Computing* 7.2, pp. 128–143.

Bozorg-Haddad, Omid, Mohammad Solgi, and Hugo A Loáiciga (2017). *Meta-heuristic and evolutionary algorithms for engineering optimization*. John Wiley & Sons.

Briš, Radim (2013). *"Evaluation of the production availability of an offshore installation by stochastic petri nets modeling"*. In: *Digital Technologies (DT), 2013 International Conference on*. IEEE, pp. 147–155.

British Standard, BS (2011). *EN 62502: 2011 Analysis techniques for dependability. Event tree analysis (ETA)*.

Cai, Baoping, Yonghong Liu, Zengkai Liu, Yuanjiang Chang, and Lei Jiang (2020). *"Risk analysis of subsea blowout preventer by mapping GO models into Bayesian networks"*. In: *Bayesian Networks for Reliability Engineering*. Springer, pp. 165–187.

Cai, Baoping, Yonghong Liu, Yunwei Zhang, Qian Fan, Zengkai Liu, and Xiaojie Tian (2013). *"A dynamic Bayesian networks modeling of human factors on offshore blowouts"*. In: *Journal of Loss Prevention in the Process Industries* 26.4, pp. 639–649.

Cai, Baoping, Yu Liu, and Min Xie (2016). *"A dynamic-Bayesian-network-based fault diagnosis methodology considering transient and intermittent faults"*. In: *IEEE Transactions on Automation Science and Engineering* 14.1, pp. 276–285.

Cai, Baoping, Min Xie, Yonghong Liu, Yiliu Liu, and Qiang Feng (2018). *"Availability-based engineering resilience metric and its corresponding evaluation methodology"*. In: *Reliability Engineering & System Safety* 172, pp. 216–224.

Čepin, Marko (2011). *"Event tree analysis"*. In: *Assessment of Power System Reliability*. Springer, pp. 89–99.

Cesare, Mark A, Carlos Santamarina, Carl Turkstra, and Erik H Vanmarcke (1992). *"Modeling bridge deterioration with Markov chains"*. In: *Journal of Transportation Engineering* 118.6, pp. 820–833.

Chambari, Amirhossain, Seyed Habib A Rahmati, Amir Abbas Najafi, et al. (2012). *"A bi-objective model to optimize reliability and cost of system with a choice of redundancy strategies"*. In: *Computers & Industrial Engineering* 63.1, pp. 109–119.

Chamberlain, GA et al. (2002). *"Controlling hydrocarbon fires in offshore structures"*. In: *Offshore Technology Conference*. Offshore Technology Conference.

Charnes, Abraham, William W Cooper, and Robert O Ferguson (1955). *"Optimal estimation of executive compensation by linear programming"*. In: *Management science* 1.2, pp. 138–151.

Chemweno, Peter, Liliane Pintelon, Peter Nganga Muchiri, and Adriaan Van Horenbeek (2018). *"Risk assessment methodologies in maintenance decision making: A*

review of dependability modelling approaches". In: *Reliability Engineering & System Safety* 173, pp. 64–77.

Chew, Samuel P, Sarah J Dunnett, and John D Andrews (2008). *"Phased mission modelling of systems with maintenance-free operating periods using simulated Petri nets"*. In: *Reliability Engineering & System Safety* 93.7, pp. 980–994.

Cho, SangJe, Jong-Ho Shin, Hong-Bae Jun, Ho-Jin Hwang, Chunghun Ha, and Jinsang Hwang (2016). *"A study on estimating the next failure time of compressor equipment in an offshore plant"*. In: *Mathematical Problems in Engineering* 2016.

Choi, In-Hwan and Daejun Chang (2016). *"Reliability and availability assessment of seabed storage tanks using fault tree analysis"*. In: *Ocean Engineering* 120, pp. 1–14.

Clarke, Keith C and Jeffrey J Hemphill (2002). *"The Santa Barbara oil spill: A retrospective"*. In: *Yearbook of the Association of Pacific Coast Geographers* 64.1, pp. 157–162.

Clemens, Pat L, Rodney J Simmons, and O Cincinnati (1998). *"System safety and risk management: A guide for engineering educators"*. In: *Lesson II Risk assessment matrix. NIOSH Instructional Module. Cincinnati, OH, USA: US Department of Health and Human Services*.

Clifton, Ericson et al. (1999). *"Fault tree analysis-a history"*. In: *Proceedings of the 17th International Systems Safety Conference*, pp. 1–9.

Colapinto, Cinzia, Raja Jayaraman, and Simone Marsiglio (2017). *"Multi-criteria decision analysis with goal programming in engineering, management and social sciences: a state-of-the art review"*. In: *Annals of Operations Research* 251.1-2, pp. 7–40.

Council, National Research (2010). *Interim Report on Causes of the Deepwater Horizon Oil Rig Blowout and Ways to Prevent Such Events*. National Academy of Engineering and National Research Council of the National Academies.

Cristaldi, Loredana, Mohamed Khalil, and Marco Faifer (2017). *"Markov process reliability model for photovoltaic module failures"*. In: *Acta IMEKO* 6.4, pp. 121–130.

Cui, Yunfei, Zhiqiang Geng, Qunxiong Zhu, and Yongming Han (2017). *"Multi-objective optimization methods and application in energy saving"*. In: *Energy* 125, pp. 681–704.

Cullen, Lord W Douglas (1993). *"The public inquiry into the Piper Alpha disaster"*. In: *Drilling Contractor;(United States)* 49.4.

DECOM (2014). *Decommissioning in the North Sea*.

DNV (2015). *Fire Protection*.

Dadashzadeh, Mohammad, Rouzbeh Abbassi, Faisal Khan, and Kelly Hawboldt (2013). *"Explosion modeling and analysis of BP Deepwater Horizon accident"*. In: *Safety science* 57, pp. 150–160.

David, René (1997). *"Modeling of hybrid systems using continuous and hybrid Petri nets"*. In: *Proceedings of the Seventh International Workshop on Petri Nets and Performance Models*. IEEE, pp. 47–58.

De Falco, Ivan, Antonio Della Cioppa, and Ernesto Tarantino (2002). *"Mutation-based genetic algorithm: performance evaluation"*. In: *Applied Soft Computing* 1.4, pp. 285–299.

Deb, Kalyanmoy (1999). *"Multi-objective genetic algorithms: Problem difficulties and construction of test problems"*. In: *Evolutionary computation* 7.3, pp. 205–230.

— (2001). *Multi-objective optimization using evolutionary algorithms*. Vol. 16. John Wiley & Sons.

— (2011). *"Multi-objective optimisation using evolutionary algorithms: an introduction"*. In: *Multi-objective evolutionary optimisation for product design and manufacturing*. Springer, pp. 3–34.

Deb, Kalyanmoy, Amrit Pratap, Sameer Agarwal, and TAMT Meyarivan (2002). *"A fast and elitist multiobjective genetic algorithm: NSGA-II"*. In: *IEEE transactions on evolutionary computation* 6.2, pp. 182–197.

Devold, Havard (2013). *Oil and gas production handbook: an introduction to oil and gas production*. Lulu. com.

Dharmaraja, Resham Vinayak S (2012). *"Semi-Markov modeling approach for deteriorating systems with preventive maintenance"*. In: *International Journal of Performability Engineering* 8.5, pp. 515–526.

Dhulipala, Somayajulu LN and Madeleine M Flint (2020). *"Series of semi-Markov processes to model infrastructure resilience under multihazards"*. In: *Reliability Engineering & System Safety* 193, p. 106659.

Elsayed, Elsayed A (2012). *Reliability engineering*. Vol. 88. John Wiley & Sons.

Ericson, Clifton A et al. (2015). *Hazard analysis techniques for system safety*. John Wiley & Sons.

Ersdal, Gerhard, Erik Hörnlund, and Hans Spilde (2011). *"Experience from Norwegian programme on ageing and life extension"*. In: *ASME 2011 30th International Conference on Ocean, Offshore and Arctic Engineering*. American Society of Mechanical Engineers, pp. 517–522.

Ever, Enver, Orhan Gemikonakli, Altan Kocyigit, and Eser Gemikonakli (2013). *"A hybrid approach to minimize state space explosion problem for the solution of two*

stage tandem queues". In: *Journal of Network and Computer Applications* 36.2, pp. 908–926.

Fenton, Norman and Martin Neil (2012). *Risk assessment and decision analysis with Bayesian networks*. Crc Press.

Fleming, Karl N (2004). *"Markov models for evaluating risk-informed in-service inspection strategies for nuclear power plant piping systems"*. In: *Reliability Engineering & System Safety* 83.1, pp. 27–45.

Foster, KJ and JD Andrews (1999). *"Techniques for modelling the frequency of explosions on offshore platforms"*. In: *Proceedings of the Institution of Mechanical Engineers, Part E: Journal of Process Mechanical Engineering* 213.2, pp. 111–119.

Freitas, Alex A (2004). *"A critical review of multi-objective optimization in data mining: a position paper"*. In: *ACM SIGKDD Explorations Newsletter* 6.2, pp. 77–86.

Friedrich, Tobias, Timo Kötzing, Martin S Krejca, and Andrew M Sutton (2016). *"The compact genetic algorithm is efficient under extreme gaussian noise"*. In: *IEEE Transactions on Evolutionary Computation* 21.3, pp. 477–490.

GEO ExPro (n.d.). *Pioneering Production from the Deep Sea*. (Accessed on 11/28/2016). URL: `http://www.geoexpro.com/articles/2008/04/pioneering-production-from-the-deep-sea`.

Gagniuc, Paul A (2017). *Markov chains: from theory to implementation and experimentation*. John Wiley & Sons.

GexCon, AS (2014). *"FLACS v10. 0 User's Manual"*. In: *GexCon AS, Bergen, Norway*.

Ghasemieh, Hamed, Anne Remke, and Boudewijn R Haverkort (2013). *"Survivability evaluation of fluid critical infrastructures using hybrid Petri nets"*. In: *2013 IEEE 19th Pacific Rim International Symposium on Dependable Computing*. IEEE, pp. 152–161.

Ghomri, Latefa and Hassane Alla (2007). *"Modeling and analysis using hybrid Petri nets"*. In: *Nonlinear Analysis: Hybrid Systems* 1.2, pp. 141–153.

Goh, Chi Keong and Kay Chen Tan (2007). *"An investigation on noisy environments in evolutionary multiobjective optimization"*. In: *IEEE Transactions on Evolutionary Computation* 11.3, pp. 354–381.

Goicoechea, Ambrose, Don R Hansen, and Lucien Duckstein (1982). *Multiobjective decision analysis with engineering and business applications*. Tech. rep. John Wiley & Sons.

Golchha, Ankita and Shahana Gajala Qureshi (2015). *"Non-dominated sorting genetic algorithm-II–A succinct survey"*. In: *International Journal of Computer Science and Information Technologies* 6.1, pp. 252–255.

Gorjian, Nima, Lin Ma, Murthy Mittinty, Prasad Yarlagadda, and Yong Sun (2010). *"A review on degradation models in reliability analysis"*. In: *Engineering Asset Lifecycle Management*. Springer, pp. 369–384.

Gowid, Samer, Roger Dixon, and Saud Ghani (2014). *"Optimization of reliability and maintenance of liquefaction system on FLNG terminals using Markov modelling"*. In: *International Journal of Quality & Reliability Management*.

Guo, Yanbao, Xiaoli Meng, Deguo Wang, Tao Meng, Shuhai Liu, and Renyang He (2016). *"Comprehensive risk evaluation of long-distance oil and gas transportation pipelines using a fuzzy Petri net model"*. In: *Journal of Natural Gas Science and Engineering* 33, pp. 18–29.

HSE (n.d.). *Fire and Gas Detection*. (Accessed on 24/03/2020). URL: `https://www.hse.gov.uk/offshore/strategy/fgdetect.htm`.

HSE (2007). *KP3: Asset integrity programme handbook*.

HSE (2009). *Guidance on management of ageing and thorough reviews of ageing installations*.

— (2010). *Plant Ageing Study*.

— (2013). *"KP4: Ageing & Life Extension Inspection Programme"*. In: *Offshore Europe*. Society of Petroleum Engineers.

Hamdani, Tarek M, Jin-Myung Won, Adel M Alimi, and Fakhri Karray (2007). *"Multi-objective feature selection with NSGA II"*. In: *International conference on adaptive and natural computing algorithms*. Springer, pp. 240–247.

Hansen, Olav R, Mathieu Ichard, and Scott G Davis (2009). *"Validation of FLACS for vapor dispersion from LNG spills: model evaluation protocol"*. In: *Proc. 2009 Mary Kay O'Connor Process Safety Symposium*.

Hokstad, Per, Solfrid Håbrekke, Roy Johnsen, and Sigbjørn Sangesland (2010). *"Ageing and life extension for offshore facilities in general and for specific systems"*. In: *SINTEF Report for the Petroleum Safety Authority Norway*.

Holmes, Tony, Stephen Connolly, Jill Wilday, John Hare, and Peter Walsh (2009). *"Managing fire and explosion hazards on offshore ageing installations"*. In: *Paper Submitted to IChemE Hazards XXI Symposium*.

Hurson, Ali R (2014). *Advances in Computers*. Academic Press.

Hwang, C-L and Abu Syed Md Masud (2012). *Multiple objective decision making methods and applications: a state-of-the-art survey*. Vol. 164. Springer Science & Business Media.

ISO (1999). *13702: Petroleum and natural gas industries — Control and mitigation of fires and explosions on offshore production installations — Requirements and guidelines.*

— (2014). *"55000: Asset management Overview, principles and terminology 2014"*. In: *Incorporating corrigendum March.*

Ishibuchi, Hisao, Noritaka Tsukamoto, and Yusuke Nojima (2008). *"Evolutionary many-objective optimization: A short review"*. In: *2008 IEEE Congress on Evolutionary Computation (IEEE World Congress on Computational Intelligence)*. IEEE, pp. 2419–2426.

Ivanov, Stanislav Y and Ajay K Ray (2014). *"Multiobjective optimization of industrial petroleum processing units using Genetic algorithms"*. In: *Procedia Chemistry* 10.2014, pp. 7–14.

Jamshidi, R and Mir Mehdi Seyyed Esfahani (2015). *"Maintenance policy determination for a complex system consisting of series and cold standby system with multiple levels of maintenance action"*. In: *The International Journal of Advanced Manufacturing Technology* 78.5-8, pp. 1337–1346.

Jensen, Kurt and Lars M Kristensen (2009). *Coloured Petri nets: modelling and validation of concurrent systems*. Springer Science & Business Media.

Jones, Dylan, Mehrdad Tamiz, et al. (2010). *Practical goal programming*. Vol. 141. Springer.

Kabir, Sohag (2017). *"An overview of fault tree analysis and its application in model based dependability analysis"*. In: *Expert Systems with Applications* 77, pp. 114–135.

Kammouh, Omar, Paolo Gardoni, and Gian Paolo Cimellaro (2020). *"Probabilistic framework to evaluate the resilience of engineering systems using Bayesian and dynamic Bayesian networks"*. In: *Reliability Engineering & System Safety* 198, p. 106813.

Khare, Vineet, Xin Yao, and Kalyanmoy Deb (2003). *"Performance scaling of multi-objective evolutionary algorithms"*. In: *International conference on evolutionary multi-criterion optimization*. Springer, pp. 376–390.

Khilwani, Nitesh, Manoj Kumar Tiwari, and Ihsan Sabuncuoglu (2011). *"Hybrid Petri-nets for modelling and performance evaluation of supply chains"*. In: *International Journal of Production Research* 49.15, pp. 4627–4656.

Kijima, Masaaki (1997). *Markov processes for stochastic modeling*. Vol. 6. CRC Press.

Kirkwood, James R (2015). *Markov processes*. Vol. 20. CRC Press.

Kita, Eisuke (2011). *Evolutionary algorithms*. InTech.

Koenig, Andreas C (2002). *"A study of mutation methods for evolutionary algorithms"*. In: *University of Missouri-Rolla*.

Kolmogoroff, Andrei (1931). *"Über die analytischen Methoden in der Wahrscheinlichkeitsrechnung"*. In: *Mathematische Annalen* 104.1, pp. 415–458.

Konak, Abdullah, David W Coit, and Alice E Smith (2006). *"Multi-objective optimization using genetic algorithms: A tutorial"*. In: *Reliability Engineering & System Safety* 91.9, pp. 992–1007.

Kujath, MF, PR Amyotte, and FI Khan (2010). *"A conceptual offshore oil and gas process accident model"*. In: *Journal of loss prevention in the process industries* 23.2, pp. 323–330.

Kundu, Tanmay and Sahidul Islam (2019). *"An interactive weighted fuzzy goal programming technique to solve multi-objective reliability optimization problem"*. In: *Journal of Industrial Engineering International*, pp. 1–10.

Labib, Ashraf (2014). *Learning from failures: decision analysis of major disasters*. Elsevier.

Langseth, Helge, Thomas D Nielsen, Rafael Rumí, and Antonio Salmerón (2009). *"Inference in hybrid Bayesian networks"*. In: *Reliability Engineering & System Safety* 94.10, pp. 1499–1509.

Langseth, Helge and Luigi Portinale (2007). *"Bayesian networks in reliability"*. In: *Reliability Engineering & System Safety* 92.1, pp. 92–108.

Le, Bryant and John Andrews (2013). *"Modelling railway bridge asset management"*. In: *Proceedings of the Institution of Mechanical Engineers, Part F: Journal of Rail and Rapid Transit* 227.6, pp. 644–656.

— (2015). *"Modelling wind turbine degradation and maintenance"*. In: *Wind Energy*.

Lees, Frank (2012). *Lees' Loss prevention in the process industries: Hazard identification, assessment and control*. Butterworth-Heinemann.

Lewthwaite, Jeni L (2006). *"Fire and explosion modelling on offshore oil and gas platforms"*. PhD thesis.

Lewthwaite, Jeni L, JD Andrews, Sarah J Dunnett, CAJ Gregory, and Roger Smith (2006). *"Risk modelling of fires and explosions in open-sided offshore platform modules"*. In: *Proceedings of the Institution of Mechanical Engineers, Part O: Journal of Risk and Reliability* 220.2, pp. 123–135.

Li, Li, Lijun Sun, and Guobao Ning (2014). *"Deterioration prediction of urban bridges on network level using Markov-chain model"*. In: *Mathematical Problems in Engineering* 2014.

Liu, Tan, Xianwen Gao, and Lina Wang (2015). *"Multi-objective optimization method using an improved NSGA-II algorithm for oil–gas production process"*. In: *Journal of the Taiwan Institute of Chemical Engineers* 57, pp. 42–53.

Liu, Zengkai, Yonghong Liu, Baoping Cai, Dawei Zhang, and Chao Zheng (2015). *"Dynamic Bayesian network modeling of reliability of subsea blowout preventer stack in presence of common cause failures"*. In: *Journal of Loss Prevention in the Process Industries* 38, pp. 58–66.

Lu, Xiaoyu, MengChu Zhou, Ahmed Chiheb Ammari, and Jingchu Ji (2016). *"Hybrid Petri nets for modeling and analysis of microgrid systems"*. In: *IEEE/CAA Journal of Automatica Sinica* 3.4, pp. 349–356.

Luo, Yi, Kaicheng Li, Yuanzheng Li, Delong Cai, Chen Zhao, and Qingxu Meng (2017). *"Three-layer Bayesian network for classification of complex power quality disturbances"*. In: *IEEE Transactions on Industrial Informatics* 14.9, pp. 3997–4006.

MNSL (1993). *"Berly 'B' Safety Case"*. In: Mobil North Sea Ltd.

Mahfoudhi, Adel, Yessine Hadj Kacem, Walid Karamti, and Mohamed Abid (2012). *"Compositional specification of real time embedded systems by priority time petri nets"*. In: *The Journal of Supercomputing* 59.3, pp. 1478–1503.

Mahmood, Yasser A, Alireza Ahmadi, Ajit Kumar Verma, Ajit Srividya, and Uday Kumar (2013). *"Fuzzy fault tree analysis: A review of concept and application"*. In: *International Journal of System Assurance Engineering and Management* 4.1, pp. 19–32.

Majdara, Aref and Toshio Wakabayashi (2009). *"Component-based modeling of systems for automated fault tree generation"*. In: *Reliability Engineering & System Safety* 94.6, pp. 1076–1086.

Markov, Andrey Andreyevich (1906). *"Extension of the law of large numbers to dependent quantities"*. In: *Izv. Fiz.-Matem. Obsch. Kazan Univ.(2nd Ser)* 15, pp. 135–156.

Marler, R Timothy and Jasbir S Arora (2004). *"Survey of multi-objective optimization methods for engineering"*. In: *Structural and multidisciplinary optimization* 26.6, pp. 369–395.

— (2010). *"The weighted sum method for multi-objective optimization: new insights"*. In: *Structural and multidisciplinary optimization* 41.6, pp. 853–862.

Marsan, M Ajmone, Gianfranco Balbo, Gianni Conte, Susanna Donatelli, and Giuliana Franceschinis (1995). *Modelling with generalized stochastic Petri nets*. Vol. 292. Wiley New York.

Marseguerra, Marzio and Enrico Zio (2000). *"Optimizing maintenance and repair policies via a combination of genetic algorithms and Monte Carlo simulation"*. In: *Reliability Engineering & System Safety* 68.1, pp. 69–83.

McCool, John I (2012). *Using the Weibull distribution: reliability, modeling, and inference*. Vol. 950. John Wiley & Sons.

McGrattan, Kevin, Bryan Klein, Simo Hostikka, and Jason Floyd (2010). *"Fire dynamics simulator (version 5), user's guide"*. In: *NIST special publication* 1019.5, pp. 1–186.

Meng, Huixing, Leïla Kloul, and Antoine Rauzy (2018). *"Production availability analysis of Floating Production Storage and Offloading (FPSO) systems"*. In: *Applied Ocean Research* 74, pp. 117–126.

Miettinen, Kaisa (2012). *Nonlinear multiobjective optimization*. Vol. 12. Springer Science & Business Media.

Mihajlovic, V and Milan Petkovic (2001). *"Dynamic bayesian networks: A state of the art"*. In: *University of Twente Document Repository*.

Mkrtchyan, Lusine, Luca Podofillini, and Vinh N Dang (2015). *"Bayesian belief networks for human reliability analysis: A review of applications and gaps"*. In: *Reliability engineering & system safety* 139, pp. 1–16.

Moghaddam, Kamran S (2013). *"Multi-objective preventive maintenance and replacement scheduling in a manufacturing system using goal programming"*. In: *International Journal of Production Economics* 146.2, pp. 704–716.

Moorhouse, J (1982). *"Scaling criteria for pool fires derived from large-scale experiments"*. In: *The Assessment of Major Hazards, Symposium Series*. Vol. 71, pp. 165–179.

Mouilleau, Yvon and Anousone Champassith (2009). *"CFD simulations of atmospheric gas dispersion using the Fire Dynamics Simulator (FDS)"*. In: *Journal of Loss Prevention in the Process Industries* 22.3, pp. 316–323.

Murata, Tadao (1989). *"Petri nets: Properties, analysis and applications"*. In: *Proceedings of the IEEE* 77.4, pp. 541–580.

Murphy, Kevin Patrick and Stuart Russell (2002). *"Dynamic bayesian networks: representation, inference and learning"*. In.

NORSOK (2008). *N-006, Assessment of Structural Integrity for Existing Offshore Load-Bearing Structures*.

National Academies of Sciences, Engineering, and Medicine and others (2016). *Strengthening the Safety Culture of the Offshore Oil and Gas Industry*. Transportation Research Board.

Noroozi, Alireza, Nima Khakzad, Faisal Khan, Scott MacKinnon, and Rouzbeh Abbassi (2013). *"The role of human error in risk analysis: Application to pre-and post-maintenance procedures of process facilities"*. In: *Reliability Engineering & System Safety* 119, pp. 251–258.

Norsk-Olje-&-Gass (2001). *"Norwegian Oil and Gas Application of IEC 61508 and IEC 61511 in the Norwegian Petroleum Industry"*. In: *Guideline for the application of IEC 61508 and IEC 61511 in the offshore industry*. Norsk-Olje-&-Gass.

OREDA (2002). *Offshore and onshore reliability data handbook*.

— (2016). *Offshore reliability data handbook*. OREDA.

Office of Response and Restoration (n.d.). *Oil Spills, Seeps, and the Early Days of Drilling Oil Along California's Coast*. (Accessed on 11/28/2016). URL: `http://response.restoration.noaa.gov/about/media/oil-spills-seeps-and-early-days-drilling-oil-along-californias-coast.html`.

Online: Offshore Energy Today (2020). *Final decommissioning of BP's Miller platform*. [Online; accessed 25. Mar. 2020]. URL: `https://www.offshoreenergytoday.com/video-final-decommissioning-of-bps-miller-platform`.

Online: Rigadvisor UK (2020). *Beryl Bravo - Rigadvisor UK*. [Online; accessed 25. Mar. 2020]. URL: `https://rigadvisor.co.uk/beryl-bravo`.

Pandey, M (2005). *"Fault tree analysis"*. In: *Diktat, University of Waterloo, Waterloo*.

Pate-Cornell, M Elisabeth (1993). *"Learning from the piper alpha accident: A post-mortem analysis of technical and organizational factors"*. In: *Risk Analysis* 13, pp. 215–215.

Pearl, Judea (1985). *"Bayesian netwcrks: A model cf self-activated memory for evidential reasoning"*. In: *Proceedings of the 7th Conference of the Cognitive Science Society, University of California, Irvine, CA, USA*, pp. 15–17.

Pedersen, Helene H and Prankul Middha (2012). *"Modelling of vented gas explosions in the CFD tool FLACS"*. In: *A publication of AIDIC. The Italian Association of Chemical Engineering Online at: www. aidic. it/cet*.

Petri, Carl Adam (1966). *"Communication with automata"*. In.

Pétrowski, Alain and Sana Ben-Hamida (2017). *Evolutionary algorithms*. Wiley Online Library.

Prescott, Darren and John Andrews (2013). *"Investigating railway track asset management using a Markov analysis"*. In: *Proceedings of the Institution of Mechanical Engineers, Part F: Journal of Rail and Rapid Transit* 229.4, pp. 402–416.

Priest, Tyler (2007). *"Extraction not creation: The history of offshore petroleum in the Gulf of Mexico"*. In: *Enterprise & Society*, pp. 227–267.

Purshouse, Robin C and Peter J Fleming (2003). *"Evolutionary many-objective optimisation: An exploratory analysis"*. In: *The 2003 Congress on Evolutionary Computation, 2003. CEC'03.* Vol. 3. IEEE, pp. 2066–2073.

Ramírez, Pedro A Pérez and Ingrid Bouwer Utne (2015). *"Use of dynamic Bayesian networks for life extension assessment of ageing systems"*. In: *Reliability Engineering & System Safety* 133, pp. 119–136.

Ramseur, Jonathan L and Curry L Hagerty (2013). *"Deepwater Horizon oil spill: Recent activities and ongoing developments"*. In: *Congressional Research Service. January* 31, p. 2013.

Ramzali, Nahid, Mohammad Reza Miri Lavasani, and Jamal Ghodousi (2015). *"Safety barriers analysis of offshore drilling system by employing fuzzy event tree analysis"*. In: *Safety science* 78, pp. 49–59.

Rao, K Durga, V Gopika, VVS Sanyasi Rao, HS Kushwaha, Ajit Kumar Verma, and Ajit Srividya (2009). *"Dynamic fault tree analysis using Monte Carlo simulation in probabilistic safety assessment"*. In: *Reliability Engineering & System Safety* 94.4, pp. 872–883.

Rausand, Marvin and Arnljot Hoyland (2003). *System reliability theory: models, statistical methods, and applications*. Vol. 396. John Wiley & Sons.

Reisig, Wolfgang (2012). *Petri nets: an introduction*. Vol. 4. Springer Science & Business Media.

Reisig, Wolfgang and Grzegorz Rozenberg (1998). *Lectures on petri nets i: basic models: advances in petri nets*. Springer Science & Business Media.

Remenyte, Rasa and John D Andrews (2006). *"A simple component connection approach for fault tree conversion to binary decision diagram"*. In: *First International Conference on Availability, Reliability and Security (ARES'06)*. IEEE, 8–pp.

Rinne, Horst (2008). *The Weibull distribution: a handbook*. CRC press.

Ruijters, Enno and Mariëlle Stoelinga (2015). *"Fault tree analysis: A survey of the state-of-the-art in modeling, analysis and tools"*. In: *Computer science review* 15, pp. 29–62.

Sadeghi, Javad, Saeid Sadeghi, and Seyed Taghi Akhavan Niaki (2014). *"Optimizing a hybrid vendor-managed inventory and transportation problem with fuzzy demand: an improved particle swarm optimization algorithm"*. In: *Information Sciences* 272, pp. 126–144.

Sandtorv, Helge A, Per Hokstad, and David W Thompson (1996). *"Practical experience with a data collection project: the OREDA project"*. In: *Reliability Engineering & System Safety* 51.2, pp. 159–167.

Santa Barbara Edible (n.d.). *1969 Santa Barbara Oil Spill Triggers Activism.* (Accessed on 11/04/2016). URL: http://ediblesantabarbara.com/1969-oil-spill/.

Schniederjans, Marc (2012). *Goal programming: Methodology and applications: Methodology and applications.* Springer Science & Business Media.

Sellami, Ilyas, Brady Manescau, Khaled Chetehouna, Charles de Izarra, Rachid Nait-Said, and Fatiha Zidani (2018). *"BLEVE fireball modeling using Fire Dynamics Simulator (FDS) in an Algerian gas industry"*. In: *Journal of Loss Prevention in the Process Industries* 54, pp. 69–84.

Shafahi, Y, P Masoudi, and R Hakhamaneshi (2008). *"Track degradation prediction models, using Markov chain, artificial neural and neuro-fuzzy network"*. In: *8th World Congress on Railway Research*, pp. 1–9.

Shang, Hui and Christophe Beŕenguer (2015). *"Delayed Maintenance Model For Deteriorating Track Using Colored Petri Nets"*. In: *IFAC-PapersOnLine* 48.21, pp. 464–469.

Shell Global (n.d.). *Perdido.* (Accessed on 09/10/2020). URL: https://www.shell.com/about-us/major-projects/perdido.html.

Sheng, Jingyu and Darren Prescott (2017). *"A hierarchical coloured Petri net model of fleet maintenance with cannibalisation"*. In: *Reliability Engineering & System Safety* 168, pp. 290–305.

Sivaraj, R and T Ravichandran (2011). *"A review of selection methods in genetic algorithm"*. In: *International journal of engineering science and technology* 3.5, pp. 3792–3797.

Skogdalen, Jon Espen, Ingrid B Utne, and Jan Erik Vinnem (2011). *"Developing safety indicators for preventing offshore oil and gas deepwater drilling blowouts"*. In: *Safety science* 49.8, pp. 1187–1199.

Smith, David J (2017). *Reliability, maintainability and risk: practical methods for engineers.* Butterworth-Heinemann.

Speight, James G (2014). *Handbook of offshore oil and gas operations.* Elsevier.

Stacey, A, M Birkinshaw, and JV Sharp (2008). *"Life extension issues for ageing offshore installations"*. In: *ASME 2008 27th International Conference on Offshore Mechanics and Arctic Engineering.* American Society of Mechanical Engineers, pp. 199–215.

Suardin, Jaffee A, A Jeff McPhate Jr, Anthony Sipkema, Matt Childs, and M Sam Mannan (2009). *"Fire and explosion assessment on oil and gas floating production storage offloading (FPSO): an effective screening and comparison tool"*. In: *Process safety and environmental protection* 87.3, pp. 147–160.

Sun, Biao, Kaihua Guo, and Vishnu K Pareek (2014). *"Computational fluid dynamics simulation of LNG pool fire radiation for hazard analysis"*. In: *Journal of Loss Prevention in the Process Industries* 29, pp. 92–102.

Syan, Chanan S and Geeta Ramsoobag (2019a). *"Maintenance applications of multi-criteria optimization: A review"*. In: *Reliability Engineering & System Safety*, p. 106520.

Syan, Chanan S. and Geeta Ramsoobag (2019b). *"Maintenance applications of multi-criteria optimization: A review"*. In: *Reliability Engineering & System Safety* 190, p. 106520.

Tauseef, SM, D Rashtchian, Tasneem Abbasi, and SA Abbasi (2011). *"A method for simulation of vapour cloud explosions based on computational fluid dynamics (CFD)"*. In: *Journal of Loss Prevention in the Process Industries* 24.5, pp. 638–647.

Thomas, PH (1963). *"The size of flames from natural fires"*. In: *Symposium (International) on Combustion*. Vol. 9. 1. Citeseer, pp. 844–859.

Tosun, Ayse, Ayse Basar Bener, and Shirin Akbarinasaji (2017). *"A systematic literature review on the applications of Bayesian networks to predict software quality"*. In: *Software Quality Journal* 25.1, pp. 273–305.

Tsoukalas, Lefteri H and Robert E Uhrig (1997). *"Fuzzy and neural approaches in engineering"*. In.

Umbarkar, AJ and PD Sheth (2015). *"Crossover operators in genetic algorithms: a review."* In: *ICTACT journal on soft computing* 6.1.

Verma, Shanu, Millie Pant, and Vaclav Snasel (2021). *"A Comprehensive Review on NSGA-II for Multi-Objective Combinatorial Optimization Problems"*. In: *IEEE Access* 9, pp. 57757–57791.

Wang, Daqing, Peng Zhang, and Liqiong Chen (2013). *"Fuzzy fault tree analysis for fire and explosion of crude oil tanks"*. In: *Journal of loss prevention in the process industries* 26.6, pp. 1390–1398.

Wang, Jiacun (2012). *Timed Petri nets: Theory and application*. Vol. 9. Springer Science & Business Media.

Wang, QJ (1997). *"Using genetic algorithms to optimise model parameters"*. In: *Environmental Modelling & Software* 12.1, pp. 27–34.

Wang, Yan Fu, Tao Qin, Biao Li, Xiao Fei Sun, and Yu Lian Li (2017). *"Fire probability prediction of offshore platform based on Dynamic Bayesian Network"*. In: *Ocean Engineering* 145, pp. 112–123.

Wang, Yan Fu, Min Xie, Kien Ming Ng, and Mohamed Salahuddin Habibullah (2011). *"Probability analysis of offshore fire by incorporating human and organizational factor"*. In: *Ocean Engineering* 38.17, pp. 2042–2055.

Wang, Yaping and Hoang Pham (2011). *"A multi-objective optimization of imperfect preventive maintenance policy for dependent competing risk systems with hidden failure"*. In: *IEEE Transactions on Reliability* 60.4, pp. 770–781.

Wang, Zhanwei, Zhiwei Wang, Xiaowei Gu, Suowei He, and Zengfeng Yan (2018). *"Feature selection based on Bayesian network for chiller fault diagnosis from the perspective of field applications"*. In: *Applied Thermal Engineering* 129, pp. 674–683.

Wikipedia (2016a). *Deepwater Horizon — Wikipedia, The Free Encyclopedia*. [Online; accessed 24-October-2016]. URL: `https://en.wikipedia.org/w/index.php?title=Deepwater_Horizon`.

— (2016b). *Piper Alpha — Wikipedia, The Free Encyclopedia*. [Online; accessed 21-October-2016]. URL: `https://en.wikipedia.org/w/index.php?title=Piper_Alpha`.

Wilder, Robert Jay (1998). *Listening to the sea: the politics of improving environmental protection*. University of Pittsburgh Pre.

Xiaozhen, Sun (2012). *Common Well Control Hazards: Identification and Countermeasures*. Gulf Professional Publishing.

Xing, Liudong and Suprasad V Amari (2008). *"Fault tree analysis"*. In: *Handbook of performability engineering*. Springer, pp. 595–620.

Yang, SK, TS Liu, et al. (1997). *"Failure analysis for an airbag inflator by Petri nets"*. In: *Quality and reliability engineering international* 13.3, pp. 139–151.

Yang, Xin-She (2014). *Nature-inspired optimization algorithms*. Elsevier.

Yuge, T, K Tagami, and S Yanagi (2006). *"Calculating top event probability of a fault tree with many repeated events"*. In: *Journal of Quality in Maintenance Engineering*.

Yuhua, Dong and Yu Datao (2005). *"Estimation of failure probability of oil and gas transmission pipelines by fuzzy fault tree analysis"*. In: *Journal of loss prevention in the process industries* 18.2, pp. 83–88.

Zhang, Qi, Chunjie Zhou, Yu-Chu Tian, Naixue Xiong, Yuanqing Qin, and Bowen Hu (2017). *"A fuzzy probability Bayesian network approach for dynamic cybersecurity risk assessment in industrial control systems"*. In: *IEEE Transactions on Industrial Informatics* 14.6, pp. 2497–2506.

Zhang, Yi, Chul-Woo Kim, and Kong Fah Tee (2017). *"Maintenance management of offshore structures using Markov process model with random transition probabilities"*. In: *Structure and Infrastructure Engineering* 13.8, pp. 1068–1080.

Zitzler, Eckart, Kalyanmoy Deb, and Lothar Thiele (2000). *"Comparison of multiobjective evolutionary algorithms: Empirical results"*. In: *Evolutionary computation* 8.2, pp. 173–195.

Zykina, Anna Vladimirovna (2004). *"A lexicographic optimization algorithm"*. In: *Automation and Remote Control* 65.3, pp. 363–368.

al., Khakzad et (2011). *"Safety analysis in process facilities: Comparison of fault tree and Bayesian network approaches"*. In: *Reliability Engineering & System Safety* 96.8, pp. 925–932.

Appendices

Appendix A

Asset Substitution Transitions

This appendix presents the asset substitution transitions for all of the assets present in the systems of this model. The layouts of these are similar, with their differences being defined by their observables and the inspections that act on them.

A.1 Production Nets

The section presents the asset substitution transitions for the assets in the production system.

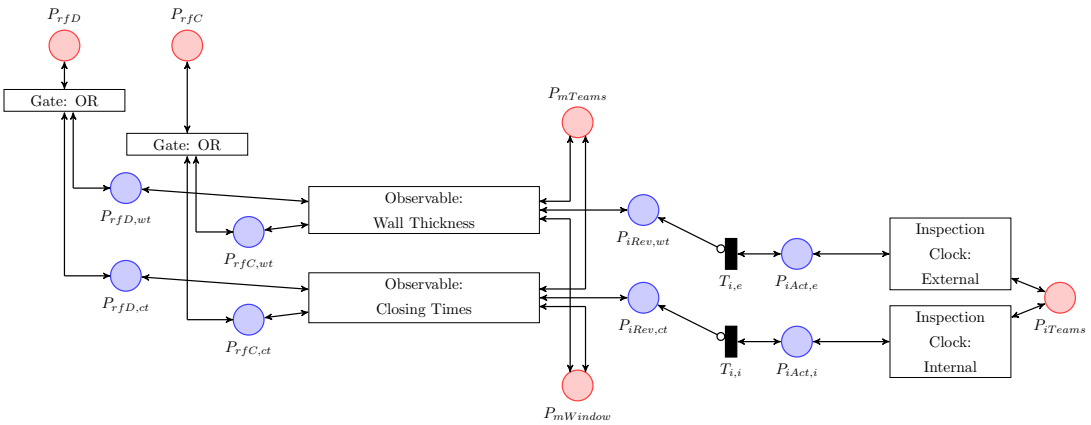

Figure A.1: Asset net for a valve.

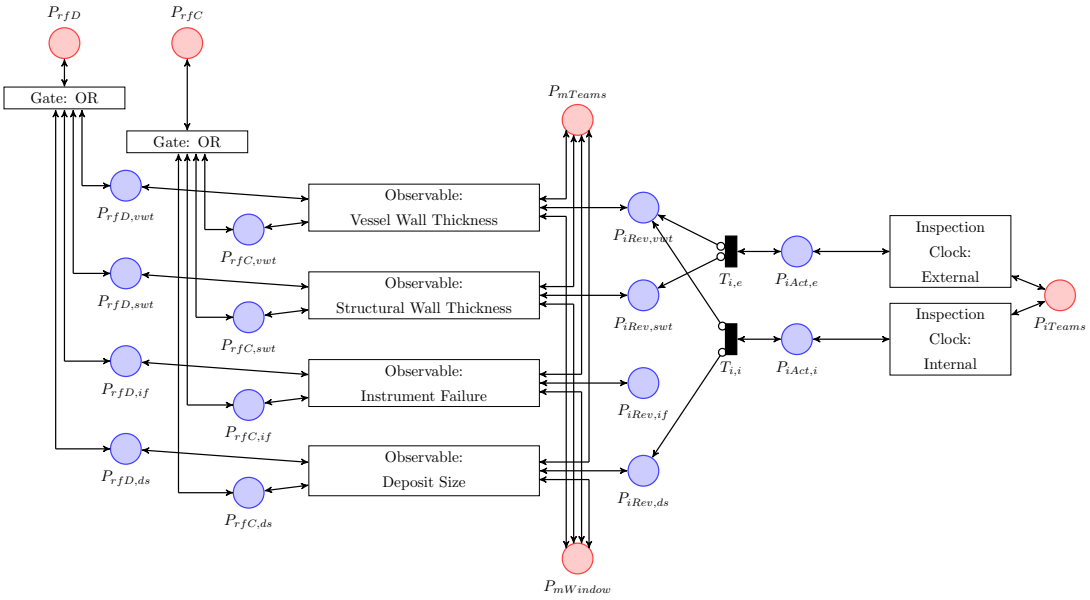

Figure A.2: Asset net for a separator.

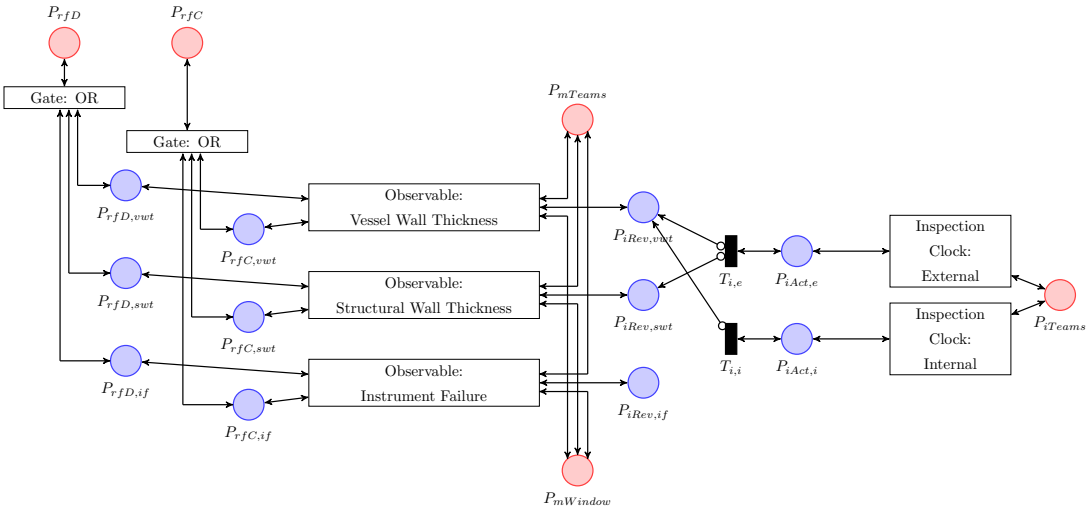

Figure A.3: Asset net for a scrubber.

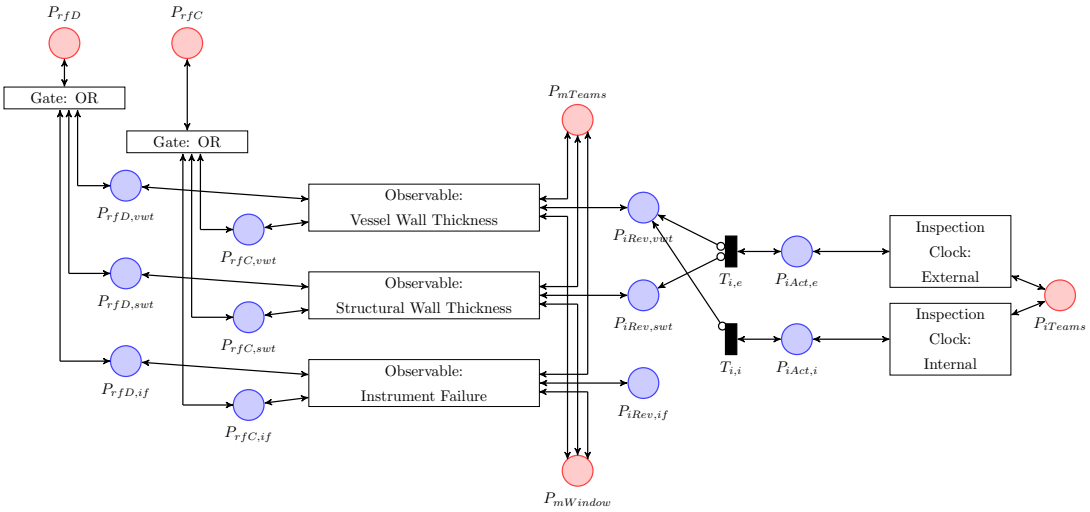

Figure A.4: Asset net for a contactor.

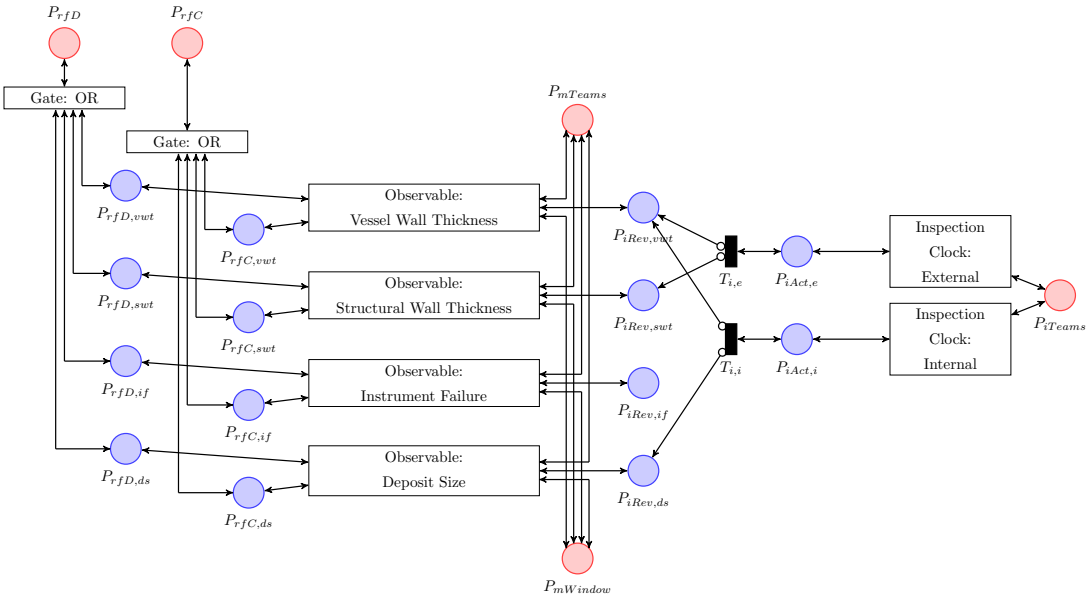

Figure A.5: Asset net for a heat exchanger.

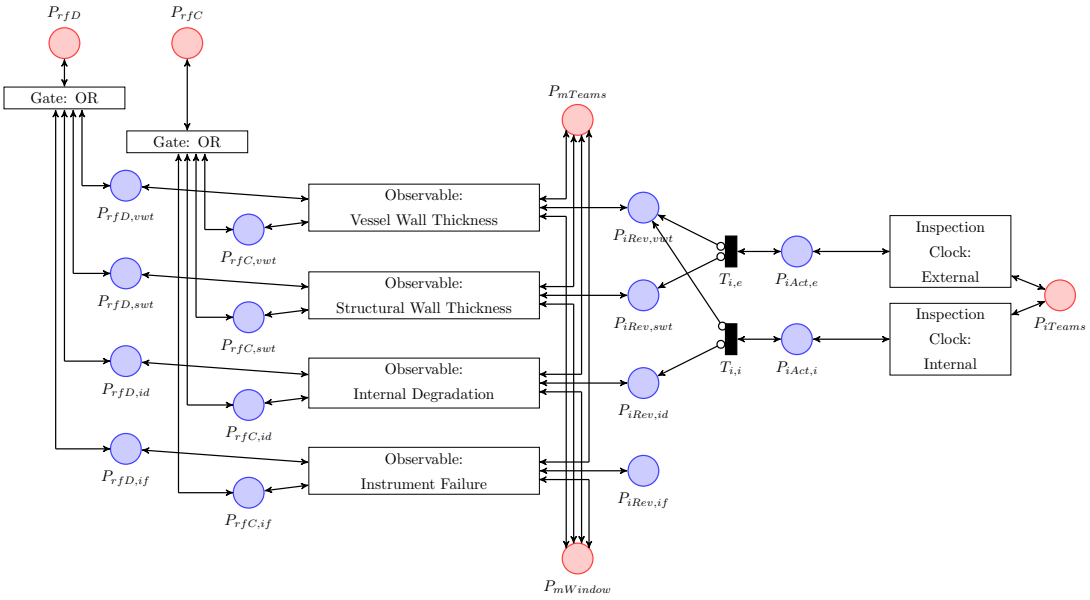

Figure A.6: Asset net for a compressor.

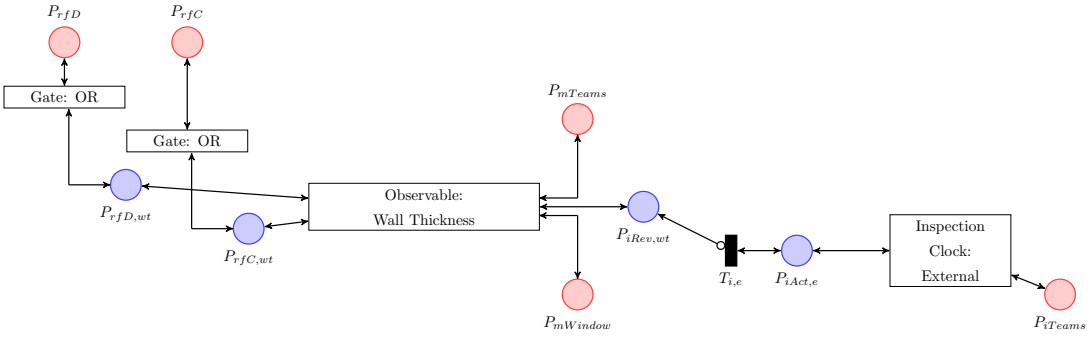

Figure A.7: Asset net for a pipe.

A.2 Firewater Deluge System

The section presents the asset substitution transitions for the assets in the firewater deluge system and the detection system.

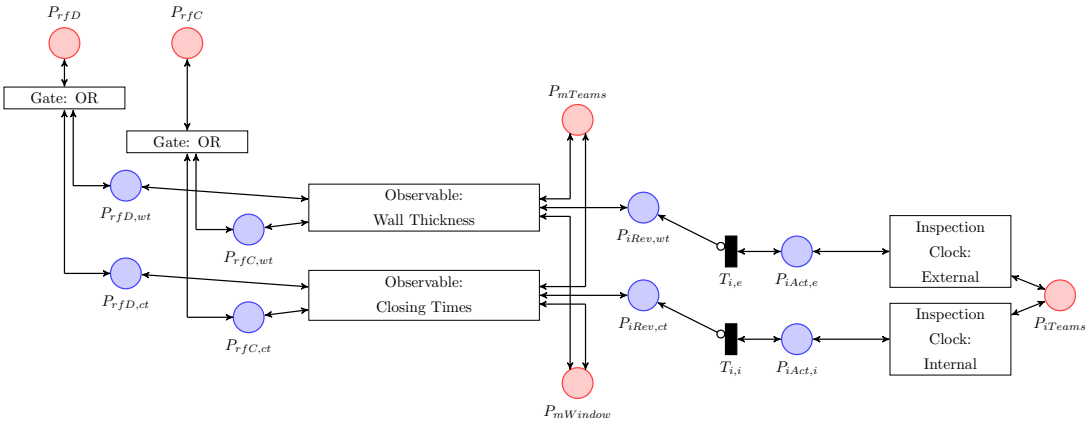

Figure A.8: Asset net for a deluge valve.

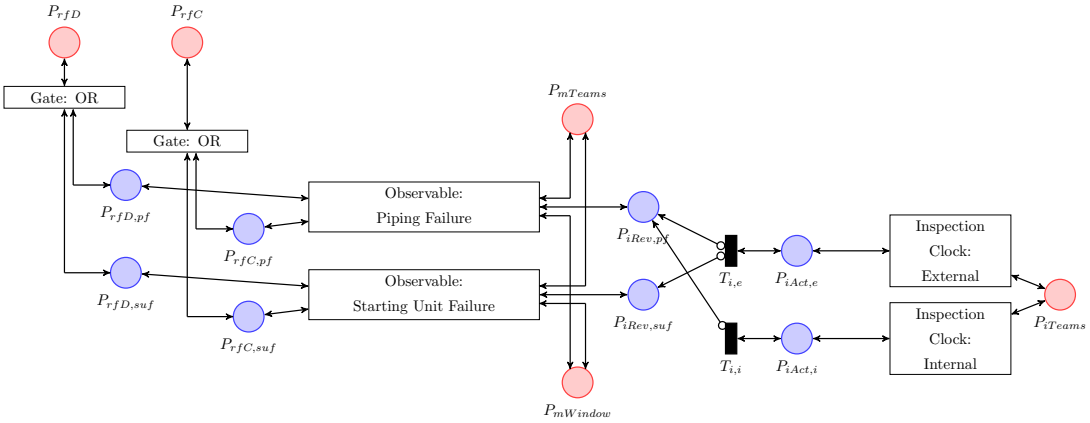

Figure A.9: Asset net for a water firefighting diesel engine.

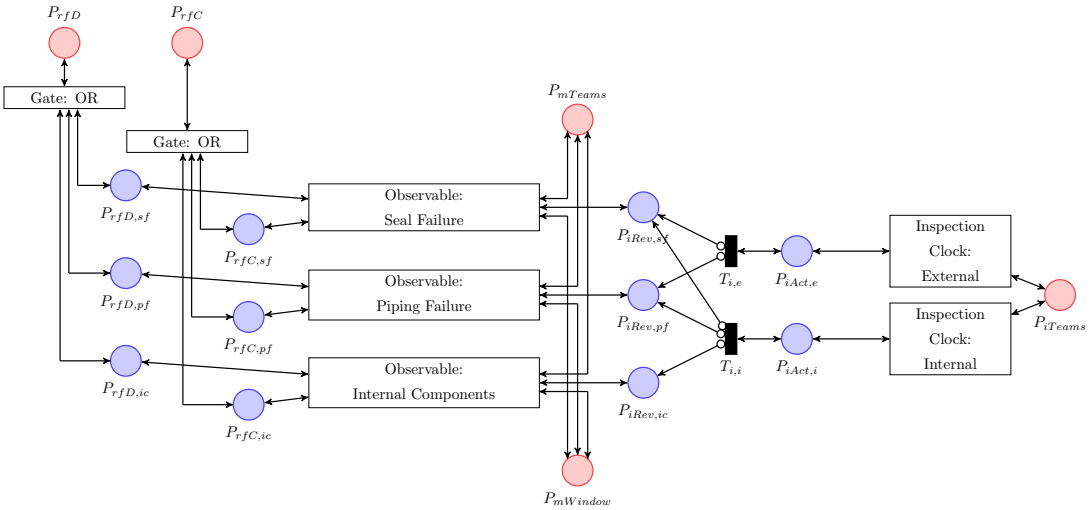

Figure A.10: Asset net for a water firefighting centrifugal pump.

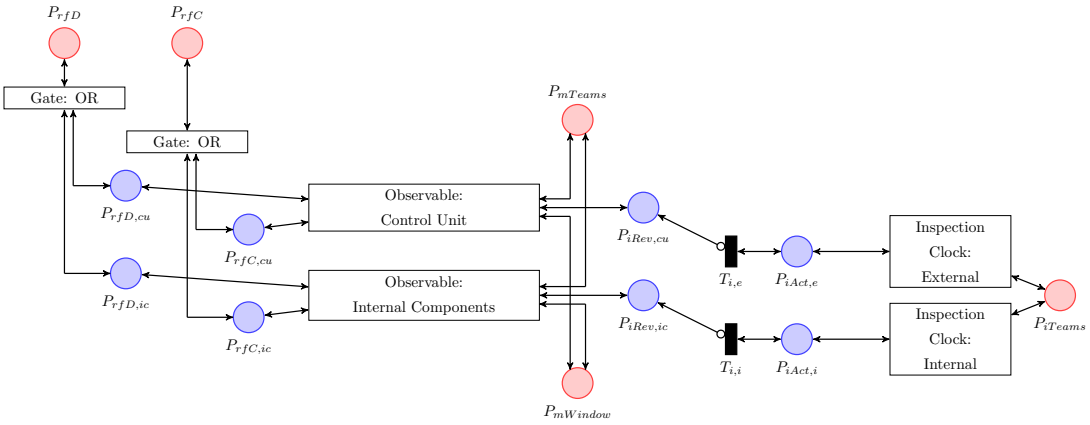

Figure A.11: Asset net for a seawaterlift electric motor.

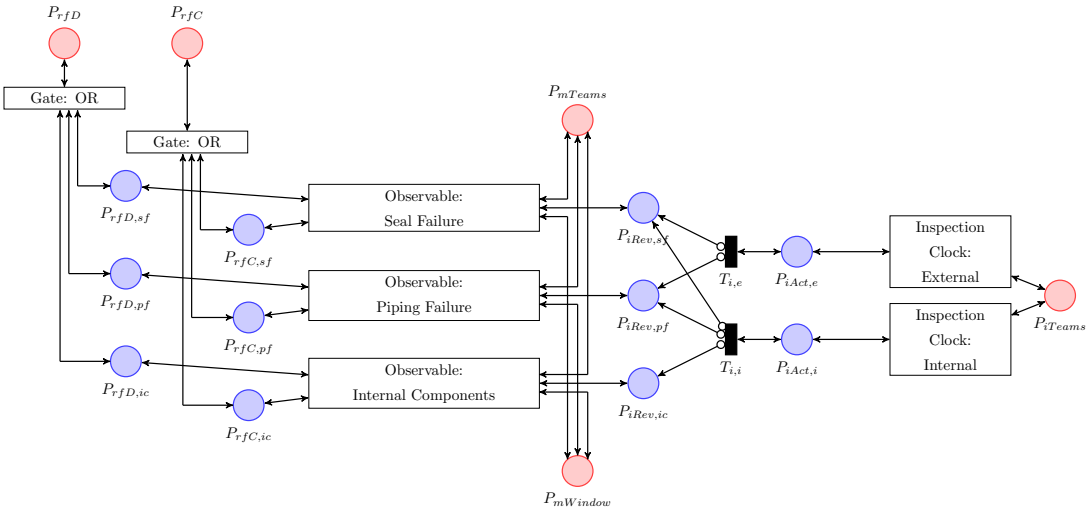

Figure A.12: Asset net for a seawaterlift centrifugal pump.

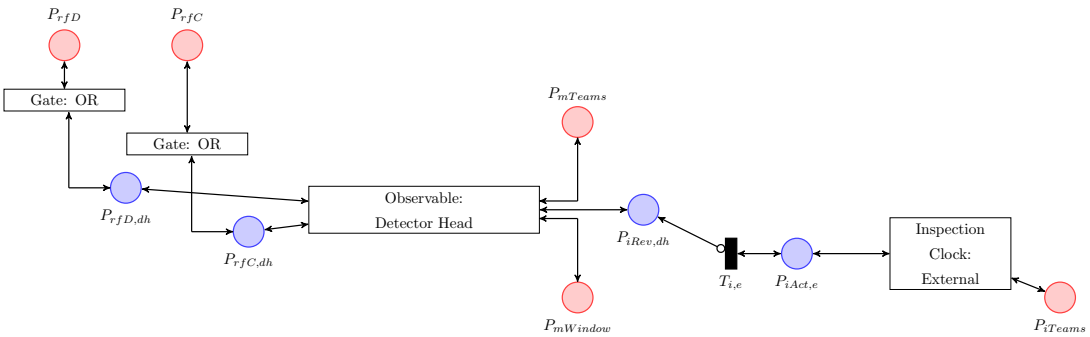

Figure A.13: Asset net for a fire or gas detector.

A.3 Power System

The section presents the asset substitution transitions for the assets in the power system.

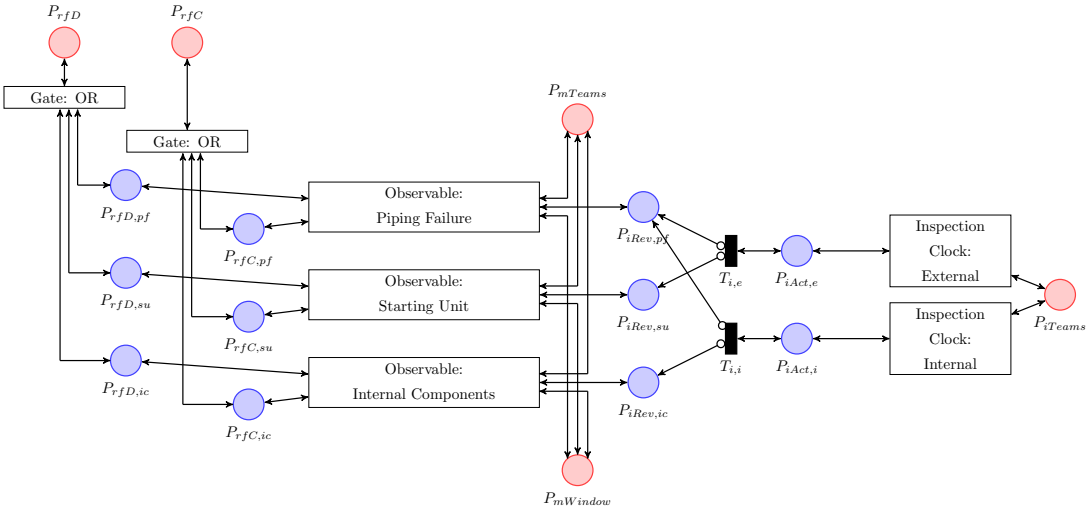

Figure A.14: Asset net for a main power gas engine.

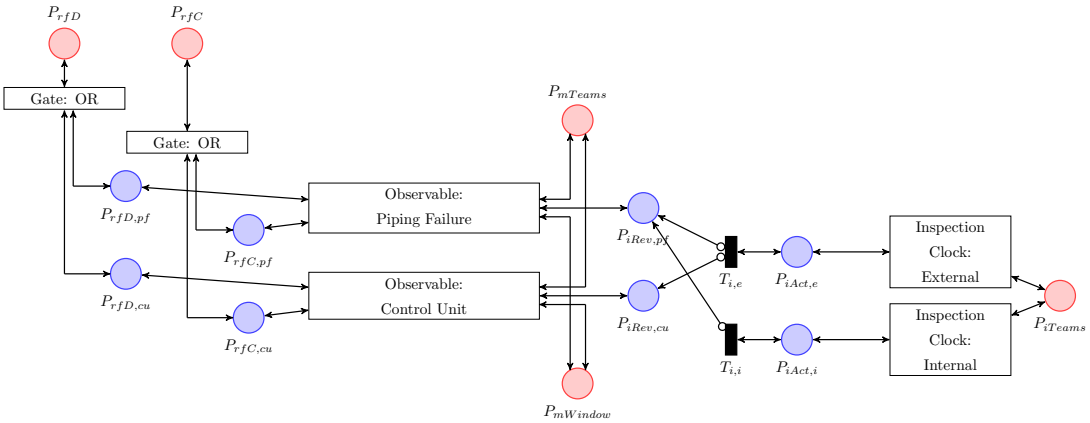

Figure A.15: Asset net for a main power gas driven electric generator.

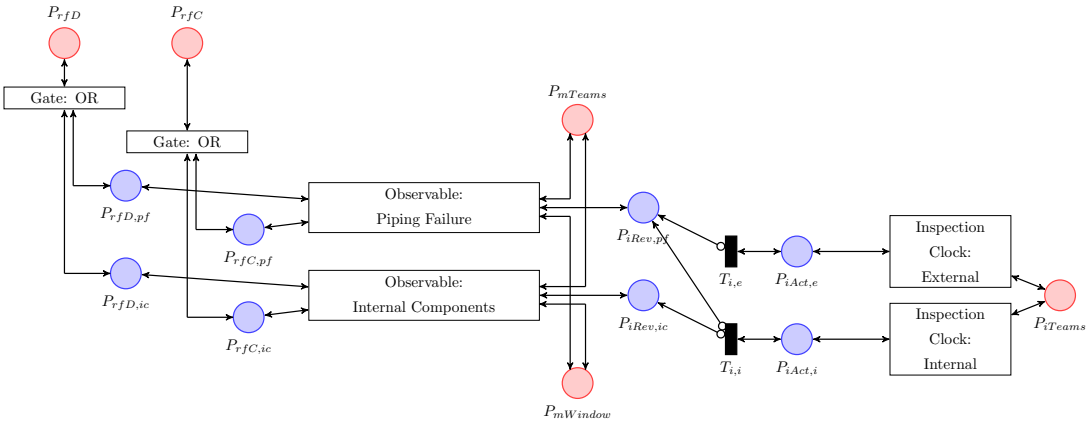

Figure A.16: Asset net for a emergency power diesel engine.

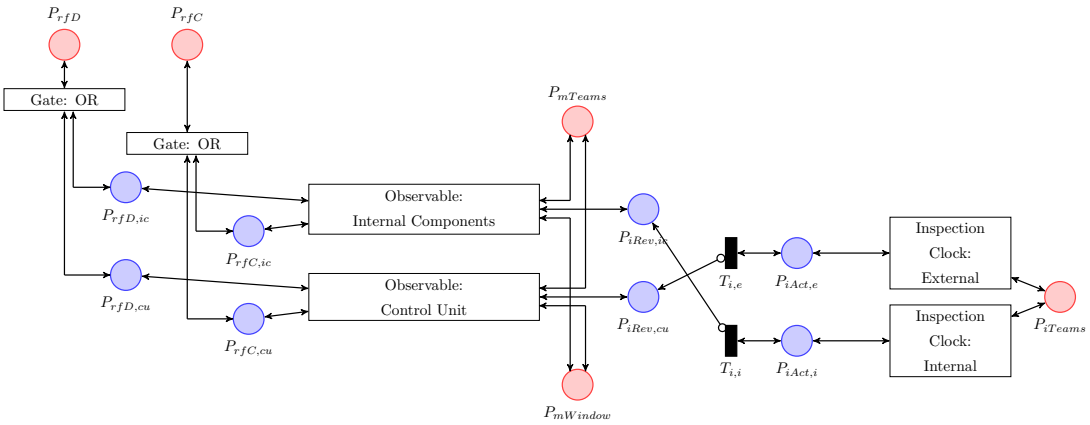

Figure A.17: Asset net for a emergency power diesel driven electric generator.

A.4 Production Train

This section gives the net for the production chain, incorporating the production substitution transitions. The structure of the net is based on the system design given in Figure 3.3. As the net is quite large it is given in a series of figures.

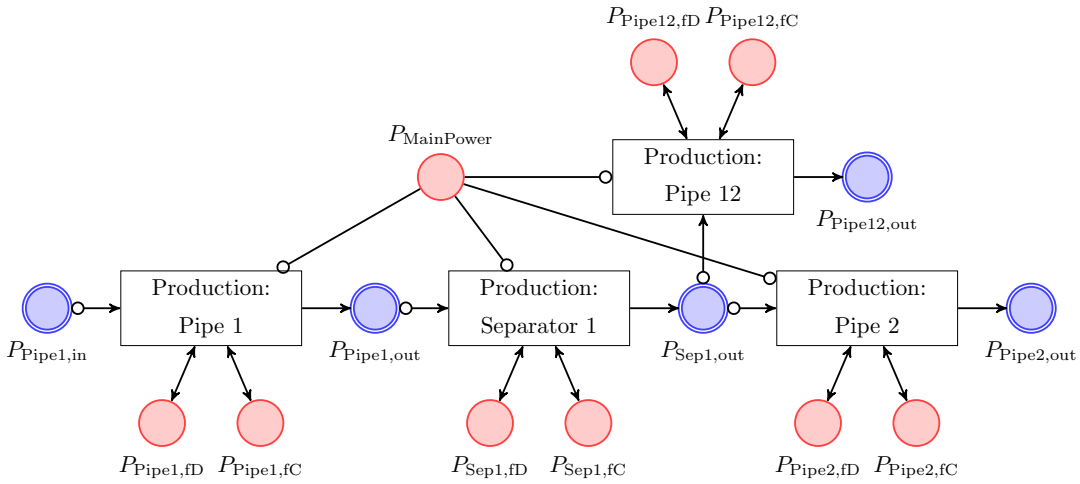

Figure A.18: Production net, part 1.

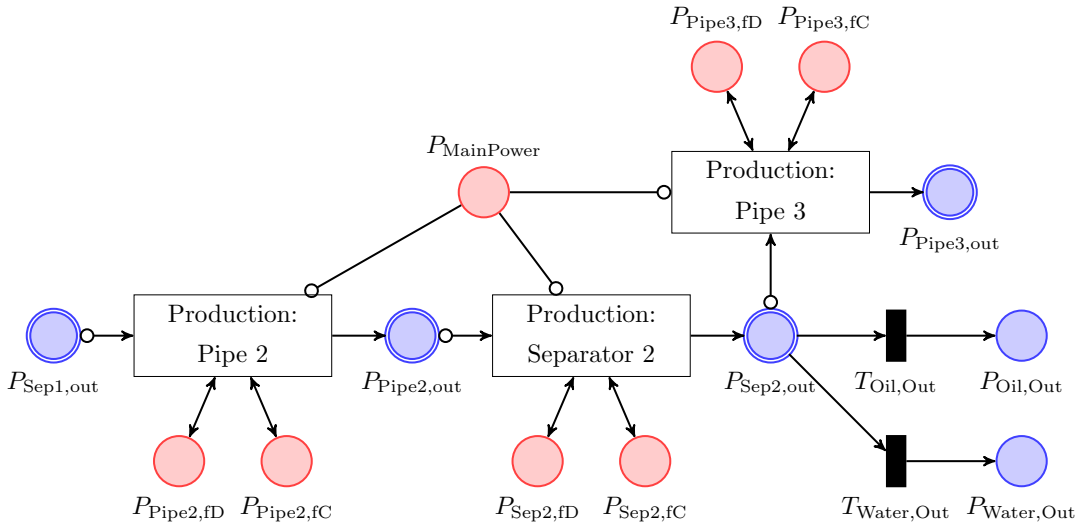

Figure A.19: Production net, part 2.

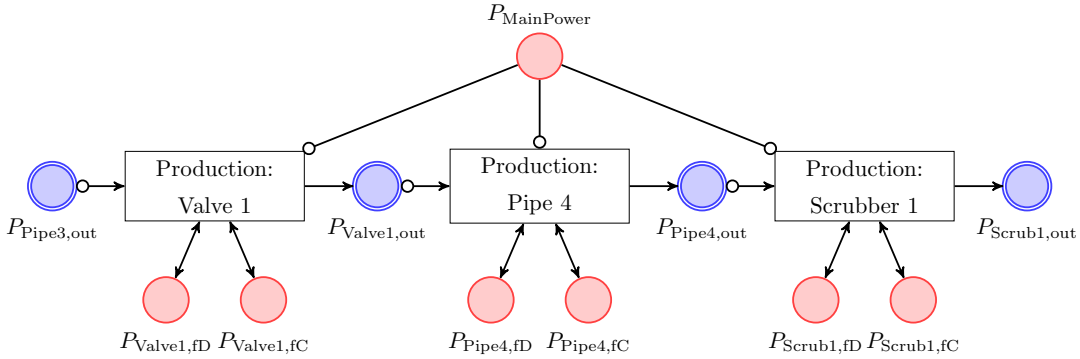

Figure A.20: Production net, part 3.

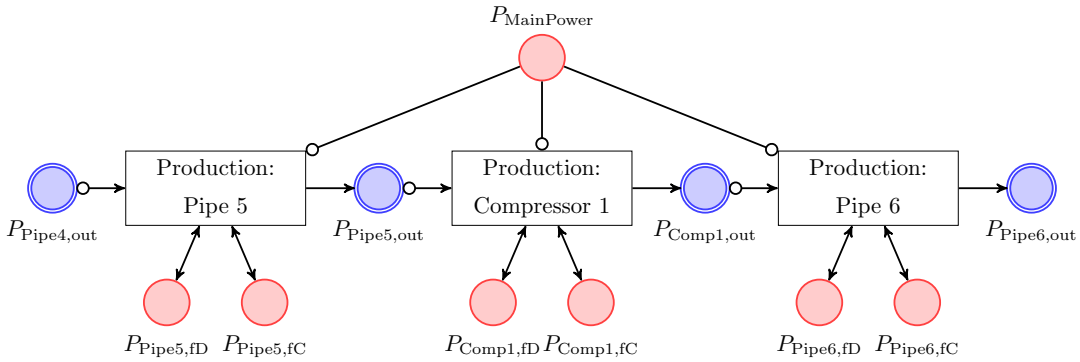

Figure A.21: Production net, part 4.

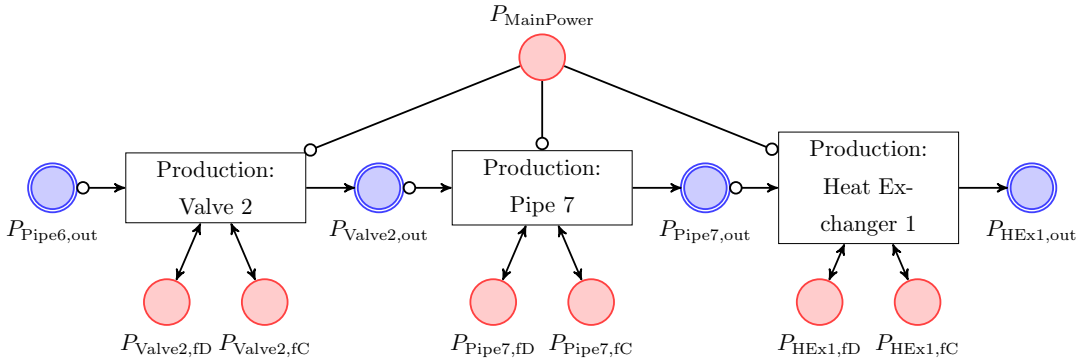

Figure A.22: Production net, part 5.

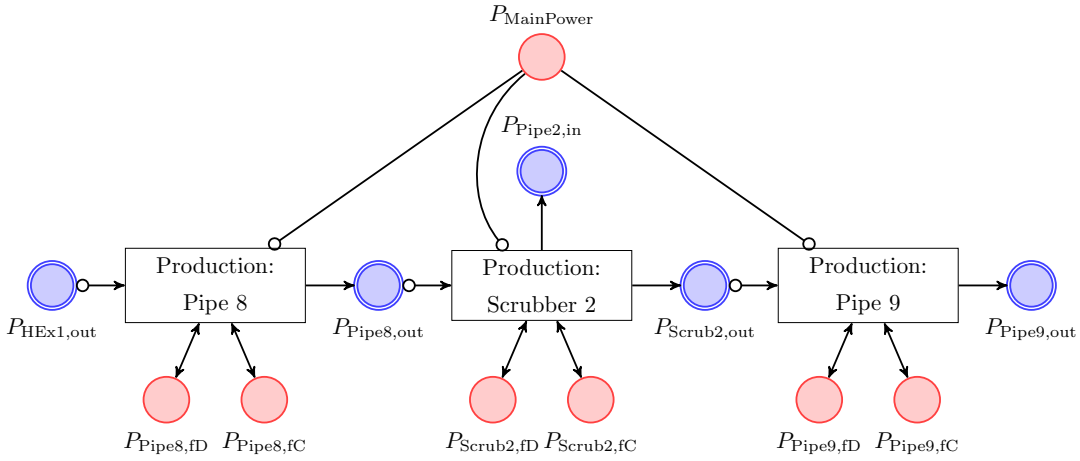

Figure A.23: Production net, part 6.

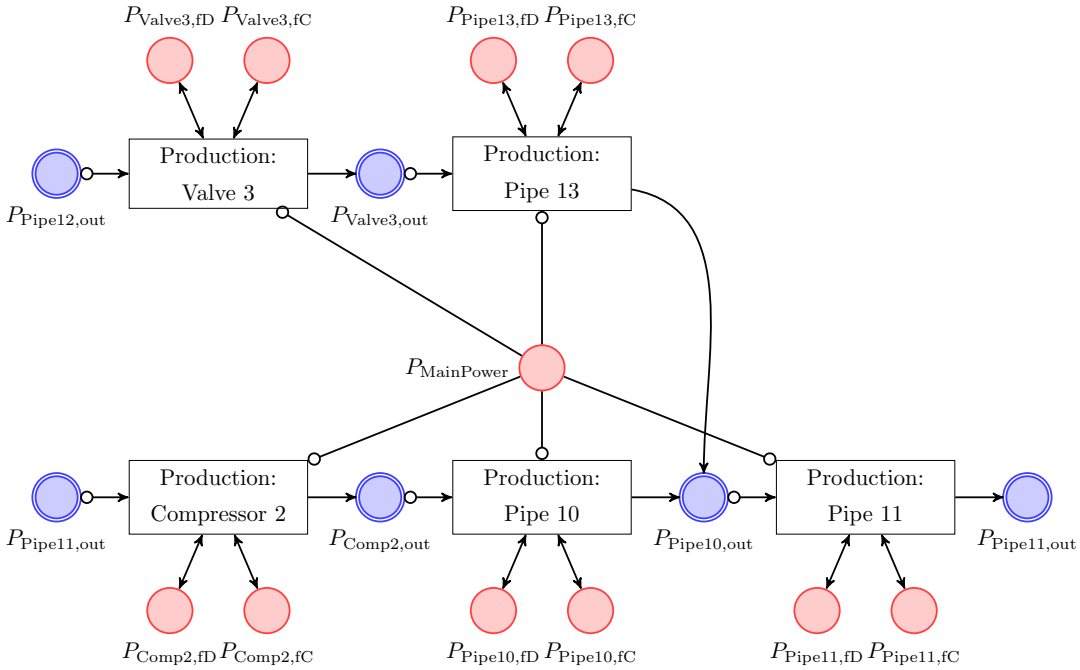

Figure A.24: Production net, part 7.

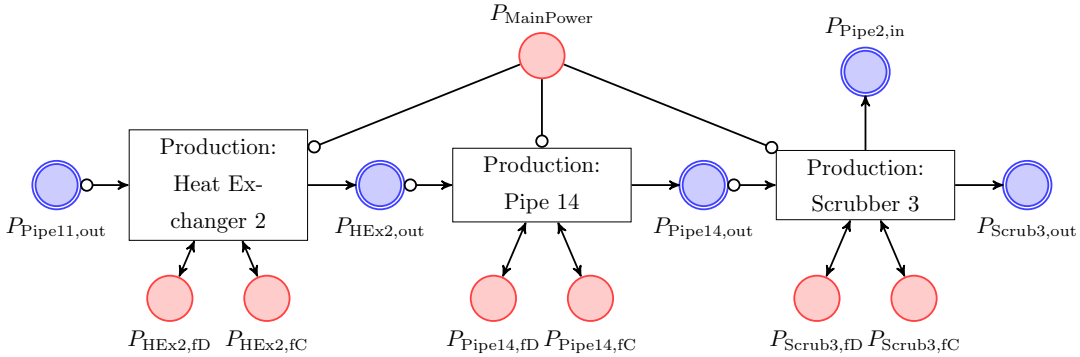

Figure A.25: Production net, part 8.

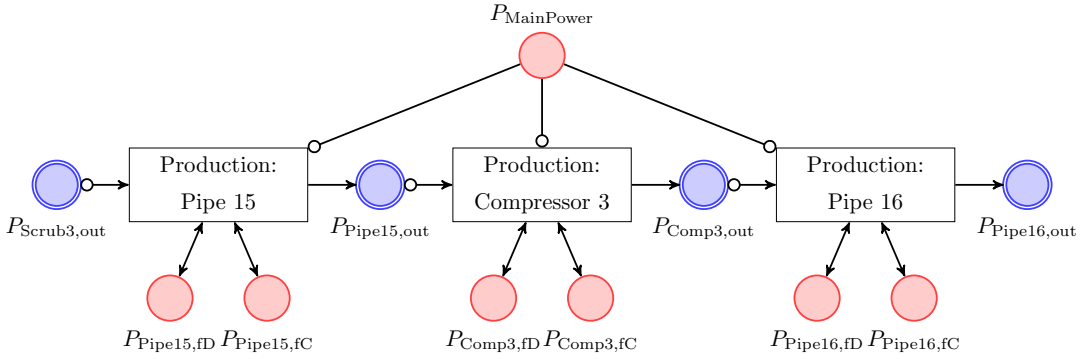

Figure A.26: Production net, part 9.

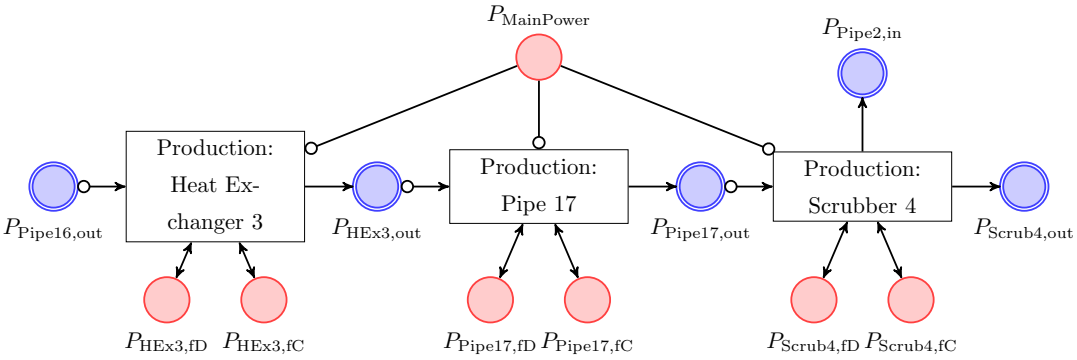

Figure A.27: Production net, part 10.

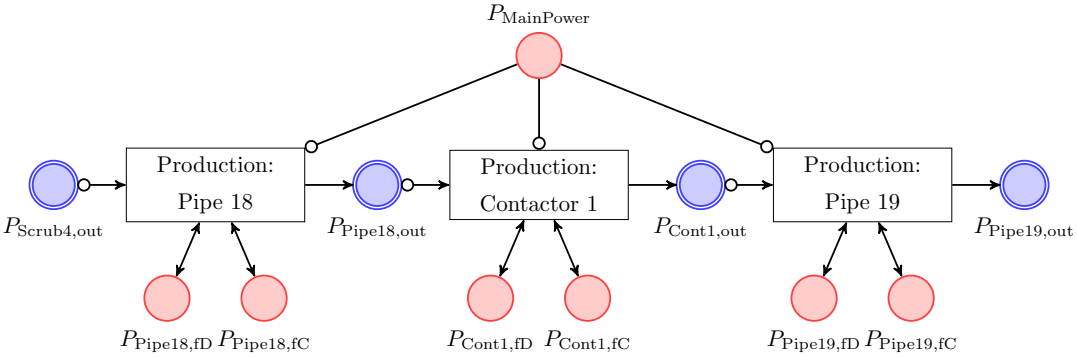

Figure A.28: Production net, part 11.

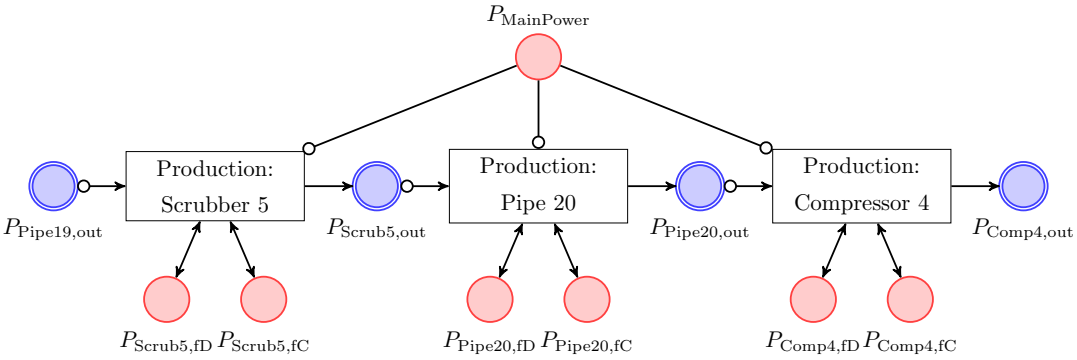

Figure A.29: Production net, part 12.

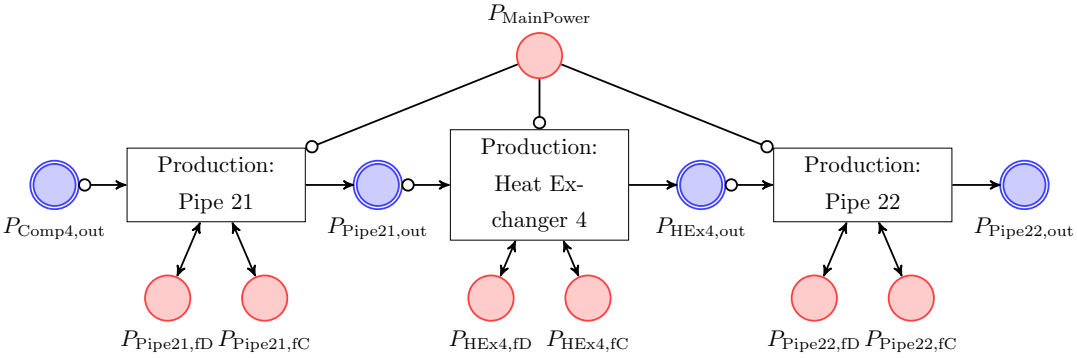

Figure A.30: Production net, part 13.

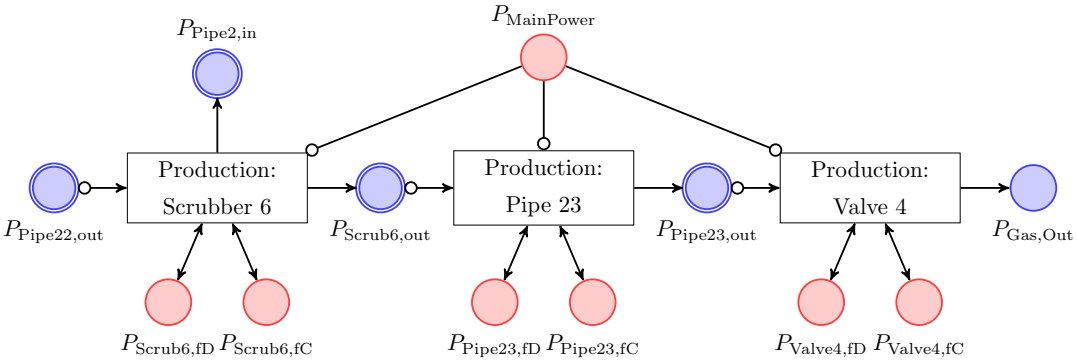

Figure A.31: Production net, part 14.

Appendix B

Asset Data

B.1 Degradation Data

This section gives data on the degradation rates between conditions for each observable in each asset.

Compressor	
Vessel Wall Thickness	
λ_1 $(10^6 h)$	19.62
k_1	1.2
λ_2 $(10^6 h)$	17.09
k_2	1.2
λ_3 $(10^6 h)$	14.89
k_3	1.2
λ_4 $(10^6 h)$	12.97
k_4	1.2
λ_5 $(10^6 h)$	11.29
k_5	1.2

Table B.1: The degradation rate data for the Vessel Wall Thickness of a Compressor.

Compressor	
Structural Wall Thickness	
λ_1 $(10^6 h)$	21.18
k_1	1.2
λ_2 $(10^6 h)$	18.45
k_2	1.2
λ_3 $(10^6 h)$	16.07
k_3	1.2
λ_4 $(10^6 h)$	14.0
k_4	1.2
λ_5 $(10^6 h)$	12.19
k_5	1.2

Table B.2: The degradation rate data for the Structural Wall Thickness of a Compressor.

Compressor	
Internal Degradation	
λ_1 $(10^6 h)$	19.13
k_1	1.2
λ_2 $(10^6 h)$	16.66
k_2	1.2
λ_3 $(10^6 h)$	14.51
k_3	1.2
λ_4 $(10^6 h)$	12.64
k_4	1.2
λ_5 $(10^6 h)$	11.01
k_5	1.2

Table B.3: The degradation rate data for the Internal Degradation of a Compressor.

Contactor	
Vessel Wall Thickness	
λ_1 $(10^6 h)$	18.57
k_1	1.2
λ_2 $(10^6 h)$	16.17
k_2	1.2
λ_3 $(10^6 h)$	14.08
k_3	1.2
λ_4 $(10^6 h)$	12.27
k_4	1.2
λ_5 $(10^6 h)$	10.68
k_5	1.2

Table B.4: The degradation rate data for the Vessel Wall Thickness of a Contactor.

Contactor	
Structural Wall Thickness	
λ_1 $(10^6 h)$	38.22
k_1	1.2
λ_2 $(10^6 h)$	33.29
k_2	1.2
λ_3 $(10^6 h)$	28.99
k_3	1.2
λ_4 $(10^6 h)$	25.25
k_4	1.2
λ_5 $(10^6 h)$	21.99
k_5	1.2

Table B.5: The degradation rate data for the Structural Wall Thickness of a Contactor.

Deluge Valve	
Wall Thickness	
λ_1 $(10^6 h)$	13.55
k_1	1.2
λ_2 $(10^6 h)$	11.8
k_2	1.2
λ_3 $(10^6 h)$	10.28
k_3	1.2
λ_4 $(10^6 h)$	8.95
k_4	1.2
λ_5 $(10^6 h)$	7.8
k_5	1.2

Table B.6: The degradation rate data for the Wall Thickness of a Deluge Valve.

Deluge Valve	
Closing Times	
λ_1 $(10^6 h)$	12.66
k_1	1.2
λ_2 $(10^6 h)$	11.03
k_2	1.2
λ_3 $(10^6 h)$	9.6
k_3	1.2
λ_4 $(10^6 h)$	8.36
k_4	1.2
λ_5 $(10^6 h)$	7.28
k_5	1.2

Table B.7: The degradation rate data for the Closing Times of a Deluge Valve.

Emergency Power Diesel Driven Electric Generator	
Internal Components	
λ_1 $(10^6 h)$	14.81
k_1	1.2
λ_2 $(10^6 h)$	12.9
k_2	1.2
λ_3 $(10^6 h)$	11.23
k_3	1.2
λ_4 $(10^6 h)$	9.78
k_4	1.2
λ_5 $(10^6 h)$	8.52
k_5	1.2

Table B.8: The degradation rate data for the Internal Components of a Emergency Power Diesel Driven Electric Generator.

Emergency Power Diesel Driven Electric Generator	
Control Unit	
λ_1 (10^6h)	15.65
k_1	1.2
λ_2 (10^6h)	13.63
k_2	1.2
λ_3 (10^6h)	11.87
k_3	1.2
λ_4 (10^6h)	10.34
k_4	1.2
λ_5 (10^6h)	9.01
k_5	1.2

Table B.9: The degradation rate data for the Control Unit of a Emergency Power Diesel Driven Electric Generator.

Emergency Power Diesel Engine	
Piping Failure	
λ_1 (10^6h)	20.77
k_1	1.2
λ_2 (10^6h)	18.09
k_2	1.2
λ_3 (10^6h)	15.75
k_3	1.2
λ_4 (10^6h)	13.72
k_4	1.2
λ_5 (10^6h)	11.95
k_5	1.2

Table B.10: The degradation rate data for the Piping Failure of a Emergency Power Diesel Engine.

Emergency Power Diesel Engine	
Internal Components	
λ_1 (10^6h)	19.14
k_1	1.2
λ_2 (10^6h)	16.67
k_2	1.2
λ_3 (10^6h)	14.52
k_3	1.2
λ_4 (10^6h)	12.64
k_4	1.2
λ_5 (10^6h)	11.01
k_5	1.2

Table B.11: The degradation rate data for the Internal Components of a Emergency Power Diesel Engine.

Fire or Gas Detector	
Detector Head	
λ_1 (10^6h)	12.45
k_1	1.2
λ_2 (10^6h)	10.84
k_2	1.2
λ_3 (10^6h)	9.44
k_3	1.2
λ_4 (10^6h)	8.23
k_4	1.2
λ_5 (10^6h)	7.16
k_5	1.2

Table B.12: The degradation rate data for the Detector Head of a Fire or Gas Detector.

Heat Exchanger	
Vessel Wall Thickness	
λ_1 $(10^6 h)$	28.64
k_1	1.2
λ_2 $(10^6 h)$	24.94
k_2	1.2
λ_3 $(10^6 h)$	21.72
k_3	1.2
λ_4 $(10^6 h)$	18.92
k_4	1.2
λ_5 $(10^6 h)$	16.48
k_5	1.2

Table B.13: The degradation rate data for the Vessel Wall Thickness of a Heat Exchanger.

Heat Exchanger	
Structural Wall Thickness	
λ_1 $(10^6 h)$	39.33
k_1	1.2
λ_2 $(10^6 h)$	34.26
k_2	1.2
λ_3 $(10^6 h)$	29.84
k_3	1.2
λ_4 $(10^6 h)$	25.99
k_4	1.2
λ_5 $(10^6 h)$	22.63
k_5	1.2

Table B.14: The degradation rate data for the Structural Wall Thickness of a Heat Exchanger.

Heat Exchanger	
Deposit Size	
λ_1 $(10^6 h)$	14.35
k_1	1.2
λ_2 $(10^6 h)$	12.5
k_2	1.2
λ_3 $(10^6 h)$	10.89
k_3	1.2
λ_4 $(10^6 h)$	9.48
k_4	1.2
λ_5 $(10^6 h)$	8.26
k_5	1.2

Table B.15: The degradation rate data for the Deposit Size of a Heat Exchanger.

Main Power Gas Driven Electric Generator	
Piping Failure	
λ_1 $(10^6 h)$	14.79
k_1	1.2
λ_2 $(10^6 h)$	12.88
k_2	1.2
λ_3 $(10^6 h)$	11.22
k_3	1.2
λ_4 $(10^6 h)$	9.77
k_4	1.2
λ_5 $(10^6 h)$	8.51
k_5	1.2

Table B.16: The degradation rate data for the Piping Failure of a Main Power Gas Driven Electric Generator.

Main Power Gas Driven Electric Generator	
Control Unit	
λ_1 (10^6h)	19.38
k_1	1.2
λ_2 (10^6h)	16.88
k_2	1.2
λ_3 (10^6h)	14.7
k_3	1.2
λ_4 (10^6h)	12.81
k_4	1.2
λ_5 (10^6h)	11.15
k_5	1.2

Table B.17: The degradation rate data for the Control Unit of a Main Power Gas Driven Electric Generator.

Main Power Gas Engine	
Piping Failure	
λ_1 (10^6h)	20.72
k_1	1.2
λ_2 (10^6h)	18.05
k_2	1.2
λ_3 (10^6h)	15.72
k_3	1.2
λ_4 (10^6h)	13.69
k_4	1.2
λ_5 (10^6h)	11.93
k_5	1.2

Table B.18: The degradation rate data for the Piping Failure of a Main Power Gas Engine.

Main Power Gas Engine	
Starting Unit	
λ_1 (10^6h)	16.86
k_1	1.2
λ_2 (10^6h)	14.68
k_2	1.2
λ_3 (10^6h)	12.79
k_3	1.2
λ_4 (10^6h)	11.14
k_4	1.2
λ_5 (10^6h)	9.7
k_5	1.2

Table B.19: The degradation rate data for the Starting Unit of a Main Power Gas Engine.

Main Power Gas Engine	
Internal Components	
λ_1 (10^6h)	15.0
k_1	1.2
λ_2 (10^6h)	13.07
k_2	1.2
λ_3 (10^6h)	11.38
k_3	1.2
λ_4 (10^6h)	9.91
k_4	1.2
λ_5 (10^6h)	8.63
k_5	1.2

Table B.20: The degradation rate data for the Internal Components of a Main Power Gas Engine.

Pipe	
Wall Thickness	
λ_1 $(10^6 h)$	19.87
k_1	1.2
λ_2 $(10^6 h)$	17.3
k_2	1.2
λ_3 $(10^6 h)$	15.07
k_3	1.2
λ_4 $(10^6 h)$	13.12
k_4	1.2
λ_5 $(10^6 h)$	11.43
k_5	1.2

Table B.21: The degradation rate data for the Wall Thickness of a Pipe.

Scrubber	
Vessel Wall Thickness	
λ_1 $(10^6 h)$	29.84
k_1	1.2
λ_2 $(10^6 h)$	25.99
k_2	1.2
λ_3 $(10^6 h)$	22.63
k_3	1.2
λ_4 $(10^6 h)$	19.71
k_4	1.2
λ_5 $(10^6 h)$	17.17
k_5	1.2

Table B.22: The degradation rate data for the Vessel Wall Thickness of a Scrubber.

Scrubber	
Structural Wall Thickness	
λ_1 $(10^6 h)$	29.84
k_1	1.2
λ_2 $(10^6 h)$	25.99
k_2	1.2
λ_3 $(10^6 h)$	22.63
k_3	1.2
λ_4 $(10^6 h)$	19.71
k_4	1.2
λ_5 $(10^6 h)$	17.17
k_5	1.2

Table B.23: The degradation rate data for the Structural Wall Thickness of a Scrubber.

Seawaterlift Centrifugal Pump	
Seal Failure	
λ_1 $(10^6 h)$	16.81
k_1	1.2
λ_2 $(10^6 h)$	14.64
k_2	1.2
λ_3 $(10^6 h)$	12.75
k_3	1.2
λ_4 $(10^6 h)$	11.11
k_4	1.2
λ_5 $(10^6 h)$	9.67
k_5	1.2

Table B.24: The degradation rate data for the Seal Failure of a Seawaterlift Centrifugal Pump.

Seawaterlift Centrifugal Pump	
Piping Failure	
λ_1 (10^6h)	15.2
k_1	1.2
λ_2 (10^6h)	13.24
k_2	1.2
λ_3 (10^6h)	11.53
k_3	1.2
λ_4 (10^6h)	10.04
k_4	1.2
λ_5 (10^6h)	8.75
k_5	1.2

Table B.25: The degradation rate data for the Piping Failure of a Seawaterlift Centrifugal Pump.

Seawaterlift Centrifugal Pump	
Internal Components	
λ_1 (10^6h)	16.42
k_1	1.2
λ_2 (10^6h)	14.3
k_2	1.2
λ_3 (10^6h)	12.46
k_3	1.2
λ_4 (10^6h)	10.85
k_4	1.2
λ_5 (10^6h)	9.45
k_5	1.2

Table B.26: The degradation rate data for the Internal Components of a Seawaterlift Centrifugal Pump.

Seawaterlift Electric Motor	
Control Unit	
λ_1 (10^6h)	19.87
k_1	1.2
λ_2 (10^6h)	17.3
k_2	1.2
λ_3 (10^6h)	15.07
k_3	1.2
λ_4 (10^6h)	13.12
k_4	1.2
λ_5 (10^6h)	11.43
k_5	1.2

Table B.27: The degradation rate data for the Control Unit of a Seawaterlift Electric Motor.

Seawaterlift Electric Motor	
Internal Components	
λ_1 (10^6h)	20.83
k_1	1.2
λ_2 (10^6h)	18.14
k_2	1.2
λ_3 (10^6h)	15.8
k_3	1.2
λ_4 (10^6h)	13.76
k_4	1.2
λ_5 (10^6h)	11.98
k_5	1.2

Table B.28: The degradation rate data for the Internal Components of a Seawaterlift Electric Motor.

Separator	
Vessel Wall Thickness	
λ_1 $(10^6 h)$	37.82
k_1	1.2
λ_2 $(10^6 h)$	32.94
k_2	1.2
λ_3 $(10^6 h)$	28.69
k_3	1.2
λ_4 $(10^6 h)$	24.98
k_4	1.2
λ_5 $(10^6 h)$	21.76
k_5	1.2

Table B.29: The degradation rate data for the Vessel Wall Thickness of a Separator.

Separator	
Structural Wall Thickness	
λ_1 $(10^6 h)$	16.79
k_1	1.2
λ_2 $(10^6 h)$	14.63
k_2	1.2
λ_3 $(10^6 h)$	12.74
k_3	1.2
λ_4 $(10^6 h)$	11.1
k_4	1.2
λ_5 $(10^6 h)$	9.66
k_5	1.2

Table B.30: The degradation rate data for the Structural Wall Thickness of a Separator.

Separator	
Deposit Size	
λ_1 $(10^6 h)$	18.16
k_1	1.2
λ_2 $(10^6 h)$	15.82
k_2	1.2
λ_3 $(10^6 h)$	13.78
k_3	1.2
λ_4 $(10^6 h)$	12.0
k_4	1.2
λ_5 $(10^6 h)$	10.45
k_5	1.2

Table B.31: The degradation rate data for the Deposit Size of a Separator.

Valve	
Wall Thickness	
λ_1 $(10^6 h)$	13.55
k_1	1.2
λ_2 $(10^6 h)$	11.8
k_2	1.2
λ_3 $(10^6 h)$	10.28
k_3	1.2
λ_4 $(10^6 h)$	8.95
k_4	1.2
λ_5 $(10^6 h)$	7.8
k_5	1.2

Table B.32: The degradation rate data for the Wall Thickness of a Valve.

Valve	
Closing Times	
λ_1 (10^6h)	12.66
k_1	1.2
λ_2 (10^6h)	11.03
k_2	1.2
λ_3 (10^6h)	9.6
k_3	1.2
λ_4 (10^6h)	8.36
k_4	1.2
λ_5 (10^6h)	7.28
k_5	1.2

Table B.33: The degradation rate data for the Closing Times of a Valve.

Water Firefighting Centrifugal Pump	
Seal Failure	
λ_1 (10^6h)	17.73
k_1	1.2
λ_2 (10^6h)	15.45
k_2	1.2
λ_3 (10^6h)	13.45
k_3	1.2
λ_4 (10^6h)	11.72
k_4	1.2
λ_5 (10^6h)	10.21
k_5	1.2

Table B.34: The degradation rate data for the Seal Failure of a Water Firefighting Centrifugal Pump.

Water Firefighting Centrifugal Pump	
Piping Failure	
λ_1 (10^6h)	17.48
k_1	1.2
λ_2 (10^6h)	15.22
k_2	1.2
λ_3 (10^6h)	13.26
k_3	1.2
λ_4 (10^6h)	11.55
k_4	1.2
λ_5 (10^6h)	10.06
k_5	1.2

Table B.35: The degradation rate data for the Piping Failure of a Water Firefighting Centrifugal Pump.

Water Firefighting Centrifugal Pump	
Internal Components	
λ_1 (10^6h)	16.1
k_1	1.2
λ_2 (10^6h)	14.02
k_2	1.2
λ_3 (10^6h)	12.21
k_3	1.2
λ_4 (10^6h)	10.64
k_4	1.2
λ_5 (10^6h)	9.26
k_5	1.2

Table B.36: The degradation rate data for the Internal Components of a Water Firefighting Centrifugal Pump.

Water Firefighting Diesel Engine	
Piping Failure	
λ_1 $(10^6 h)$	18.02
k_1	1.2
λ_2 $(10^6 h)$	15.69
k_2	1.2
λ_3 $(10^6 h)$	13.67
k_3	1.2
λ_4 $(10^6 h)$	11.9
k_4	1.2
λ_5 $(10^6 h)$	10.37
k_5	1.2

Table B.37: The degradation rate data for the Piping Failure of a Water Firefighting Diesel Engine.

Water Firefighting Diesel Engine	
Starting Unit Failure	
λ_1 $(10^6 h)$	15.95
k_1	1.2
λ_2 $(10^6 h)$	13.89
k_2	1.2
λ_3 $(10^6 h)$	12.1
k_3	1.2
λ_4 $(10^6 h)$	10.54
k_4	1.2
λ_5 $(10^6 h)$	9.18
k_5	1.2

Table B.38: The degradation rate data for the Starting Unit Failure of a Water Firefighting Diesel Engine.

Compressor							
Vessel Wall Thickness							
Failure from Condition	**With Incipient (True/False)**	**Incipient**		**Degraded**		**Critical**	
		λ $(10^6 h)$	k	λ $(10^6 h)$	k	λ $(10^6 h)$	k
1	False	443.52	1.2	535.68	1.2	583.68	1.2
	True	N/A	N/A	133.92	1.2	145.92	1.2
2	False	390.45	1.2	453.44	1.2	474.31	1.2
	True	N/A	N/A	113.36	1.2	118.58	1.2
3	False	278.72	1.2	311.7	1.2	312.46	1.2
	True	N/A	N/A	77.92	1.2	78.11	1.2
4	False	168.89	1.2	182.13	1.2	174.63	1.2
	True	N/A	N/A	45.53	1.2	43.66	1.2
5	False	88.57	1.2	92.22	1.2	84.41	1.2
	True	N/A	N/A	23.06	1.2	21.1	1.2
6	False	40.69	1.2	40.96	1.2	35.7	1.2
	True	N/A	N/A	10.24	1.2	8.93	1.2

Table B.39: The failure rate data for the Vessel Wall Thickness of a Compressor.

B.2 Failure Rate Date

This section gives data on the failures rates from different conditions for each observable in each asset.

Compressor							
Structural Wall Thickness							
Failure from Condition	**With Incipient (True/False)**	**Incipient**		**Degraded**		**Critical**	
		λ $(10^6 h)$	k	λ $(10^6 h)$	k	λ $(10^6 h)$	k
1	False	493.44	1.2	568.96	1.2	616.96	1.2
	True	N/A	N/A	142.24	1.2	154.24	1.2
2	False	434.4	1.2	481.61	1.2	501.36	1.2
	True	N/A	N/A	120.4	1.2	125.34	1.2
3	False	310.09	1.2	331.06	1.2	330.27	1.2
	True	N/A	N/A	82.77	1.2	82.57	1.2
4	False	187.9	1.2	193.44	1.2	184.59	1.2
	True	N/A	N/A	48.36	1.2	46.15	1.2
5	False	98.54	1.2	97.95	1.2	89.22	1.2
	True	N/A	N/A	24.49	1.2	22.31	1.2
6	False	45.27	1.2	43.5	1.2	37.74	1.2
	True	N/A	N/A	10.88	1.2	9.43	1.2

Table B.40: The failure rate data for the Structural Wall Thickness of a Compressor.

Compressor							
Internal Degradation							
Failure from Condition	**With Incipient (True/False)**	**Incipient**		**Degraded**		**Critical**	
		λ (10^6h)	k	λ (10^6h)	k	λ (10^6h)	k
1	False	427.97	1.2	525.31	1.2	573.31	1.2
	True	N/A	N/A	131.33	1.2	143.33	1.2
2	False	376.76	1.2	444.67	1.2	465.89	1.2
	True	N/A	N/A	111.17	1.2	116.47	1.2
3	False	268.95	1.2	305.67	1.2	306.91	1.2
	True	N/A	N/A	76.42	1.2	76.73	1.2
4	False	162.97	1.2	178.6	1.2	171.53	1.2
	True	N/A	N/A	44.65	1.2	42.88	1.2
5	False	85.47	1.2	90.44	1.2	82.91	1.2
	True	N/A	N/A	22.61	1.2	20.73	1.2
6	False	39.27	1.2	40.17	1.2	35.07	1.2
	True	N/A	N/A	10.04	1.2	8.77	1.2

Table B.41: The failure rate data for the Internal Degradation of a Compressor.

Compressor							
Instrument Failure							
Failure from Condition	**With Incipient (True/False)**	**Incipient**		**Degraded**		**Critical**	
		λ (10^6h)	k	λ (10^6h)	k	λ (10^6h)	k
1	False	341.76	1.2	467.84	1.2	515.84	1.2
	True	N/A	N/A	116.96	1.2	128.96	1.2

Table B.42: The failure rate data for the Instrument Failure of a Compressor.

Contactor							
Vessel Wall Thickness							
Failure from Condition	**With Incipient (True/False)**	**Incipient**		**Degraded**		**Critical**	
		λ $(10^6 h)$	k	λ $(10^6 h)$	k	λ $(10^6 h)$	k
1	False	410.11	1.2	513.41	1.2	561.41	1.2
	True	N/A	N/A	128.35	1.2	140.35	1.2
2	False	361.04	1.2	434.59	1.2	456.21	1.2
	True	N/A	N/A	108.65	1.2	114.05	1.2
3	False	257.72	1.2	298.74	1.2	300.54	1.2
	True	N/A	N/A	74.68	1.2	75.13	1.2
4	False	156.17	1.2	174.55	1.2	167.97	1.2
	True	N/A	N/A	43.64	1.2	41.99	1.2
5	False	81.9	1.2	88.39	1.2	81.19	1.2
	True	N/A	N/A	22.1	1.2	20.3	1.2
6	False	37.63	1.2	39.26	1.2	34.34	1.2
	True	N/A	N/A	9.81	1.2	8.59	1.2

Table B.43: The failure rate data for the Vessel Wall Thickness of a Contactor.

Contactor							
Structural Wall Thickness							
Failure from Condition	**With Incipient (True/False)**	**Incipient**		**Degraded**		**Critical**	
		λ (10^6h)	k	λ (10^6h)	k	λ (10^6h)	k
1	False	1064.06	1.2	949.38	1.2	997.38	1.2
	True	N/A	N/A	237.34	1.2	249.34	1.2
2	False	936.74	1.2	803.63	1.2	810.49	1.2
	True	N/A	N/A	200.91	1.2	202.62	1.2
3	False	668.68	1.2	552.42	1.2	533.92	1.2
	True	N/A	N/A	138.1	1.2	133.48	1.2
4	False	405.19	1.2	322.78	1.2	298.41	1.2
	True	N/A	N/A	80.69	1.2	74.6	1.2
5	False	212.5	1.2	163.44	1.2	144.23	1.2
	True	N/A	N/A	40.86	1.2	36.06	1.2
6	False	97.63	1.2	72.59	1.2	61.01	1.2
	True	N/A	N/A	18.15	1.2	15.25	1.2

Table B.44: The failure rate data for the Structural Wall Thickness of a Contactor.

Contactor							
Instrument Failure							
Failure from Condition	**With Incipient (True/False)**	**Incipient**		**Degraded**		**Critical**	
		λ (10^6h)	k	λ (10^6h)	k	λ (10^6h)	k
1	False	1173.12	1.2	1022.08	1.2	1070.08	1.2
	True	N/A	N/A	255.52	1.2	267.52	1.2

Table B.45: The failure rate data for the Instrument Failure of a Contactor.

Deluge Valve							
Wall Thickness							
Failure from Condition	**With Incipient (True/False)**	**Incipient**		**Degraded**		**Critical**	
		λ $(10^6 h)$	k	λ $(10^6 h)$	k	λ $(10^6 h)$	k
1	False	259.2	1.2	412.8	1.2	460.8	1.2
	True	N/A	N/A	103.2	1.2	115.2	1.2
2	False	228.18	1.2	349.43	1.2	374.46	1.2
	True	N/A	N/A	87.36	1.2	93.61	1.2
3	False	162.89	1.2	240.2	1.2	246.68	1.2
	True	N/A	N/A	60.05	1.2	61.67	1.2
4	False	98.7	1.2	140.35	1.2	137.87	1.2
	True	N/A	N/A	35.09	1.2	34.47	1.2
5	False	51.76	1.2	71.07	1.2	66.64	1.2
	True	N/A	N/A	17.77	1.2	16.66	1.2
6	False	23.78	1.2	31.56	1.2	28.19	1.2
	True	N/A	N/A	7.89	1.2	7.05	1.2

Table B.46: The failure rate data for the Wall Thickness of a Deluge Valve.

Deluge Valve							
Closing Times							
Failure from Condition	**With Incipient (True/False)**	**Incipient**		**Degraded**		**Critical**	
		λ $(10^6 h)$	k	λ $(10^6 h)$	k	λ $(10^6 h)$	k
1	False	234.24	1.2	396.16	1.2	444.16	1.2
	True	N/A	N/A	99.04	1.2	111.04	1.2
2	False	206.21	1.2	335.34	1.2	360.93	1.2
	True	N/A	N/A	83.84	1.2	90.23	1.2
3	False	147.2	1.2	230.52	1.2	237.77	1.2
	True	N/A	N/A	57.63	1.2	59.44	1.2
4	False	89.2	1.2	134.69	1.2	132.89	1.2
	True	N/A	N/A	33.67	1.2	33.22	1.2
5	False	46.78	1.2	68.2	1.2	64.23	1.2
	True	N/A	N/A	17.05	1.2	16.06	1.2
6	False	21.49	1.2	30.29	1.2	27.17	1.2
	True	N/A	N/A	7.57	1.2	6.79	1.2

Table B.47: The failure rate data for the Closing Times of a Deluge Valve.

Emergency Power Diesel Driven Electric Generator							
Internal Components							
Failure from Condition	**With Incipient (True/False)**	**Incipient**		**Degraded**		**Critical**	
		λ (10^6h)	k	λ (10^6h)	k	λ (10^6h)	k
1	False	295.68	1.2	437.12	1.2	485.12	1.2
	True	N/A	N/A	109.28	1.2	121.28	1.2
2	False	260.3	1.2	370.01	1.2	394.22	1.2
	True	N/A	N/A	92.5	1.2	98.55	1.2
3	False	185.81	1.2	254.35	1.2	259.7	1.2
	True	N/A	N/A	63.59	1.2	64.92	1.2
4	False	112.59	1.2	148.62	1.2	145.14	1.2
	True	N/A	N/A	37.15	1.2	36.29	1.2
5	False	59.05	1.2	75.25	1.2	70.15	1.2
	True	N/A	N/A	18.81	1.2	17.54	1.2
6	False	27.13	1.2	33.42	1.2	29.67	1.2
	True	N/A	N/A	8.36	1.2	7.42	1.2

Table B.48: The failure rate data for the Internal Components of a Emergency Power Diesel Driven Electric Generator.

Emergency Power Diesel Driven Electric Generator

Control Unit							
Failure from Condition	**With Incipient (True/False)**	**Incipient**		**Degraded**		**Critical**	
		λ (10^6h)	k	λ (10^6h)	k	λ (10^6h)	k
1	False	320.64	1.2	453.76	1.2	501.76	1.2
	True	N/A	N/A	113.44	1.2	125.44	1.2
2	False	282.27	1.2	384.1	1.2	407.74	1.2
	True	N/A	N/A	96.02	1.2	101.94	1.2
3	False	201.5	1.2	264.03	1.2	268.6	1.2
	True	N/A	N/A	66.01	1.2	67.15	1.2
4	False	122.1	1.2	154.27	1.2	150.12	1.2
	True	N/A	N/A	38.57	1.2	37.53	1.2
5	False	64.03	1.2	78.12	1.2	72.56	1.2
	True	N/A	N/A	19.53	1.2	18.14	1.2
6	False	29.42	1.2	34.69	1.2	30.69	1.2
	True	N/A	N/A	8.67	1.2	7.67	1.2

Table B.49: The failure rate data for the Control Unit of a Emergency Power Diesel Driven Electric Generator.

Emergency Power Diesel Engine							
Piping Failure							
Failure from Condition	**With Incipient (True/False)**	**Incipient**		**Degraded**		**Critical**	
		λ $(10^6 h)$	k	λ $(10^6 h)$	k	λ $(10^6 h)$	k
1	False	480.0	1.2	560.0	1.2	608.0	1.2
	True	N/A	N/A	140.0	1.2	152.0	1.2
2	False	422.56	1.2	474.03	1.2	494.07	1.2
	True	N/A	N/A	118.51	1.2	123.52	1.2
3	False	301.64	1.2	325.85	1.2	325.48	1.2
	True	N/A	N/A	81.46	1.2	81.37	1.2
4	False	182.78	1.2	190.4	1.2	181.91	1.2
	True	N/A	N/A	47.6	1.2	45.48	1.2
5	False	95.86	1.2	96.41	1.2	87.92	1.2
	True	N/A	N/A	24.1	1.2	21.98	1.2
6	False	44.04	1.2	42.82	1.2	37.19	1.2
	True	N/A	N/A	10.7	1.2	9.3	1.2

Table B.50: The failure rate data for the Piping Failure of a Emergency Power Diesel Engine.

Emergency Power Diesel Engine							
Internal Components							
Failure from Condition	**With Incipient (True/False)**	**Incipient**		**Degraded**		**Critical**	
		λ (10^6h)	k	λ (10^6h)	k	λ (10^6h)	k
1	False	428.16	1.2	525.44	1.2	573.44	1.2
	True	N/A	N/A	131.36	1.2	143.36	1.2
2	False	376.93	1.2	444.78	1.2	465.99	1.2
	True	N/A	N/A	111.19	1.2	116.5	1.2
3	False	269.07	1.2	305.74	1.2	306.98	1.2
	True	N/A	N/A	76.43	1.2	76.74	1.2
4	False	163.04	1.2	178.65	1.2	171.57	1.2
	True	N/A	N/A	44.66	1.2	42.89	1.2
5	False	85.5	1.2	90.46	1.2	82.93	1.2
	True	N/A	N/A	22.61	1.2	20.73	1.2
6	False	39.29	1.2	40.18	1.2	35.08	1.2
	True	N/A	N/A	10.04	1.2	8.77	1.2

Table B.51: The failure rate data for the Internal Components of a Emergency Power Diesel Engine.

Fire or Gas Detector							
Detector Head							
Failure from Condition	**With Incipient (True/False)**	**Incipient**		**Degraded**		**Critical**	
		λ (10^6h)	k	λ (10^6h)	k	λ (10^6h)	k
1	False	228.48	1.2	392.32	1.2	440.32	1.2
	True	N/A	N/A	98.08	1.2	110.08	1.2
2	False	201.14	1.2	332.09	1.2	357.81	1.2
	True	N/A	N/A	83.02	1.2	89.45	1.2
3	False	143.58	1.2	228.28	1.2	235.71	1.2
	True	N/A	N/A	57.07	1.2	58.93	1.2
4	False	87.0	1.2	133.39	1.2	131.74	1.2
	True	N/A	N/A	33.35	1.2	32.94	1.2
5	False	45.63	1.2	67.54	1.2	63.68	1.2
	True	N/A	N/A	16.89	1.2	15.92	1.2
6	False	20.96	1.2	30.0	1.2	26.93	1.2
	True	N/A	N/A	7.5	1.2	6.73	1.2

Table B.52: The failure rate data for the Detector Head of a Fire or Gas Detector.

Heat Exchanger							
Vessel Wall Thickness							
Failure from Condition	**With Incipient (True/False)**	**Incipient**		**Degraded**		**Critical**	
		λ $(10^6 h)$	k	λ $(10^6 h)$	k	λ $(10^6 h)$	k
1	False	739.2	1.2	732.8	1.2	780.8	1.2
	True	N/A	N/A	183.2	1.2	195.2	1.2
2	False	650.75	1.2	620.3	1.2	634.5	1.2
	True	N/A	N/A	155.08	1.2	158.62	1.2
3	False	464.53	1.2	426.4	1.2	417.98	1.2
	True	N/A	N/A	106.6	1.2	104.5	1.2
4	False	281.48	1.2	249.15	1.2	233.61	1.2
	True	N/A	N/A	62.29	1.2	58.4	1.2
5	False	147.62	1.2	126.16	1.2	112.91	1.2
	True	N/A	N/A	31.54	1.2	28.23	1.2
6	False	67.82	1.2	56.03	1.2	47.76	1.2
	True	N/A	N/A	14.01	1.2	11.94	1.2

Table B.53: The failure rate data for the Vessel Wall Thickness of a Heat Exchanger.

Heat Exchanger							
Structural Wall Thickness							
Failure from Condition	**With Incipient (True/False)**	**Incipient**		**Degraded**		**Critical**	
		λ $(10^6 h)$	k	λ $(10^6 h)$	k	λ $(10^6 h)$	k
1	False	1102.08	1.2	974.72	1.2	1022.72	1.2
	True	N/A	N/A	243.68	1.2	255.68	1.2
2	False	970.21	1.2	825.08	1.2	831.09	1.2
	True	N/A	N/A	206.27	1.2	207.77	1.2
3	False	692.57	1.2	567.16	1.2	547.49	1.2
	True	N/A	N/A	141.79	1.2	136.87	1.2
4	False	419.66	1.2	331.4	1.2	305.99	1.2
	True	N/A	N/A	82.85	1.2	76.5	1.2
5	False	220.09	1.2	167.81	1.2	147.9	1.2
	True	N/A	N/A	41.95	1.2	36.97	1.2
6	False	101.12	1.2	74.53	1.2	62.56	1.2
	True	N/A	N/A	18.63	1.2	15.64	1.2

Table B.54: The failure rate data for the Structural Wall Thickness of a Heat Exchanger.

Heat Exchanger							
Instrument Failure							
Failure from Condition	**With Incipient (True/False)**	**Incipient**		**Degraded**		**Critical**	
		λ $(10^6 h)$	k	λ $(10^6 h)$	k	λ $(10^6 h)$	k
1	False	341.76	1.2	467.84	1.2	515.84	1.2
	True	N/A	N/A	116.96	1.2	128.96	1.2

Table B.55: The failure rate data for the Instrument Failure of a Heat Exchanger.

Heat Exchanger							
Deposit Size							
Failure from Condition	**With Incipient (True/False)**	**Incipient**		**Degraded**		**Critical**	
		λ $(10^6 h)$	k	λ $(10^6 h)$	k	λ $(10^6 h)$	k
1	False	282.24	1.2	428.16	1.2	476.16	1.2
	True	N/A	N/A	107.04	1.2	119.04	1.2
2	False	248.47	1.2	362.43	1.2	386.94	1.2
	True	N/A	N/A	90.61	1.2	96.73	1.2
3	False	177.37	1.2	249.14	1.2	254.9	1.2
	True	N/A	N/A	62.28	1.2	63.72	1.2
4	False	107.47	1.2	145.57	1.2	142.46	1.2
	True	N/A	N/A	36.39	1.2	35.62	1.2
5	False	56.36	1.2	73.71	1.2	68.86	1.2
	True	N/A	N/A	18.43	1.2	17.21	1.2
6	False	25.9	1.2	32.74	1.2	29.13	1.2
	True	N/A	N/A	8.18	1.2	7.28	1.2

Table B.56: The failure rate data for the Deposit Size of a Heat Exchanger.

Main Power Gas Driven Electric Generator

Piping Failure							
Failure from	**With Incipient**	**Incipient**		**Degraded**		**Critical**	
Condition	**(True/False)**	λ (10^6h)	k	λ (10^6h)	k	λ (10^6h)	k
1	False	295.18	1.2	436.79	1.2	484.79	1.2
	True	N/A	N/A	109.2	1.2	121.2	1.2
2	False	259.86	1.2	369.73	1.2	393.95	1.2
	True	N/A	N/A	92.43	1.2	98.49	1.2
3	False	185.5	1.2	254.16	1.2	259.52	1.2
	True	N/A	N/A	63.54	1.2	64.88	1.2
4	False	112.4	1.2	148.5	1.2	145.04	1.2
	True	N/A	N/A	37.13	1.2	36.26	1.2
5	False	58.95	1.2	75.2	1.2	70.11	1.2
	True	N/A	N/A	18.8	1.2	17.53	1.2
6	False	27.08	1.2	33.4	1.2	29.65	1.2
	True	N/A	N/A	8.35	1.2	7.41	1.2

Table B.57: The failure rate data for the Piping Failure of a Main Power Gas Driven Electric Generator.

Main Power Gas Driven Electric Generator

Control Unit							
Failure from Condition	**With Incipient (True/False)**	**Incipient**		**Degraded**		**Critical**	
		λ (10^6h)	k	λ (10^6h)	k	λ (10^6h)	k
1	False	435.84	1.2	530.56	1.2	578.56	1.2
	True	N/A	N/A	132.64	1.2	144.64	1.2
2	False	383.69	1.2	449.11	1.2	470.15	1.2
	True	N/A	N/A	112.28	1.2	117.54	1.2
3	False	273.89	1.2	308.72	1.2	309.72	1.2
	True	N/A	N/A	77.18	1.2	77.43	1.2
4	False	165.96	1.2	180.39	1.2	173.1	1.2
	True	N/A	N/A	45.1	1.2	43.28	1.2
5	False	87.04	1.2	91.34	1.2	83.67	1.2
	True	N/A	N/A	22.84	1.2	20.92	1.2
6	False	39.99	1.2	40.57	1.2	35.39	1.2
	True	N/A	N/A	10.14	1.2	8.85	1.2

Table B.58: The failure rate data for the Control Unit of a Main Power Gas Driven Electric Generator.

Main Power Gas Engine							
Piping Failure							
Failure from	**With Incipient**	**Incipient**		**Degraded**		**Critical**	
Condition	**(True/False)**	λ $(10^6 h)$	k	λ $(10^6 h)$	k	λ $(10^6 h)$	k
1	False	478.66	1.2	559.1	1.2	607.1	1.2
	True	N/A	N/A	139.78	1.2	151.78	1.2
2	False	421.38	1.2	473.27	1.2	493.35	1.2
	True	N/A	N/A	118.32	1.2	123.34	1.2
3	False	300.8	1.2	325.33	1.2	325.0	1.2
	True	N/A	N/A	81.33	1.2	81.25	1.2
4	False	182.27	1.2	190.09	1.2	181.64	1.2
	True	N/A	N/A	47.52	1.2	45.41	1.2
5	False	95.59	1.2	96.25	1.2	87.79	1.2
	True	N/A	N/A	24.06	1.2	21.95	1.2
6	False	43.92	1.2	42.75	1.2	37.14	1.2
	True	N/A	N/A	10.69	1.2	9.28	1.2

Table B.59: The failure rate data for the Piping Failure of a Main Power Gas Engine.

Main Power Gas Engine							
Starting Unit							
Failure from Condition	**With Incipient (True/False)**	**Incipient**		**Degraded**		**Critical**	
		λ (10^6h)	k	λ (10^6h)	k	λ (10^6h)	k
1	False	357.12	1.2	478.08	1.2	526.08	1.2
	True	N/A	N/A	119.52	1.2	131.52	1.2
2	False	314.39	1.2	404.69	1.2	427.5	1.2
	True	N/A	N/A	101.17	1.2	106.88	1.2
3	False	224.42	1.2	278.18	1.2	281.62	1.2
	True	N/A	N/A	69.55	1.2	70.41	1.2
4	False	135.99	1.2	162.54	1.2	157.4	1.2
	True	N/A	N/A	40.64	1.2	39.35	1.2
5	False	71.32	1.2	82.31	1.2	76.08	1.2
	True	N/A	N/A	20.58	1.2	19.02	1.2
6	False	32.77	1.2	36.55	1.2	32.18	1.2
	True	N/A	N/A	9.14	1.2	8.04	1.2

Table B.60: The failure rate data for the Starting Unit of a Main Power Gas Engine.

Main Power Gas Engine							
Internal Components							
Failure from Condition	**With Incipient (True/False)**	**Incipient**		**Degraded**		**Critical**	
		λ (10^6h)	k	λ (10^6h)	k	λ (10^6h)	k
1	False	301.4	1.2	440.93	1.2	488.93	1.2
	True	N/A	N/A	110.23	1.2	122.23	1.2
2	False	265.34	1.2	373.24	1.2	397.32	1.2
	True	N/A	N/A	93.31	1.2	99.33	1.2
3	False	189.41	1.2	256.57	1.2	261.74	1.2
	True	N/A	N/A	64.14	1.2	65.43	1.2
4	False	114.77	1.2	149.91	1.2	146.29	1.2
	True	N/A	N/A	37.48	1.2	36.57	1.2
5	False	60.19	1.2	75.91	1.2	70.71	1.2
	True	N/A	N/A	18.98	1.2	17.68	1.2
6	False	27.65	1.2	33.71	1.2	29.91	1.2
	True	N/A	N/A	8.43	1.2	7.48	1.2

Table B.61: The failure rate data for the Internal Components of a Main Power Gas Engine.

Pipe							
Wall Thickness							
Failure from Condition	**With Incipient (True/False)**	**Incipient**		**Degraded**		**Critical**	
		λ $(10^6 h)$	k	λ $(10^6 h)$	k	λ $(10^6 h)$	k
1	False	451.2	1.2	540.8	1.2	588.8	1.2
	True	N/A	N/A	135.2	1.2	147.2	1.2
2	False	397.21	1.2	457.78	1.2	478.47	1.2
	True	N/A	N/A	114.44	1.2	119.62	1.2
3	False	283.54	1.2	314.68	1.2	315.2	1.2
	True	N/A	N/A	78.67	1.2	78.8	1.2
4	False	171.81	1.2	183.87	1.2	176.16	1.2
	True	N/A	N/A	45.97	1.2	44.04	1.2
5	False	90.11	1.2	93.1	1.2	85.15	1.2
	True	N/A	N/A	23.28	1.2	21.29	1.2
6	False	41.4	1.2	41.35	1.2	36.02	1.2
	True	N/A	N/A	10.34	1.2	9.0	1.2

Table B.62: The failure rate data for the Wall Thickness of a Pipe.

Scrubber							
Vessel Wall Thickness							
Failure from Condition	**With Incipient (True/False)**	**Incipient**		**Degraded**		**Critical**	
		λ $(10^6 h)$	k	λ $(10^6 h)$	k	λ $(10^6 h)$	k
1	False	779.52	1.2	759.68	1.2	807.68	1.2
	True	N/A	N/A	189.92	1.2	201.92	1.2
2	False	686.24	1.2	643.06	1.2	656.34	1.2
	True	N/A	N/A	160.76	1.2	164.08	1.2
3	False	489.87	1.2	442.04	1.2	432.37	1.2
	True	N/A	N/A	110.51	1.2	108.09	1.2
4	False	296.83	1.2	258.28	1.2	241.65	1.2
	True	N/A	N/A	64.57	1.2	60.41	1.2
5	False	155.67	1.2	130.78	1.2	116.8	1.2
	True	N/A	N/A	32.7	1.2	29.2	1.2
6	False	71.52	1.2	58.09	1.2	49.4	1.2
	True	N/A	N/A	14.52	1.2	12.35	1.2

Table B.63: The failure rate data for the Vessel Wall Thickness of a Scrubber.

Scrubber							
Structural Wall Thickness							
Failure from Condition	**With Incipient (True/False)**	**Incipient**		**Degraded**		**Critical**	
		λ (10^6h)	k	λ (10^6h)	k	λ (10^6h)	k
1	False	779.52	1.2	759.68	1.2	807.68	1.2
	True	N/A	N/A	189.92	1.2	201.92	1.2
2	False	686.24	1.2	643.06	1.2	656.34	1.2
	True	N/A	N/A	160.76	1.2	164.08	1.2
3	False	489.87	1.2	442.04	1.2	432.37	1.2
	True	N/A	N/A	110.51	1.2	108.09	1.2
4	False	296.83	1.2	258.28	1.2	241.65	1.2
	True	N/A	N/A	64.57	1.2	60.41	1.2
5	False	155.67	1.2	130.78	1.2	116.8	1.2
	True	N/A	N/A	32.7	1.2	29.2	1.2
6	False	71.52	1.2	58.09	1.2	49.4	1.2
	True	N/A	N/A	14.52	1.2	12.35	1.2

Table B.64: The failure rate data for the Structural Wall Thickness of a Scrubber.

Scrubber							
Instrument Failure							
Failure from Condition	**With Incipient (True/False)**	**Incipient**		**Degraded**		**Critical**	
		λ (10^6h)	k	λ (10^6h)	k	λ (10^6h)	k
1	False	485.76	1.2	563.84	1.2	611.84	1.2
	True	N/A	N/A	140.96	1.2	152.96	1.2

Table B.65: The failure rate data for the Instrument Failure of a Scrubber.

Seawaterlift Centrifugal Pump							
Seal Failure							
Failure from Condition	**With Incipient (True/False)**	**Incipient**		**Degraded**		**Critical**	
		λ $(10^6 h)$	k	λ $(10^6 h)$	k	λ $(10^6 h)$	k
1	False	355.78	1.2	477.18	1.2	525.18	1.2
	True	N/A	N/A	119.3	1.2	131.3	1.2
2	False	313.2	1.2	403.93	1.2	426.78	1.2
	True	N/A	N/A	100.98	1.2	106.69	1.2
3	False	223.58	1.2	277.66	1.2	281.14	1.2
	True	N/A	N/A	69.42	1.2	70.29	1.2
4	False	135.48	1.2	162.24	1.2	157.13	1.2
	True	N/A	N/A	40.56	1.2	39.28	1.2
5	False	71.05	1.2	82.15	1.2	75.95	1.2
	True	N/A	N/A	20.54	1.2	18.99	1.2
6	False	32.64	1.2	36.49	1.2	32.12	1.2
	True	N/A	N/A	9.12	1.2	8.03	1.2

Table B.66: The failure rate data for the Seal Failure of a Seawaterlift Centrifugal Pump.

Seawaterlift Centrifugal Pump							
Piping Failure							
Failure from Condition	**With Incipient (True/False)**	**Incipient**		**Degraded**		**Critical**	
		λ (10^6h)	k	λ (10^6h)	k	λ (10^6h)	k
1	False	307.2	1.2	444.8	1.2	492.8	1.2
	True	N/A	N/A	111.2	1.2	123.2	1.2
2	False	270.44	1.2	376.52	1.2	400.46	1.2
	True	N/A	N/A	94.13	1.2	100.12	1.2
3	False	193.05	1.2	258.82	1.2	263.81	1.2
	True	N/A	N/A	64.7	1.2	65.95	1.2
4	False	116.98	1.2	151.23	1.2	147.44	1.2
	True	N/A	N/A	37.81	1.2	36.86	1.2
5	False	61.35	1.2	76.58	1.2	71.27	1.2
	True	N/A	N/A	19.14	1.2	17.82	1.2
6	False	28.19	1.2	34.01	1.2	30.14	1.2
	True	N/A	N/A	8.5	1.2	7.54	1.2

Table B.67: The failure rate data for the Piping Failure of a Seawaterlift Centrifugal Pump.

Seawaterlift Centrifugal Pump							
Internal Components							
Failure from Condition	**With Incipient (True/False)**	**Incipient**		**Degraded**		**Critical**	
		λ (10^6h)	k	λ (10^6h)	k	λ (10^6h)	k
1	False	343.87	1.2	469.25	1.2	517.25	1.2
	True	N/A	N/A	117.31	1.2	129.31	1.2
2	False	302.72	1.2	397.21	1.2	420.33	1.2
	True	N/A	N/A	99.3	1.2	105.08	1.2
3	False	216.1	1.2	273.04	1.2	276.9	1.2
	True	N/A	N/A	68.26	1.2	69.22	1.2
4	False	130.94	1.2	159.54	1.2	154.76	1.2
	True	N/A	N/A	39.89	1.2	38.69	1.2
5	False	68.67	1.2	80.78	1.2	74.8	1.2
	True	N/A	N/A	20.2	1.2	18.7	1.2
6	False	31.55	1.2	35.88	1.2	31.64	1.2
	True	N/A	N/A	8.97	1.2	7.91	1.2

Table B.68: The failure rate data for the Internal Components of a Seawaterlift Centrifugal Pump.

Seawaterlift Electric Motor							
Control Unit							
Failure from Condition	**With Incipient (True/False)**	**Incipient**		**Degraded**		**Critical**	
		λ (10^6h)	k	λ (10^6h)	k	λ (10^6h)	k
1	False	451.2	1.2	540.8	1.2	588.8	1.2
	True	N/A	N/A	135.2	1.2	147.2	1.2
2	False	397.21	1.2	457.78	1.2	478.47	1.2
	True	N/A	N/A	114.44	1.2	119.62	1.2
3	False	283.54	1.2	314.68	1.2	315.2	1.2
	True	N/A	N/A	78.67	1.2	78.8	1.2
4	False	171.81	1.2	183.87	1.2	176.16	1.2
	True	N/A	N/A	45.97	1.2	44.04	1.2
5	False	90.11	1.2	93.1	1.2	85.15	1.2
	True	N/A	N/A	23.28	1.2	21.29	1.2
6	False	41.4	1.2	41.35	1.2	36.02	1.2
	True	N/A	N/A	10.34	1.2	9.0	1.2

Table B.69: The failure rate data for the Control Unit of a Seawaterlift Electric Motor.

Seawaterlift Electric Motor							
Internal Components							
Failure from Condition	**With Incipient (True/False)**	**Incipient**		**Degraded**		**Critical**	
		λ $(10^6 h)$	k	λ $(10^6 h)$	k	λ $(10^6 h)$	k
1	False	481.92	1.2	561.28	1.2	609.28	1.2
	True	N/A	N/A	140.32	1.2	152.32	1.2
2	False	424.25	1.2	475.11	1.2	495.11	1.2
	True	N/A	N/A	118.78	1.2	123.78	1.2
3	False	302.85	1.2	326.59	1.2	326.16	1.2
	True	N/A	N/A	81.65	1.2	81.54	1.2
4	False	183.51	1.2	190.83	1.2	182.29	1.2
	True	N/A	N/A	47.71	1.2	45.57	1.2
5	False	96.24	1.2	96.63	1.2	88.11	1.2
	True	N/A	N/A	24.16	1.2	22.03	1.2
6	False	44.22	1.2	42.92	1.2	37.27	1.2
	True	N/A	N/A	10.73	1.2	9.32	1.2

Table B.70: The failure rate data for the Internal Components of a Seawaterlift Electric Motor.

Separator							
Vessel Wall Thickness							
Failure from Condition	**With Incipient (True/False)**	**Incipient**		**Degraded**		**Critical**	
		λ $(10^6 h)$	k	λ $(10^6 h)$	k	λ $(10^6 h)$	k
1	False	1050.24	1.2	940.16	1.2	988.16	1.2
	True	N/A	N/A	235.04	1.2	247.04	1.2
2	False	924.57	1.2	795.83	1.2	803.0	1.2
	True	N/A	N/A	198.96	1.2	200.75	1.2
3	False	660.0	1.2	547.05	1.2	528.99	1.2
	True	N/A	N/A	136.76	1.2	132.25	1.2
4	False	399.92	1.2	319.65	1.2	295.65	1.2
	True	N/A	N/A	79.91	1.2	73.91	1.2
5	False	209.74	1.2	161.86	1.2	142.9	1.2
	True	N/A	N/A	40.46	1.2	35.73	1.2
6	False	96.36	1.2	71.89	1.2	60.44	1.2
	True	N/A	N/A	17.97	1.2	15.11	1.2

Table B.71: The failure rate data for the Vessel Wall Thickness of a Separator.

Separator							
Structural Wall Thickness							
Failure from Condition	**With Incipient (True/False)**	**Incipient**		**Degraded**		**Critical**	
		λ $(10^6 h)$	k	λ $(10^6 h)$	k	λ $(10^6 h)$	k
1	False	355.2	1.2	476.8	1.2	524.8	1.2
	True	N/A	N/A	119.2	1.2	131.2	1.2
2	False	312.7	1.2	403.6	1.2	426.46	1.2
	True	N/A	N/A	100.9	1.2	106.62	1.2
3	False	223.22	1.2	277.44	1.2	280.94	1.2
	True	N/A	N/A	69.36	1.2	70.23	1.2
4	False	135.26	1.2	162.11	1.2	157.02	1.2
	True	N/A	N/A	40.53	1.2	39.25	1.2
5	False	70.93	1.2	82.08	1.2	75.89	1.2
	True	N/A	N/A	20.52	1.2	18.97	1.2
6	False	32.59	1.2	36.46	1.2	32.1	1.2
	True	N/A	N/A	9.11	1.2	8.03	1.2

Table B.72: The failure rate data for the Structural Wall Thickness of a Separator.

Separator							
Instrument Failure							
Failure from Condition	**With Incipient (True/False)**	**Incipient**		**Degraded**		**Critical**	
		λ $(10^6 h)$	k	λ $(10^6 h)$	k	λ $(10^6 h)$	k
1	False	1132.8	1.2	995.2	1.2	1043.2	1.2
	True	N/A	N/A	248.8	1.2	260.8	1.2

Table B.73: The failure rate data for the Instrument Failure of a Separator.

Separator							
Deposit Size							
Failure from Condition	**With Incipient (True/False)**	**Incipient**		**Degraded**		**Critical**	
		λ (10^6h)	k	λ (10^6h)	k	λ (10^6h)	k
1	False	397.44	1.2	504.96	1.2	552.96	1.2
	True	N/A	N/A	126.24	1.2	138.24	1.2
2	False	349.88	1.2	427.44	1.2	449.35	1.2
	True	N/A	N/A	106.86	1.2	112.34	1.2
3	False	249.76	1.2	293.82	1.2	296.01	1.2
	True	N/A	N/A	73.46	1.2	74.0	1.2
4	False	151.34	1.2	171.68	1.2	165.44	1.2
	True	N/A	N/A	42.92	1.2	41.36	1.2
5	False	79.37	1.2	86.93	1.2	79.96	1.2
	True	N/A	N/A	21.73	1.2	19.99	1.2
6	False	36.47	1.2	38.61	1.2	33.82	1.2
	True	N/A	N/A	9.65	1.2	8.46	1.2

Table B.74: The failure rate data for the Deposit Size of a Separator.

Valve							
Wall Thickness							
Failure from Condition	**With Incipient (True/False)**	**Incipient**		**Degraded**		**Critical**	
		λ $(10^6 h)$	k	λ $(10^6 h)$	k	λ $(10^6 h)$	k
1	False	259.2	1.2	412.8	1.2	460.8	1.2
	True	N/A	N/A	103.2	1.2	115.2	1.2
2	False	228.18	1.2	349.43	1.2	374.46	1.2
	True	N/A	N/A	87.36	1.2	93.61	1.2
3	False	162.89	1.2	240.2	1.2	246.68	1.2
	True	N/A	N/A	60.05	1.2	61.67	1.2
4	False	98.7	1.2	140.35	1.2	137.87	1.2
	True	N/A	N/A	35.09	1.2	34.47	1.2
5	False	51.76	1.2	71.07	1.2	66.64	1.2
	True	N/A	N/A	17.77	1.2	16.66	1.2
6	False	23.78	1.2	31.56	1.2	28.19	1.2
	True	N/A	N/A	7.89	1.2	7.05	1.2

Table B.75: The failure rate data for the Wall Thickness of a Valve.

Valve							
Closing Times							
Failure from Condition	**With Incipient (True/False)**	**Incipient**		**Degraded**		**Critical**	
		λ (10^6h)	k	λ (10^6h)	k	λ (10^6h)	k
1	False	234.24	1.2	396.16	1.2	444.16	1.2
	True	N/A	N/A	99.04	1.2	111.04	1.2
2	False	206.21	1.2	335.34	1.2	360.93	1.2
	True	N/A	N/A	83.84	1.2	90.23	1.2
3	False	147.2	1.2	230.52	1.2	237.77	1.2
	True	N/A	N/A	57.63	1.2	59.44	1.2
4	False	89.2	1.2	134.69	1.2	132.89	1.2
	True	N/A	N/A	33.67	1.2	33.22	1.2
5	False	46.78	1.2	68.2	1.2	64.23	1.2
	True	N/A	N/A	17.05	1.2	16.06	1.2
6	False	21.49	1.2	30.29	1.2	27.17	1.2
	True	N/A	N/A	7.57	1.2	6.79	1.2

Table B.76: The failure rate data for the Closing Times of a Valve.

Water Firefighting Centrifugal Pump

Seal Failure							
Failure from Condition	**With Incipient (True/False)**	**Incipient**		**Degraded**		**Critical**	
		λ (10^6h)	k	λ (10^6h)	k	λ (10^6h)	k
1	False	384.19	1.2	496.13	1.2	544.13	1.2
	True	N/A	N/A	124.03	1.2	136.03	1.2
2	False	338.22	1.2	419.96	1.2	442.17	1.2
	True	N/A	N/A	104.99	1.2	110.54	1.2
3	False	241.44	1.2	288.68	1.2	291.28	1.2
	True	N/A	N/A	72.17	1.2	72.82	1.2
4	False	146.3	1.2	168.68	1.2	162.8	1.2
	True	N/A	N/A	42.17	1.2	40.7	1.2
5	False	76.72	1.2	85.41	1.2	78.69	1.2
	True	N/A	N/A	21.35	1.2	19.67	1.2
6	False	35.25	1.2	37.93	1.2	33.28	1.2
	True	N/A	N/A	9.48	1.2	8.32	1.2

Table B.77: The failure rate data for the Seal Failure of a Water Firefighting Centrifugal Pump.

Water Firefighting Centrifugal Pump

Piping Failure							
Failure from Condition	**With Incipient (True/False)**	**Incipient**		**Degraded**		**Critical**	
		λ (10^6h)	k	λ (10^6h)	k	λ (10^6h)	k
1	False	376.32	1.2	490.88	1.2	538.88	1.2
	True	N/A	N/A	122.72	1.2	134.72	1.2
2	False	331.29	1.2	415.52	1.2	437.91	1.2
	True	N/A	N/A	103.88	1.2	109.48	1.2
3	False	236.49	1.2	285.63	1.2	288.48	1.2
	True	N/A	N/A	71.41	1.2	72.12	1.2
4	False	143.3	1.2	166.9	1.2	161.23	1.2
	True	N/A	N/A	41.72	1.2	40.31	1.2
5	False	75.15	1.2	84.51	1.2	77.93	1.2
	True	N/A	N/A	21.13	1.2	19.48	1.2
6	False	34.53	1.2	37.53	1.2	32.96	1.2
	True	N/A	N/A	9.38	1.2	8.24	1.2

Table B.78: The failure rate data for the Piping Failure of a Water Firefighting Centrifugal Pump.

Water Firefighting Centrifugal Pump							
Internal Components							
Failure from Condition	**With Incipient (True/False)**	**Incipient**		**Degraded**		**Critical**	
		λ (10^6h)	k	λ (10^6h)	k	λ (10^6h)	k
1	False	334.08	1.2	462.72	1.2	510.72	1.2
	True	N/A	N/A	115.68	1.2	127.68	1.2
2	False	294.1	1.2	391.68	1.2	415.02	1.2
	True	N/A	N/A	97.92	1.2	103.76	1.2
3	False	209.94	1.2	269.24	1.2	273.4	1.2
	True	N/A	N/A	67.31	1.2	68.35	1.2
4	False	127.21	1.2	157.32	1.2	152.8	1.2
	True	N/A	N/A	39.33	1.2	38.2	1.2
5	False	66.72	1.2	79.66	1.2	73.86	1.2
	True	N/A	N/A	19.92	1.2	18.46	1.2
6	False	30.65	1.2	35.38	1.2	31.24	1.2
	True	N/A	N/A	8.85	1.2	7.81	1.2

Table B.79: The failure rate data for the Internal Components of a Water Firefighting Centrifugal Pump.

Water Firefighting Diesel Engine

Piping Failure

Failure from Condition	With Incipient (True/False)	Incipient		Degraded		Critical	
		λ $(10^6 h)$	k	λ $(10^6 h)$	k	λ $(10^6 h)$	k
1	False	393.02	1.2	502.02	1.2	550.02	1.2
	True	N/A	N/A	125.5	1.2	137.5	1.2
2	False	346.0	1.2	424.95	1.2	446.96	1.2
	True	N/A	N/A	106.24	1.2	111.74	1.2
3	False	246.99	1.2	292.11	1.2	294.44	1.2
	True	N/A	N/A	73.03	1.2	73.61	1.2
4	False	149.66	1.2	170.68	1.2	164.56	1.2
	True	N/A	N/A	42.67	1.2	41.14	1.2
5	False	78.49	1.2	86.43	1.2	79.54	1.2
	True	N/A	N/A	21.61	1.2	19.88	1.2
6	False	36.06	1.2	38.38	1.2	33.64	1.2
	True	N/A	N/A	9.6	1.2	8.41	1.2

Table B.80: The failure rate data for the Piping Failure of a Water Firefighting Diesel Engine.

Water Firefighting Diesel Engine							
Starting Unit Failure							
Failure from Condition	**With Incipient (True/False)**	**Incipient**		**Degraded**		**Critical**	
		λ $(10^6 h)$	k	λ $(10^6 h)$	k	λ $(10^6 h)$	k
1	False	329.66	1.2	459.78	1.2	507.78	1.2
	True	N/A	N/A	114.94	1.2	126.94	1.2
2	False	290.22	1.2	389.19	1.2	412.63	1.2
	True	N/A	N/A	97.3	1.2	103.16	1.2
3	False	207.17	1.2	267.53	1.2	271.82	1.2
	True	N/A	N/A	66.88	1.2	67.96	1.2
4	False	125.53	1.2	156.32	1.2	151.92	1.2
	True	N/A	N/A	39.08	1.2	37.98	1.2
5	False	65.83	1.2	79.15	1.2	73.43	1.2
	True	N/A	N/A	19.79	1.2	18.36	1.2
6	False	30.25	1.2	35.15	1.2	31.06	1.2
	True	N/A	N/A	8.79	1.2	7.77	1.2

Table B.81: The failure rate data for the Starting Unit Failure of a Water Firefighting Diesel Engine.

Asset	Inspection		Failure Mode		
	Internal	**External**	**Preventative**	**Degraded**	**Critical**
Compressor	100	25	200	1000	2000
			200	1000	2000
			200	1000	2000
			200	1000	2000
Contactor	200	15	400	2000	4000
			400	2000	4000
			400	2000	4000

Table B.82: Asset management strategy expenditures, part 1.

B.3 Asset Management Expenditures

This section gives the AM expenditures for inspection and maintenance actions for each asset type.

Asset	Inspection		Failure Mode		
	Internal	**External**	**Preventative**	**Degraded**	**Critical**
Deluge Valve	20	5	20	100	200
			20	100	
Emergency Power Diesel Driven Electric Generator	100	25	20	100	200
			20	100	
Emergency Power Diesel Engine	100	25	20	100	200
			20	100	
Fire or Gas Detector	N/A	2	20	100	200

Table B.83: Asset management strategy expenditures, part 2.

Asset	Inspection		Failure Mode		
	Internal	**External**	**Preventative**	**Degraded**	**Critical**
Heat Exchanger	100	25	200	1000	2000
			200	1000	2000
			200	1000	2000
			200	1000	2000
Main Power Gas Driven Electric Generator	100	25	20	100	200
			20	100	
Main Power Gas Engine	100	25	20	100	200
			20	100	200
			20	100	200

Table B.84: Asset management strategy expenditures, part 3.

	Inspection		Failure Mode		
Asset	**Internal**	**External**	**Preventative**	**Degraded**	**Critical**
Pipe	N/A	5	20	100	200
Scrubber	200	50	400	2000	4000
			400	2000	4000
			400	2000	4000
Seawaterlift Centrifugal Pump	100	25	20	100	200
			20	100	200
			20	100	200

Table B.85: Asset management strategy expenditures, part 4.

	Inspection		Failure Mode		
Asset	**Internal**	**External**	**Preventative**	**Degraded**	**Critical**
Seawaterlift Electric Motor	100	25	20	100	200
			20	100	
Separator	200	25	400	2000	4000
			400	2000	4000
			400	2000	4000
			400	2000	4000
Valve	20	5	20	100	200
			20	100	

Table B.86: Asset management strategy expenditures, part 5.

	Inspection		Failure Mode		
Asset	**Internal**	**External**	**Preventative**	**Degraded**	**Critical**
Water Firefighting Centrifugal Pump	100	25	20	100	200
			20	100	200
			20	100	200
Water Firefighting Diesel Engine	100	25	20	100	200
			20	100	

Table B.87: Asset management strategy expenditures, part 6.

	Maintenance	**Inspection**
Teams	5000	5000

Table B.88: Asset management strategy expenditures for teams.

Asset	Inspection Interval (weeks)		Observable	Maintenance Decision Condition
	Internal	External		
Compressor	104	13	Vessel Wall Thickness	4
			Structural Wall Thickness	4
			Internal Degradation	4
			Instrument Failure	4
Contactor	104	13	Vessel Wall Thickness	4
			Structural Wall Thickness	4
			Instrument Failure	4

Table B.89: Asset management strategy 'A' inspection intervals and first condition that maintenance is performed on, part 1.

B.4 Asset Management Strategies

This section tables three AM strategies that are used as example strategies in this work. The inspection intervals and maintenance decisions are defined by asset type. However, the AM strategy can be specified for individually for each asset instance. The optimisation has decision variables associated with these parameters for each asset instance.

B.4.1 Strategy A

Asset	Inspection Interval (weeks)		Observable	Maintenance Decision Condition
	Internal	**External**		
Deluge Valve	104	13	Wall Thickness	4
			Closing Times	4
Emergency Power Diesel Driven Electric Generator	26	13	Internal Components	4
			Control Unit	4
Emergency Power Diesel Engine	26	13	Piping Failure	4
			Internal Components	4
Fire or Gas Detector	-	26	Detector Head	4

Table B.90: Asset management strategy 'A' inspection intervals and first condition that maintenance is performed on, part 2.

Asset	Inspection Interval (weeks)		Observable	Maintenance Decision Condition
	Internal	External		
Heat Exchanger	104	13	Vessel Wall Thickness	4
			Structural Wall Thickness	4
			Instrument Failure	4
			Deposit Size	4
Main Power Gas Driven Electric Generator	26	13	Piping Failure	4
			Control Unit	4
Main Power Gas Engine	104	26	Piping Failure	4
			Starting Unit	4
			Internal Components	4

Table B.91: Asset management strategy 'A' inspection intervals and first condition that maintenance is performed on, part 3.

Asset	Inspection Interval (weeks)		Observable	Maintenance Decision Condition
	Internal	External		
Pipe	-	104	Wall Thickness	4
Scrubber	104	26	Vessel Wall Thickness	4
			Structural Wall Thickness	4
			Instrument Failure	4
Seawaterlift Centrifugal Pump	104	26	Seal Failure	4
			Piping Failure	4
			Internal Components	4

Table B.92: Asset management strategy 'A' inspection intervals and first condition that maintenance is performed on, part 4.

Asset	Inspection Interval (weeks)		Observable	Maintenance Decision Condition
	Internal	External		
Seawaterlift Electric Motor	104	26	Control Unit	4
			Internal Components	4
Separator	104	13	Vessel Wall Thickness	4
			Structural Wall Thickness	4
			Instrument Failure	4
			Deposit Size	4
Valve	104	13	Wall Thickness	4
			Closing Times	4

Table B.93: Asset management strategy 'A' inspection intervals and first condition that maintenance is performed on, part 5.

Asset	Inspection Interval (weeks)		Observable	Maintenance Decision Condition
	Internal	External		
Water Firefighting Centrifugal Pump	104	26	Seal Failure	4
			Piping Failure	4
			Internal Components	4
Water Firefighting Diesel Engine	104	26	Piping Failure	4
			Starting Unit Failure	4

Table B.94: Asset management strategy 'A' inspection intervals and first condition that maintenance is performed on, part 6.

	Maintenance	Inspection
Teams	4	4

Table B.95: Asset management strategy 'A' number of maintenance and inspection teams.

Asset	Inspection Interval (weeks)		Observable	Maintenance Decision Condition
	Internal	External		
Compressor	104	13	Vessel Wall Thickness	3
			Structural Wall Thickness	3
			Internal Degradation	3
			Instrument Failure	3
Contactor	104	13	Vessel Wall Thickness	3
			Structural Wall Thickness	3
			Instrument Failure	3

Table B.96: Asset management strategy 'B' inspection intervals and first condition that maintenance is performed on, part 1.

B.4.2 Strategy B

Asset	Inspection Interval (weeks)		Observable	Maintenance Decision Condition
	Internal	External		
Deluge Valve	104	13	Wall Thickness	3
			Closing Times	3
Emergency Power Diesel Driven Electric Generator	26	13	Internal Components	3
			Control Unit	3
Emergency Power Diesel Engine	26	13	Piping Failure	3
			Internal Components	3
Fire or Gas Detector	-	26	Detector Head	3

Table B.97: Asset management strategy 'B' inspection intervals and first condition that maintenance is performed on, part 2.

Asset	Inspection Interval (weeks)		Observable	Maintenance Decision Condition
	Internal	External		
Heat Exchanger	104	13	Vessel Wall Thickness	3
			Structural Wall Thickness	3
			Instrument Failure	3
			Deposit Size	3
Main Power Gas Driven Electric Generator	26	13	Piping Failure	3
			Control Unit	3
Main Power Gas Engine	104	26	Piping Failure	3
			Starting Unit	3
			Internal Components	3

Table B.98: Asset management strategy 'B' inspection intervals and first condition that maintenance is performed on, part 3.

Asset	Inspection Interval (weeks)		Observable	Maintenance Decision Condition
	Internal	External		
Pipe	-	104	Wall Thickness	3
Scrubber	104	26	Vessel Wall Thickness	3
			Structural Wall Thickness	3
			Instrument Failure	3
Seawaterlift Centrifugal Pump	104	26	Seal Failure	3
			Piping Failure	3
			Internal Components	3

Table B.99: Asset management strategy 'B' inspection intervals and first condition that maintenance is performed on, part 4.

Asset	Inspection Interval (weeks)		Observable	Maintenance Decision Condition
	Internal	External		
Seawaterlift Electric Motor	104	26	Control Unit	3
			Internal Components	3
Separator	104	13	Vessel Wall Thickness	3
			Structural Wall Thickness	3
			Instrument Failure	3
			Deposit Size	3
Valve	104	13	Wall Thickness	3
			Closing Times	3

Table B.100: Asset management strategy 'B' inspection intervals and first condition that maintenance is performed on, part 5.

Asset	Inspection Interval (weeks)		Observable	Maintenance Decision Condition
	Internal	External		
Water Firefighting Centrifugal Pump	104	26	Seal Failure	3
			Piping Failure	3
			Internal Components	3
Water Firefighting Diesel Engine	104	26	Piping Failure	3
			Starting Unit Failure	3

Table B.101: Asset management strategy 'B' inspection intervals and first condition that maintenance is performed on, part 6.

	Maintenance	Inspection
Teams	4	4

Table B.102: Asset management strategy 'B' number of maintenance and inspection teams.

Asset	Inspection Interval (weeks)		Observable	Maintenance Decision Condition
	Internal	External		
Compressor	104	13	Vessel Wall Thickness	5
			Structural Wall Thickness	5
			Internal Degradation	5
			Instrument Failure	5
Contactor	104	13	Vessel Wall Thickness	5
			Structural Wall Thickness	5
			Instrument Failure	5

Table B.103: Asset management strategy 'C' inspection intervals and first condition that maintenance is performed on, part 1.

B.4.3 Strategy C

Asset	Inspection Interval (weeks)		Observable	Maintenance Decision Condition
	Internal	**External**		
Deluge Valve	104	13	Wall Thickness	5
			Closing Times	5
Emergency Power Diesel Driven Electric Generator	26	13	Internal Components	5
			Control Unit	3
Emergency Power Diesel Engine	26	13	Piping Failure	5
			Internal Components	5
Fire or Gas Detector	-	26	Detector Head	5

Table B.104: Asset management strategy 'C' inspection intervals and first condition that maintenance is performed on, part 2.

Asset	Inspection Interval (weeks)		Observable	Maintenance Decision Condition
	Internal	External		
Heat Exchanger	104	13	Vessel Wall Thickness	5
			Structural Wall Thickness	5
			Instrument Failure	5
			Deposit Size	5
Main Power Gas Driven Electric Generator	26	13	Piping Failure	5
			Control Unit	5
Main Power Gas Engine	104	26	Piping Failure	5
			Starting Unit	5
			Internal Components	5

Table B.105: Asset management strategy 'C' inspection intervals and first condition that maintenance is performed on, part 3.

Asset	Inspection Interval (weeks)		Observable	Maintenance Decision Condition
	Internal	External		
Pipe	-	104	Wall Thickness	5
Scrubber	104	26	Vessel Wall Thickness	5
			Structural Wall Thickness	5
			Instrument Failure	5
Seawaterlift Centrifugal Pump	104	26	Seal Failure	5
			Piping Failure	5
			Internal Components	5

Table B.106: Asset management strategy 'C' inspection intervals and first condition that maintenance is performed on, part 4.

Asset	Inspection Interval (weeks)		Observable	Maintenance Decision Condition
	Internal	External		
Seawaterlift Electric Motor	104	26	Control Unit	5
			Internal Components	5
Separator	104	13	Vessel Wall Thickness	5
			Structural Wall Thickness	5
			Instrument Failure	5
			Deposit Size	5
Valve	104	13	Wall Thickness	5
			Closing Times	5

Table B.107: Asset management strategy 'C' inspection intervals and first condition that maintenance is performed on, part 5.

Asset	Inspection Interval (weeks)		Observable	Maintenance Decision Condition
	Internal	External		
Water Firefighting Centrifugal Pump	104	26	Seal Failure	5
			Piping Failure	5
			Internal Components	5
Water Firefighting Diesel Engine	104	26	Piping Failure	5
			Starting Unit Failure	5

Table B.108: Asset management strategy 'C' inspection intervals and first condition that maintenance is performed on, part 6.

	Maintenance	Inspection
Teams	4	4

Table B.109: Asset management strategy 'C' number of maintenance and inspection teams.

Appendix C

Consequence Analysis Data

C.1 Constants

This sections gives values of the constants used in the consequence analysis.

Symbol	Variable	Value
g	Gravitational acceleration	$9.81ms^{-1}$
p_a	Atmospheric gas pressure	$101325Pa$
$\rho_{g,\text{atmo}}$	Atmospheric gas density	$1.225kgm^{-3}$
$\rho_{o,\text{atmo}}$	Atmospheric oil density	$900kgm^{-3}$
A	Overpressure A with Deluge	-18.215
A	Overpressure A without Deluge	-19.693
B	Overpressure B with Deluge	1.007
B	Overpressure B without Deluge	1.0563
$O_{\max}$	Overpressure Maximum	8.7
C_s	Stoichiometric concentration	0.0888
R_B	Mass burn rate	0.035 kgs^{-1}
C_{LFL}	Lower Flammable Limit	0.05
C_{UFL}	Upper Flammable Limit	0.15

Table C.1: A table of constants used in the consequence analysis.

Symbol	Variable	Value
$p_{I,\text{Explosion}}$	Probability of ignition of an explosion per unit time	$1/90s^{-1}$
$p_{I,\text{JetFire}}$	Probability of ignition of a jet fire per unit time	$1/270s^{-1}$
$p_{I,\text{PoolFire}}$	Probability of ignition of a pool fire per unit time	$1/180s^{-1}$

Table C.2: A table of the probability of ignition per unit time for each consequent event.

C.2 Vessel data

This section contains data on the vessel's and their contents for each production vessel.

Vessel Type	Index	Module	Volume (m^3)	Height (m)	Gas Pressure (bar)	Oil (%)	Gas (%)
Valve	1	Separation	14.5	0.5	13.0	0.0	100.0
	2	Compression	9.8	0.5	49.0	28.57	71.43
	3	Separation	37.5	0.5	186.0	30.67	69.33
	4	Compression	5.8	0.5	1780.0	0.0	100.0
Separator	1	Separation	166	10	20.7	53.01	46.99
	2	Separation	109	10	1.6	52.29	47.71
Scrubber	1	Compression	14.5	15	13.0	0.0	100.0
	2	Compression	9.8	15	49.0	28.57	71.43
	3	Compression	37.5	15	186.0	30.67	69.33
	4	Compression	18.5	15	493.0	24.32	75.68
	5	Compression	10.8	15	490.0	0.0	100.0
	6	Compression	5.8	15	1780.0	0.0	100.0
Contactor	1	Compression	21.5	15	492.0	0.0	100.0
	2	Compression	18.6	15	492.0	0.0	100.0
Heat Exchanger	1	Compression	9.8	5	49.0	28.57	71.43
	2	Compression	37.5	5	186.0	30.67	69.33
	3	Compression	18.5	5	493.0	24.32	75.68
	4	Compression	5.8	5	1780.0	0.0	100.0

Table C.3: A table of data on the production vessel for use by the consequence analysis (Part 1 of 2)

Vessel Type	**Index**	**Module**	**Volume** (m^3)	**Height** (m)	**Gas Pressure (bar)**	**Oil** (%)	**Gas** (%)
Compressor	1	Compression	9.8	5	49.0	28.57	71.43
	2	Compression	37.5	5	186.0	30.67	69.33
	3	Compression	18.5	5	493.0	24.32	75.68
	4	Compression	5.8	5	1780.0	0.0	100.0
Pipe	1	Compression	166	0.5	20.7	53.01	46.99
	2	Compression	109	0.5	1.6	52.29	47.71
	3	Separation	14.5	0.5	13.0	0.0	100.0
	4	Separation	14.5	0.5	13.0	0.0	100.0
	5	Separation	9.8	0.5	49.0	28.57	71.43
	6	Compression	9.8	0.5	49.0	28.57	71.43
	7	Compression	9.8	0.5	49.0	28.57	71.43
	8	Compression	9.8	0.5	49.0	28.57	71.43
	9	Compression	37.5	0.5	186.0	30.67	69.33
	10	Compression	37.5	0.5	186.0	30.67	69.33
	11	Compression	37.5	0.5	186.0	30.67	69.33
	12	Compression	37.5	0.5	186.0	30.67	69.33
	13	Compression	37.5	0.5	186.0	30.67	69.33
	14	Separation	37.5	0.5	186.0	30.67	69.33
	15	Compression	18.5	0.5	493.0	24.32	75.68
	16	Compression	18.5	0.5	493.0	24.32	75.68
	17	Compression	18.5	0.5	493.0	24.32	75.68
	18	Compression	21.5	0.5	492.0	0.0	100.0
	19	Compression	10.8	0.5	490.0	0.0	100.0
	20	Compression	5.8	0.5	1780.0	0.0	100.0
	21	Compression	5.8	0.5	1780.0	0.0	100.0
	22	Compression	5.8	0.5	1780.0	0.0	100.0
	23	Compression	5.8	0.5	1780.0	0.0	100.0

Table C.4: A table of data on the production vessel for use by the consequence analysis (Part 2 of 2).

C.3 Consequence Event Frequencies

Figure C.1 gives the probability of the different escalation events for the production assets for their degraded failure modes. The counter part figure for their critical failure modes was given in Figure 6.11.

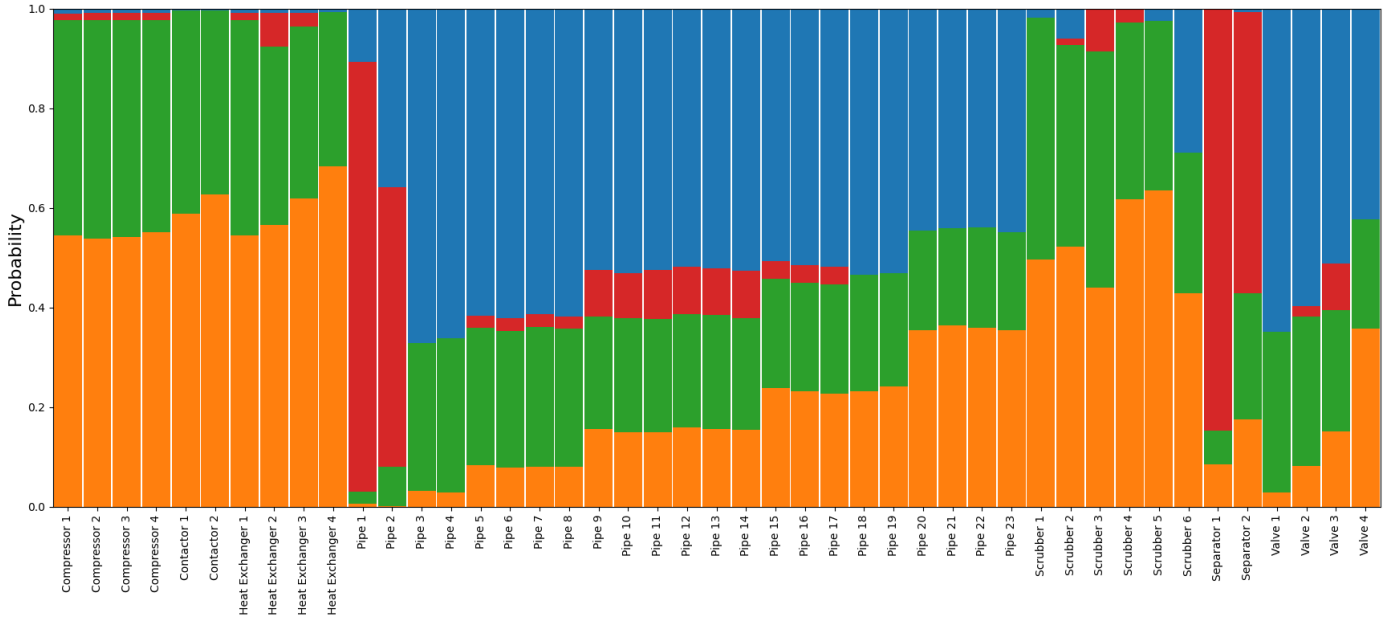

Figure C.1: The probability of escalation events for all of the production assets for their degraded failure modes. Explosion, Jet fire, Pool fire, No escalation.